

CRANFIELD UNIVERSITY

Lisa Dicken

PASSIVE BLOODSTAINS ON COTTON FABRICS

DEFENCE ACADEMY  
CENTRE FOR DEFENCE ENGINEERING

PhD THESIS  
Academic Year: 2018 - 2019

Supervisor: Dr. Clare Knock  
February 2019

CRANFIELD UNIVERSITY

DEFENCE ACADEMY  
CENTRE FOR DEFENCE ENGINEERING

PhD THESIS

Academic Year 2018 - 2019

Lisa Dicken

PASSIVE BLOODSTAINS ON COTTON FABRICS

Supervisor: Dr. Clare Knock  
February 2019

© Cranfield University 2019. All rights reserved. No part of this publication may be reproduced without the written permission of the copyright owner.

## ABSTRACT

Bloodstains on finished fabrics are frequently found at crime scenes, however there has been limited work on the creation mechanisms and interaction of blood and fabric. The initial aim of this research was to verify the use of a micro computed tomography ( $\mu$ CT) scanner for blood pattern analysis (BPA) research. The pilot study confirmed it was possible to visualise the form of the bloodstain inside the fabric in the CT scans, providing additional information to what could be learnt from examination of the external bloodstains alone.

Bloodstains were created on three mass per unit areas (85.1, 163.5 and 224.6 g/m<sup>2</sup>) of laundered 100% cotton plain woven calico from six impact velocities (1.7, 2.9, 4.1, 4.9, 5.1 and 5.4 ms<sup>-1</sup>). The bloodstains were examined with external photographs, area measurements, a  $\mu$ CT scanner and a scanning electron microscope (SEM). The fabric with the lightest mass per unit area (85.1 g/m<sup>2</sup>) generally produced the largest bloodstains. The blood was able to coat the yarns owing to the high porosity of the fabric and wick along the low linear density yarns. For the fabrics with the middle (163.5 g/m<sup>2</sup>) and heaviest (224.6 g/m<sup>2</sup>) mass per unit areas less wicking occurred. Dry bloodstain area increased with impact velocity due to the increase in lateral spreading at impact with greater impact velocities. The yarn linear density, sett and yarn twist altered the way in which blood interacted with the fabrics.

Bloodstains were then created on the calico fabrics following reactive dyeing or digital printing. The dry bloodstain areas increased for the dyed fabric owing to the swelling of the fibres following dyeing, reducing the intra-yarn spaces to a more optimum size for wicking. The digital printing increased the wettability of the fabric, most likely with a reduction in surface roughness. This allowed the blood to spread more easily on the surface of the fabric, before wicking into and along the intra-yarn spaces. The differences seen among the dry bloodstains for the different treatments emphasise the importance of not comparing bloodstains between fabrics with different finishing treatments.

**Keywords:**

Micro computed tomography

Scanning electron microscopy

Wetting

Wicking

Plain woven

Reactively dyed

Impact velocity

Mass per unit area

Linear density

Digital printing

## **ACKNOWLEDGEMENTS**

The task of completing a PhD is not something which anyone undertakes likely, and it would not have been possible without the support and guidance of a number of people.

Firstly, I would like to thank Dr. Clare Knock, my primary supervisor. Clare has supported me unwaveringly throughout my studies and given me a push when necessary. Secondly, Dr. Debra Carr, who taught me everything I know about fabrics, and was suitably pleased when I finally learnt which way around warp and weft went. Despite not remaining at Cranfield for the duration of my studies, she continued to provide support and advice, for which I am grateful. Dr. Sophie Beckett, who was my advisor on all things CT-related, for her patience in teaching me to use the CT scanner. Dr. Jon Painter, for helping me with, and teaching me to use, the scanning electron microscope. Clare Pratchett and Media Services for designing the images for my discussion.

Lastly, my husband, David Dicken, for his unquestioning support and advice throughout this journey, but most importantly for putting up with my complaints after a bad day in the office!

# CONTENTS

ABSTRACT .....	i
ACKNOWLEDGEMENTS .....	iii
LIST OF FIGURES .....	ix
LIST OF TABLES .....	xiv
LIST OF EQUATIONS .....	xvi
GLOSSARY AND ABBREVIATIONS .....	xvii
1 INTRODUCTION .....	1
1.1 Background.....	1
1.2 Aims and Objectives.....	5
1.2.1 Aim .....	5
1.2.2 Objectives.....	6
1.3 Thesis layout.....	6
1.4 References.....	11
2 The use of micro computed tomography to ascertain the morphology of bloodstains on fabric. ....	14
2.1 Abstract .....	14
2.2 Keywords.....	14
2.3 Highlights.....	14
2.4 Introduction .....	15
2.5 Materials and methods .....	17
2.5.1 Materials .....	17
2.5.2 Method.....	18
2.6 Results .....	20
2.6.1 General Observations.....	20
2.6.2 Bloodstain Area .....	21
2.6.3 Warp and wale measurements .....	28
2.7 Discussion.....	30
2.7.1 The use of the CT scanner .....	30

2.7.2	Shape of the bloodstain .....	30
2.7.3	Effect of impact velocity and fabric type.....	31
2.8	Conclusions .....	32
2.9	References.....	33
3	The effect of fabric mass per unit area and blood impact velocity on bloodstain morphology.....	36
3.1	Abstract .....	36
3.2	Keywords.....	37
3.3	Highlights.....	37
3.4	Introduction .....	37
3.5	Materials and methods .....	39
3.5.1	Materials .....	39
3.5.2	Method.....	42
3.6	Results and Discussion .....	45
3.6.1	1.7 ms <sup>-1</sup> .....	49
3.6.2	2.9, 4.1 and 4.9 ms <sup>-1</sup> .....	55
3.6.3	5.1 ms <sup>-1</sup> .....	62
3.6.4	5.4 ms <sup>-1</sup> :.....	67
3.7	Conclusions .....	73
3.8	Ethical Statement .....	74
3.9	References.....	75
4	Investigating bloodstain dynamics at impact on the technical rear of fabric.....	79
4.1	Abstract .....	79
4.2	Keywords.....	79
4.3	Highlights.....	80
4.4	Introduction .....	80
4.5	Materials and methods .....	82
4.5.1	Materials .....	82
4.5.2	Methods .....	83
4.6	Results .....	85

4.6.1	Impact dynamics .....	85
4.6.2	Effect of fabric mass per unit area .....	89
4.6.3	Dry technical face and technical rear area.....	91
4.7	Discussion.....	92
4.8	Conclusion .....	97
4.9	Ethical Statement .....	97
4.10	References.....	97
5	The effect of reactive dyeing of fabric on the morphology of passive bloodstains .....	100
5.1	Abstract .....	100
5.2	Keywords.....	100
5.3	Highlights.....	101
5.4	Introduction .....	101
5.5	Materials and Method.....	104
5.5.1	Materials .....	104
5.5.2	Method.....	105
5.6	Results and discussion.....	107
5.6.1	Bloodstains on dyed fabric.....	107
5.6.1.1	Overall trends.....	107
5.6.1.2	Bloodstain formation .....	108
5.6.1.3	Fabric and velocity effects.....	110
5.6.2	Effect of dyeing.....	117
5.6.3	Comparison to bloodstains on not-coloured fabric .....	119
5.7	Conclusions .....	124
5.8	References.....	124
6	The effect of the digital printing of fabric on the morphology of passive bloodstains....	128
6.1	Abstract .....	128
6.2	Keywords.....	128
6.3	Highlights.....	129
6.4	Introduction .....	129
6.5	Materials and Method.....	131



6.5.1	Materials .....	131
6.5.2	Method.....	133
6.6	Results .....	135
6.6.1	Wet impact face bloodstains.....	136
6.6.2	Dry impact face bloodstains.....	139
6.6.3	Dry penetrated face bloodstain .....	141
6.6.4	CT printed face bloodstains.....	144
6.6.5	SEM printed face bloodstains.....	147
6.7	Discussion.....	148
6.7.1	Bloodstains from blood drops on the PF.....	148
6.7.2	Comparison between bloodstains from blood drops on the PF and NPF.....	150
6.7.3	Effect of printing on the bloodstains.....	151
6.7.4	Comparison to not-coloured and dyed calico .....	153
6.8	Conclusion.....	160
6.9	References.....	161
7	Discussion .....	164
7.1	Bloodstain formation .....	164
7.1.1	Wetting.....	164
7.1.2	Penetration.....	166
7.1.3	Wicking.....	166
7.2	Effect of yarn and fabric properties on the wicking of blood .....	167
7.2.1	Summary of interaction of blood and fabric.....	167
7.2.2	Intra-yarn capillary spaces.....	167
7.2.3	Twist .....	169
7.2.4	Yarn linear density.....	171
7.2.5	Inter-yarn spaces.....	173
7.3	Advantages and disadvantages of the $\mu$ CT and SEM .....	174
7.4	Impact for forensic science .....	177
7.5	References.....	179

8	Conclusions.....	181
8.1	Summary .....	181
8.1.1	Objective one – to investigate the applicability of the use of the $\mu$ CT and SEM to BPA. 181	
8.1.2	Objective two – to investigate the effect of fabric mass per unit area and thickness on bloodstain morphology. ....	182
8.1.3	Objective three – to investigate the effect of the impact velocity of the blood drop on the bloodstain morphology. ....	182
8.1.4	Objective four – to investigate how reactive dyeing affects the resultant bloodstains. ....	183
8.1.5	Objective five – to investigate how digital printing affects the resultant bloodstains. ....	183
8.2	Limitations and suggestions for future work .....	183
	Appendix A – Poster Presentation from International Association of Bloodstain Pattern Analysts Conference Rome 2015. ....	185
	Appendix B – Presentation from International Association of Bloodstain Pattern Analysts Warsaw 2017. Presented by Dr. Clare Knock on the work done in Chapter 3 by the author. .	186
	Appendix C – Fabric testing.....	195
	Appendix D - Post-processing .....	204
	Appendix E - Using the Micro Computed Tomography Scanner ( $\mu$ CT) .....	210
	Appendix F - Scanning electron microscope (SEM).....	214
	Appendix G - Raw data for the not-coloured calico.....	216
	Appendix H – Raw data for the dyed calico .....	220
	Appendix I – Raw data for the printed calico drops on the printed face.....	223
	Appendix J – Raw data for the printed calico drops on the not printed face .....	226

## LIST OF FIGURES

Figure 1-1 how different surfaces affect the resulting contact angle.....	4
Figure 1-2 illustrating the different sizes of capillary spaces which alter the amount of wicking which can occur. Each circle is a representation of an individual fibre within a single yarn.....	5
Figure 1-3 outline of the relationship between the chapters and the objectives each chapter contributes to.....	9
Figure 2-1 a technical drawing of the resultant specimens, indicating the direction of the warp (woven) and wales (knitted) (fig 2-1a), and a possible cross-section of a specimen, indicating the two faces of the fabrics (2-1b).....	18
Figure 2-2 the direction of the measurements taken from the bloodstain. The area measurements were taken on the cross-sections marked in figure 2-2a from the technical face to the technical rear in direction z. The resultant images were approximately circular, as seen in figure 2-2b, and measurements were taken in the y (wale or warp) and x (course or weft) direction on the cross-section with the largest area. ....	20
Figure 2-3 an example of a cross-sectional slice in the z-axis from the rib knit from a depth of 0.8mm (2-3a) and bull drill from a depth of 0.6mm (2-3b). An example of a blood-void section is indicated by 'A', an example of an area of denser blood is indicated by 'B' .....	21
Figure 2-4 The mean and standard deviation of the area of the parent bloodstain for cross-sections taken every 0.1 mm throughout the depth of the bloodstain in the z-direction for three velocities ( $3.2 \text{ ms}^{-1}$ , $4.5 \text{ ms}^{-1}$ and $5.3 \text{ ms}^{-1}$ ) on rib knit fabric.....	22
Figure 2-5 The mean and standard deviation of the area of the parent bloodstain for cross-sections taken every 0.1 mm throughout the depth of the bloodstain in the z-direction for three velocities ( $2.9 \text{ ms}^{-1}$ , $4.2 \text{ ms}^{-1}$ and $5.0 \text{ ms}^{-1}$ ) on bull drill fabric. ....	23
Figure 2-6 The mean of the area of the parent bloodstain for cross-sections taken every 0.1 mm throughout the depth of the bloodstain in the z-direction for three velocities for both rib knit and bull drill fabrics.....	24
Figure 2-7 The first three cross-sections (0.1 mm, 0.2 mm and 0.3 mm) in the z-direction (through the depth of the bloodstain) for a specimen for each velocity for the rib knit fabric. ....	26
Figure 2-8 the mean and standard deviation measurements for rib knit and bull drill fabrics for all velocities for the x (course or weft) and y (wale or warp) measurements from the cross section with the largest area.....	29
Figure 3-1 SEM images of the light, medium and heavy calicos at 50x magnification, and of warp and weft yarns removed from the fabric at 75x magnification. ....	41
Figure 3-2 direction of the 2D images saved from the CT data. Cross-sections were saved at a slice distance of 0.05 mm in each of the warp and weft directions. ....	44
Figure 3-3 mean wet and dry bloodstain area at each velocity for all fabrics.....	46
Figure 3-4 Typical example of a blood drop impacting the light calico at $1.9 \text{ ms}^{-1}$ (images from work undertaken for [27] but not used in the publication).....	49

Figure 3-5 Typical example of a wet bloodstain on each calico formed at 1.7 ms <sup>-1</sup> . Scale is 10 mm. ....	50
Figure 3-6 The CT data from a typical example of a light calico specimen formed at 1.7 ms <sup>-1</sup> ..	52
Figure 3-7 a typical example of a cross-section in the warp and weft directions on the medium and heavy calico formed at 1.7 ms <sup>-1</sup> . 'A' indicates an example blood-soaked warp yarn, 'B' an example blood-soaked weft yarn and 'C' the blood remaining on the surface of the fabric. ....	54
Figure 3-8 a typical example of a dry bloodstain on each calico formed at 1.7 ms <sup>-1</sup> . 'B' indicates the coffee ring effect in part of the bloodstains. Scale is 10 mm. ....	55
Figure 3-9 a typical example of a technical face wet and dry and technical rear dry bloodstain on each calico formed at 4.1 ms <sup>-1</sup> . Scale is 10 mm. ....	56
Figure 3-10 a typical example of a CT cross section in the warp and weft directions and an SEM image (x 42) on each calico formed at 4.1 ms <sup>-1</sup> . ....	61
Figure 3-11 a typical example of a CT cross section in the warp and weft directions and an SEM image (x42) on each calico formed at 5.1 ms <sup>-1</sup> . 'A' indicates the blood soaked warp yarns, and 'B' the blood soaked weft yarns.....	65
Figure 3-12 a typical example of a dry technical face and technical rear bloodstain on each calico formed at 5.1 ms <sup>-1</sup> . Scale is 10 mm. ....	67
Figure 3-13 a typical example of a wet and dry technical face and dry technical rear bloodstain (scale: 10 mm) and 2D of the 3D CT reconstruction on each calico formed at 5.4 ms <sup>-1</sup> .....	69
Figure 3-14 a typical example of a CT cross section in the warp and weft directions and an SEM image (x42) on each calico formed at 5.4 ms <sup>-1</sup> . ....	73
Figure 4-1 camera set-up .....	83
Figure 4-2 measuring the area of an example technical rear bloodstain image. The darkest central area is where the blood has passed through to the technical rear of the fabric, while the light surrounding area is blood on the surface of the fabric. ....	85
Figure 4-3 impact stages on the technical face and technical rear of the light calico of a single specimen from 4.2 ms <sup>-1</sup> . The technical face and technical rear bloodstains are orientated to the same angle but appear as mirror images owing to being filmed from the top and bottom respectively. The additional technical rear image at 0.335 ms is between two technical face frames. Scale is 20 mm.....	88
Figure 4-4 a typical example of a high speed video still from each fabric and each velocity from 1 ms after impact. The light areas surrounding the darker technical rear bloodstains is the blood on the surface of the fabric, which can be seen from the technical rear. Scale is 2 cm. .	90
Figure 4-5 an example dry technical rear bloodstain on each fabric from 4.2 ms <sup>-1</sup> . Scale is 1cm. ....	92
Figure 4-6 a timeline of what dynamics occurred following drop impact. ....	94
Figure 5-1 dry bloodstain areas plotted against velocity for all three mass per unit areas of calico. ....	108

Figure 5-2 stills from filming the fabric technical face at impact on all three calicos from 1.9 ms<sup>-1</sup> and 4.2 ms<sup>-1</sup>. Scale is 2 cm. .... 109

Figure 5-3 a typical example of a wet and dry bloodstain on the dyed light calico. 'A' indicates where the blood has continued to wick along the warp yarns beyond the main bloodstain. Scale is 2 cm. .... 112

Figure 5-4 a typical example of a wet and dry bloodstain (scale: 2 cm) and SEM image at 42x magnification and CT cross section on the dyed medium and heavy calicos from an impact velocity of 1.7 ms<sup>-1</sup>. 'A' is an example of blood in the warp and weft yarns at the centre of the bloodstain. 'B' is the blood in the centre of the bloodstain inside the yarns. 'C' is the blood at the edge of the bloodstain which remained on the surface of the fabric. .... 114

Figure 5-5 a typical example of a wet and dry bloodstain (scale: 2 cm) and CT cross-section in the weft direction from the medium and heavy calico from 4.1 ms<sup>-1</sup> impact. .... 116

Figure 5-6 a typical example of a 2D image of the 3D CT reconstruction of a light calico specimen from an impact velocity of 4.1 ms<sup>-1</sup> and 4.9 ms<sup>-1</sup>. .... 116

Figure 5-7 a typical example of a dry bloodstain on the light calico from impact velocities of 4.9 and 5.3 ms<sup>-1</sup>. Scale is 2 cm. .... 117

Figure 5-8 SEM images of the dyed and not-coloured [10] medium calico. .... 119

Figure 5-9 Dry bloodstain area for the not-coloured calicos [10] and the mean dry bloodstain area and range for the dyed calicos plotted against impact velocity ..... 120

Figure 5-10 a typical example of a high speed video still from 2ms following impact on a light dyed and not-coloured calico [20] from 4.2 ms<sup>-1</sup>. Scale is 2 cm. .... 121

Figure 5-11 an example wet and dry bloodstain photograph (scale: 2 cm), SEM image at 42x magnification and CT cross-section in the weft direction on the medium dyed and not-coloured calico (images taken for research done in [10] but not used in publication) from 4.1 ms<sup>-1</sup> .... 123

Figure 6-1 example SEM images of the printed calicos at 50x and 250x magnification. .... 132

Figure 6-2 a high speed video still of the maximum spread of the blood drop following impact onto each fabric from each velocity. Scale is 20 mm. .... 136

Figure 6-3 an example wet impact face bloodstain on each of the three printed fabrics from drops onto both the PF and NPF from 4.1 ms<sup>-1</sup>. Scale is 20 mm. .... 137

Figure 6-4 the wet bloodstain areas from the blood drops on the PF and NPF of the light, medium and heavy calicos. .... 138

Figure 6-5 an example dry impact face bloodstain on each of the three printed fabrics from drops onto both the PF and NPF from 4.1 ms<sup>-1</sup>. Scale is 20 mm. .... 139

Figure 6-6 the dry bloodstain areas from the blood drops on the PF and NPF of the light, medium and heavy calicos. .... 140

Figure 6-7 an example dry penetrated face bloodstain on each of the three printed fabrics from drops onto both the PF and NPF from 4.1 ms<sup>-1</sup>. Scale is 20 mm. .... 142

Figure 6-8 stills from filming the penetrated face of the fabric at impact on each printed fabric PF following impact from $4.3 \text{ ms}^{-1}$ . Scale is 15 mm.....	143
Figure 6-9 a typical example of a light calico (PF) penetrated face bloodstain (translucent, red) superimposed on the equivalent impact face bloodstain (opaque, black) from $1.9 \text{ ms}^{-1}$ , $4.1 \text{ ms}^{-1}$ and $5.4 \text{ ms}^{-1}$ showing the similarity in shape between the two bloodstains. ....	144
Figure 6-10 A 2D image of the complete 3D reconstruction and cross-sections from a specimen from the printed calico from $4.1 \text{ ms}^{-1}$ . 'A' is a blood-soaked warp yarn, 'B' a blood-soaked weft yarn. 'C' is an example of the denser blood at the edge of the bloodstain. ....	146
Figure 6-11 a typical example of an SEM image of a bloodstain on each fabric from $4.1 \text{ ms}^{-1}$	147
Figure 6-12 the dry impact face bloodstain areas for all specimens from blood drops on the PF and NPF of the printed calico, dyed [10] and not-coloured [6] calicos. ....	154
Figure 6-13 High speed video stills showing the maximum area of spreading on the dyed (image taken for research done in [10] but not used in publication) and printed heavy calico from a drop impact at $1.8 \text{ ms}^{-1}$ . Scale: 15 mm. ....	154
Figure 6-14 a typical example of a wet and dry bloodstain on each of the medium not-coloured, dyed and printed calicos from $4.1 \text{ ms}^{-1}$ [6,10]. Scale 20 mm.....	156
Figure 6-15 a typical example of a penetrated face bloodstain from an impact velocity of $4.1 \text{ ms}^{-1}$ on each mass per unit area and treatment of fabric [6,10] (figure 6-15d not used in publication). Scale 20 mm. ....	158
Figure 7-1 illustrating the different twist levels of yarns. In figure 7-1a, the blood is able to enter the capillary spaces between the fibres owing to the reduction in twist, while the blood cannot easily enter the capillary spaces when the fabric is more highly twisted (figure 7-1b). ....	170
Figure 7-2 the effect of yarn linear density on wicking with a finite reservoir. Only a small volume of blood is required to wet and wick into the yarn with a low linear density (figure 7-2b), but the same volume of blood cannot as easily wet and wick into a yarn with a higher linear density (figure 7-2a). ....	172
Figure 7-3 illustrating the effect of yarn linear density on the fabric construction. The greater the yarn linear density, assuming the sett is kept the same, the lower the fabric porosity. ...	173
Figure C-1 measuring the mass of a fabric specimen.....	196
Figure C-2 a fabric sample on the thickness gauge .....	200
Figure C-3 measuring the linear density of ten yarns .....	202
Figure D-1 calibrating the software with the ruler.....	204
Figure D-2 measuring the diameter of a blood drop .....	205
Figure D-3 measuring the impact velocity of a blood drop.....	206
Figure D-4 measuring an example technical face dry bloodstain .....	207
Figure D-5 measuring the technical rear bloodstains on the heavy calico. ....	208

Figure D-6 measuring the area of an example technical rear bloodstain image to measure the area. The darkest central area is where the blood has passed through to the technical rear of the fabric, while the light surrounding area is blood on the surface of the fabric. ....	209
Figure E-1 A sample in VGStudio Max which has been registered and cropped .....	213
Figure F-1 Drawing of the main components on a scanning electron microscope. Recreated from [2]. ....	214

## LIST OF TABLES

Table 1-1 the publications from each chapter, the objectives they contributed to and any conferences they were presented at .....	10
Table 2-1 fabric properties after six laundering cycles [9].....	17
Table 3-1 mean fabric properties and standard deviations where available (n=5).....	40
Table 3-2 the drop heights and subsequent velocities measured from the high-speed video ..	42
Table 3-3 the values at which all three masses of calico were scanned in the micro CT scanner and reconstructed.....	43
Table 3-4 a summary of the way in which blood is interacting with each fabric (light: 85.1 g/m <sup>2</sup> ; medium: 163.5 g/m <sup>2</sup> ; heavy: 224.6 g/m <sup>2</sup> ) for each velocity category .....	48
Table 4-1 mean fabric properties and standard deviations where available (n = 5). .....	82
Table 4-2 the setting for the high speed cameras. ....	84
Table 4-3 the mean and standard deviation dry technical face and technical rear bloodstains for all fabrics and velocities.....	92
Table 5-1 mean fabric properties and standard deviation. *taken from Dicken et al. [10]. ....	105
Table 5-2 the mean and standard deviation impact velocity resulting from each drop height	105
Table 5-3 $\mu$ CT scanner parameters .....	106
Table 5-4 the R <sup>2</sup> values for each of the not-coloured [10] and dyed fabrics .....	120
Table 6-1 mean fabric properties and standard deviation. *1 [10] *2 [6].....	133
Table 6-2 the mean and standard deviation impact velocity resulting from each drop height. ....	134
Table 6-3 $\mu$ CT scanner parameters. ....	135
Table 6-4 results of ANOVA on the wet impact face bloodstain area. ....	138
Table 6-5 results of ANOVA on the dry impact face bloodstain area .....	141
Table 6-6 results of ANOVA on the dry penetrated face bloodstain area .....	141
Table 6-7 the mean penetrated face bloodstain area for each fabric state and each mass per unit area [6,10].....	157
Table C-1 calculating the mass per unit area for each specimen and the mean and standard deviation for each not-coloured fabric. ....	197
Table C-2 calculating the mass per unit area for each specimen and the mean and standard deviation for each dyed fabric. ....	198



Table C-3 calculating the mass per unit area for each specimen and the mean and standard deviation for each printed fabric. ....	199
Table C-4 the thickness measurements for all specimens and the mean and standard deviation for each not-coloured fabric. ....	200
Table C-5 the thickness measurements for all specimens and the mean and standard deviation for each dyed fabric.....	201
Table C-6 the thickness measurements for all specimens and the mean and standard deviation for each printed fabric.....	201
Table C-7 the sett for each specimen and the mean and standard deviation for each fabric.....	201
Table C-8 the weight of 10 yarns from each fabric and the resultant tex. ....	202
Table D-1 the velocities measured and transformed from the technical face filming. ....	206
Table E-1 Specification of the CT scanner [3].....	210
Table E-2 the CT settings for each of the fabrics.....	212

## LIST OF EQUATIONS

Equation C-1 calculating the mass per unit area of a fabric specimen .....	196
Equation C-2 calculating the linear density of the yarns.....	202
Equation D-1 transforming the impact velocity taking into account the angle of recording.....	206

## GLOSSARY AND ABBREVIATIONS

μA	Microamps
μCT	Micro Computed Tomography
ANOVA	Analysis of variation
Bloodstain	“A deposit of blood on a surface” [1]
Bloodstain pattern	“A grouping or distribution of bloodstains that indicates through regular or repetitive form, order or arrangement the manner in which the pattern was distributed” [1]
BPA	Blood Pattern Analysis
Calico	“A generic term for plain cotton fabric, generally heavier than muslin but lighter than canvas” [2]
Computed tomography	“A technique of x-ray photography in which a single plane is photographed, with the outline of structures in other planes eliminated. The 2D slices are then put together using an algorithm to generate a 3D volume” [3]
Course	“A row of loops (i) across the width of a flat fabric, or (ii) around the circumference of a circular fabric” [2]
CV	Coefficient of variation $CV = \left( \frac{\text{standard deviation}}{\text{mean}} \right) \times 100$
Desize	“The removal of size from woven fabrics” [2]
End	“An individual warp thread” [2]
Fibre	“Textile raw material, generally characterised by flexibility, fineness and a high ratio of length to thickness” [2]
Inter-yarn	The spaces between the yarns

Intra-yarn	The spaces between the fibres, within the yarns.
ISO	International Organization for Standardization
kV	Kilovolts
Loom-state	“Any woven fabric as it leaves the loom before it receives any subsequent processing” [2]
Mercerised	“The treatment of cellulosic fibres...with a concentrated solution of caustic alkali whereby fibres are swollen, the moisture regain, strength and dye affinity of the materials are increased” [2]
Non-newtonian	Fluids which do not obey Newton’s law of viscosity, in which shear stress is not linearly related to velocity gradient [4]
Optical brightening agent	“A substance that when added to a substrate increases the apparent reflectance in the visible region...and so increases the whiteness or brightness” [2]
Parent stain	“A bloodstain from which a satellite spatter originated” [1]
Pick	“A single weft thread in a fabric as woven” [2]
Plain woven	“The simplest of all weave interlacings in which the odd warp threads operate over one and under one weft thread throughout the fabric with the even warp threads reversing this order to under one, over one, throughout” [2]
Plasma	The liquid component of blood [5]
R <sup>2</sup>	The coefficient of variation. It explains the amount of variation in one variable accounted for by the other variable [6]
Reactive dye	Water soluble dye where the aim is to achieve a dye-fibre covalent bond [7]

Red blood cells	The major particulate fraction of blood [5]
Satellite stain	“A smaller bloodstain that originated during the formation of the parent stain as a result of blood impacting a solid surface” [1]
Scoured	“The treatment of textile materials in aqueous or other media in order to remove natural fats, waxes, proteins and other constituents” [2]
SEM	Scanning electron microscope
Sett	“A term used to indicate the density of ends or picks or both in a woven fabric, usually expressed as the number of threads per centimetre” [2]
Singe	“To remove, in a flame, or by infra-red radiation, or by burning against a hot plate, unwanted surface fibres” [2]
Size	“A gelatinous film-forming substance...applied normally to warps but sometimes to wefts, generally before weaving, to protect the yarns from abrasion...; to strengthen them; and...to lubricate them” [2]
Spines	“...pointed-edge characteristics of a bloodstain that radiate away from the central area of the stain” [8]
Twist	“The condition of a yarn when the component elements have a helical disposition such as results from relative rotation of the yarn ends. Twist is measured in turns per unit length” [2]
Viscosity	Measure of the resistance of a fluid to flow
Wale	“A column of loops along the length of a [knitted] fabric” [2]
Warp	“Threads lengthways in a fabric as woven” [2]

Weft	“Threads widthways in a fabric as woven” [2]
Wetting	“A solid surface is wettable when a liquid adheres to the solid more strongly than the liquid coheres to itself” [2]
Wicking	“...spontaneous displacement of a solid-air interface with a solid-liquid interface in a capillary system” [9]
Yarn	“A product of substantial length and relatively small cross-section consisting of fibres and/or filaments with or without twist” [2]
Yarn linear density	“The mass per unit length of linear textile material (preferred unit is tex)” [2]

## References

- [1] Scientific Working Group on Bloodstain Pattern Analysis, Recommended Terminology, (2015). <http://www.swgstain.org/resources> (accessed September 12, 2018).
- [2] M.J. Denton, P.N. Daniels, Textile Terms and Definitions, 11th Edition, The Textile Institute, Manchester, 2002.
- [3] J. Hsieh, Computed Tomography: Principles, Design, Artefacts, and Recent Advances, Third Edit, Society of Photo-Optical Instrument Engineers, Washington, 2015.
- [4] J. Douglas, J. Gasiorek, J. Swaffield, Fluid Mechanics, Longman, London, 1995.
- [5] A. Wonder, Blood Dynamics, Academic Press, London, 2001.
- [6] F.L. Coolidge, Statistics: A Gentle Introduction, Sage Publications, California, 2006.
- [7] D.M. Lewis, Dyestuff-fibre interactions, Rev. Prog. Color. 28 (1998) 12–17.
- [8] S. James, P. Kish, T. Sutton, Principles of Bloodstain Pattern Analysis: Theory and Practice, CRC Press, Florida, 2005.

- [9] A. Patnaik, R.S. Rengasamy, V.K. Kothari, A. Ghosh, Wetting and Wicking in Fibrous Materials, *Text. Prog.* 1 (2006) 1–105. doi:10.1533/tepr.2006.0001.

# 1 INTRODUCTION

## 1.1 Background

Blood pattern analysis (BPA) is the study of bloodstains at crime scenes in an attempt to recreate the events which may have caused the blood to be shed [1]. The use of bloodstains at crime scenes to help recreate the crime was developed as early as 1895 by Dr Eduard Piotrowski [2]. In 1955 the evidence of Paul Leeland Kirk, which included an assessment of the blood patterns at a crime scene, helped acquit the defendant in *State of Ohio vs Samuel H. Sheppard* [3]. Since then, BPA has become a recognised methodology within forensic science. However, in recent times the reliability of many of the standard practises, as well as consistency among practitioners within forensic science, has been questioned. In a recent report, it was stated:

*'The uncertainties associated with blood pattern analysis are enormous'. [4, p179]*

In 2016 a study was undertaken to assess the reliability of bloodstain classification on three rigid non-absorbent surfaces [5] and three fabric substrates [6]. Various blood patterns were created on each of the substrates, with a number of experts being asked to identify the patterns. For the non-absorbent surfaces incorrect classifications were made 13% of the time, while for the fabric surfaces incorrect classifications were made 23% of the time [5,6]. These studies provided a base-line for the error rate within BPA, even among experts, and showed the additional complexities of interpreting bloodstains on fabrics.

A comprehensive study of bloodstains on fabrics was not undertaken until 1986 [7] despite the fact that the clothing of any perpetrator, victim or bystander within a violent crime could be bloodstained as well as household furnishings such as carpets, upholstery, cushions and curtains. White's 1986 [7] work involved dropping human blood from six heights onto fifteen fabrics at five angles. This work provided an overview of bloodstains which may be produced on different fabrics, and indicated the



difficulty of calculating the angle of impact from bloodstains on fabrics. However, the use of so many fabrics, dropping heights and angles meant it was only possible to briefly discuss each fabric. Little insight was provided as to why the different fabrics produced the bloodstains which they did. No comparison or statistics were undertaken to compare the different fabrics and drop heights.

The early work discussing BPA on fabrics [8–10] produced very little scientific evidence for the conclusions drawn. Similar to White [7], Slemko [8] attempted to investigate the reliability of calculating the angle of impact from bloodstains on fabrics, using 22 different fabrics. The conclusions to Slemko's [8] work were qualitative, merely stating the degree of distortion of the bloodstain varied depending on the absorption properties and surface texture of the fabric, and, as White [7] concluded, assessing the impact angle of a bloodstain on fabric is misleading. Both Karger et al. [9] and Holbrook [10] attempted to differentiate between contact and spatter stains on fabric, but as their work is qualitative the interpretation of the examiner is important. Although this early research [8–10] pointed to the complexities of understanding bloodstains on fabric, a more scientific approach was needed to begin to understand the interaction of blood and fabric.

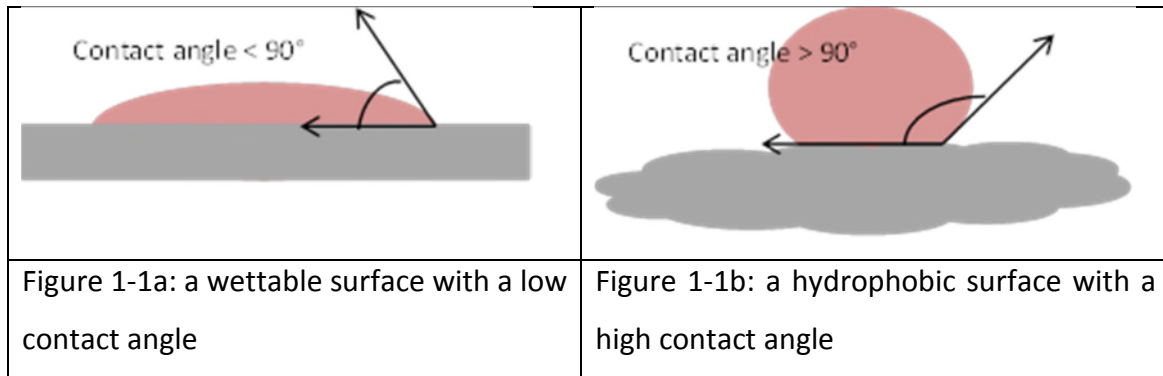
A number of cases in the courts have also pointed to the complexities of interpreting bloodstained fabrics. In *Indiana vs. David Camm* [11], four experts for the State testified that the bloodstains on the shirt of the defendant were from high-velocity impact spatter. Four bloodstain pattern experts for the defence then testified that the bloodstains on the defendant's shirt were from transfer. Camm was eventually exonerated after 13 years in prison. In the *McLeod-Lindsay* case [12], the defendant was charged with the attempted murder of his wife and son on the basis of bloodstains, interpreted as spatter stains, on his coat. However, in 1991, twenty-six years after his original conviction, the bloodstain evidence was re-examined and concluded it could have come from blood coughed up by his wife.

Therefore, more research needs to be undertaken within BPA on fabrics to better understand this complex field. In recent years, this topic has gained some momentum

and more research is being undertaken to better understand the interaction of blood and fabrics [13–20]. This work has shown the huge number of variables which affect the resultant bloodstains due to blood interacting with fabrics. These include the construction of the fabric [13,14,21], the yarn construction [17] and the fibre type [14,21]. However, there are still some methodological problems and little consistency amongst researchers. For example, the treatment of the fabric prior to experimentation varies from being not stated [9,20] to being sourced from a second hand store so unknown [10] to laundered for one [17,18] or more [13,14] cycles. The fabric properties (e.g. mass per unit area, thickness, set, yarn linear density and twist) are not always stated [8,9,19,20], which makes it difficult to compare and collate the research.

As well as this, in much of the research the science behind the conclusions is still lacking. Not only is there a lack of quantitative measurements and statistical analysis, but only a small number of the research papers provide a solid explanation for the results seen [14,21], centred around the wetting and wicking properties of different fabrics. These phenomena are well understood within textile science.

Wetting occurs when the attractive forces between the solid surface and the liquid drop overcome the cohesive forces between the liquid molecules, and the liquid therefore spreads on the surface of the solid [22]. The wettability of a surface can be measured by the contact angle, which is the angle between the solid-liquid interface and the tangent to the liquid-vapour interface [23] (figure 1-1). If a surface is hydrophilic, a low contact angle will result (figure 1-1a). Wetting cannot occur if the solid surface is hydrophobic, which results in a large contact angle between the liquid drop and the solid surface (figure 1-1b).






**Figure 1-1** how different surfaces affect the resulting contact angle

Following wetting, when the liquid has spread laterally across the surface of the solid, wicking can occur. Wicking is the transport of the liquid through the inter-yarn (the spaces between the yarns) and intra-yarn (the spaces within the yarns, between the fibres) capillary spaces [23]. The amount of wicking which occurs within a yarn is affected by the size of the capillary spaces between the fibres [24–26]. Altering the size of the capillary spaces between the fibres within an individual yarn (figure 1-2) alters the amount of wicking which occurs along the yarn [24–26]. If the capillary spaces are too small, in a vertical wicking test drag may be created to slow the rise in liquid height. On the other hand, too large capillary spaces will reduce capillary pressure and therefore also decrease the rise in the liquid [23]. The size, number and continuity of the capillary spaces can be affected by variables such as twist<sup>1</sup> and yarn linear density<sup>2</sup> [27,28]. Wetting and wicking are not referred to in BPA as often as they should be, indicating the lack of conversation between the textile science and forensic communities.

<sup>1</sup> ‘The condition of a yarn or similar structure when the component elements have a helical structure such as results...from relative rotation of the yarn ends...measured in turns per unit length.’ Textile Terms and Definitions (2002) 11<sup>th</sup> edition (revised) edited by Denton, M.J. and Daniels, P.N.

<sup>2</sup> ‘The mass per unit length of linear textile material.’ Textile Terms and Definitions (2002) 11<sup>th</sup> edition (revised) edited by Denton, M.J. and Daniels, P.N.

		
<p>Figure 1-2a: smaller than optimum capillary spaces</p>	<p>Figure 1-2b: optimum capillary spaces</p>	<p>Figure 1-2c: larger than optimum capillary spaces</p>

**Figure 1-2 illustrating the different sizes of capillary spaces which alter the amount of wicking which can occur. Each circle is a representation of an individual fibre within a single yarn.**

Therefore, a systematic study of how blood interacts with fabric, with reference to research in textile science, needs to be undertaken. In order to fully realise what is happening when a blood drop impacts an absorbent surface, such as a fabric, where the blood is within the fabric and the yarns must be understood. A novel technique within BPA which will be introduced in the work in this thesis is the use of a micro-computed tomography scanner ( $\mu$ CT) to examine the internal morphology of the bloodstain within the fabric. The  $\mu$ CT exploits the differences in density between the lower density air-filled fabric and the higher density iron-rich blood allowing visualisation of the blood within the fabric. The greater the amount of particulates within the blood (most notably iron), the denser the blood will appear on the  $\mu$ CT images. The knowledge of where the blood is within the fabric will assist in understanding the mechanisms which occurred following impact to result in that particular bloodstain. Combining the research undertaken in this way with current understanding of the way fabrics absorb, wet and wick liquids should result in a detailed understanding of the interaction of blood and fabrics.

## **1.2 Aims and Objectives**

### **1.2.1 Aim**

The overall aim of this research is to improve understanding of the interaction of blood and fabric. A thorough investigation into what occurs when a blood drop impacts a 100% cotton plain woven fabric will be undertaken using novel techniques.

### **1.2.2 Objectives**

- 1) To investigate the applicability of the use of the micro computed tomography scanner and scanning electron microscope to BPA.
- 2) To investigate the effect of fabric mass per unit area and thickness on bloodstain morphology.
- 3) To investigate the effect of the impact velocity of the blood drop on the bloodstain morphology.
- 4) To investigate how reactive dyeing affects the resultant bloodstains.
- 5) To investigate how digital printing affects the resultant bloodstains.

### **1.3 Thesis layout**

This thesis is presented as a series of chapters formatted as journal papers. All experimental work was carried out by Lisa Dicken. All papers were written by the primary author, Lisa Dicken, and edited by Clare Knock, Debra Carr and Sophie Beckett, where appropriate. Samples for the work undertaken in chapter two (The use of micro computed tomography to ascertain the morphology of bloodstains on fabric) were previously prepared by Therese deCastro and Tania Nickson [21]. A list of publications is given in table 1-1. A diagrammatic representation of the links between the chapters and the aims they contribute to is given in figure 1-3.

The work presented in chapter two was undertaken to assess the suitability and applicability of the use of  $\mu$ CT scanner to BPA. Work on the external bloodstains on the specimens used in this research had previously been published [21]. Therefore, the specimens were used to ascertain whether anything additional could be learnt about the bloodstains with the use of the  $\mu$ CT. This work was published in Forensic Science International.

L. Dicken, C. Knock, S. Beckett, T.C. de Castro, T. Nickson, D.J. Carr, The use of micro computed tomography to ascertain the morphology of bloodstains on fabric, *Forensic Sci. Int.* 257 (2015) 369-375. doi:10.1016/j.forsciint.2015.10.006.

The work undertaken in chapter two confirmed that the use of a  $\mu$ CT was able to provide additional information as to the morphology of bloodstains on fabric. Therefore, this was a novel technique to BPA which was suitable to be taken forward for further research.

The work in chapter three was undertaken to build on the use of a  $\mu$ CT and undertake a thorough examination of the interaction of bloodstains on fabric. A simple 100% cotton, plain woven fabric was chosen to remove the variables of fabric structure and fibre type. This allowed other variables, such as mass per unit area and yarn linear density to be assessed. The multi-faceted approach to this research, with the addition of the  $\mu$ CT and scanning electron microscope (SEM) to the analysis of the external wet and dry bloodstains, enabled the bloodstains to be examined in considerable detail. Differences in the interaction of blood and the fabrics amongst both the fabric mass per unit area and impact velocities were revealed.

L. Dicken, C. Knock, S. Beckett, D.J. Carr, The effect of fabric mass per unit area and blood impact velocity on bloodstain morphology, (2018) Submitted for publication in *Forensic Science International*, July 2018.

The relationship between drop impact velocity and dry bloodstain areas seen in chapter three (The effect of fabric mass per unit area and impact velocity of bloodstain morphology) raised a question as to how the impact dynamics of a drop differed depending on the impact velocity. The work undertaken in chapter four involved filming the technical rear and technical face of the fabric at impact to understand specifically how the impact of the blood drop varied depending on the impact velocity, and what dynamics were occurring on the technical rear of the fabric in this time. What occurs on the technical rear of the fabric at impact has not been previously

investigated. The work in this chapter aided the understanding of why the bloodstains varied at different impact velocities.

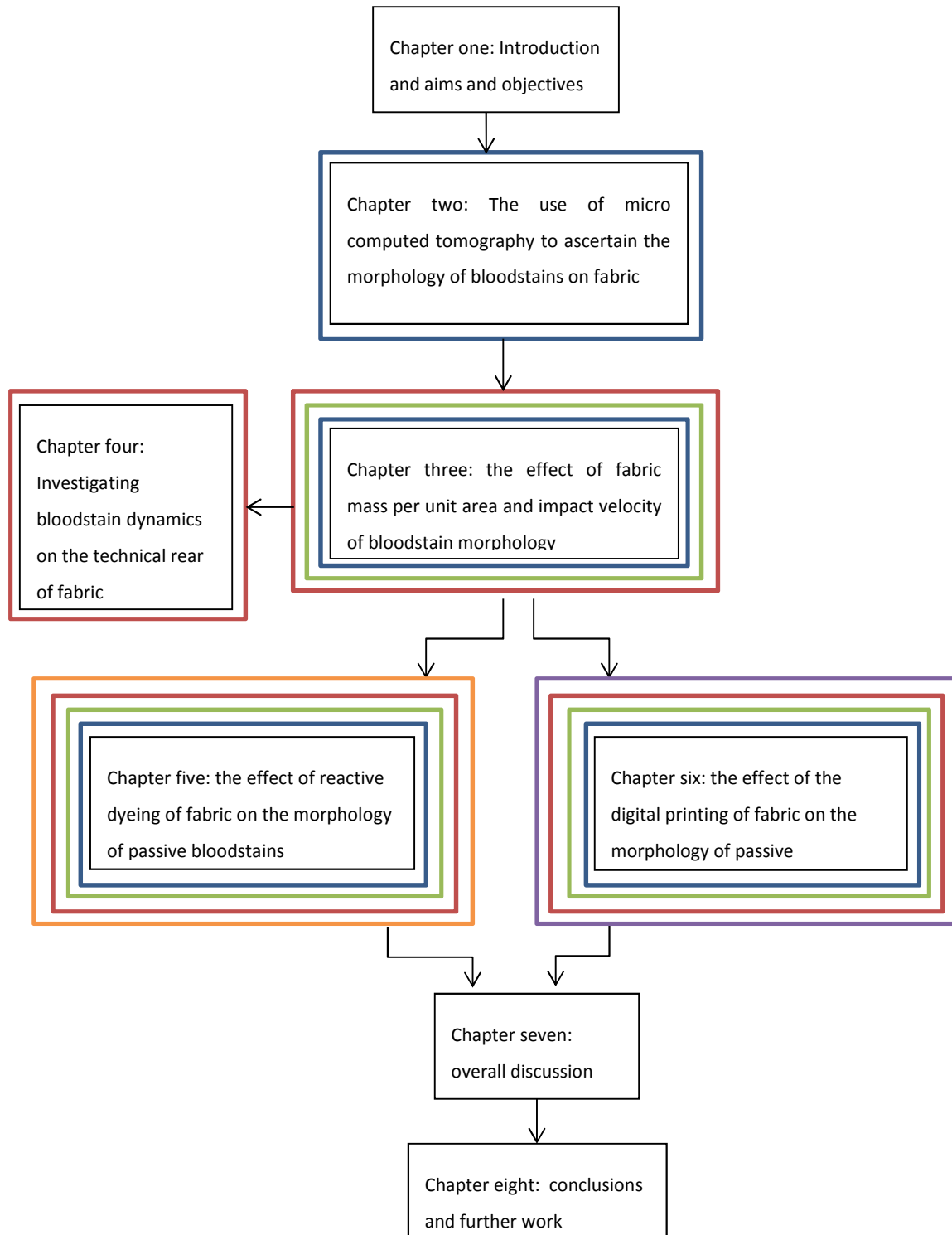
L. Dicken, C. Knock, D.J. Carr, S. Beckett, Investigating bloodstain dynamics at impact on the technical rear of fabric, (2018) Submitted for publication in Forensic Science International, July 2018.

The calico fabrics used in chapters three and four were chosen for their simplicity, as any understanding must start from the basics and build from there. As the fabrics used were not subjected to any finishing treatments, the next stage of research involved reactively dyeing (chapter five) or digitally printing (chapter six) the fabrics. The effect of finishing treatments on bloodstains on fabric is not something which has been previously considered within BPA. This helped to set the research in a more true-to-life setting, as blood-stained fabrics at crime scenes are likely to have been dyed or subjected to a finishing treatment of some manner. The same fabric was used in this research as in chapters three and four, to allow comparison of the data.

L. Dicken, C. Knock, D.J. Carr, S. Beckett, The effect of reactive dyeing of fabric on the morphology of passive bloodstains, (2018) Prepared for International Journal of Legal Medicine.

L. Dicken, C. Knock, D.J. Carr, S. Beckett, The effect of the digital printing of fabric on the morphology of passive bloodstains, (2018) Prepared for Textile Research Journal.

Chapter seven is an overall discussion of the research, focusing on the effect of yarn and fabric properties on the wicking of blood. Finally, chapter eight provides the conclusions for the work, as well as limitations and suggestions for how these could be addressed in further research. Appendices C-F provide further details on the methods used in this research.



Key	
Objective one	
Objective two	
Objective three	
Objective four	
Objective five	

Figure 1-3 outline of the relationship between the chapters and the objectives each chapter contributes to



Chapter	Objective	Publication	Conference
2	1	Dicken, L, Knock, C, Beckett, S, de Castro, T, Nickson, T and Carr, D. J. (2015) 'The use of micro computed tomography to ascertain the morphology of bloodstains on fabric.' <i>Forensic Science International</i> 257, 369-375.	The 5 <sup>th</sup> European IABPA conference 2015 Poster presentation (Appendix A).
3	1, 2, 3	Dicken, L, Knock, C, Carr, DJ and Beckett, S (2018) 'The effect of fabric mass per unit area and impact velocity of bloodstain morphology'. Submitted for publication in <i>Forensic Science International</i> , July 2018.	The 6 <sup>th</sup> European IABPA conference 2017 Presented by Dr. Clare Knock (Appendix B).
4	3	Dicken, L, Knock, C, Carr, DJ and Beckett, S (2018) 'Investigating bloodstain dynamics on the technical rear of fabric'. Submitted for publication in <i>Forensic Science International</i> , July 2018.	
5	1, 2, 3, 4	Dicken, L, Knock, C, Carr, DJ and Beckett, S (2018) 'the effect of reactive dyeing of fabric on the morphology of passive bloodstains'. Prepared for <i>International Journal of Legal Medicine</i> .	
6	1, 2, 3, 5	Dicken, L, Knock, C, Carr, DJ and Beckett, S (2018) 'the effect of the digital printing of fabric on the morphology of passive bloodstains'. Prepared for <i>Textile Research Journal</i> .	

**Table 1-1 the publications from each chapter, the objectives they contributed to and any conferences they were presented at**

## 1.4 References

- [1] T. Bevel, R.M. Gardner, *Blood Pattern Analysis with an Introduction to Crime Scene Reconstruction*, Third Edit, CRC Press, Florida, 2008.
- [2] S. James, P. Kish, T. Sutton, Impact spatter mechanisms, *Princ. Bloodstain Pattern Anal. Theory Pract.* (2005) 119–148.
- [3] P.L. Kirk, *Ohio vs Samuel H. Sheppard: Affidavit of Paul Leland Kirk*, 1955.
- [4] National Research Council, *Strengthening Forensic Science in the United States: A Path Forwards*, Washington, 2009.
- [5] M.C. Taylor, T.L. Laber, P.E. Kish, G. Owens, N.K.P. Osborne, M. Sc, G. Owens, N.K.P. Osborne, The Reliability of Pattern Classification in Bloodstain Pattern Analysis, Part 1: Bloodstain Patterns on Rigid Non-absorbent Surfaces, *J. Forensic Sci.* (2016) 1–6. doi:10.1111/1556-4029.13091.
- [6] M.C. Taylor, T.L. Laber, P.E. Kish, G. Owens, N.K.P. Osborne, The Reliability of Pattern Classification in Bloodstain Pattern Analysis, Part 2: Bloodstain patterns on fabric surfaces, *J. Forensic Sci.* 61 (2016) 1461–1466. doi:10.1111/1556-4029.13091.
- [7] B. White, Bloodstain pattern on fabrics: the effect of drop volume, dropping height and impact angle, *Can. Soc. Forensic Sci. J.* 19 (1986) 3–36.
- [8] J. Slemko, *Bloodstains on fabric- the effects of droplet velocity and fabric Composition*, (1999).
- [9] B. Karger, S.P. Rand, B. Brinkmann, Experimental bloodstains on fabric from contact and from droplets, *Int. J. Legal Med.* 111 (1998) 17–21. doi:10.1007/s004140050104.
- [10] M. Holbrook, Evaluation of Blood Deposition on Fabric: Distinguishing Spatter and Transfer Stains, *Int. Assoc. Bloodstain Pattern Anal. News.* 26 (2010) 3–12.
- [11] Indiana Supreme Court, *David R. Camm V. State of Indiana*, (2009).
- [12] M. Brown, P. Wilson, *Justice and nightmares: successes and failures of forensic science*, Burlington, 1992.
- [13] T.C. de Castro, M.C. Taylor, J.A. Kieser, D.J. Carr, W. Duncan, Systematic investigation of drip stains on apparel fabrics: The effects of prior-laundering, fibre content and fabric structure on final stain appearance, *Forensic Sci. Int.* 250 (2015) 98–109. doi:10.1016/j.forsciint.2015.03.004.
- [14] T.C. De Castro, D.J. Carr, M.C. Taylor, J.A. Kieser, W. Duncan, Drip bloodstain appearance on inclined apparel fabrics: Effect of prior-laundering, fibre content and fabric structure, *Forensic Sci. Int.* 266 (2016) 488–501. doi:10.1016/j.forsciint.2016.07.008.

- [15] E.M.P. Williams, M. Dodds, M.C. Taylor, J. Li, S. Michielsen, Impact dynamics of porcine drip bloodstains on fabrics, *Forensic Sci. Int.* 262 (2016) 66–72. doi:10.1016/j.forsciint.2016.02.037.
- [16] J. Li, X. Li, S. Michielsen, Alternative method for determining the original drop volume of bloodstains on knit fabrics, *Forensic Sci. Int.* 263 (2016) 194–203. doi:10.1016/j.forsciint.2016.04.018.
- [17] X. Li, J. Li, S. Michielsen, Effect of yarn structure on wicking and its impact on bloodstain pattern analysis (BPA) on woven cotton fabrics, *Forensic Sci. Int.* 276 (2017) 41–50. doi:10.1016/j.forsciint.2017.04.011.
- [18] J.Y.M. Chang, S. Michielsen, Effect of fabric mounting method and backing material on bloodstain patterns of drip stains on textiles, *Int. J. Legal Med.* (2016). doi:10.1007/s00414-015-1314-z.
- [19] H.F. Miles, R.M. Morgan, J.E. Millington, The influence of fabric surface characteristics on satellite bloodstain morphology, *Sci. Justice.* 54 (2014) 262–266. doi:10.1016/j.scijus.2014.04.002.
- [20] Y. Cho, F. Springer, F.A. Tulleners, W.D. Ristenpart, Quantitative bloodstain analysis: Differentiation of contact transfer patterns versus spatter patterns on fabric via microscopic inspection, *Forensic Sci. Int.* 249 (2015) 233–240. doi:10.1016/j.forsciint.2015.01.021.
- [21] T. De Castro, T. Nickson, D. Carr, C. Knock, Interpreting the formation of bloodstains on selected apparel fabrics, *Int. J. Legal Med.* 127 (2013) 251–258. doi:10.1007/s00414-012-0717-3.
- [22] E. Kissa, Wetting and Wicking, *Text. Res. J.* 66 (1996) 660–668. doi:10.1177/004051759606601008.
- [23] A. Patnaik, R.S. Rengasamy, V.K. Kothari, A. Ghosh, Wetting and Wicking in Fibrous Materials, *Text. Prog.* 1 (2006) 1–105. doi:10.1533/tepr.2006.0001.
- [24] Q. Li, J.J. Wang, C.J. Hurren, A Study on Wicking in Natural Staple Yarns, *J. Nat. Fibers.* 14 (2017) 400–409. doi:10.1080/15440478.2016.1212763.
- [25] H. Rhee, R.A. Young, A.M. Sarmadi, The Effect of Functional Finishes and Laundering on Textile Materials Part II: Characterization of Liquid Flow, *J. Text. Inst.* 84 (1993) 406–418.
- [26] N. Erdumlu, C. Saricam, Wicking and drying properties of conventional ring- and vortex-spun cotton yarns and fabrics, *J. Text. Inst.* 104 (2013) 1284–1291. doi:10.1080/00405000.2013.799258.
- [27] N. Hollies, M. Kaessinger, H. Bogarty, Water Transport Mechanisms in Textile Materials Part I: The Role of Yarn Roughness in Capillary-Type Penetration, *Text. Res. J.* 26 (1956) 829–835.

- [28] M. Taheri, M. Vadood, M.S. Johari, Investigating the effect of yarn count and twist factor on the packing density and wicking height of lyocell ring-spun yarns, *Fibers Polym.* 14 (2013) 1548–1555. doi:10.1007/s12221-013-1548-7.

## **2 The use of micro computed tomography to ascertain the morphology of bloodstains on fabric.**

**Dicken, L., Knock, C., Beckett, S., de Castro, T. C., Nickson, T., Carr, D. J.**

**Publication: Forensic Science International (2015) 257, 369-375**

### **2.1 Abstract**

Very little is known about the interactions of blood and fabric and how bloodstains on fabric are formed. Whereas the bloodstain size for non-absorbent surfaces depends on impact velocity, previous work has suggested that for fabrics the bloodstain size is independent of impact velocity when the drop size is kept constant. Therefore, a greater understanding of the interaction of blood and fabric is required. This paper explores the possibility of using a micro computed tomography (CT) scanner to study bloodstain size and shape throughout fabrics. Two different fabrics were used: 100% cotton rib knit and 100% cotton bull drill. Bloodstains were created by dropping blood droplets from three heights; 500 mm, 1000 mm and 1500 mm. Results from the CT scanner clearly showed the bloodstain shape throughout the fabric. The blood was found to form a diamond shaped stain, with the maximum cross-sectional area 0.3mm to 0.5mm below the surface. The bloodstain morphology depended on both the impact velocity and fabric structure.

### **2.2 Keywords**

- Wicking
- Wetting
- Absorbent surfaces

### **2.3 Highlights**

- The use of the micro CT scanner to detect blood in fabric
- Size of bloodstain in fabric initially increases with depth
- Bloodstain forms a diamond shape in the fabric

## 2.4 Introduction

When blood hits a surface, a bloodstain is formed. Bloodstains are important to forensic science as, when present at the scene of a crime, they can help to provide important information on the character, number and chain of events which occurred [1]. The main bloodstain is known as the parent bloodstain [2]. Spines may form, which are linear characteristics around the circumference of the bloodstain. These are created when the surface tension can no longer hold the bloodstain as an integral entity [3]. Satellite stains can also be formed. These are separate bloodstains formed by secondary droplets, which detach when the large drop impacts the surface [3]. The formation of bloodstains on less- and non-absorbent surfaces such as glass, stainless steel, laminate [4], drywall and wood [5] and paper [6] has been extensively reported. The aim of such experiments was to ascertain the drop diameter and velocity from variables such as parent stain area and number of spines. If the impact velocity is known, it is then possible to include the effect of gravity on the flight of the droplet and hence more accurately estimate the position of the source of the droplet [6]. When a non-absorbent surface is impacted, higher velocity impact of blood droplets results in larger bloodstains and more spines [5,6].

There is a paucity of information in the literature regarding the interaction of blood and absorbent surfaces, such as fabrics. Reported work has focused on the visible bloodstain on the fabric surface, treating it in much the same way as a bloodstain on a non-absorbent surface by looking at, for example, the number of satellite bloodstains or the parent stain area [7–9]. The scarcity of literature in this area does not correlate with the importance of understanding bloodstains on fabric. When bloody clothing is examined following a crime, there is a need to be able to distinguish between the clothing worn by the assailant and a bystander. In *Indiana v. Camm* [10] blood spatter which was found on the defendant's clothing was believed by four prosecution expert witnesses to be consistent with high-velocity impact spatter. However, four experts for the defence stated that it was instead consistent with transfer stains, caused by the defendant finding the bodies rather than committing the murders. A greater

understanding of the interaction of blood and fabrics would prevent situations such as this from arising.

In contrast with non-absorbent surfaces, the size of the parent bloodstain on fabrics is not reportedly affected by impact velocity when the drop size is kept constant [9]. A greater understanding of the interaction of blood and fabric, both in terms of the internal morphology of the bloodstain and the mechanisms by which the blood is soaking in to the fabric is required. Merely assessing bloodstains on the surface of a fabric, as with bloodstains on non-absorbent surfaces, may not provide sufficient understanding of these mechanisms.

The movement of liquids into and through a fabric has to be understood with reference to wetting and wicking, as this will allow a greater understanding to be gained of why the blood soaks into the fabric. These two mechanisms are well understood in textile science, generally in the context of the movement of water and water-vapour into and through a fabric. Wetting is the displacement of the solid-air interface with the solid-liquid interface. The surface energy of a liquid would usually keep a drop of that liquid in a spherical shape. If this energy is overcome by the attractive forces between the liquid molecules and the surface on which the liquid is placed, wetting occurs [11]. Wetting is a dynamic and complex process in a fibrous assembly. The surface fibres must be wetted [11] before the liquid can then be transported through the inter-fibre and inter-yarn pores by means of capillary action, known as wicking [12]. Wicking can only occur when a wetted material has capillary spaces in between the fibres [12].

Wicking and wetting mechanisms are beginning to be considered within the context of blood on fabrics [13]. It has been shown that the fibre content within a plain woven fabric affects the resultant parent stain area, and therefore most likely the wetting and wicking properties. A cotton/ polyester blend was found to result in larger parent stain areas than either 100% cotton or 100% polyester, possibly owing to larger inter-fibre pore-size. 100% polyester produced larger bloodstains than 100% cotton, most likely owing to the continuous polyester fibres producing capillary action, wicking the blood

along the fibres but not into them [13]. As wetting and wicking will only occur on absorbent surfaces they therefore need to be treated differently to non-absorbent surfaces.

Thus a greater understanding of the internal morphology of the bloodstain is required to inform the mechanisms by which blood moves through a fabric’s structure. The aim of the work summarised in this paper was to investigate the use of a micro computed tomography (CT) scanner to examine the morphology of the bloodstain inside fabrics.

## 2.5 Materials and methods

### 2.5.1 Materials

Two fabric specimens were used in this research. They were i) 100% cotton rib knit fabric and ii) 100% cotton bull drill (a woven fabric) [9] (table 2-1).

	Mass per unit area (g/m <sup>2</sup> )			Thickness (mm)		
	<i>Mean</i>	<i>Standard deviation</i>	<i>Coefficient of variation (%)</i>	<i>Mean</i>	<i>Standard deviation</i>	<i>Coefficient of variation (%)</i>
100% cotton 1x1 rib knit	201.3	3.3	1.64	0.98	0.02	2.46
100% cotton drill	383.92	9.93	2.59	0.79	0.01	1.27

**Table 2-1 fabric properties after six laundering cycles [9]**

In the work of de Castro et al. [9], bloodstains were created on each fabric specimen by vertically dropping a single blood drop from a Pasteur pipette from heights of i) 500 mm, ii) 1000 mm and iii) 1500 mm; five specimens of each fabric / height combination were used [9] resulting in a total of 30 specimens. The drops were filmed using a Phantom V12 high speed video (3000 fps and exposure 100 μs) and subsequently analysed using Phantom Camera Control software to measure the drop diameter and



velocity [9]. The three heights resulted in slightly different impact velocities for the two fabrics. For rib knit the mean impact velocities were: i)  $3.2 \text{ ms}^{-1}$ , ii)  $4.5 \text{ ms}^{-1}$  and iii)  $5.3 \text{ ms}^{-1}$ ; for the bull drill they were i)  $2.9 \text{ ms}^{-1}$  ii)  $4.2 \text{ ms}^{-1}$  and iii)  $5.0 \text{ ms}^{-1}$ . It has previously found to be the case that the effects of air resistance need to be taken into consideration when calculating velocity from drop height [14]. Therefore, as the mean drop diameter for the rib knit was  $4.1 \text{ mm}$  (s.d. =  $0.01 \text{ mm}$ ), but for the bull drill it was  $3.4 \text{ mm}$  (s.d. =  $0.01 \text{ mm}$ ), this is the most likely explanation for the differences in the velocities between the two fabrics. Velocity and blood drop diameter were consistent for each height for each fabric excepting one replicate which was removed from the current analysis. A technical drawing of the resultant specimens can be seen in figure 2-1.

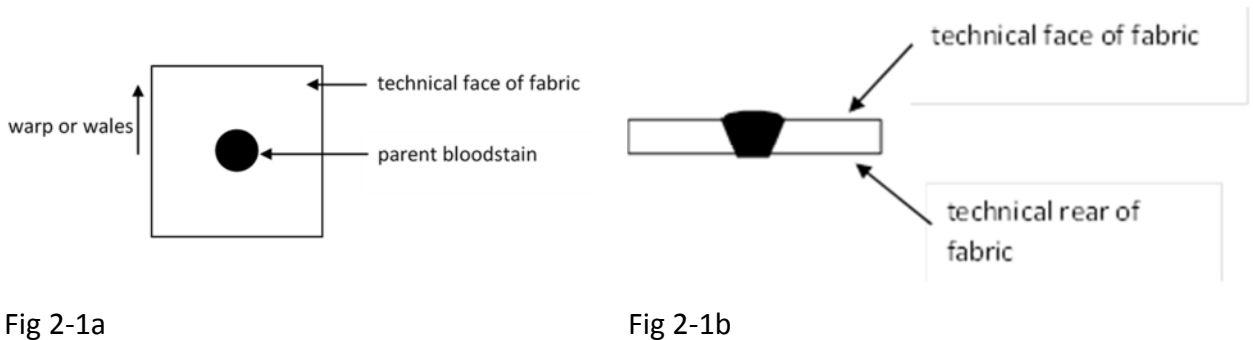


Figure 2-1 a technical drawing of the resultant specimens, indicating the direction of the warp (woven) and wales (knitted) (fig 2-1a), and a possible cross-section of a specimen, indicating the two faces of the fabrics (2-1b).

### 2.5.2 Method

The specimens, for which previously only the external visible bloodstain had been analysed [9], were examined using a Nikon XTH225 micro CT scanner<sup>3</sup>, with an Open Tube UltraFocus Reflection Target X-Ray source, a Tungsten target, a max kV of 225 and power rating of 225W. The x-ray spot size was  $3\mu\text{m}$ , with a geometric magnification of  $>150\times$  and a Varian 2520 flat panel detector [15].

The micro CT scanner exploited the difference in density between the higher density dried blood and the lower density air-filled fabric. The two fabrics were analysed using different voltage (kV), current ( $\mu\text{A}$ ) and exposure (ms) settings to optimise contrast;

<sup>3</sup> Nikon Metrology UK, Tring Business Centre, Icknield Way, Tring, Hertfordshire, HP23 4JX, UK.

the two fabrics were not compared to each other. This difference was due to the differences in the structure of the fabrics used in the work (knits are typically between 85-95% air whilst tight woven fabrics such as drills are typically between 60-90% air [16]). The samples were analysed between 30 – 35 kV, 30 – 330  $\mu$ A and 500 – 1000 ms exposure.

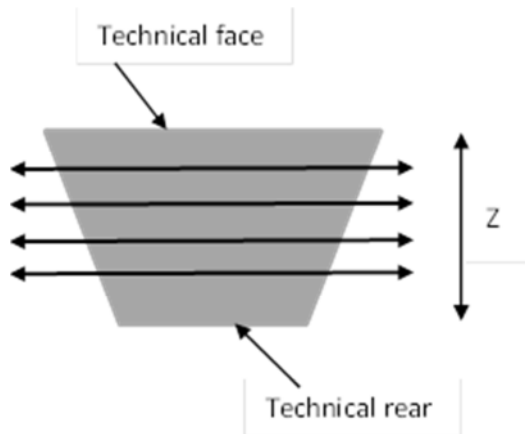
Scanning data was manually reconstructed using CT Pro<sup>4</sup>, and then two-dimensional and three-dimensional data were gathered using VGStudio Max<sup>5</sup>. The cross-sectional data were saved at 0.1mm intervals in the vertical (z) direction. The interval of 0.1mm was decided upon to be able to visualise the bloodstain at small intervals without having an excessive number of cross-sections (figure 2-2). The data was then imported into ImageJ<sup>6</sup> to measure i) area ii) length in the y (wale or warp) direction iii) length in the x (course or weft) direction. The built-in tools in ImageJ were used for each of these measurements. The area was measured using a freehand drawing tool around the external edge of each parent stain. The first area measurement was taken from the first cross-section in the z-direction where blood was visible, on the side of the fabric the blood impacted. At this point depth = 0 mm. This will not necessarily correspond to the technical face of the fabric, as blood may be raised above the surface of the fabric.

---

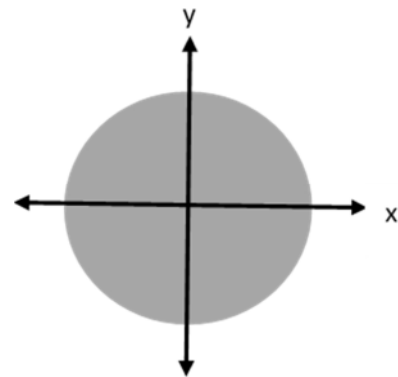
<sup>4</sup> CT Pro is an offline 3D computer tomography reconstruction programme (Metris, CT Pro User Manual 2008).

<sup>5</sup> VGStudio Max is high-end software for the visualisation and analysis of CT data (Volume Graphics, VGStudio Max 3.0, 2014).

<sup>6</sup> ImageJ is a public domain Java image processing programme (<http://imagej.nih.gov/ij/docs/intro.html> accessed 20th Jan 2015)



2-2a



2-2b

Figure 2-2 the direction of the measurements taken from the bloodstain. The area measurements were taken on the cross-sections marked in figure 2-2a from the technical face to the technical rear in direction z. The resultant images were approximately circular, as seen in figure 2-2b, and measurements were taken in the y (wale or warp) and x (course or weft) direction on the cross-section with the largest area.

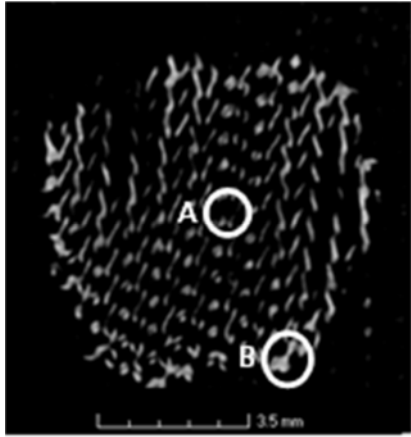
To determine whether the impact velocity had a statistically significant effect on the area and the length in the y (wale or warp) and x (course or weft) directions of the bloodstain an analysis of variance (ANOVA) and Tukey's HSD test (IBM SPSS statistics version 22) was carried out. To ensure that these statistical tests were viable, equality of variances and normality of data were checked.

## 2.6 Results

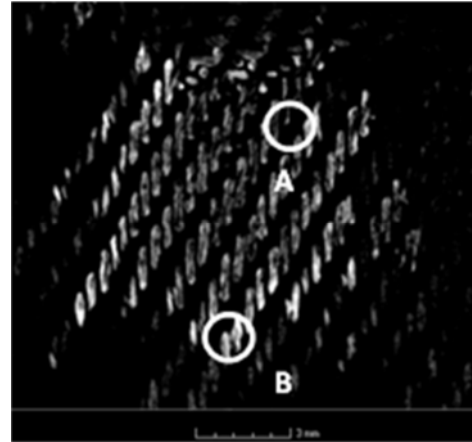
### 2.6.1 General Observations

Figure 3 shows a typical cross-section from the micro CT in the z-direction of the bloodstains formed on the rib knit and bull drill fabrics. From these images it is possible to see the blood-soaked areas and blood-void areas (labelled A in figure 2-3), the latter of which are most likely the air spaces between the yarns. There are more of these voids in the knit fabric (2-3a) than the bull drill (2-3b). It is also possible to see some variation in the intensity of the blood, with the external edges having a brighter colouration (labelled B in figure 2-3), suggesting denser blood in these areas. There is a possibility this is caused by the 'coffee-ring' effect. This is when a colloidal fluid cannot shrink during drying, causing liquid evaporating from the edge to be replaced by liquid from the interior of the drop; hence, much of the dispersed material ends up at the

edge [17]. This higher concentration of particulates would account for the brighter colouration seen in the CT scans.



2-3a



2-3b

Figure 2-3 an example of a cross-sectional slice in the z-axis from the rib knit from a depth of 0.8mm (2-3a) and bull drill from a depth of 0.6mm (2-3b). An example of a blood-void section is indicated by 'A', an example of an area of denser blood is indicated by 'B'

### 2.6.2 Bloodstain Area

The variation of the area with depth (z-direction) for each impact velocity is given in figure 4 for the rib knit and figure 5 for the bull drill fabric. For both fabrics and all impact velocities the bloodstain initially showed an increase in area with depth. The maximum area is reached between 0.3 mm and 0.5 mm below the technical face (figure 2-4, 2-5 and 2-6). Thereafter the mean area decreases with depth towards the technical rear of the fabric.

The coefficient of variation (CV) for each cross-sectional area through the fabrics varied. For both fabrics at all velocities the CV was smaller (between 2 and 11%) at the centre of the bloodstain in the z-direction, between 0.5 mm and 0.7 mm from the technical face. This suggested there was more variation in the area of the bloodstain towards the technical face and the technical rear of the fabric, than there was in the middle of the bloodstain in the z-direction.

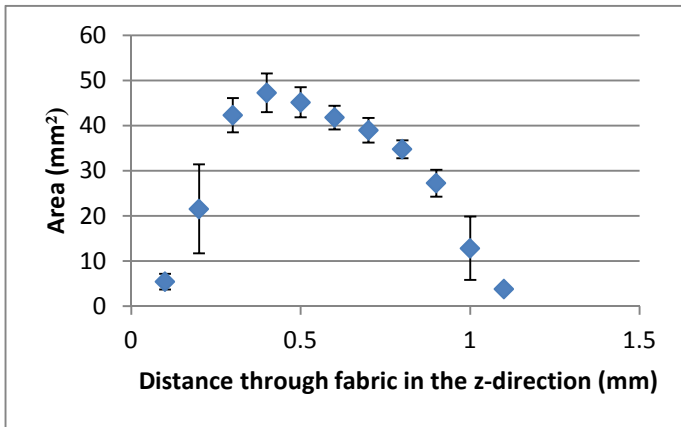


Fig 2-4a: the rib knit from 3.2 ms<sup>-1</sup>

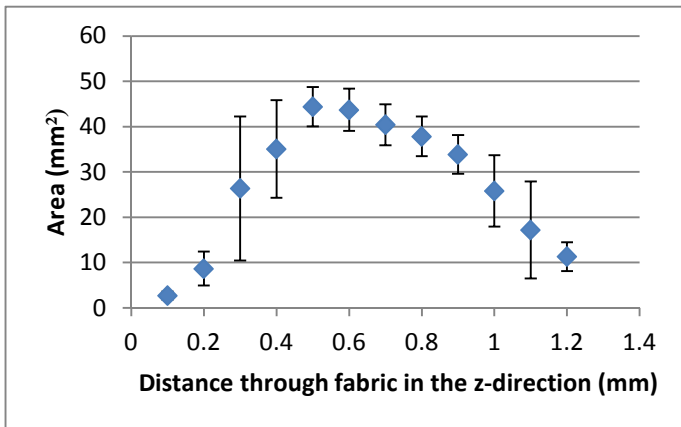


Fig 2-4b: the rib knit from 4.5 ms<sup>-1</sup>

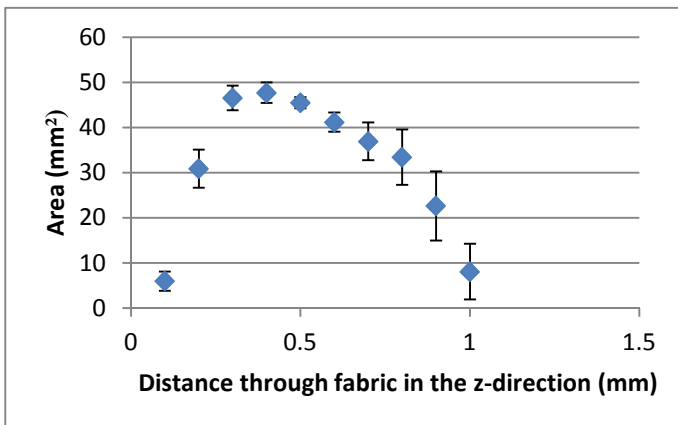


Fig 2-4c: the rib knit from 5.3 ms<sup>-1</sup>

Figure 2-4 The mean and standard deviation of the area of the parent bloodstain for cross-sections taken every 0.1 mm throughout the depth of the bloodstain in the z-direction for three velocities (3.2 ms<sup>-1</sup>, 4.5 ms<sup>-1</sup> and 5.3 ms<sup>-1</sup>) on rib knit fabric.

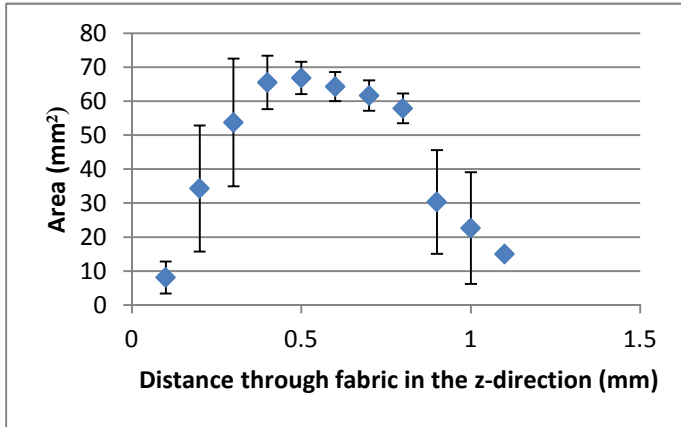


Fig 2-5a: the bull drill from 2.9 ms<sup>-1</sup>

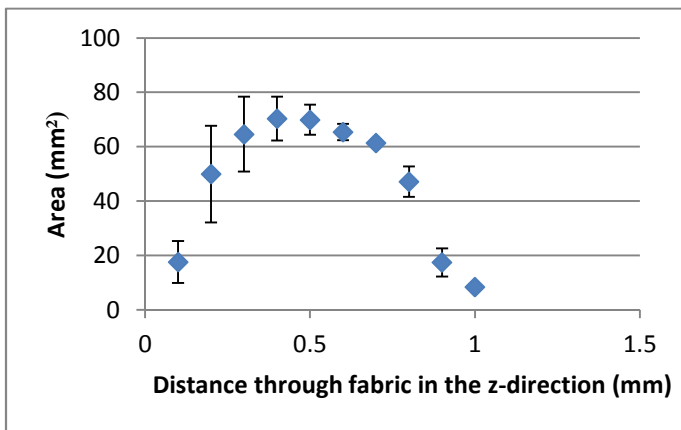


Fig 2-5b: the bull drill from 4 ms<sup>-1</sup>

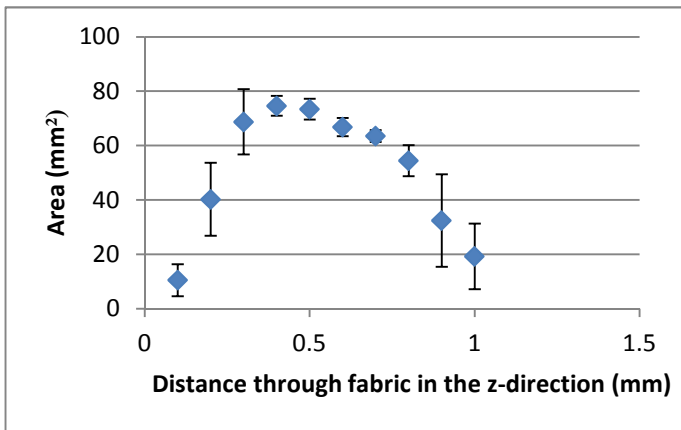


Fig 2-5c: the bull drill from 5.0 ms<sup>-1</sup>

Figure 2-5 The mean and standard deviation of the area of the parent bloodstain for cross-sections taken every 0.1 mm throughout the depth of the bloodstain in the z-direction for three velocities (2.9 ms<sup>-1</sup>, 4.2 ms<sup>-1</sup> and 5.0 ms<sup>-1</sup>) on bull drill fabric.

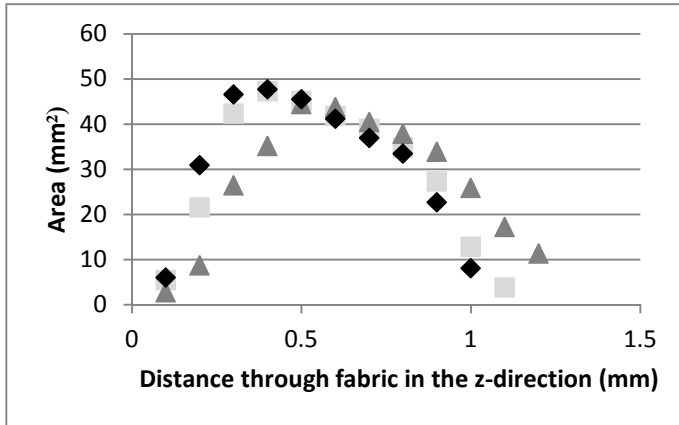


Fig 2-6a: the mean area for all impact velocities for the rib knit ( $3.2 \text{ ms}^{-1} = \blacksquare$ ,  $4.5 \text{ ms}^{-1} = \blacktriangle$ ,  $5.3 \text{ ms}^{-1} = \blacklozenge$ )

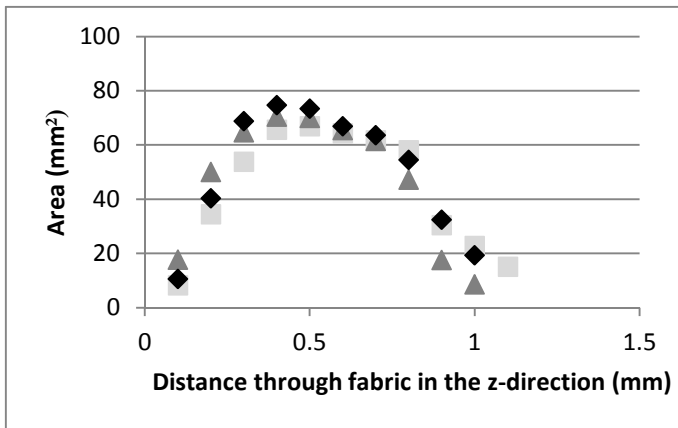


Fig 2-6b: the mean area for all impact velocities for the bull drill ( $2.9 \text{ ms}^{-1} = \blacksquare$ ,  $4.2 \text{ ms}^{-1} = \blacktriangle$ ,  $5.0 \text{ ms}^{-1} = \blacklozenge$ )

Figure 2-6 The mean of the area of the parent bloodstain for cross-sections taken every 0.1 mm throughout the depth of the bloodstain in the z-direction for three velocities for both rib knit and bull drill fabrics.

The impact velocity affected the area of the bloodstain throughout the thickness of the fabric (i.e. in the z-direction, figure 2-2a).

Bloodstains formed on the rib knit fabric from the middle impact velocity of  $4.5 \text{ ms}^{-1}$  (1000 mm) produced the smallest maximum area at the deepest point into the fabric (i.e. further away from the technical face of the fabric). The fastest impact velocity of  $5.3 \text{ ms}^{-1}$  (1500 mm) and slowest impact velocity of  $3.2 \text{ ms}^{-1}$  (500 mm) both produced larger maximum areas at a shallower depth than the middle velocity (figure 2-4, 2-6a).

Bloodstains formed from an impact velocity of  $5.3 \text{ ms}^{-1}$  (1500 mm) had thinner bloodstains (1 mm thick) than the other impact velocities. Specimens formed from  $4.5 \text{ ms}^{-1}$  (1000 mm) had the thickest bloodstains (1.2 mm). Figure 2-7 shows the first three cross sections for a specimen for all three velocities for the rib knit fabric. From figure 2-7a and 2-7c it is possible to see that for the specimens from  $3.2 \text{ ms}^{-1}$  and  $5.3 \text{ ms}^{-1}$  respectively, the bloodstain has largely formed by a depth of 0.2 mm; there is blood apparent over the vast majority of the area which will be covered when the bloodstain reaches its maximum extent. However, figure 2-7b shows the specimen from  $4.5 \text{ ms}^{-1}$  has not formed to as great an extent as the other two specimens within that same depth. In figure 2-7b, for all three cross-sections, blood is only visible around the edge of the bloodstain, suggesting these sections are therefore raised above the external visible bloodstain.



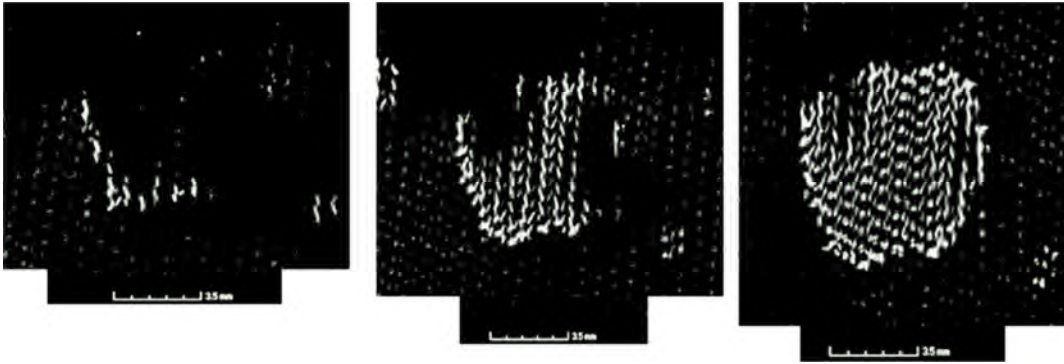


Figure 2-7a: the first three cross-sections in the z-direction for a specimen from  $3.2 \text{ ms}^{-1}$



Figure 2-7b: the first three cross-sections in the z-direction for a specimen from  $4.5 \text{ ms}^{-1}$

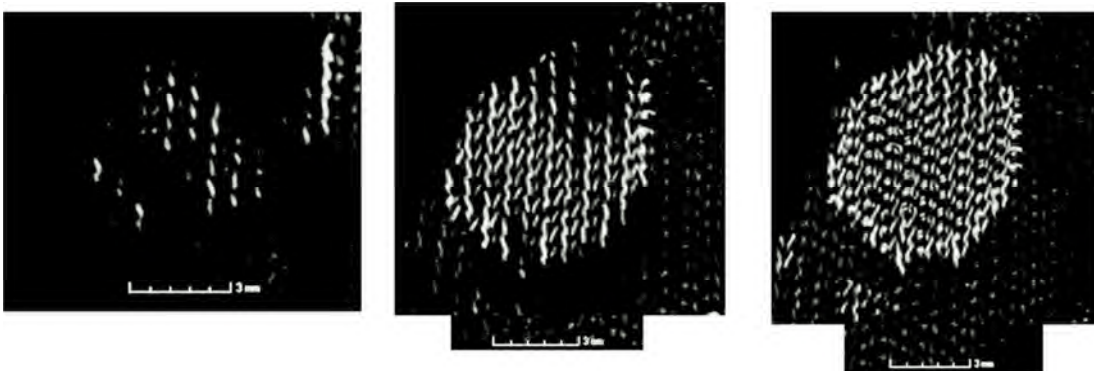


Figure 2-7c: the first three cross-sections in the z-direction for a specimen from  $5.3 \text{ ms}^{-1}$

**Figure 2-7 The first three cross-sections (0.1 mm, 0.2 mm and 0.3 mm) in the z-direction (through the depth of the bloodstain) for a specimen for each velocity for the rib knit fabric.**

For the drill fabric (figure 2-5, 2-6b) a different pattern was observed. The largest mean area was at the same distance (0.4 mm) from the technical face for the specimens from the middle impact velocity of  $4.2\text{ms}^{-1}$  (1000 mm) and the fastest impact velocity of  $5\text{ms}^{-1}$  (1500 mm). The largest mean area for the slowest impact velocity of  $2.9\text{ms}^{-1}$  (500 mm) was seen at a greater depth (0.5 mm).

The bloodstains formed at a velocity of  $4.2\text{ms}^{-1}$  produced the largest mean areas in the first two cross sections from the technical face. The area was around 40% greater than the other two velocities at a depth of 0.1 mm, and between 10% and 30% greater at a depth of 0.2 mm, although the large CV at these depths (between 33% and 58%) negates some of this variability. Towards the middle of the bloodstain in the z-direction (between a depth of 0.3 mm and 0.7 mm) the bloodstains from  $5.0\text{ms}^{-1}$  produced the largest areas, although at most they were only  $15\text{mm}^2$  greater than the areas for the other two velocities. The differences among the areas were greater towards the technical rear of the fabric; the specimens created from the middle velocity of  $4.2\text{ms}^{-1}$  (1000 mm) produced the smallest mean area at a depth of 0.7 – 1 mm.

Univariate ANOVA was undertaken on the first area on the technical face, the maximum area and the last area at the technical rear of the cross-sections in the z-direction. ANOVA revealed only one statistically significant difference due to impact velocity. This was for the area of the cross-section on the technical face for the knit fabric ( $F_{2,11} = 5.523$ ,  $p = \leq 0.05$ ). Tukeys HSD analysis revealed a significant difference between only two of the means;  $4.5\text{ms}^{-1}$  ( $2.7\text{mm}^2$ ) and  $5.3\text{ms}^{-1}$  ( $6\text{mm}^2$ ). No significant difference was found between either of these two means and the mean area of the bloodstain formed at  $3.2\text{ms}^{-1}$  ( $5.4\text{mm}^2$ ).

For the bloodstain area formed on the technical face of the drill fabric the data was transformed as it was not normal (log10), but no significant difference was found ( $F_{2,12} = 3.803$ ,  $p = \text{NS}$ ). No significant difference was found for the maximum bloodstain area (knit:  $F_{2,11} = 1.66$ ,  $p = \text{NS}$ ; drill:  $F_{2,12} = 2.088$ ,  $p = \text{NS}$ ) or the area of the last bloodstain cross-section at the technical rear (knit:  $F_{2,11} = 0.454$ ,  $p = \text{NS}$ ; drill:  $F_{2,12} = 0.058$ ,  $p = \text{NS}$ ).

### **2.6.3 Warp and wale measurements**

Figure 2-8 shows the mean and standard deviation of measurements taken in the y (wale or warp) and x (course or weft) directions for the largest cross-section in the z-direction for each of the three impact velocities for each fabric. The coefficient of variation is largest for the x (weft) measurements for the bull drill, and smallest for the y (warp) measurements for this same fabric. For the rib knit the CV was similar for both the x (course) and y (wale) measurements. A greater difference between the x and y measurements is seen for the bull drill fabric, as well as a suggestion of a pattern, with the x (weft) measurement decreasing with impact velocity and the y (warp) measurement increasing.

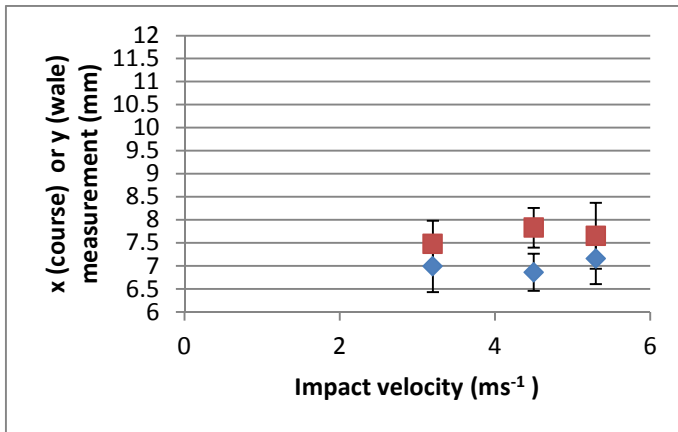


Figure 2-8a: the mean and standard deviation x (course) ( ◆ ) and y (wale) ( ■ ) measurement for each impact velocity for the rib knit fabric

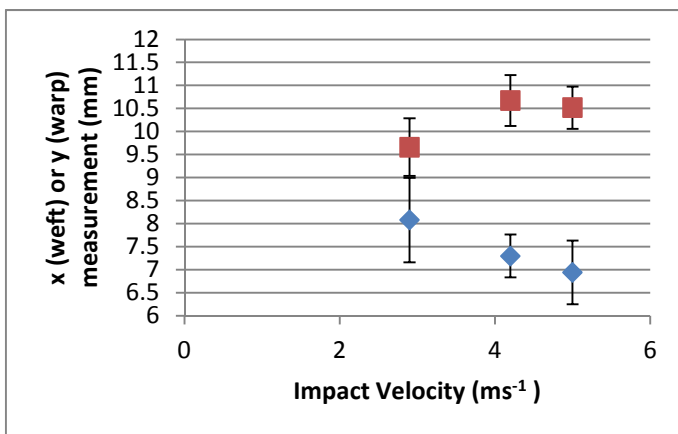


Figure 2-8b: the mean and standard deviation x (weft) ( ◆ ) and y (warp) ( ■ ) measurement for each impact velocity for the bull drill fabric.

Figure 2-8 the mean and standard deviation measurements for rib knit and bull drill fabrics for all velocities for the x (course or weft) and y (wale or warp) measurements from the cross section with the largest area.

Impact velocity did not affect either the y (wale) or x (course) measurements for the rib knit fabric (wale:  $F_{2,11} = 0.512$ ,  $p = \text{NS}$ ; course:  $F_{2,11} = 0.38$ ,  $p = \text{NS}$ ). For the drill fabric, impact velocity affected the y (warp) measurement ( $F_{2,12} = 4.911$ ,  $p = \leq 0.05$ ). Tukeys HSD analysis revealed a significant difference between only two of the means;  $2.9 \text{ ms}^{-1}$  (9.7 mm) and  $4.2 \text{ ms}^{-1}$  (10.7 mm). No significant difference was found between either of these two means and the mean y (warp) measurement from  $5 \text{ ms}^{-1}$  (10.5 mm). Impact velocity did not affect the x (weft) measurement ( $F_{2,12} = 3.307$ ,  $p = \text{NS}$ ).

## **2.7 Discussion**

Four key points were examined in this paper: (1) the use of the CT scanner to study bloodstains, (2) the shape of the bloodstain (3) the effect of impact velocity on the bloodstain (4) the effect of fabric structure on the bloodstain.

### **2.7.1 The use of the CT scanner**

Gaining a greater understanding of the morphology of a bloodstain on fabric has proved difficult by examining the external parent stain [9]. The use of the micro CT scanner has enabled the internal morphology of the bloodstain to be examined, by showing the shape which the blood forms within the fabric and therefore indicating how the blood has moved through the fabric.

### **2.7.2 Shape of the bloodstain**

For all impact velocities and both fabrics the combination of wetting and wicking resulted in a diamond shaped stain. The cross-sectional area of the bloodstain initially increased with depth, before decreasing towards the rear of the fabric. When the blood initially hit the fabric it spread, wetting the top of the fabric and allowing wicking to occur. The largest cross-sectional area was always below the technical face of the fabric (figures 2-4 and 2-5). In all cases the largest cross-sectional area was always within 0.5mm of the first cross-section of the bloodstain.

For the rib knit fabric, the first cross-sectional area measured was always less than the cross sectional area of the original blood drop (e.g. for an impact velocity of  $3.2 \text{ ms}^{-1}$  the mean cross-sectional area of the bloodstain was  $5.44 \text{ mm}^2$  for a blood drop diameter of 4.1 mm giving a cross-sectional area of the droplet of  $13.2 \text{ mm}^2$ ). This could be as a result of the 'coffee ring' effect (as shown in figure 2-7), whereby the particulates at the edge of the bloodstain have built up above the central bloodstain. This section is therefore seen in an earlier cross-section than the remainder of the bloodstain.

The mass of the remaining drop resulted in capillary action through the depth of the fabric, which did not occur around the extremities. In figures 2-4, 2-5 and 2-6 this is shown as the gradually decreasing area towards the technical rear of the fabric; as the blood travelled towards the technical rear, there was less liquid to spread.

### **2.7.3 Effect of impact velocity and fabric type**

Previous studies on absorbent surfaces have suggested that the impact velocity does not affect the surface morphology of bloodstains when the drop size remains constant [9]. In this work there were some suggestions of variability among the impact velocities for the two fabrics. The shape of the bloodstain through the fabric thickness (figures 2-4 and 2-6a) varied with velocity for the rib knit fabric. The cross-sectional areas for the fastest ( $5.3 \text{ ms}^{-1}$ ) velocity reached their greatest extent closer to the technical face of the fabric than the middle velocity ( $4.5 \text{ ms}^{-1}$ ). The first cross-sectional area for the fastest velocity ( $5.3 \text{ ms}^{-1}$ ) was only marginally smaller than the cross-sectional area of the original blood drop ( $10.7 \text{ mm}^2$  compared to  $13.2 \text{ mm}^2$ ). Both of these findings were most likely due to the higher velocity forcing the blood through the capillaries between and among the yarns and fibres, not allowing much blood to remain on the surface. The faster velocity resulted in a bloodstain which had a larger maximum cross-sectional area, but penetrated a shorter distance into the fabric resulting in a shallower depth, suggesting sideways wicking is dominating at this velocity.

The middle velocity ( $4.5 \text{ ms}^{-1}$ ) resulted in the smallest maximum area. It also had the deepest maximum area,  $0.5 \text{ mm}$  compared to  $0.4 \text{ mm}$  for the  $3.2 \text{ ms}^{-1}$  and  $5.3 \text{ ms}^{-1}$  impact velocities. This suggested sideways wicking was less dominant at this velocity, allowing more capillary action. However, why the lowest velocity ( $3.2 \text{ ms}^{-1}$ ) had a maximum area only  $1 \text{ mm}^2$  smaller at the same depth into the fabric as the highest velocity ( $5.3 \text{ ms}^{-1}$ ) raises further questions. The lowest velocity may have allowed the blood to wick to a greater extent than the middle velocity.

A statistically significant difference was seen between the areas on the technical face of the rib knit fabric for the specimens from  $4.5 \text{ ms}^{-1}$  and  $5.3 \text{ ms}^{-1}$ . This pattern was

not observed for the maximum area or the technical rear, indicating the greatest differentiation between these two groups of specimens was present on the technical face of the fabric. This was not a differentiation seen in the original external analysis of the parent stain [9] as the technical face area measurement from the CT cross-sections was different to the area of the visible parent stain on the external surface. This can be seen in figure 2-7, in that the bloodstain in the first cross-section for all three specimens is only a small percentage of the maximum area of the bloodstain, and the external visible bloodstain. This is something which would not have been apparent in the original external analysis of the bloodstain.

The lack of variability among the cross sectional areas depending on velocity seen in the bull drill fabric was most likely owing to the smaller capillary spaces than in the rib knit fabric. This meant the blood could not dissipate to a great extent regardless of the velocity [11]. However, a statistically significant difference was seen in the warp measurement of the bloodstain for the bull drill fabric (figure 2-8b) for specimens from  $2.9 \text{ ms}^{-1}$  and  $4.2 \text{ ms}^{-1}$ . These measurements were taken from the largest cross-section in the z-direction; however, the area measurements of this same cross-section revealed no statistically significant differences. This suggests that it is the warp measurement which varies most with velocity for this fabric. The pattern which is seen in figure 2-8b, where the weft decreased as the warp increased, helped explain why there was no statistically significant difference in the areas for the bull drill. As the warp was increasing as the weft decreased, the area would remain approximately similar throughout. However, no significant difference was seen among the weft measurements, most likely owing to the greater CV, pointing to the fact that the variation among specimens within a velocity was greater than for the warp measurement.

## **2.8 Conclusions**

This pilot study has demonstrated that micro CT scanning may aid understanding of the morphology of bloodstains on and within fabrics. The technique has allowed extra measurements to be taken regarding the size and shape of the bloodstain inside the

fabric. The results have shown that the maximum cross-sectional area occurs below the surface of the fabric and the bloodstain therefore formed a diamond shape within the fabric as a result of wetting and wicking occurring.

This work has identified some variability regarding the bloodstain morphology on two common fabrics due to impact velocity, for example the variation in the area of the cross-sections throughout the depth of the bloodstain. This work has also suggested that the structure of the fabrics themselves did have an effect on the bloodstain morphology.

## **2.9 References**

- [1] B. Karger, S. Rand, T. Fracasso, H. Pfeiffer, Bloodstain pattern analysis-Casework experience, *Forensic Sci. Int.* 181 (2008) 15–20. doi:10.1016/j.forsciint.2008.07.010.
- [2] Scientific Working Group on Bloodstain Pattern Analysis, Recommended Terminology, (2015). <http://www.swgstain.org/resources> (accessed September 12, 2018).
- [3] T. Bevel, R.M. Gardner, *Blood Pattern Analysis with an Introduction to Crime Scene Reconstruction*, Third Edition, CRC Press, Florida, 2008.
- [4] L. Hulse-Smith, N.Z. Mehdizadeh, S. Chandra, Deducing drop size and impact velocity from circular bloodstains, *J. Forensic Sci.* 50 (2005) 54–63. doi:10.1520/JFS2003224.
- [5] L. Hulse-Smith, M. Illes, A blind trial evaluation of a crime scene methodology for deducing impact velocity and droplet size from circular bloodstains, *J. Forensic Sci.* 52 (2007) 65–69. doi:10.1111/j.1556-4029.2006.00298.x.
- [6] C. Knock, M. Davison, Predicting the position of the source of blood stains for angled impacts, *J. Forensic Sci.* 52 (2007) 1044–1049. doi:10.1111/j.1556-4029.2007.00505.x.



- [7] B. White, Bloodstain pattern on fabrics: the effect of drop volume, dropping height and impact angle, *Can. Soc. Forensic Sci. J.* 19 (1986) 3–36.
- [8] B. Karger, S.P. Rand, B. Brinkmann, Experimental bloodstains on fabric from contact and from droplets, *Int. J. Legal Med.* 111 (1998) 17–21. doi:10.1007/s004140050104.
- [9] T. De Castro, T. Nickson, D. Carr, C. Knock, Interpreting the formation of bloodstains on selected apparel fabrics, *Int. J. Legal Med.* 127 (2013) 251–258. doi:10.1007/s00414-012-0717-3.
- [10] Indiana Supreme Court, *David R. Camm V. State of Indiana*, (2009).
- [11] E. Kissa, Wetting and Wicking, *Text. Res. J.* 66 (1996) 660–668. doi:10.1177/004051759606601008.
- [12] A. Patnaik, R.S. Rengasamy, V.K. Kothari, A. Ghosh, Wetting and wicking in fibrous materials, *Text. Prog.* 1 (2006) 1–105. doi:10.1533/tepr.2006.0001.
- [13] T.C. de Castro, M.C. Taylor, J.A. Kieser, D.J. Carr, W. Duncan, Systematic investigation of drip stains on apparel fabrics: The effects of prior-laundering, fibre content and fabric structure on final stain appearance, *Forensic Sci. Int.* 250 (2015) 98–109. doi:10.1016/j.forsciint.2015.03.004.
- [14] C.D. Adam, Fundamental studies of bloodstain formation and characteristics, *Forensic Sci. Int.* 219 (2012) 76–87. doi:10.1016/j.forsciint.2011.12.002.
- [15] Nikon Metrology, *XT H Series X-ray and CT technology for industrial applications*, (2010).
- [16] A.M. Schneider, B.V. Holcombe, The role of radiation in fabric warmth, in: G.A. Carnaby, E.J. Wood, L.F. Story (Eds.), *Adv. Work. Appl. Math. Phys. Wool Ind. Proceeding*, Lincoln, 1988: pp. 488–502.

[17] R.D. Deegan, O. Bakajin, T.F. Dupont, G. Huber, S.R. Nagel, T.A. Witten, Capillary flow as the cause of ring stains from dried liquid drops, *Nature*. 389 (1997) 827–829. doi:10.1038/39827.

### **3 The effect of fabric mass per unit area and blood impact velocity on bloodstain morphology.**

**Dicken, L., Knock, C., Beckett, S., Carr, D. J.**

**Submitted for publication in Forensic Science International, July 2018.**

#### **3.1 Abstract**

This paper discusses the effect of thickness and mass per unit area of calico fabrics (100% cotton, plain woven) on bloodstains. Horse blood was dropped vertically onto three calico fabrics with different mass per unit areas (85.1 g/m<sup>2</sup>, 163.5 g/m<sup>2</sup> and 224.6 g/m<sup>2</sup>). Six different impact velocities were used (1.7 ms<sup>-1</sup>, 2.9 ms<sup>-1</sup>, 4.1 ms<sup>-1</sup>, 4.9 ms<sup>-1</sup>, 5.1 ms<sup>-1</sup> and 5.4 ms<sup>-1</sup>). The dry bloodstains were largest on the calico with the lightest mass per unit area. The low yarn linear density and large inter-yarn spaces meant that the blood could wick into the yarns from all directions and along the intra-yarn spaces. The calico with the middle mass per unit area had the smallest mean dry bloodstain area for four out of the six velocities. The twist level for this calico was greater than for the calicos with a heavier or lighter mass per unit area. This reduced the amount of wicking which occurred along the yarns due to the tighter yarn structure. The calico with the heaviest mass per unit area had the highest yarn linear density resulting in a thicker fabric, so the blood could not as easily penetrate into the fabric. This resulted in a thicker wet blood layer remaining on the fabric surface, where it gradually wicked vertically into the yarns under gravity. Less wicking along the yarns occurred, resulting in a smaller bloodstain than on the fabric with the lightest mass per unit area. The correlation between impact velocity and mean dry bloodstain area was greater for the calicos with the medium and heaviest mass per unit area than for the calico with the lightest mass per unit area. For the calicos with the medium and heaviest mass per unit area, the amount of lateral spreading at impact, which increased with the increase in impact velocity, had a greater influence on the dry bloodstain area than the amount of wicking.

### **3.2 Keywords**

- Bloodstain analysis
- Absorbent surfaces
- Yarn linear density
- Micro-computed tomography
- Scanning electron microscopy
- Wicking

### **3.3 Highlights**

- The fabric mass per unit area affected the morphology of the bloodstain formed.
- Bloodstain area increased with blood impact velocity for all fabrics.
- CT scans aided the understanding of bloodstain morphology in the fabrics.

### **3.4 Introduction**

Although Bloodstain Pattern Analysis (BPA) has been used by crime scene investigators for over a century [1], questions have been raised on the scientific validity of the work [2]. The premise of BPA is that the pattern that blood creates when impacting a surface will enable the observer to gain an idea of the events which occurred to cause the bloodshed. However, the wide variety of creation mechanisms, drop sizes, impact velocities and target surfaces result in a complex topic [3]. The reliability of pattern classification of five bloodstain patterns on non-absorbent rigid surfaces [4] and fabric surfaces [5] by expert BPA analysts has been considered. On non-absorbent surfaces incorrect classifications were made 13.1% of the time [4] and on fabric surfaces incorrect classifications were made 23.4% of the time [5].

As such, more research is being undertaken on the understanding of the interaction of blood drops with a variety of surfaces. Work has been carried out on non-absorbent surfaces (e.g. steel and plastic [6]) and partially absorbent surfaces (e.g. paper and wood [7–9]). Methods have resulted that use the bloodstain size and number of spines

to back-calculate the impact velocity and assist in determination of the source of the bloodstain [7–9].

Bloodstains on household and clothing fabrics often found at crime scenes are also being researched. To understand bloodstains on fabrics, it is important to consider wetting and wicking. Wetting and wicking are the mechanisms by which liquids move into and through a fabric [10]. Wetting occurs when the surface energy of a solid overcomes the surface tension of a liquid, allowing the liquid to spread on the surface [10]. Once a fabric has been wetted, wicking can occur. Wicking is the spontaneous transport of a liquid into a porous system by capillary forces. The rate at which the wicking occurs is dependent on the dimensions of the capillaries within the substrate, and the viscosity of the liquid [11].

Fibre content and fabric structure affect the wetting and wicking properties of a fabric [12,13]. A 65% polyester / 35% cotton plain woven fabric produced larger bloodstains than either 100% cotton or 100% polyester plain woven fabrics. De Castro et al. [12,13] hypothesised that this may be in part due to the random mixture of cotton staple and cut polyester fibres which are spun together in a blend. This may have created larger interstitial spaces which resulted in more capillary action. Differences in capillary forces within 100% cotton plain woven and single jersey knitted fabrics may have resulted in the larger parent bloodstain area for the former [12].

When otherwise identical 100% cotton plain weave fabrics were manufactured from yarns which were either ring, rotor open end or Murata vortex air jet spun, porcine blood wicked only into the fabric woven from ring spun yarn [14]. When porcine blood was dropped vertically on to a commercially woven bed sheet, the elliptical bloodstains created were attributed to the warp yarns being ring spun, which wicked blood, and the weft yarns being Murata vortex spun, which did not. Therefore, even fabrics which appear identical may not result in similar bloodstains if the yarn manufacturing technique is different.

Scanning bloodstains with the use of a micro computed tomography ( $\mu$ CT) scanner provided a greater insight into the internal structure of bloodstains on fabric [15]. For 100% cotton rib knit fabric sideways wicking dominated at the fastest impact velocity ( $5.3 \text{ ms}^{-1}$ ), resulting in larger, shallower bloodstains [15]. However, for 100% cotton drill fabric, little variation was seen as the velocity increased from  $2.9 \text{ ms}^{-1}$  to  $5.3 \text{ ms}^{-1}$ . A suggested explanation was that the small capillary spaces for the drill fabric resulted in the blood not spreading regardless of velocity.

Previous work has had inconsistent methodology which precludes the ability to compare and conglomerate the research. There is often inconsistency in the treatment of the fabric prior to experimentation, for example not stated [16,17], from a second-hand store so unknown [18] and sometimes laundered, although not always for the same number of cycles [19,20]. In a number of articles, the fabric properties (e.g. mass per unit area, thickness, sett, yarn linear density and twist) are not provided [16,17,19,21].

Whilst work has been published on the effects of fabric and fibre content on bloodstain morphology, the effect of mass per unit area has not been extensively studied. The aim of the current work was to understand the effects of fabric mass per unit area and blood impact velocity on the resultant parent bloodstain formed on three 100% cotton plain woven fabrics.

### **3.5 Materials and methods**

#### **3.5.1 Materials**

To ensure the research was relevant to BPA, the fabrics used were 'household textiles'. Three calico fabrics (100% cotton, plain woven) were used to study the effect of different mass per unit areas ( $85.1 \text{ g/m}^2$  (light),  $163.5 \text{ g/m}^2$  (medium) and  $224 \text{ g/m}^2$  (heavy)) on passive bloodstains (table 3-1).

Dimensionally stable fabrics were created by washing the fabrics for six cycles in a domestic washing machine<sup>7</sup> before line drying [22]. The fabrics were ironed under the same conditions using a PSP-202E digital steam press on the cotton setting to remove creases. 100 mm x 100 mm specimens (n = 90) were cut from the fabrics, and were conditioned to 20 ± 2 °C and 65 ± 4% R.H. for 24 hours [23].

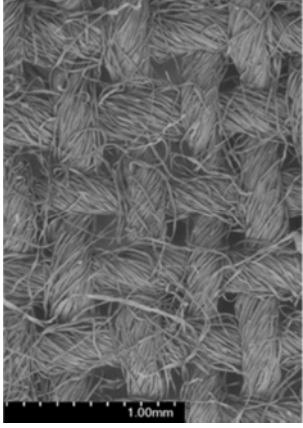
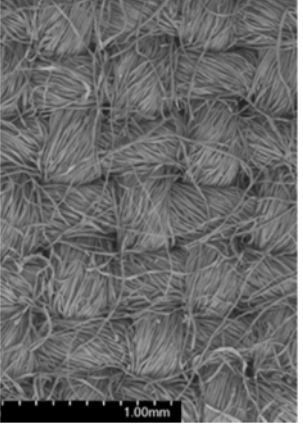
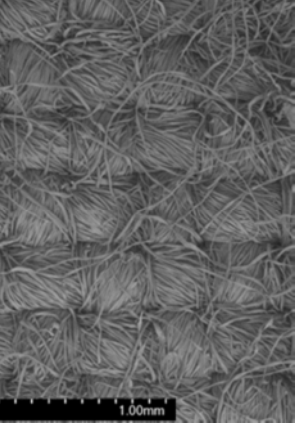
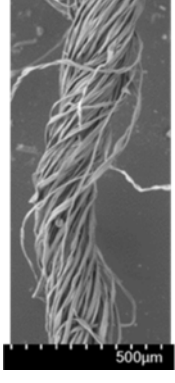
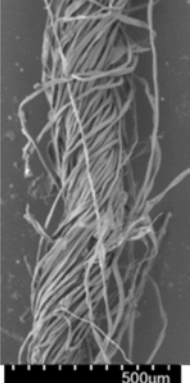
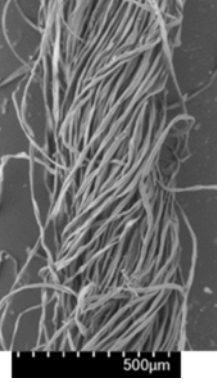
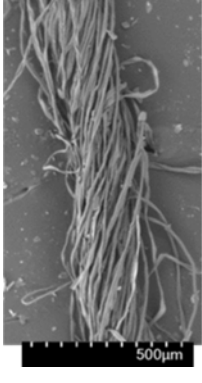
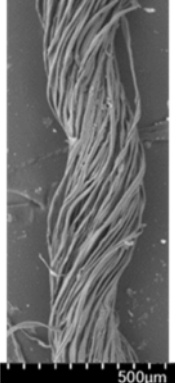
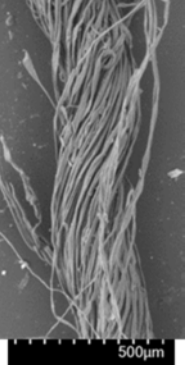
Fabric thickness (mm) [24], mass per unit area (g/m<sup>2</sup>) [25] and sett [26] were measured. Yarn linear density was estimated by the removal of ten 1 m long yarns from the fabric and weighing them using an Oxford A2204 balance accurate to four decimal places (appendix C). The twist level and yarn type were provided by the fabric supplier<sup>8</sup> (table 3-1). SEM images of the fabrics at 50x magnification and the warp and weft yarns at 75x magnification can be seen in figure 3-1.

	Light calico		Medium calico		Heavy calico	
Thickness (mm)	0.38 ± 0.03		0.46 ± 0.02		0.56 ± 0.03	
Mass per unit area (g/m <sup>2</sup> )	85.1 ± 1.54		163.5 ± 2.26		224.6 ± 1.56	
Sett (yarns per 10 mm)	27 x 23		25 x 26		26 x 26	
Yarn type	Ring spun		Ring spun		Ring spun	
	Warp:	Weft:	Warp:	Weft:	Warp:	Weft:
Twist (turns per m)	650	650	756	756	650	624
Linear density (tex)	14	18	33	31	43	47

**Table 3-1 mean fabric properties and standard deviations where available (n=5).**

<sup>7</sup> Samsung Ecobubble at 40°C cotton cycle.

<sup>8</sup> Whaleys Bradford Ltd, Harris Court, Great Horton, Bradford, West Yorkshire, BD7 4EQ  
<http://www.whaleys-bradford.ltd.uk/>

		
<p>Figure 3-1a: SEM image of the light calico at 50x magnification</p>	<p>Figure 3-1b: SEM image of the medium calico at 50x magnification</p>	<p>Figure 3-1c: SEM image of the heavy calico at 50x magnification</p>
		
<p>Figure 3-1d: SEM image of a weft yarn from the light calico at 75x magnification</p>	<p>Figure 3-1e: SEM image of a weft yarn from the medium calico 75x magnification</p>	<p>Figure 3-1f: SEM image of a weft yarn from the heavy calico 75x magnification</p>
		
<p>Figure 3-1g: SEM image of a warp yarn from the light calico 75x magnification</p>	<p>Figure 3-1h: SEM image of a warp yarn from the medium calico 75x magnification</p>	<p>Figure 3-1i: SEM image of a warp yarn from the heavy calico 75x magnification</p>

**Figure 3-1 SEM images of the light, medium and heavy calicos at 50x magnification, and of warp and weft yarns removed from the fabric at 75x magnification.**



Defibrinated horse blood sourced from Southern Group Laboratory<sup>9</sup> was used to create the bloodstains. The blood was stored below 4 °C, and used within one week of delivery.

### 3.5.2 Method

The horse blood was heated to 37 °C in a water bath to simulate a blood-letting event at body temperature. All drops were filmed using a Phantom V12 high-speed video (6273 fps and exposure 70 µs). The high-speed video was subsequently analysed using Phantom Camera Control software<sup>10</sup> to measure the droplet diameter and impact velocity for each drop height (table 3-2). The mean diameter of the drops for all experiments was 3.3 ± 0.17 mm. Five repeats were taken at each velocity on each fabric resulting in a total of 90 specimens.

Drop height (mm)	Mean velocity and standard deviation (ms <sup>-1</sup> )
200	1.7 ± 0.01
500	2.9 ± 0.06
1000	4.1 ± 0.04
1500	4.9 ± 0.04
2000	5.1 ± 0.2
2500	5.4 ± 0.2

**Table 3-2 the drop heights and subsequent velocities measured from the high-speed video**

<sup>9</sup> E-H Cavendish Courtyard, Sallow Road, Weldon North Industrial Estate, Corby, Northants  
www.sglab.co.uk

<sup>10</sup> <https://www.phantomhighspeed.com/resourcesandsupport/phantomresources/pccsoftware>  
page accessed 27<sup>th</sup> September 2018.

Bloodstains were photographed using a Nikon D3300 camera under the following conditions: wet ( $\leq 30$  s following the drop event) and dry on the technical face and technical rear of the fabric ( $\geq 24$  hours later).

Dry specimens were analysed using a Nikon XTH225 micro Computed Tomography ( $\mu$ CT) scanner<sup>11</sup>. For the  $\mu$ CT scans, the fabric specimens were cropped to a width just greater than the parent bloodstain to increase the resolution of the scans, and mounted on a foam block. Foam was used as it was a different density from the fabric, and so the scanned image of the foam could easily be removed from the CT data during post-processing.

The  $\mu$ CT data was manually reconstructed in CT pro 3D<sup>12</sup> (table 3-3). The reconstructed data was then analysed in VGStudio Max<sup>13</sup> and a 2D image of the 3D reconstruction of the bloodstain saved. Two-dimensional cross-sections were saved with a slice distance of 0.05 mm. Cross sections were obtained through the depth of the fabric in the warp and weft directions (figure 3-2).

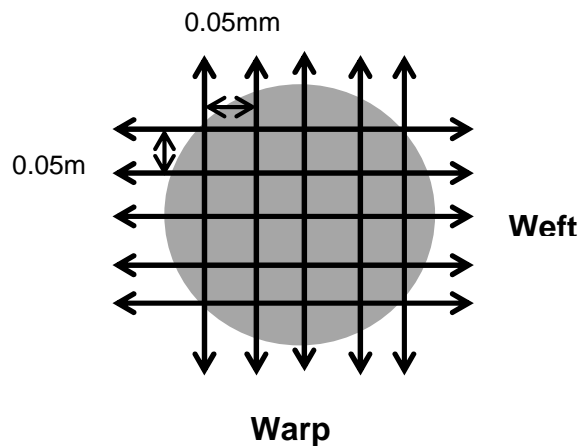
Scanning Values						Reconstruction	
<i>Target</i>	<i>Voltage (kV)</i>	<i>Current (<math>\mu</math>A)</i>	<i>Exposure (ms)</i>	<i>Projections</i>	<i>Frames per projection</i>	<i>Beam hardening</i>	<i>Noise reduction</i>
Tungsten	120	30	500	1080	2	1	1

**Table 3-3 the values at which all three masses of calico were scanned in the micro CT scanner and reconstructed.**

<sup>11</sup> Nikon Metrology UK, Tring Business Centre, Icknield Way, Tring, Hertfordshire, HP23 4JX

<sup>12</sup> CT pro is 3D CT reconstruction software [30]

<sup>13</sup> VGStudio Max enables the visualisation, examination and processing of CT data [31]



**Figure 3-2** direction of the 2D images saved from the CT data. Cross-sections were saved at a slice distance of 0.05 mm in each of the warp and weft directions.

The areas of the wet and dry technical face and technical rear parent bloodstains were obtained using the in-built tools in ImageJ<sup>14</sup> (appendix D). Briefly, the image was converted to binary so the parent bloodstains was black against the white background. The area of the bloodstain was measured using the ‘analyse particles’ function. The outline of the measured area was compared to the original photograph to ensure spatter not connected to the parent bloodstain was not included in the measurement.

Two specimens from each fabric and velocity combination were examined using a Hitachi SU3500 SEM with the EDAX TEAM microanalysis system<sup>15</sup> (15 kV, 60 Pa). Background images were taken of the fabric (x50) and of a yarn removed from the fabric (x75) (figure 3-1) as well as of the dry bloodstains (x42 and x250).

To determine whether the blood drop impact velocity or fabric mass per unit area had a statistically significant effect on the wet and dry bloodstain areas, an analysis of variance (ANOVA) (IBM SPSS statistics version 22) was carried out. Interaction results are only reported in the results section if significant. Tukey’s HSD test identified which

<sup>14</sup> ImageJ is a public domain Java image processing programme  
(<https://imagej.nih.gov/ij/docs/intro.html> page accessed 27th September 2018)

<sup>15</sup> <https://www.edax.com/products/eds/team-eds-system-for-the-sem> Page accessed 27<sup>th</sup> September 2018

variables or levels contributed towards any significant effects. To ensure that these statistical tests were viable, equality of variances and normality of data were checked.

### **3.6 Results and Discussion**

The resultant bloodstains from the passive blood drops were examined to compare the interaction between the blood and the fabric among the different fabrics and velocities.

Overall, the light calico produced the largest mean dry bloodstain area, and the medium the smallest, although this is not true across all velocities (figure 3-3). For the medium and heavy calico, a straight line fitted to the mean data using a least square fit gave a strong correlation for both wet (medium:  $R^2 = 0.98$ ; heavy:  $R^2 = 0.92$ ) and dry (medium:  $R^2 = 0.93$ ; heavy:  $R^2 = 0.94$ ) bloodstain area with velocity. The correlation was lower for the light calico (wet:  $R^2 = 0.6$ ; dry:  $R^2 = 0.74$ ). Univariate analysis of variance (ANOVA) revealed impact velocity affected wet bloodstain area ( $F_{17,72} = 49.314, p \leq 0.01$ ) and dry bloodstain area ( $F_{17,72} = 37.459, p \leq 0.01$ ), the details of which are given in table 3-4.

The results showed four groupings of velocities (table 3-4). The specimens from  $1.7 \text{ ms}^{-1}$  had dry bloodstains which were small and dense, and so the specimens from this velocity were looked at individually. The specimens from 2.9, 4.1 and  $4.9 \text{ ms}^{-1}$  were grouped together as all fabrics had a gradual increase in mean dry bloodstain area with velocity. The medium calico had the smallest mean dry bloodstain area and the light the largest. Within a fabric, the bloodstains appeared visually similar. The specimens from  $5.1 \text{ ms}^{-1}$  were looked at individually as the medium calico had the largest mean dry bloodstain area, and the light calico the smallest, which only occurred at this velocity. Lastly, the specimens from  $5.4 \text{ ms}^{-1}$  were also looked at individually. This velocity resulted in a large increase in mean dry bloodstain area for the light and heavy calicos.

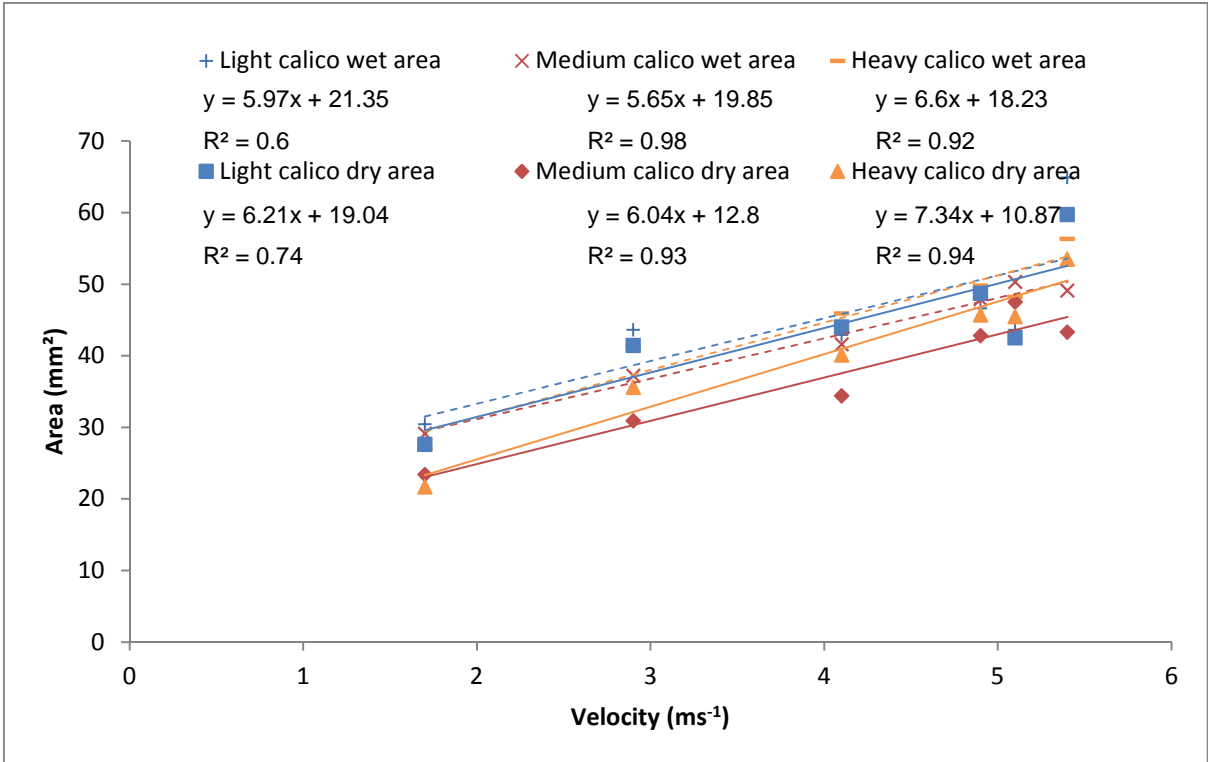


Figure 3-3 mean wet and dry bloodstain area at each velocity for all fabrics.

Velocity category (ms <sup>-1</sup> )	Mean dry bloodstain area and standard deviation (mm <sup>2</sup> )	Light Calico	Medium Calico	Heavy Calico	Statistics
1.7	L: 27.6 ± 4.4 M: 23.4 ± 4.7 H: 21.7 ± 3.2	<ul style="list-style-type: none"> <li>- Blood pooled on the surface of the fabric when wet, filling the inter-yarn spaces (figure 3-5a)</li> <li>- Blood surrounded yarns and wicked into the yarns from all sides</li> <li>- Pooled blood provided a reservoir for blood to wick along the intra-yarn spaces (figure 3-6a and b)</li> <li>- Bloodstain dried in the manner of the coffee ring effect (figure 3-8a)</li> </ul>	<ul style="list-style-type: none"> <li>- Blood remained pooled on the surface of the fabric (figures 3-5b and c)</li> <li>- Blood wicked vertically through the yarns under gravity</li> <li>- Only a small amount of wicking along the intra-yarn spaces</li> <li>- Large volume of blood dried on the surface of the fabric (figures 3-8b and c)</li> </ul>		Technical face wet and dry bloodstain areas statistically significantly smaller than all other velocities.
2.9	L: 41.4 ± 3.6 M: 30.9 ± 5.6 H: 35.6 ± 7.8	<ul style="list-style-type: none"> <li>- No wet blood pooled on the fabric technical face (figure 3-9a)</li> <li>- Blood penetrated the fabric at impact through to the technical rear</li> </ul>	<ul style="list-style-type: none"> <li>- Blood remained pooled on the surface in specimens from 2.9 and 4.1 ms<sup>-1</sup> (figure 3-9b)</li> <li>- Blood wicked vertically into the warp and weft yarns (figure 3-10d and e)</li> <li>- Wicking along the intra-yarn spaces impeded owing to the greater twist than for the light and heavy calicos</li> </ul>	<ul style="list-style-type: none"> <li>- Blood remaining pooled on the surface in specimens from 2.9 and 4.1 ms<sup>-1</sup> (figure 3-9c)</li> <li>- Blood dried before penetrating through the thickness of the yarns (figure 3-10 g and h)</li> <li>- A large volume of blood dried on the surface of the fabric (figure 3-9f)</li> </ul>	<p>Technical face wet and dry bloodstain area for 2.9 ms<sup>-1</sup> statistically significantly smaller than 4.9 ms<sup>-1</sup>, 5.1 ms<sup>-1</sup> and 5.4 ms<sup>-1</sup>.</p> <p>Technical face wet bloodstain area for 4.1 ms<sup>-1</sup> and 4.9 ms<sup>-1</sup> is statistically significantly smaller than 5.4 ms<sup>-1</sup>. Technical face dry bloodstain area for 4.1 ms<sup>-1</sup> statistically significantly smaller than 5.4 ms<sup>-1</sup>.</p>
4.1	L: 44 ± 6.9 M: 34.4 ± 3.9 H: 40.1 ± 6.3	<ul style="list-style-type: none"> <li>- Wicking occurred along the intra-yarn spaces and removed iron-rich blood from the centre of the bloodstain (figure 3-10a and b)</li> </ul>			
4.9	L: 48.7 ± 12 M: 42.8 ± 5.7 H: 45.7 ± 4.5	<ul style="list-style-type: none"> <li>- Very little blood dried on the surface of the fabric (figure 3-9d)</li> </ul>			
5.1	L: 42.5 ± 3.4 M: 47.5 ± 8.8 H: 45.5 ± 4.3	<ul style="list-style-type: none"> <li>- No wet blood pooled on the fabric technical face</li> <li>- Blood penetrated the yarns at impact - very little blood in the inter-yarn spaces (figure 3-11a-c)</li> </ul>	<ul style="list-style-type: none"> <li>- No wet blood pooled on the fabric technical face</li> <li>- Blood penetrated the yarns at impact (figure 3-11d-f)</li> <li>- Blood penetrated through to the</li> </ul>	<ul style="list-style-type: none"> <li>- No wet blood pooled on the fabric technical face</li> <li>- Blood penetrated the yarns at impact (figure 3-11g-i)</li> <li>- Less blood available for lateral</li> </ul>	Technical face wet and dry bloodstain area statistically significantly smaller than 5.4 ms <sup>-1</sup> .

		- With no blood pooled on the surface further wicking along the intra-yarn spaces could not take place.	technical rear of the fabric (figure 3-12e) - Some wicking occurred along the intra-yarn spaces.	spreading - Greater yarn linear density of the heavy calico meant blood could not wick easily along the yarns	
5.4	L: 59.7 ± 6.4 M: 43.3 ± 4.1 H: 53.5 ± 7.3	- No wet blood pooled on the fabric technical face (figure 3-13a) - Large amount of spreading on the technical face at impact - Penetration through to the technical rear at impact - Blood wicked into the warp yarns, but only coated the weft yarns (figure 3-14a and b) - Once the blood was either in or around the yarns, it then wicked along the intra-yarn spaces.	- Small amount of blood remained on the surface following impact (figure 3-13b) - Blood penetrated through to technical rear at impact (figure 3-13h) - Blood coating the warp and weft yarns (figure 3-14d and e) – Small amount of wicking occurred - Wicking limited owing to blood drying on the surface and the greater twist of the medium calico.	- Small amount of blood remained on the surface following impact (figure 3-13c) - No penetration through to the technical rear of the fabric at impact (figure 3-13i) - Blood spread laterally across the surface of the fabric	Technical face wet bloodstain area statistically significantly larger than all other velocities. Technical face dry bloodstain area statistically significantly larger than 1.7 ms <sup>-1</sup> , 2.9 ms <sup>-1</sup> , 4.1 ms <sup>-1</sup> and 5.1 ms <sup>-1</sup> .

**Table 3-4 a summary of the way in which blood is interacting with each fabric (light: 85.1 g/m<sup>2</sup>; medium: 163.5 g/m<sup>2</sup>; heavy: 224.6 g/m<sup>2</sup>) for each velocity category**

### 3.6.1 1.7 ms<sup>-1</sup>

At an impact velocity of 1.7 ms<sup>-1</sup> a small amount of lateral spreading occurred following the initial impact with little satellite stain and ligament formation (figure 3-4a-c). The amount the blood drop spread on the surface of the fabric following impact depended on the kinetic energy at impact. The kinetic energy was converted to surface energy to cause the spreading [20]. From 1.7 ms<sup>-1</sup>, there was little kinetic energy at impact, therefore little spreading. The blood then retracted to form a small bloodstain (figure 3-4d).

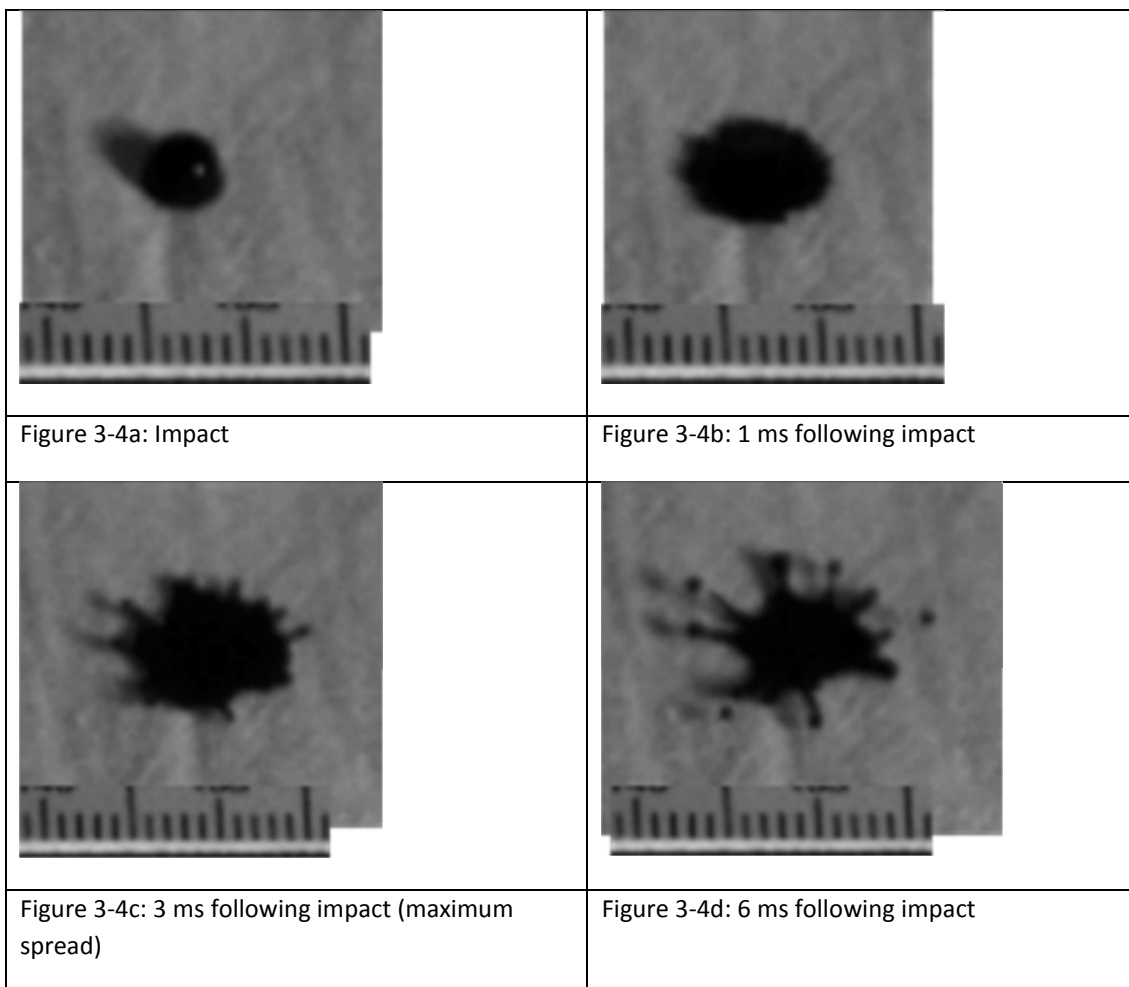
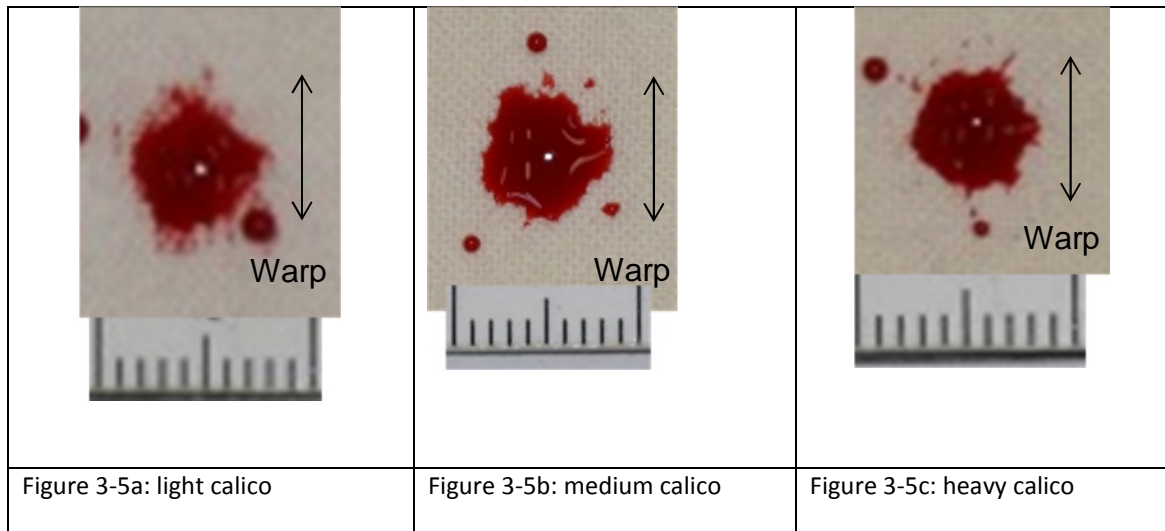


Figure 3-4 Typical example of a blood drop impacting the light calico at 1.9 ms<sup>-1</sup> (images from work undertaken for [27] but not used in the publication)

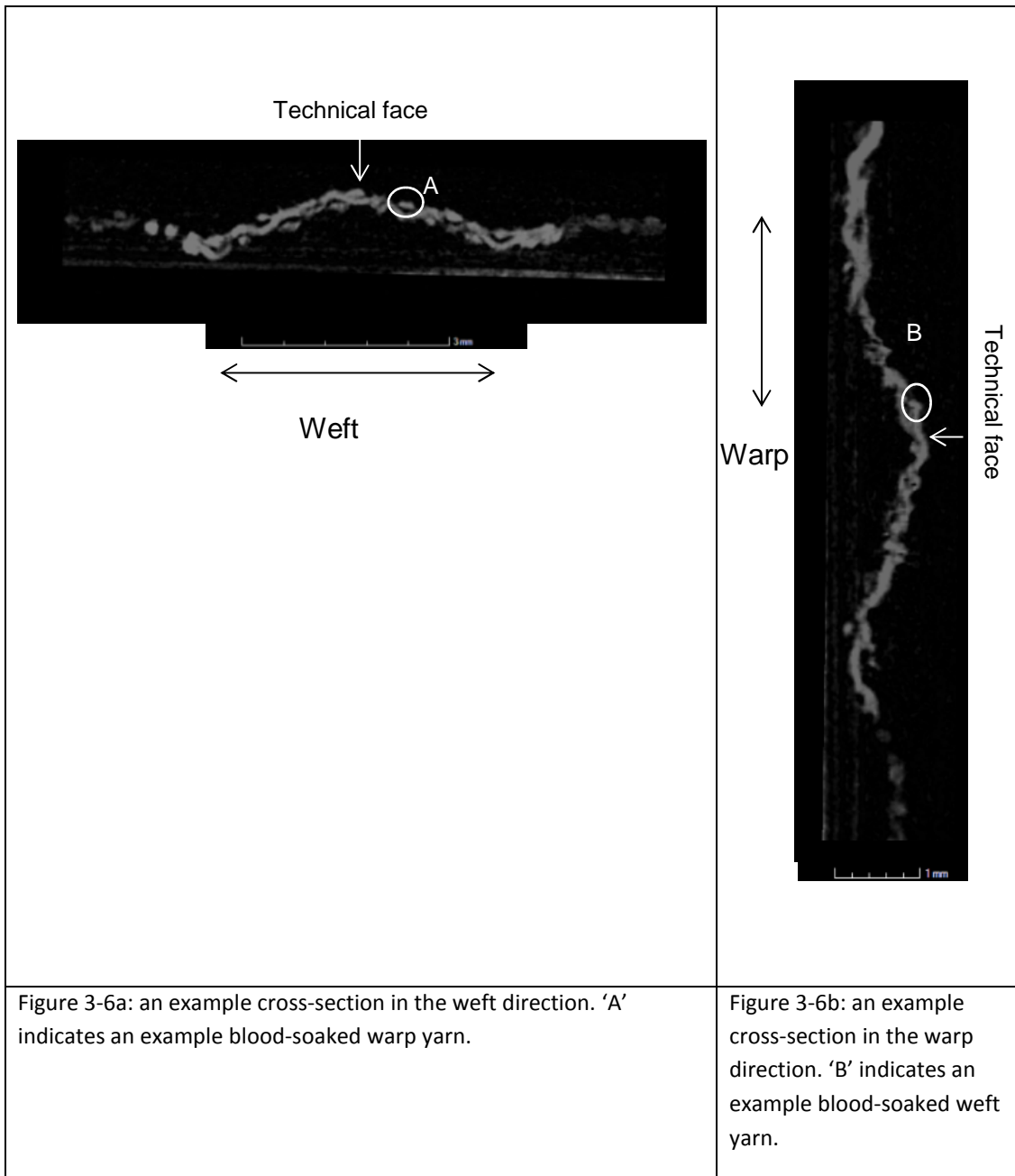


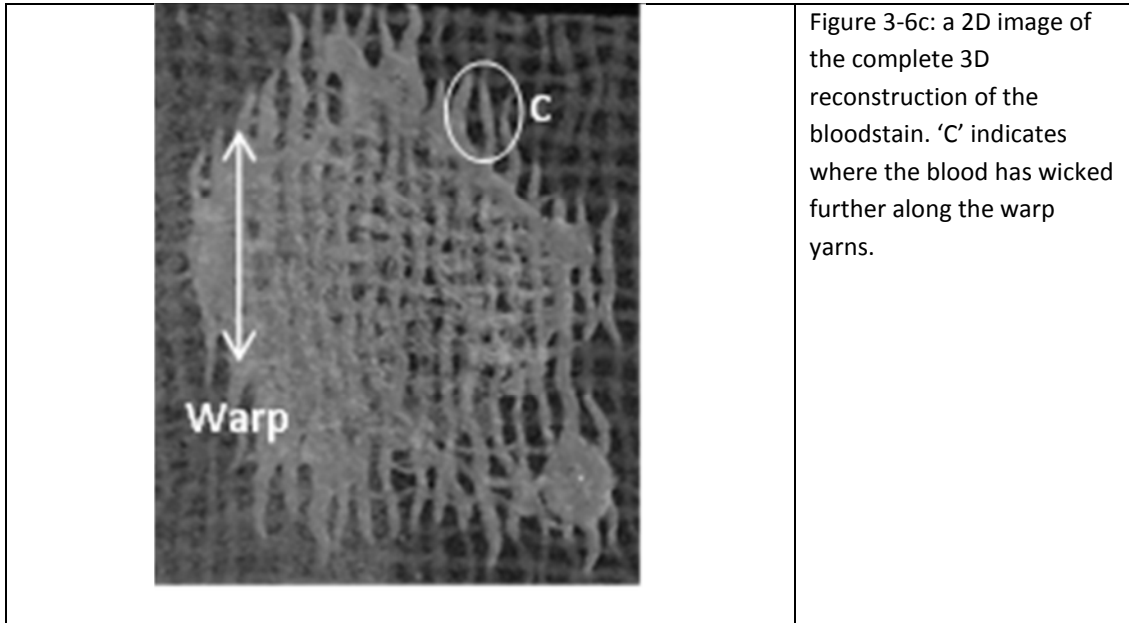
The small amount of initial spreading resulted in the blood remaining pooled on the surface of all fabrics in the wet bloodstain photographs (figure 3-5).



**Figure 3-5 Typical example of a wet bloodstain on each calico formed at  $1.7 \text{ ms}^{-1}$ . Scale is 10 mm.**

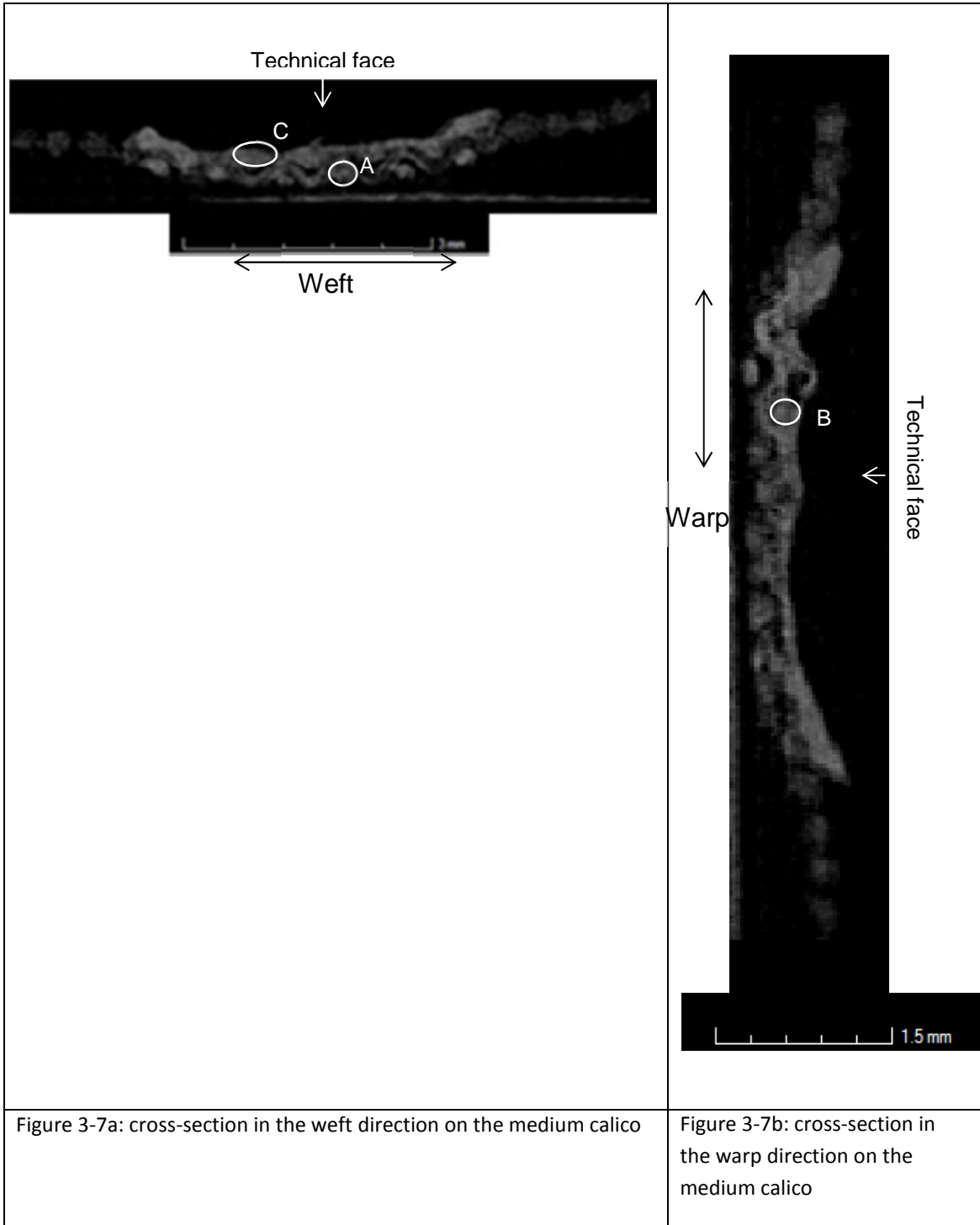
A key finding in the current work was the effect of the different fabric structures between the light, and the medium and heavy calicos on the bloodstains resulting from the  $1.7 \text{ ms}^{-1}$  impacts (table 3-4). On the light calico blood pooled in the large inter-yarn spaces. The blood then wicked into the yarns from all sides, filling the intra-yarn spaces. In the CT cross-sections (figures 3-6a and b), both the warp (marked 'A') and weft (marked 'B') yarns are soaked in iron-rich blood. The volume of blood on the fabric surface, and in the inter-yarn spaces, then provided a reservoir for the blood to wick along the yarns after wetting. The lower linear density of the warp yarns (14 tex) than the weft yarns (18 tex) increased the amount of wicking in the former (figures 3-6c, marked 'C' and 3-8a marked 'A'). The lower yarn linear density meant less blood was required to wet the yarn, and then fill the volume of the yarn, so the blood was able to wick further.





**Figure 3-6** The CT data from a typical example of a light calico specimen formed at  $1.7 \text{ ms}^{-1}$

On the medium and heavy calicos more blood dried on the surface of the fabric than for the light calico (figure 3-8a-c). The higher yarn linear density and smaller inter-yarn spaces of the medium and heavy calico meant it was more difficult for the blood to fill the inter-yarn spaces and surround the yarns. The blood pooled on the surface of the fabric and then wicked vertically through the yarns under gravity from the technical face towards the technical rear. This resulted in both the warp (marked 'A') and weft (marked 'B') yarns being soaked in iron-rich blood (figure 3-7), with blood also remaining on the surface of the fabric (figure 3-7, marked 'C'). Although the blood was in the intra-yarn spaces, it did not wick along the yarns to the same extent as the light calico. This was owing to the amount of time it would take to fully wet the high linear density yarns of the medium and heavy calico as the blood was only soaking through from the technical face of the fabric. The blood therefore dried on the surface before it was able to wick along the yarns.  $1.7 \text{ ms}^{-1}$  is the only velocity where the heavy calico specimens had the smallest mean dry bloodstain area (figure 3-3), owing to the greater yarn linear density of this fabric than either the medium or light calico.



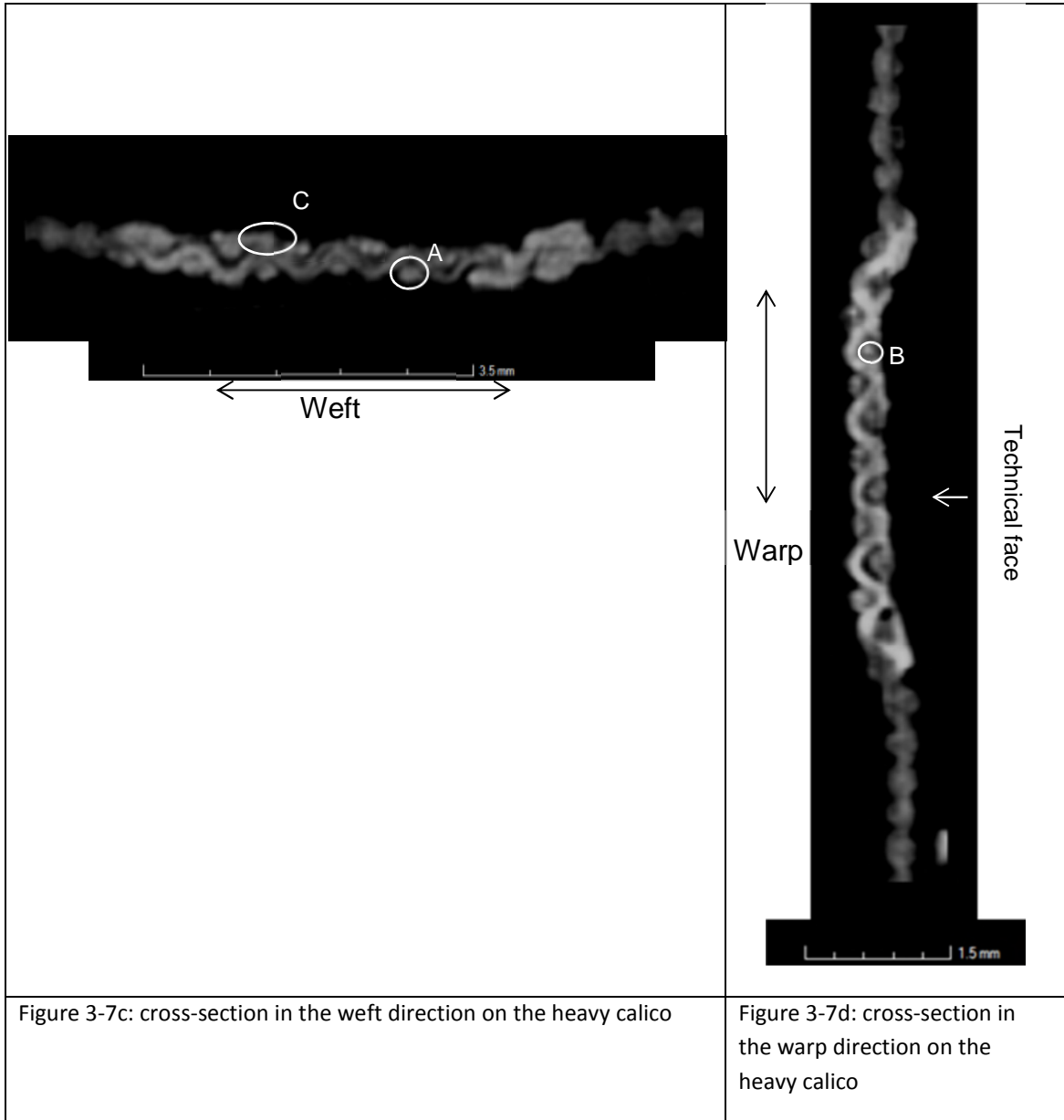


Figure 3-7 a typical example of a cross-section in the warp and weft directions on the medium and heavy calico formed at  $1.7 \text{ ms}^{-1}$ . 'A' indicates an example blood-soaked warp yarn, 'B' an example blood-soaked weft yarn and 'C' the blood remaining on the surface of the fabric.

On all three fabrics for  $1.7 \text{ ms}^{-1}$  impacts the blood which remained on the surface of the fabric dried in the manner of the coffee ring effect (figure 3-8a-c, marked 'B'). The coffee ring effect occurs in many colloidal fluids when the solutes move to the pinned edge of the liquid drop to compensate for evaporative losses [28]. This results in a higher concentration of particulates at the edge of the drop than the centre, and is evidenced by a ring of dense blood surrounding the parent bloodstain.

As a larger volume of blood remained on the surface of the medium and heavy calicos than the light calico, the coffee ring effect was more pronounced. The coffee ring effect occurred more extensively for  $1.7 \text{ ms}^{-1}$  impacts as blood pooled on the surface of all fabrics following impact and dried before it could wick away.

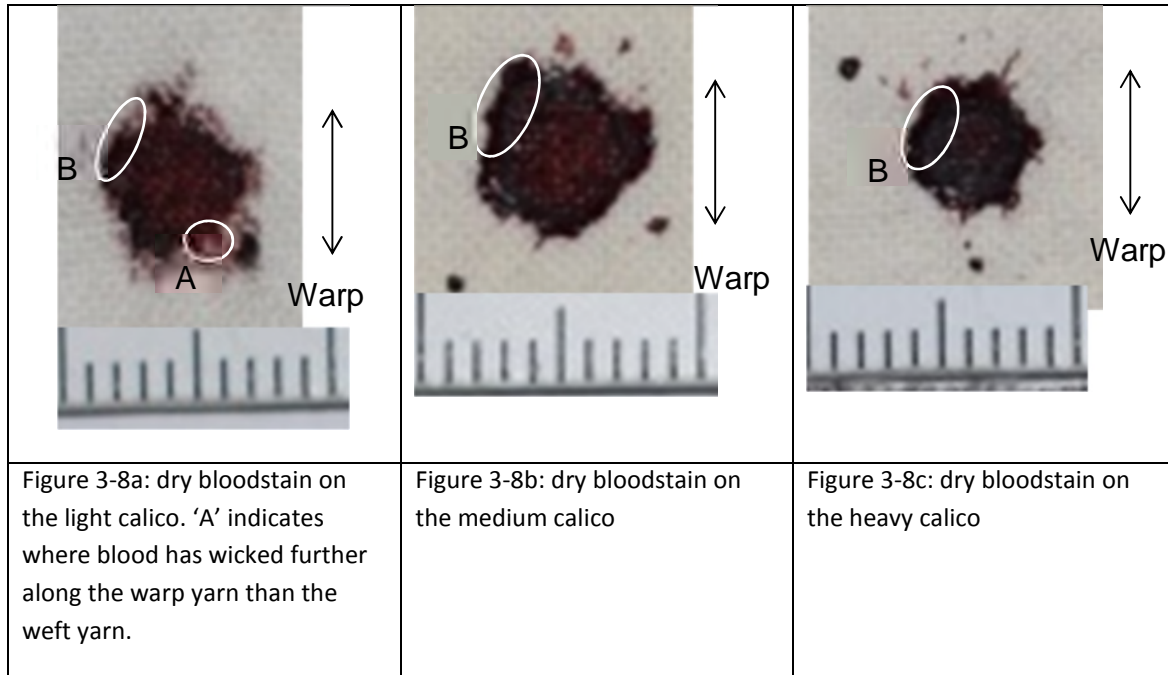


Figure 3-8 a typical example of a dry bloodstain on each calico formed at  $1.7 \text{ ms}^{-1}$ . 'B' indicates the coffee ring effect in part of the bloodstains. Scale is 10 mm.

### 3.6.2 2.9, 4.1 and $4.9 \text{ ms}^{-1}$

On the light calico there was a large increase in mean dry bloodstain area from  $27.6 \text{ mm}^2$  at  $1.7 \text{ ms}^{-1}$  to  $41.4 \text{ mm}^2$  at  $2.9 \text{ ms}^{-1}$  (figure 3-3) owing to the increase in lateral spreading following impact due to the increase in velocity (table 3-4). This increase in lateral spreading resulted in no blood remaining pooled on the surface of the light calico (figure 3-9a). The blood instead penetrated the yarns through to the technical rear of the light calico (figure 3-9g, marked 'A') some of which occurred closely following impact [27], with wicking further increasing the technical rear bloodstain area. The amount of blood which penetrated to the technical rear following impact has previously been found to increase with an increase in impact velocity from  $1.9 \text{ ms}^{-1}$  to  $4.2 \text{ ms}^{-1}$  ( $7.2 \text{ mm}^2$  to  $18.6 \text{ mm}^2$ ) [27].

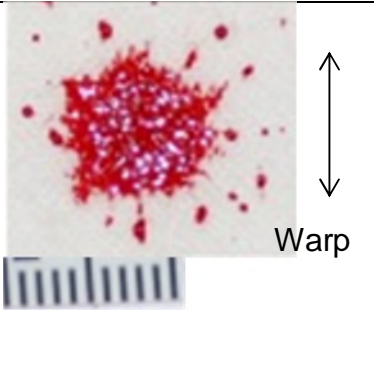
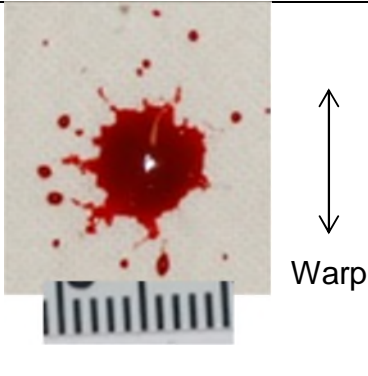
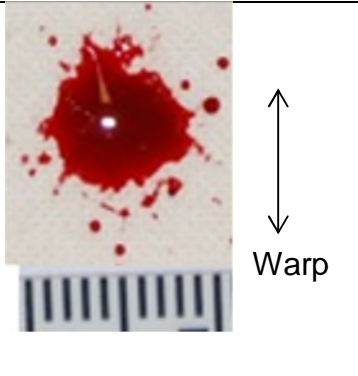
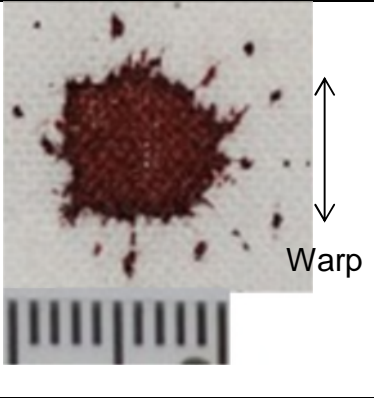
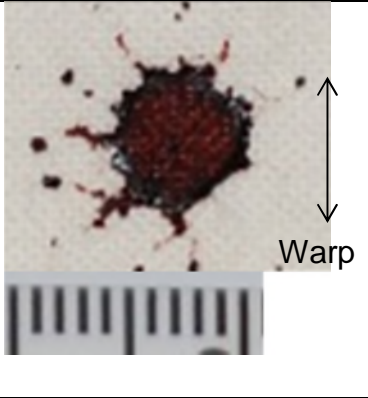
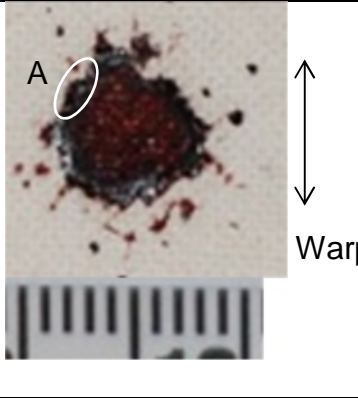
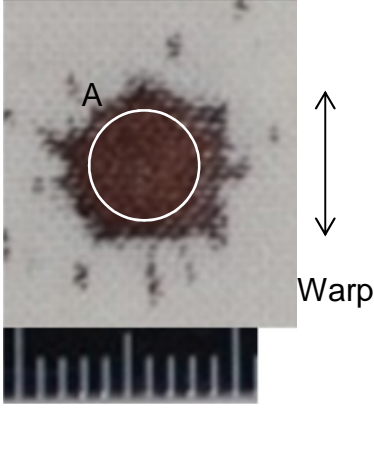
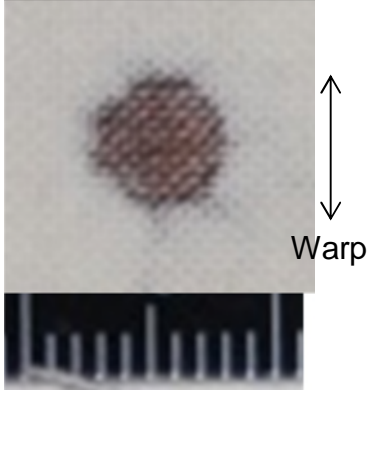
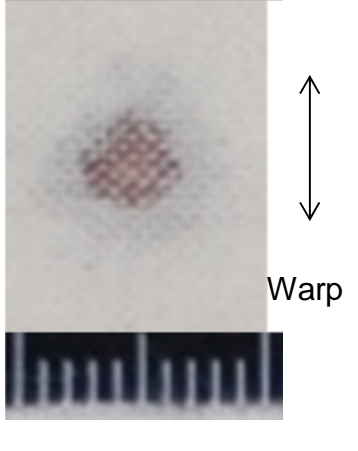
		
<p>Figure 3-9a: light calico wet bloodstain</p>	<p>Figure 3-9b: medium calico wet bloodstain</p>	<p>Figure 3-9c: heavy calico wet bloodstain</p>
		
<p>Figure 3-9d: light calico dry bloodstain</p>	<p>Figure 3-9e: medium calico dry bloodstain</p>	<p>Figure 3-9f: heavy calico dry bloodstain. 'A' indicates the dense dry blood at the edge of the bloodstain.</p>
		
<p>Figure 3-9g: light calico technical rear dry bloodstain. 'A' indicates where the blood has penetrated both the warp and weft yarns.</p>	<p>Figure 3-9h: medium calico technical rear dry bloodstain</p>	<p>Figure 3-9i: heavy calico technical rear dry bloodstain</p>

Figure 3-9 a typical example of a technical face wet and dry and technical rear dry bloodstain on each calico formed at  $4.1 \text{ ms}^{-1}$ . Scale is 10 mm.

For the light calico neither the warp nor weft yarns contained a large amount of iron-rich blood (figure 3-10a and b), with only a patchy area in the centre of the bloodstain (marked 'A'). At the edge of the bloodstain there is iron-rich blood primarily on the warp yarns (marked 'B'). Once the blood penetrated the intra-yarn spaces of the light calico, wicking occurred along them to remove the particulates (red blood cells, white blood cells and platelets) from the centre of the bloodstain towards the edge, removing any blood which was originally pooled in the inter-yarn spaces (figure 3-10c, marked 'C'). Any particulates which remained in the centre of the bloodstain were spread out owing to the larger dry bloodstain areas at these velocities than at  $1.7 \text{ ms}^{-1}$ . The amount of wicking which was occurring at  $2.9$ ,  $4.1$  and  $4.9 \text{ ms}^{-1}$  on the light calico resulted in similar mean dry bloodstain areas at these three velocities ( $41.4$ ,  $44.0$  and  $48.7 \text{ mm}^2$  respectively) and reduced the correlation of mean dry bloodstain area and velocity.

The dry bloodstains formed on the light (thinnest) calico specimens from impact velocities of  $2.9$ ,  $4.1$  and  $4.9 \text{ ms}^{-1}$  had a larger mean area than the medium and heavy calico specimens (figure 3-3, table 3-4). However, there was only one statistically significant difference in dry bloodstain area among the fabrics at any of these three velocities. From an impact velocity of  $2.9 \text{ ms}^{-1}$  ( $F_{2,12} = 3.951$ ,  $p \leq 0.05$ ), the light calico was statistically significantly larger than the medium calico. A larger bloodstain on a thinner fabric was also seen when bloodstains on a blend (65% polyester / 35% cotton) plain woven fabric were compared to those on 100% cotton and 100% polyester fabrics which had greater thickness and mass per unit area [12]. Although fibre content may also have had an effect in this previous work, it was suggested that the large bloodstain size was caused by the blood spreading laterally over the fabric, rather than over and through the fabric [12].

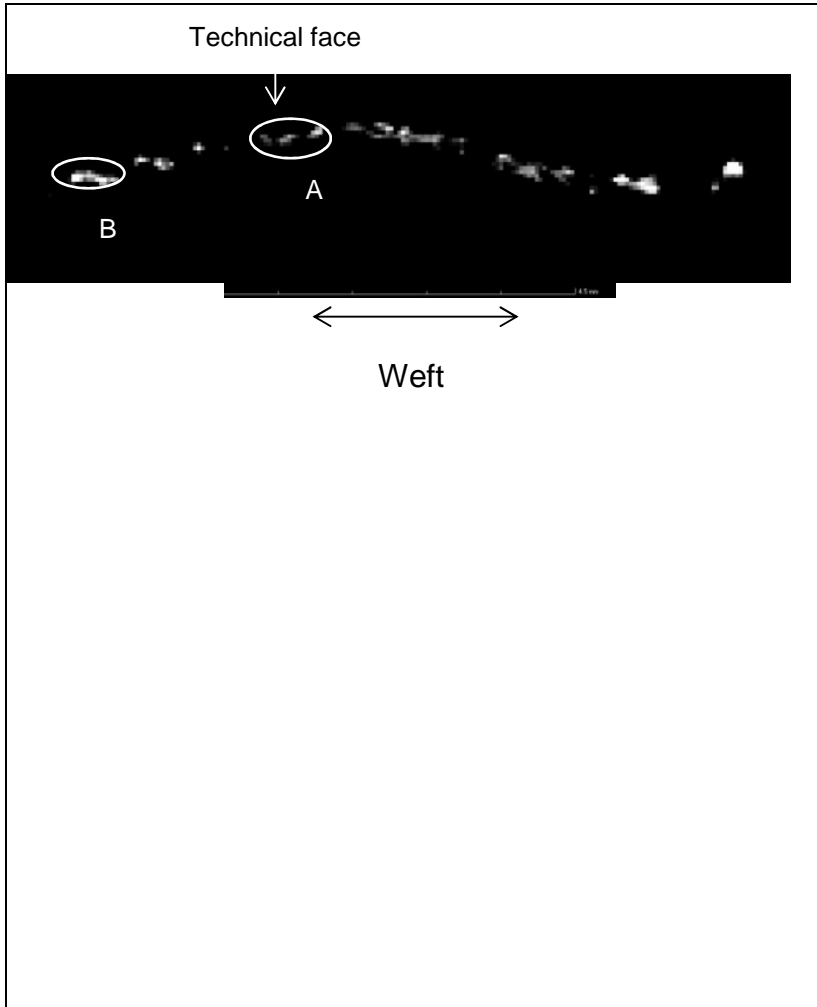
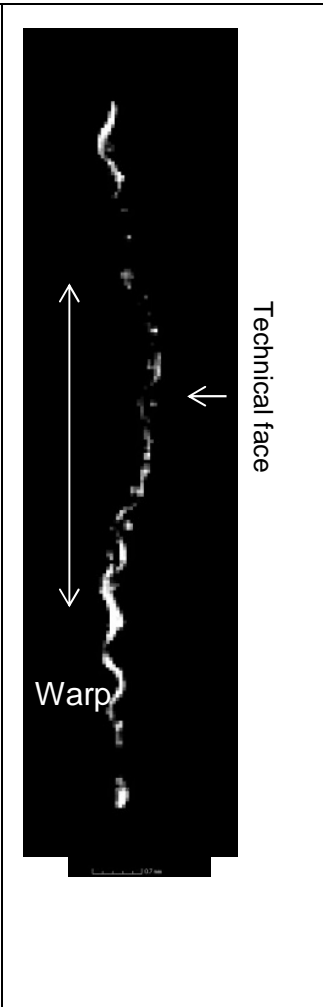
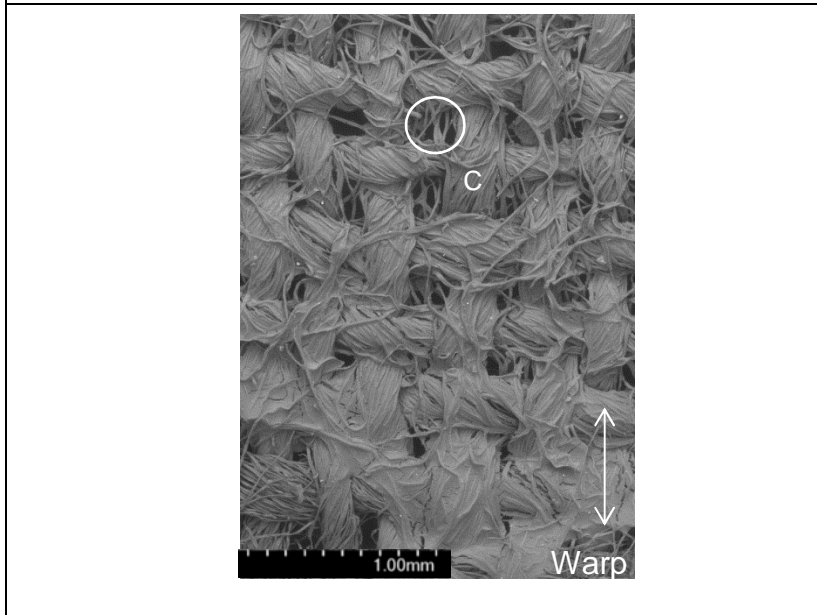
For the medium and heavy calico, blood remained pooled on the surface of the fabric when the blood impacted at a velocity of  $2.9 \text{ ms}^{-1}$  or  $4.1 \text{ ms}^{-1}$  (figure 3-9b and c). At an impact velocity of  $4.9 \text{ ms}^{-1}$  no blood remained pooled on the fabric surface owing to



the greater amount of lateral spreading. The increase in lateral spreading also increased the mean dry bloodstain area with velocity (figure 3-3, table 3-4).

Although the blood could not penetrate the medium calico as easily as the light calico owing to the smaller inter-yarn spaces, iron-rich blood did wick into both the warp and weft yarns. This occurred primarily on the sections of the yarns which were on the technical face of the fabric (figure 3-10d and e, marked 'A'). The blood was therefore penetrating the yarns from the reservoir pooled on the surface of the fabric. However, the high twist level of the medium calico (756/756) compared to the heavy calico (650/624) impeded the wicking of the blood along the intra-yarn spaces, resulting in the smallest mean dry bloodstain area at each of these velocities.

The  $\mu$ CT cross-sections for the heavy calico indicated very little iron-rich blood in the centre of the bloodstain (figures 3-10g and h). Any iron-rich blood which is in the centre of the bloodstain (marked 'A') is primarily on the warp yarns, with the blood not soaked all the way through to the centre of the yarns. This is indicative of the higher linear density for the heavy than the light and medium calicos. The blood dried before penetrating to the centre of the yarns, shown by the volume of dry blood which remained on the surface of the fabric (figure 3-9f, marked 'A', figure 3-10i marked 'B'), filling the inter-yarn spaces (figure 3-10i, marked 'C'). At an impact velocity of  $4.2 \text{ ms}^{-1}$  it has previously been found that no blood penetrated through to the technical rear of the heavy calico at impact, while blood did penetrate both the medium and light calicos [27].

	
<p>Figure 3-10a: light calico in the weft direction. 'A' indicates a patchy area of iron-rich blood. 'B' indicates denser iron-rich blood on the warp yarns.</p>	<p>Figure 3-10b: light calico in the warp direction</p>
	<p>Figure 3-10c: light calico SEM image at 42x magnification. 'C' indicates an inter-yarn space with no blood pooled inside.</p>

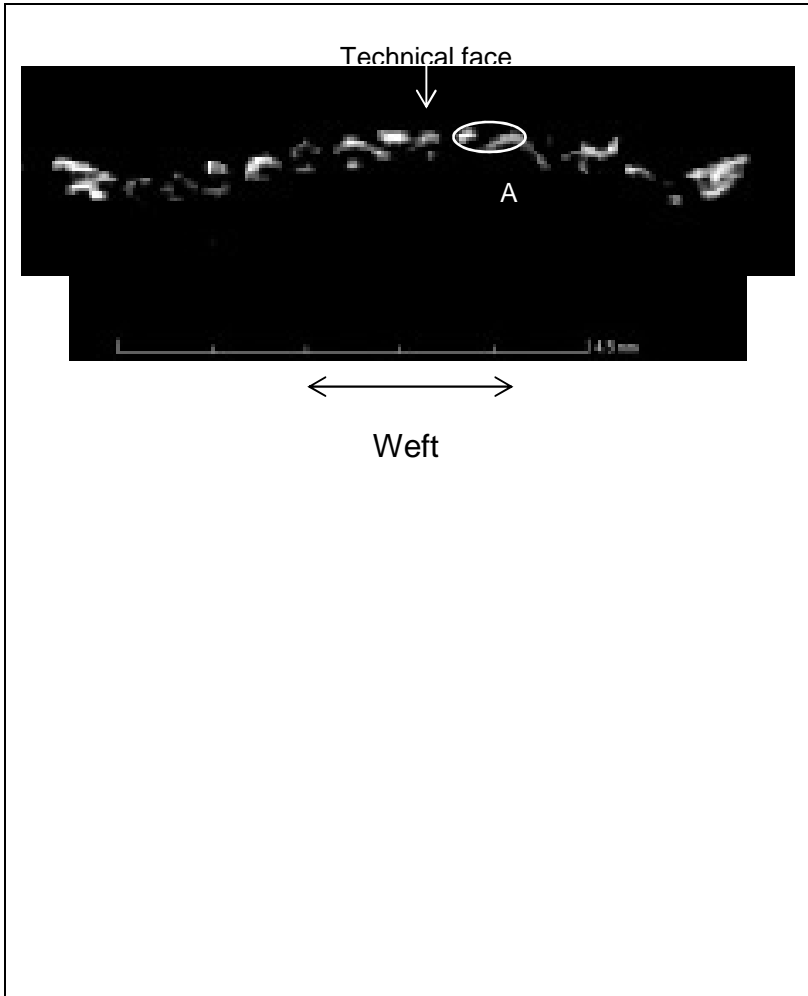


Figure 3-10d: medium calico in the weft direction. 'A' indicates blood-soaked yarns on the technical face of the fabric.

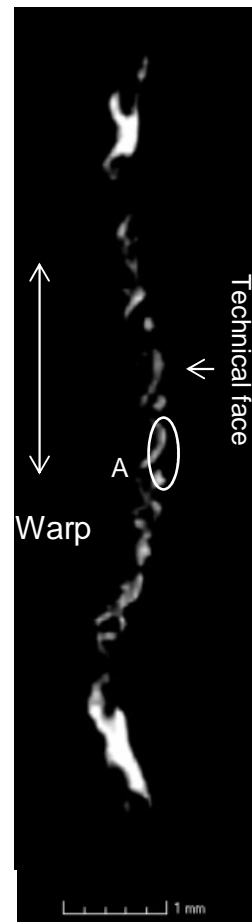


Figure 3-10e: medium calico in the warp direction. 'A' indicates blood-soaked yarns on the technical face of the fabric.

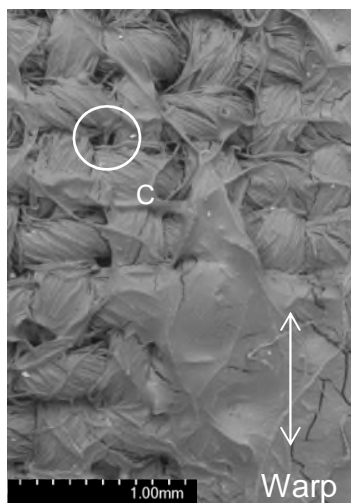


Figure 3-10f: medium calico SEM image at 42x magnification. 'C' is an inter-yarn space.

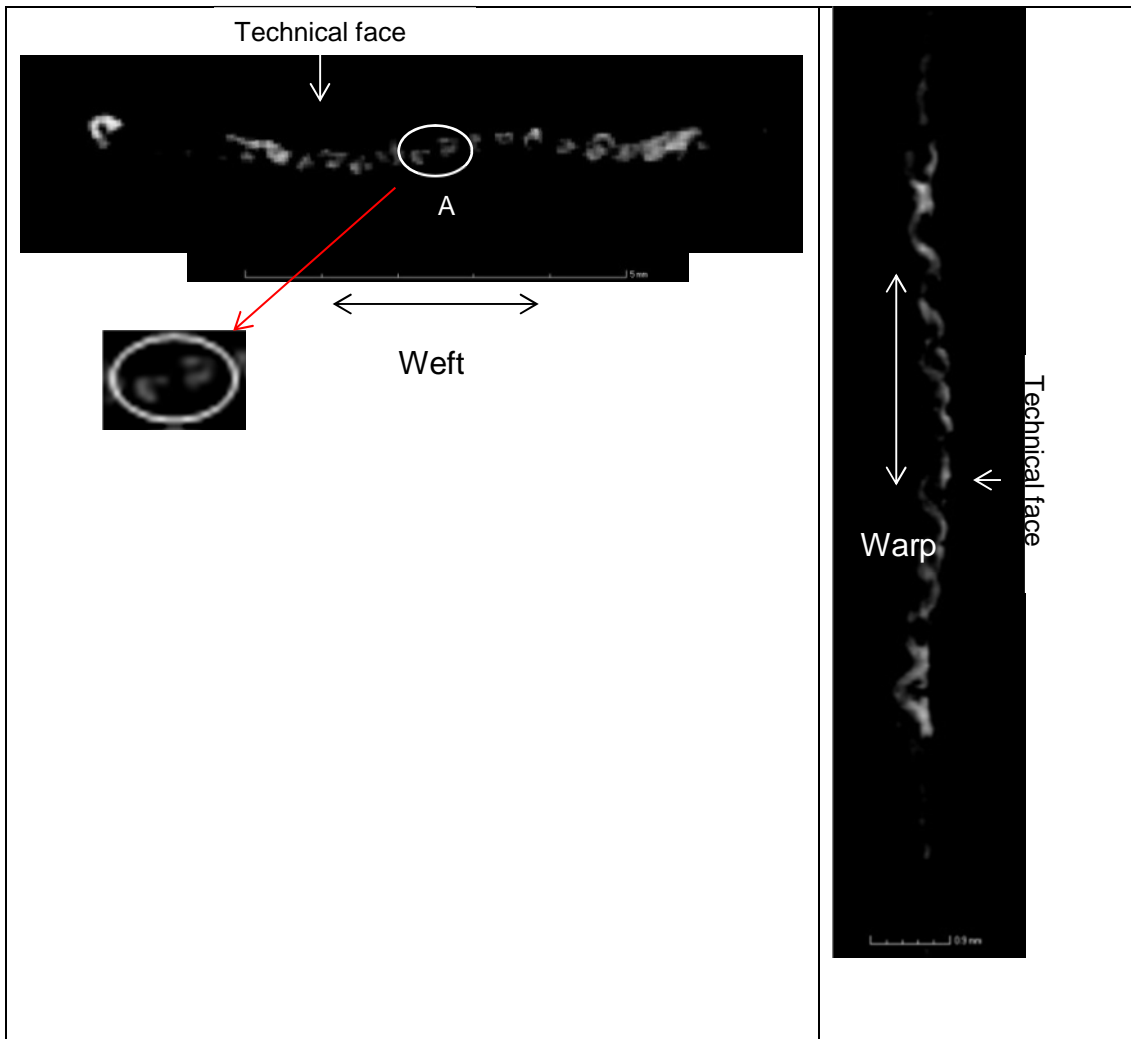


Figure 3-10g: heavy calico in the weft direction. 'A' indicates the iron-rich blood on the warp yarn which has not reached the centre of the yarn.

Figure 3-10h: heavy calico in the warp direction

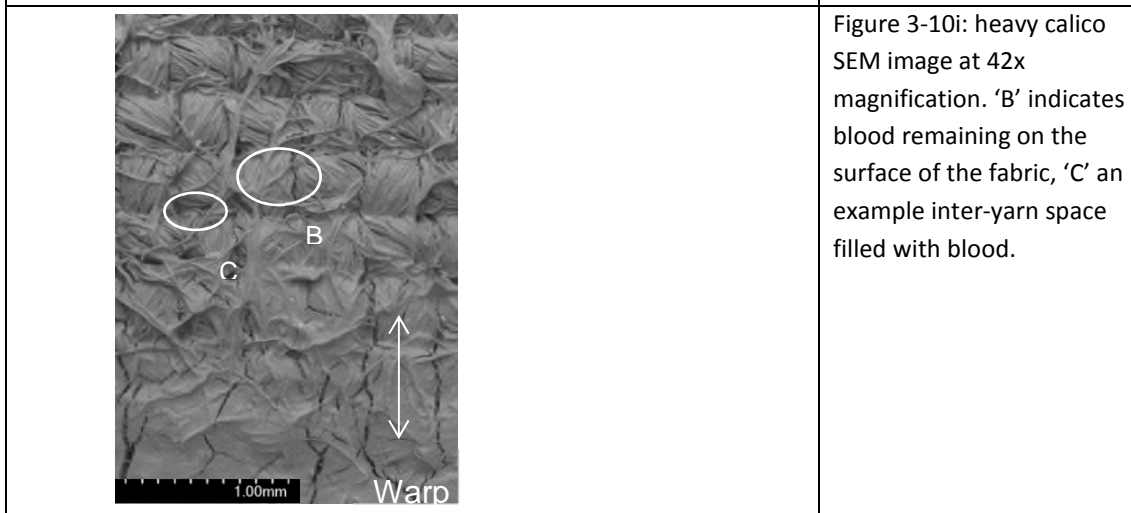


Figure 3-10i: heavy calico SEM image at 42x magnification. 'B' indicates blood remaining on the surface of the fabric, 'C' an example inter-yarn space filled with blood.

Figure 3-10 a typical example of a CT cross section in the warp and weft directions and an SEM image (x 42) on each calico formed at  $4.1 \text{ ms}^{-1}$ .

### 3.6.3 5.1 ms<sup>-1</sup>

5.1 ms<sup>-1</sup> was the only velocity where the largest mean dry bloodstain area was on the medium calico, and the smallest on the light calico (figure 3-3, table 3-4). The difference in mean dry bloodstain area at 5.1 ms<sup>-1</sup> was not statistically significant (the difference between the medium and light calico was only 5 mm<sup>2</sup>).

For all specimens from an impact velocity of 5.1 ms<sup>-1</sup> both the warp (marked 'A') and weft (marked 'B') yarns were almost completely soaked in iron-rich blood (figure 3-11a, b, d, e, g and h). With the increase in velocity to 5.1 ms<sup>-1</sup> the blood penetrated into the yarns at impact, filling the intra-yarn spaces. There was less blood on the surface of the yarns at 5.1 ms<sup>-1</sup> (figure 3-11c, f, i) than at 4.1 ms<sup>-1</sup> (figure 3-10c, f, i), as it was inside the yarns.

On the light calico the mean dry bloodstain area decreased from 48.7 mm<sup>2</sup> at 4.9 ms<sup>-1</sup> to 42.5 mm<sup>2</sup> at 5.1 ms<sup>-1</sup>. The coefficient of variation (CV) for the light calico at 5.1 ms<sup>-1</sup> (8%) was lower than at 4.9 ms<sup>-1</sup> (25%). This was possibly due to a greater amount of wicking at 4.9 ms<sup>-1</sup> increasing the variability in the dry bloodstain area. The amount of wicking in a specimen would be dependent on variations within the fabric and yarns [29] and therefore would differ between specimens. When the area of the bloodstain is more dependent on wicking than on the amount of lateral spreading at impact, greater variability among specimens within that velocity will be seen. The reduced wicking at 5.1 ms<sup>-1</sup>, indicated by less variability among specimens, resulted in the smaller mean dry bloodstain area at this velocity.

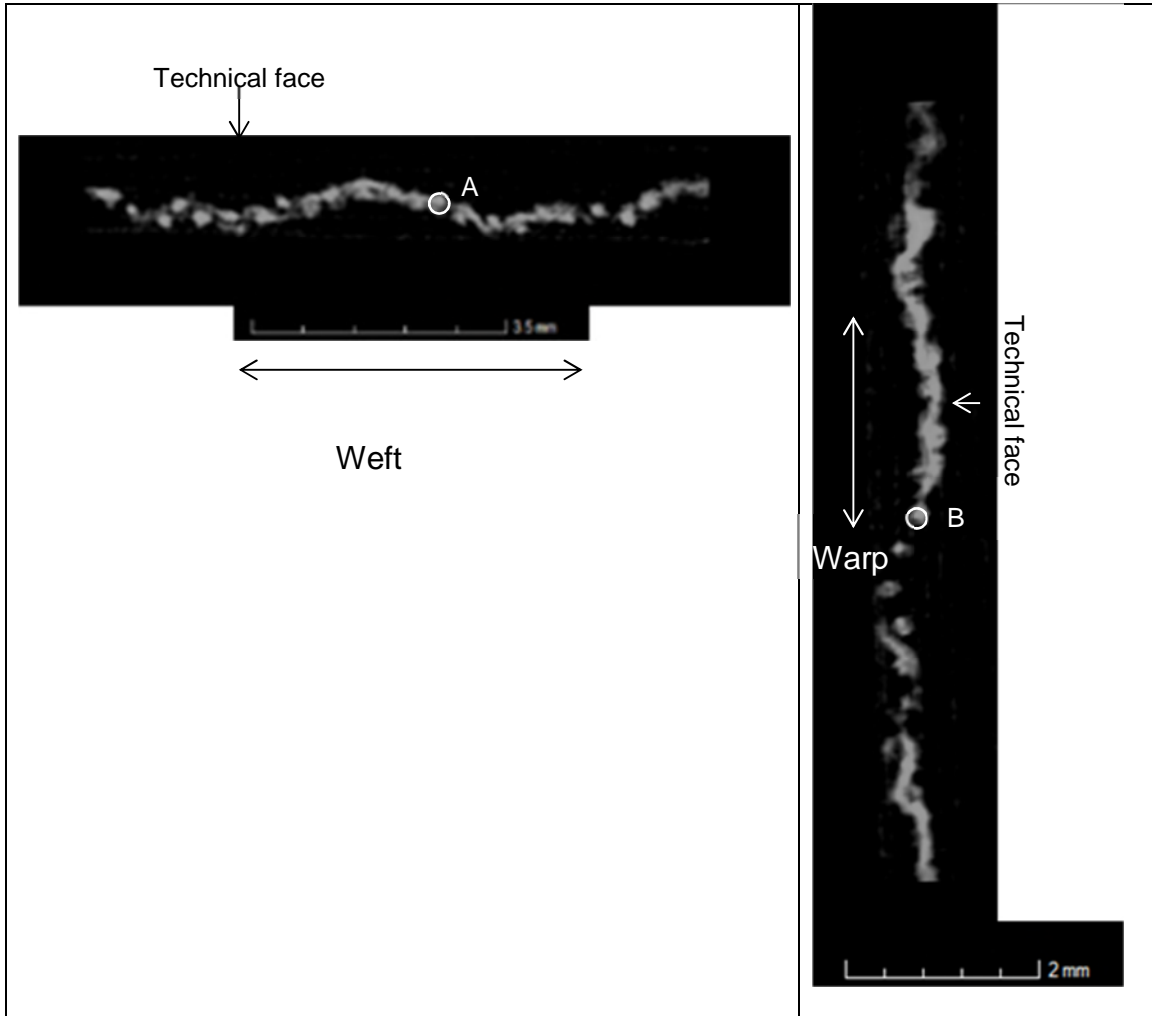


Figure 3-11a: light calico in the weft direction

Figure 3-11b: light calico in the warp direction

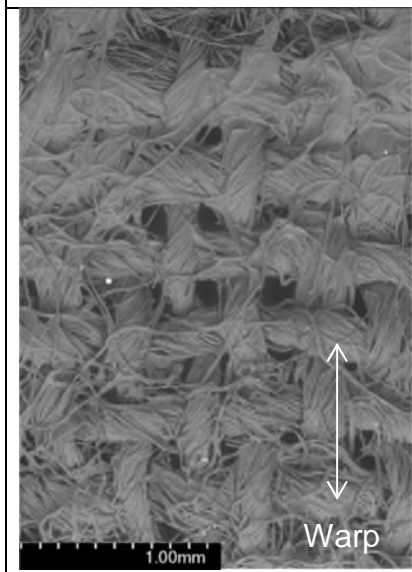
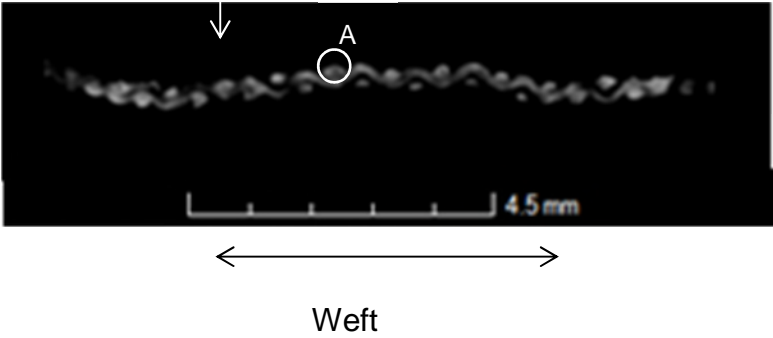
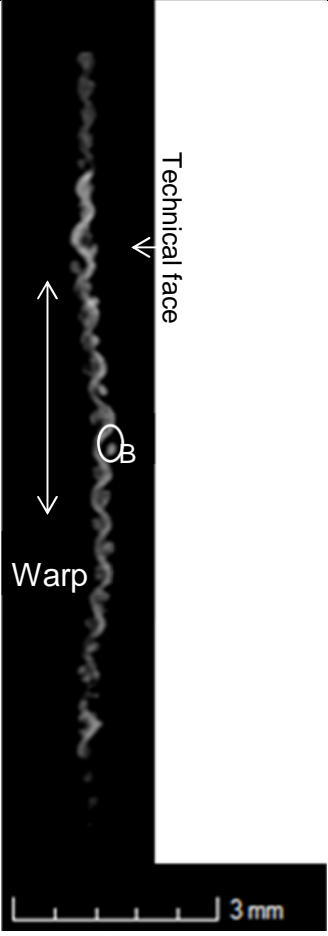
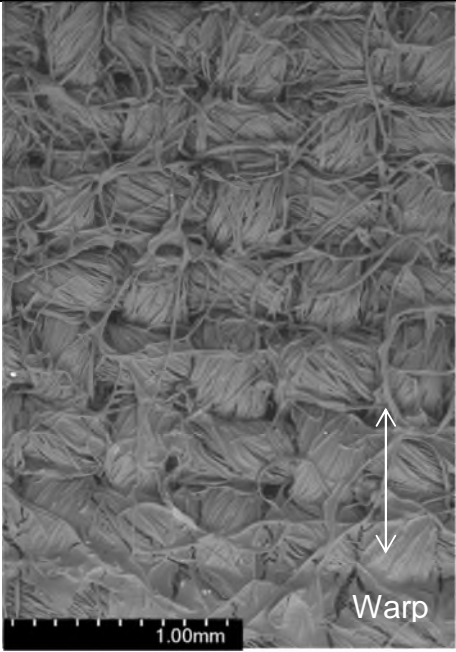


Figure 3-11c: light calico SEM image at 42x magnification

	
<p>Figure 3-11d: medium calico in the weft direction</p>	<p>Figure 3-11e: medium calico in the warp direction</p>
	<p>Figure 3-11f: medium calico SEM image at 42x magnification</p>

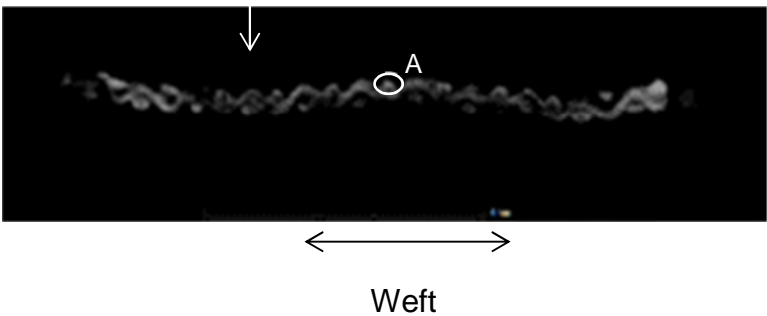
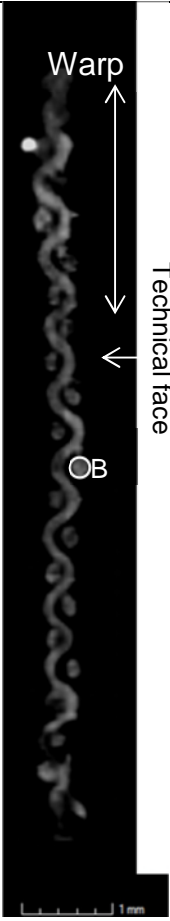
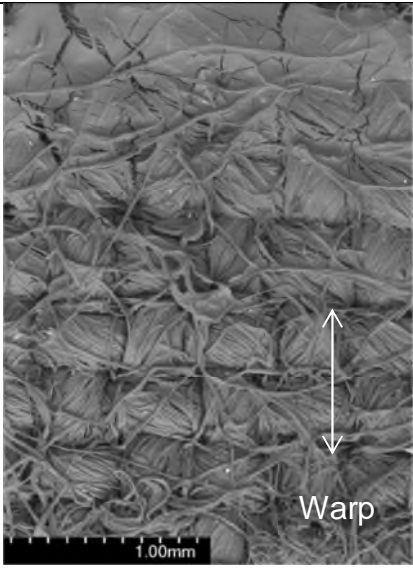
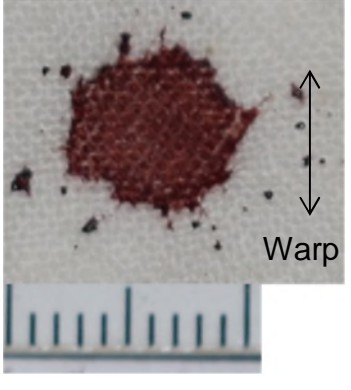
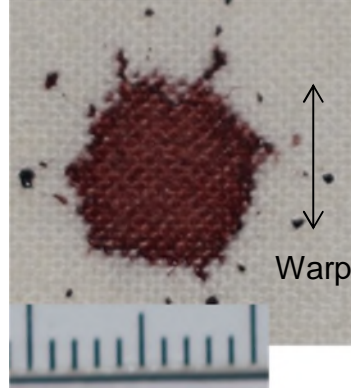
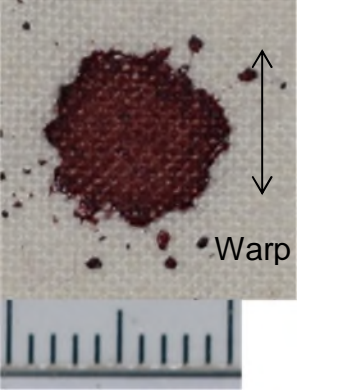
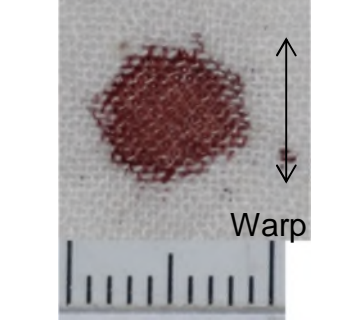
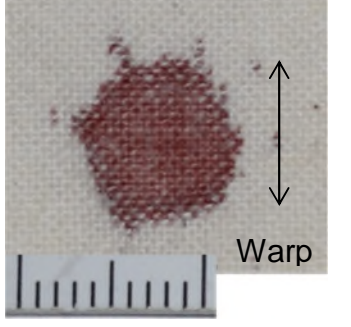
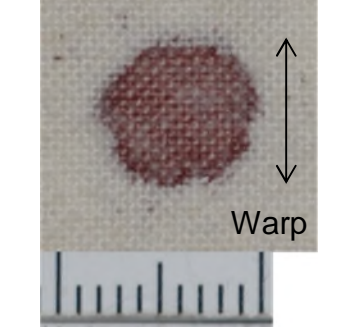
	
<p>Figure 3-11g: heavy calico in the weft direction</p>	<p>Figure 3-11h: heavy calico in the warp direction</p>
	<p>Figure 3-11i: heavy calico SEM image at 42x magnification</p>

Figure 3-11 a typical example of a CT cross section in the warp and weft directions and an SEM image (x42) on each calico formed at  $5.1 \text{ ms}^{-1}$ . 'A' indicates the blood soaked warp yarns, and 'B' the blood soaked weft yarns.



The mean dry bloodstain area on the heavy calico decreased slightly despite the increase in impact velocity from 45.7 mm<sup>2</sup> at 4.9 ms<sup>-1</sup> to 45.5 mm<sup>2</sup> at 5.1 ms<sup>-1</sup>. There is little evidence of dense blood on the surface of the heavy calico in the dry bloodstains (figure 3-12c). This was due to the blood penetrating the yarns rather than remaining on the surface of the fabric. Although the blood was then in the intra-yarn spaces, the high yarn linear density of the heavy calico precluded a large amount of wicking.

The medium calico was the only fabric where the mean dry bloodstain area increased with the increase in velocity from 42.8 mm<sup>2</sup> at 4.9 ms<sup>-1</sup> to 47.5 mm<sup>2</sup> at 5.1 ms<sup>-1</sup>. The CV also increased from 13% to 19% suggesting a greater amount of wicking was occurring, as this would increase the inconsistency of the dry bloodstain area among specimens [29]. The largest technical rear bloodstain on the medium calico was seen on the specimens from a velocity of 5.1 ms<sup>-1</sup> (figure 3-12e). Blood penetrated the yarns through to the technical rear of the medium calico across the entire bloodstain and then wicked along the yarns as the blood was already in the intra-yarn spaces. The lower yarn linear density for the medium than the heavy calico meant more wicking occurred in the former.

		
<p>Figure 3-12a: light calico technical face</p>	<p>Figure 3-12b: medium calico technical face</p>	<p>Figure 3-12c: heavy calico technical face</p>
		
<p>Figure 3-12d: light calico technical rear</p>	<p>Figure 3-12e: medium calico technical rear</p>	<p>Figure 3-12f: heavy calico technical rear</p>

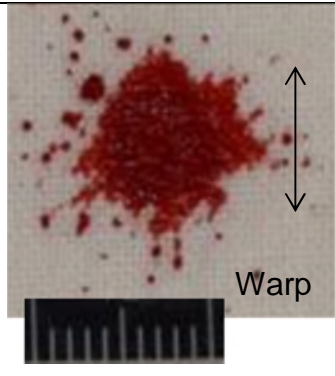
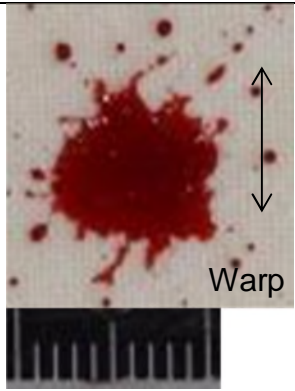
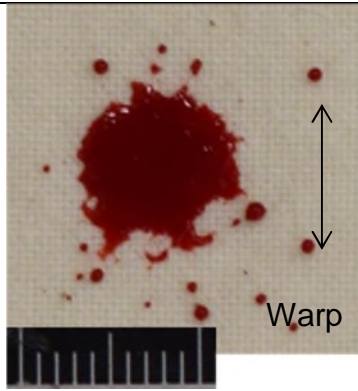
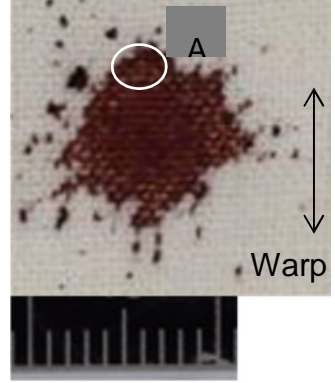
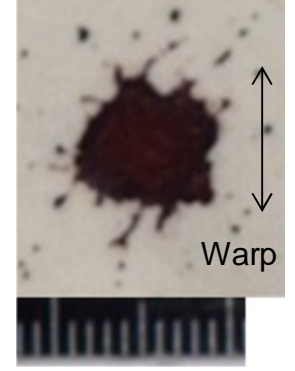
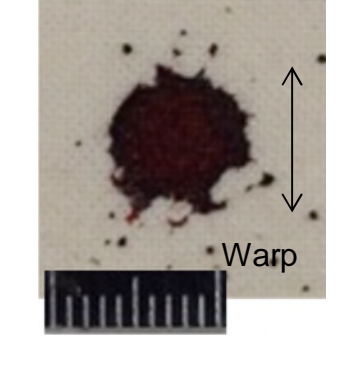
**Figure 3-12 a typical example of a dry technical face and technical rear bloodstain on each calico formed at  $5.1 \text{ ms}^{-1}$ . Scale is 10 mm.**

#### **3.6.4 $5.4 \text{ ms}^{-1}$ :**

The light calico specimens had the largest mean dry bloodstain area and the medium the smallest from a velocity of  $5.4 \text{ ms}^{-1}$  (figure 3-3, table 3-4). The difference in mean dry bloodstain area among fabrics at  $5.4 \text{ ms}^{-1}$  was statistically significantly different ( $F_{2,12} = 9.32, p \leq 0.01$ ). The mean dry bloodstain area for the light calico ( $59.7 \text{ mm}^2$ ) was significantly larger than the medium ( $43.3 \text{ mm}^2$ ). The mean dry bloodstain area for the heavy calico ( $53.5 \text{ mm}^2$ ) was not significantly different.

For the light calico specimens from  $5.4 \text{ ms}^{-1}$ , a large amount of spreading occurred at impact shown in the increase in mean wet bloodstain area from  $43.6 \text{ mm}^2$  at  $5.1 \text{ ms}^{-1}$  to  $64.9 \text{ mm}^2$  at  $5.4 \text{ ms}^{-1}$ . No blood remained pooled on the surface of the light calico specimens from  $5.4 \text{ ms}^{-1}$  impacts (figure 3-13a). A large amount of blood penetrated

through to the technical rear of the fabric (figure 3-13g). Iron-rich blood penetrated through the entire thickness of the warp yarns (figure 3-14a, marked 'A') while only coating the weft yarns (figure 3-14b, marked 'B'). The predilection for the warp yarns owing to their lower linear density (14 compared to 18 tex) can be seen around the edge of the dry technical face (figure 3-13d marked 'A') and technical rear (figure 3-13g marked 'A') bloodstain and the 2D image of the 3D CT reconstruction (figure 3-13j). As the warp yarn on the light calico was soaked in blood it was possible for the blood to wick along the intra-yarn spaces within the yarns, increasing the bloodstain area.

		
<p>Figure 3-13a: light calico wet bloodstain</p>	<p>Figure 3-13b: medium calico wet bloodstain</p>	<p>Figure 3-13c: heavy calico wet bloodstain</p>
		
<p>Figure 3-13d: light calico dry bloodstain. 'A' indicates where the blood has wicked along the warp yarns beyond the edge of the bloodstain.</p>	<p>Figure 3-13e: medium calico dry bloodstain</p>	<p>Figure 3-13f: heavy calico dry bloodstain</p>

<p>Figure 3-13g: light calico technical rear. 'A' indicates where the blood has wicked along the warp yarns beyond the edge of the bloodstain.</p>	<p>Figure 3-13h: medium calico technical rear. 'B' indicates where the blood has penetrated the fabric.</p>	<p>Figure 3-13i: heavy calico technical rear</p>
<p>Figure 3-13j: light calico CT reconstruction</p>	<p>Figure 3-13k: medium calico CT reconstruction</p>	<p>Figure 3-13l: heavy calico CT reconstruction</p>

**Figure 3-13 a typical example of a wet and dry technical face and dry technical rear bloodstain (scale: 10 mm) and 2D of the 3D CT reconstruction on each calico formed at  $5.4 \text{ ms}^{-1}$**

The mean technical rear bloodstain area for the medium calico decreased from  $27.8 \text{ mm}^2$  at  $5.1 \text{ ms}^{-1}$  to  $15.1 \text{ mm}^2$  at  $5.4 \text{ ms}^{-1}$ . However, the specimens from an impact velocity of  $5.4 \text{ ms}^{-1}$  were the only specimens on the medium calico where the blood completely penetrated to the technical rear of the fabric (figure 3-13h, marked 'B'). The blood coated the warp and weft yarns (figure 3-13d and e, marked 'A') rather than penetrating through to the centre of them. Therefore, the blood on the technical rear of the medium calico was forced through the inter-yarn spaces and around the yarns at impact. Some blood also remained pooled on the surface of the medium calico (figure 3-13b). The blood on the surface dried before being able to fully wick into the intra-yarn spaces, therefore reducing the amount of wicking which occurred along

them. The greater yarn twist of the medium than the heavy and the light calicos reduced the ability of the blood to wick into and along the intra-yarn spaces, reducing the dry bloodstain area.

For the heavy, as for the medium calico, iron-rich blood coated both the warp and weft yarns (figure 3-14g and h), although no blood was forced through to the technical rear of the fabric at impact (figure 3-13i). The blood remained more on the surface of the heavy calico than either the medium or light calicos owing to the higher yarn linear density. This is evidenced by a greater amount of iron-rich blood towards the technical face of the fabric in the  $\mu$ CT cross-sections (figure 3-14g and h) and the ring of dense blood which occurred on the surface of the fabric (figure 3-13l). Therefore, with the increase in impact velocity to  $5.4 \text{ ms}^{-1}$  the blood spread laterally across the surface of the heavy calico, as opposed to penetrating through to the technical rear of the fabric as for the medium calico. This resulted in a larger mean dry bloodstain area for the heavy than the medium calico.

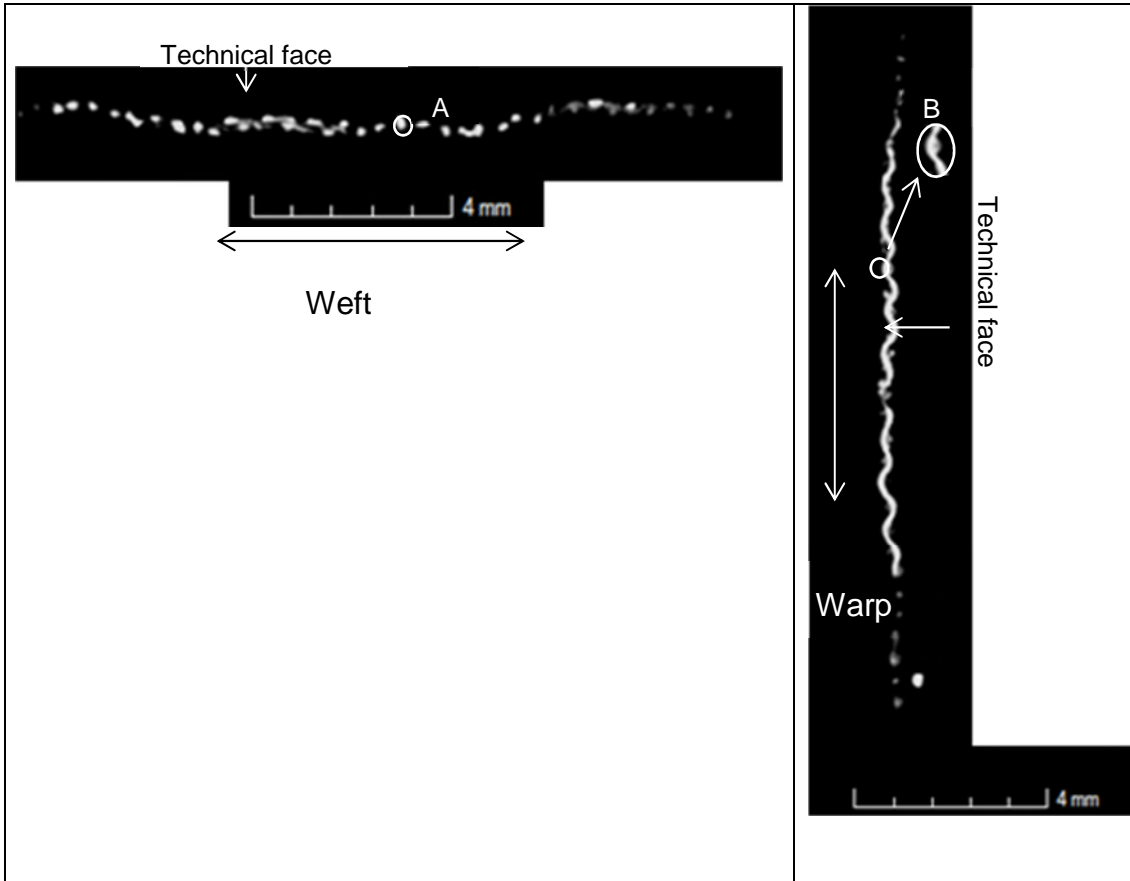


Figure 3-14a: light calico cross section in the weft direction. 'A' indicates a blood-soaked warp yarn.

Figure 3-14b: light calico cross section in the warp direction. 'B' indicates a weft yarn coated in blood.

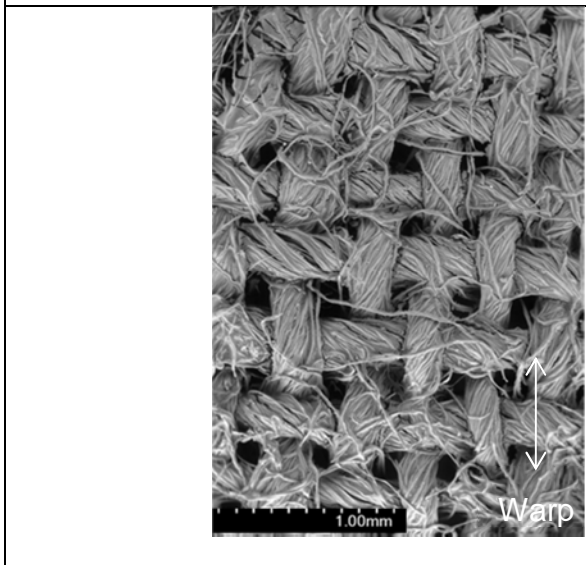


Figure 3-14c: light calico SEM image at 42x magnification

<p>Figure 3-14d: medium calico cross section in the weft direction. 'A' shows a blood-coated warp yarn; the darker circle in the centre indicates where the blood has not penetrated through to the centre of the yarn.</p>	<p>Figure 3-14e: medium calico cross section in the warp direction. 'A' shows a blood-coated weft yarn; the darker circle in the centre indicates where the blood has not penetrated through to the centre of the yarn.</p>
	<p>Figure 3-14f: medium calico SEM image at 42x magnification</p>

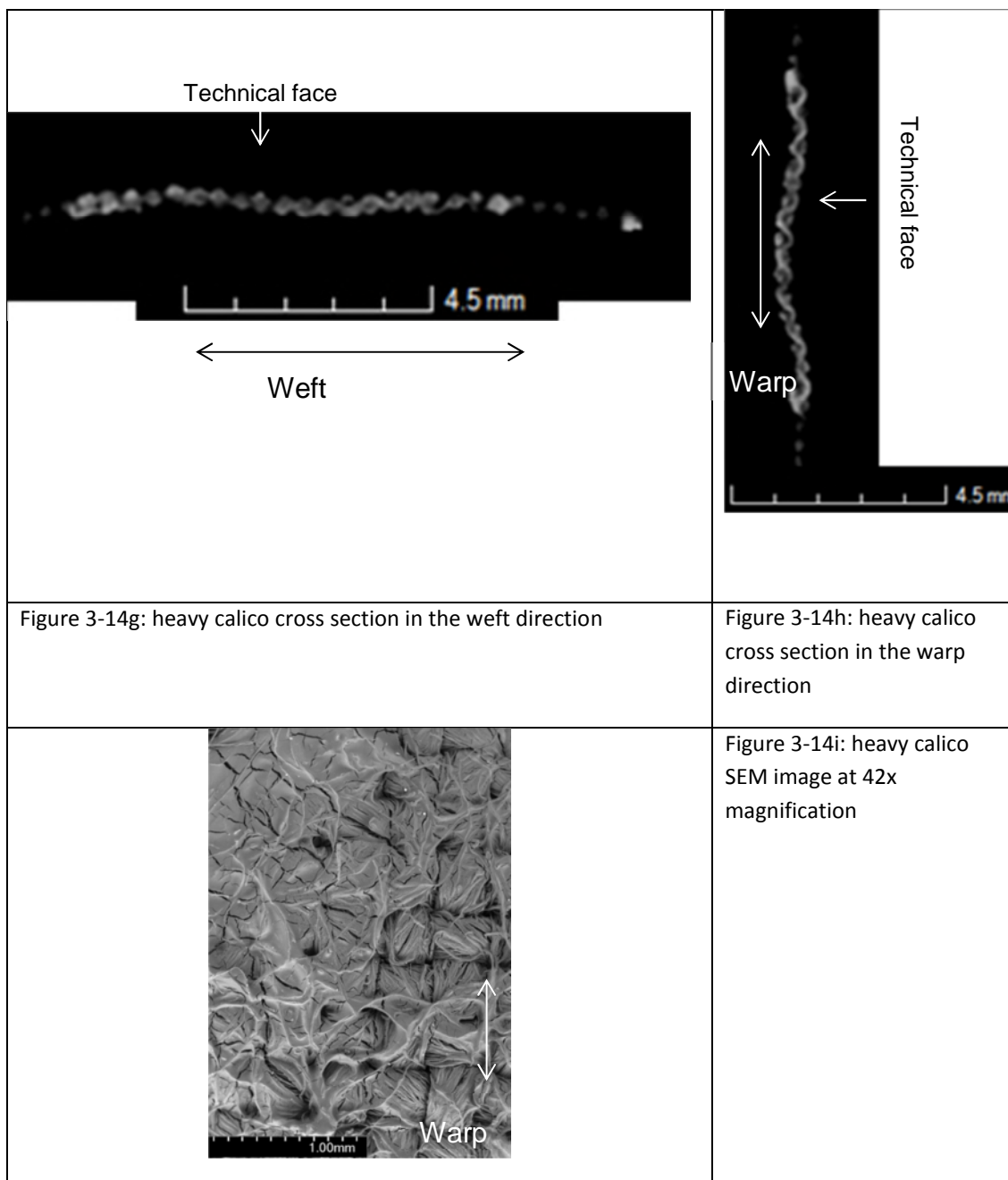


Figure 3-14 a typical example of a CT cross section in the warp and weft directions and an SEM image (x42) on each calico formed at  $5.4 \text{ ms}^{-1}$ .

### 3.7 Conclusions

Passive bloodstains were created on three mass per unit areas (light:  $85 \text{ g/m}^2$ , medium:  $164 \text{ g/m}^2$  and heavy:  $225 \text{ g/m}^2$ ) of 100% cotton plain woven calico. Six drop heights were used, resulting in six impact velocities ( $1.7, 2.9, 4.1, 4.9, 5.1$  and  $5.4 \text{ ms}^{-1}$ ). The use of  $\mu\text{CT}$  enabled the internal structure of the bloodstains to be assessed. This provided an understanding of where the blood was within the bloodstain, and whether



it had penetrated or coated the yarns, which was imperative to understanding the interaction of the blood and the fabric.

The bloodstains varied depending on the type of fabric and the velocity with which the blood impacted. Overall, dry bloodstain area increased with impact velocity, although this was not consistent across all three fabrics. The light calico generally had the largest mean dry bloodstain area but had a lower correlation with velocity. This was due to the low yarn linear density of the light calico which reduced the volume the blood had to fill; therefore the blood wicked further along the yarns. The correlation with velocity was greater for the medium and heavy calicos. Less wicking along the intra-yarn spaces occurred, and so the dry bloodstain area was more dependent on the amount of lateral spreading following impact, which increased with the increase in impact velocity. At a slow impact velocity ( $1.7 \text{ ms}^{-1}$ ) the blood pooled on the surface of the fabric wicked slowly into the warp and weft yarns under gravity, while at a faster impact velocity (e.g.  $4.1 \text{ ms}^{-1}$ ) the particulates were more spread out within the bloodstain, resulting in very different CT scans between fast and slow impact velocities. This is important to note for forensic science, as in some circumstances it may be possible to ascertain something of the area of origin of the bloodstain on the basis of a fast or slow impact velocity.

For forensic science, it is also important to note that fabric mass per unit area needs to be taken into account when analysing bloodstains on fabrics. When comparing bloodstains between two fabrics of identical fibre content and weave structure, the fabric with the lower mass per unit area may produce a larger bloodstain than that of the higher mass per unit area irrespective of the velocity with which the blood impacted.

### **3.8 Ethical Statement**

All applicable international, national and institutional guidelines for the care and use of animals were followed.

### 3.9 References

- [1] S.H. James, P.E. Kish, T.P. Sutton, Principles of Bloodstain pattern analysis: Theory and Practice, CRC Press, Florida, 2005.
- [2] National Research Council, Strengthening Forensic Science in the United States: A Path Forwards, Washington, 2009.
- [3] T. Bevel, R.M. Gardner, Blood Pattern Analysis with an Introduction to Crime Scene Reconstruction, Third Edition, CRC Press, Florida, 2008.
- [4] M.C. Taylor, T.L. Laber, P.E. Kish, G. Owens, N.K.P. Osborne, The Reliability of Pattern Classification in Bloodstain Pattern Analysis, Part 1: Bloodstain Patterns on Rigid Non-absorbent Surfaces, *J. Forensic Sci.* (2016) 1–6. doi:10.1111/1556-4029.13091.
- [5] M.C. Taylor, T.L. Laber, P.E. Kish, G. Owens, N.K.P. Osborne, The Reliability of Pattern Classification in Bloodstain Pattern Analysis, Part 2: Bloodstain patterns on fabric surfaces, *J. Forensic Sci.* 61 (2016) 1461–1466. doi:10.1111/1556-4029.13091.
- [6] B.A.J. Larkin, C.E. Banks, Bloodstain pattern analysis: looking at impacting blood from a different angle, *Aust. J. Forensic Sci.* 45 (2013) 85–102. doi:10.1080/00450618.2012.721134.
- [7] L. Hulse-Smith, M. Illes, A blind trial evaluation of a crime scene methodology for deducing impact velocity and droplet size from circular bloodstains, in: *J. Forensic Sci.*, 2007: pp. 65–69. doi:10.1111/j.1556-4029.2006.00298.x.
- [8] L. Hulse-Smith, N.Z. Mehdizadeh, S. Chandra, Deducing drop size and impact velocity from circular bloodstains, *J. Forensic Sci.* 50 (2005) 54–63. doi:10.1520/JFS2003224.
- [9] C. Knock, M. Davison, Predicting the position of the source of blood stains for angled impacts, *J. Forensic Sci.* 52 (2007) 1044–1049. doi:10.1111/j.1556-

4029.2007.00505.x.

- [10] A. Patnaik, R.S. Rengasamy, V.K. Kothari, A. Ghosh, Wetting and Wicking in Fibrous Materials, *Text. Prog.* 1 (2006) 1–105. doi:10.1533/tepr.2006.0001.
- [11] E. Kissa, Wetting and Wicking, *Text. Res. J.* 66 (1996) 660–668. doi:10.1177/004051759606601008.
- [12] T.C. de Castro, M.C. Taylor, J.A. Kieser, D.J. Carr, W. Duncan, Systematic investigation of drip stains on apparel fabrics: The effects of prior-laundering, fibre content and fabric structure on final stain appearance, *Forensic Sci. Int.* 250 (2015) 98–109. doi:10.1016/j.forsciint.2015.03.004.
- [13] T.C. De Castro, D.J. Carr, M.C. Taylor, J.A. Kieser, W. Duncan, Drip bloodstain appearance on inclined apparel fabrics: Effect of prior-laundering, fibre content and fabric structure, *Forensic Sci. Int.* 266 (2016) 488–501. doi:10.1016/j.forsciint.2016.07.008.
- [14] X. Li, J. Li, S. Michielsen, Effect of yarn structure on wicking and its impact on bloodstain pattern analysis (BPA) on woven cotton fabrics, *Forensic Sci. Int.* 276 (2017) 41–50. doi:10.1016/j.forsciint.2017.04.011.
- [15] L. Dicken, C. Knock, S. Beckett, T.C. de Castro, T. Nickson, D.J. Carr, The use of micro computed tomography to ascertain the morphology of bloodstains on fabric, *Forensic Sci. Int.* 257 (2015) 369–375. doi:10.1016/j.forsciint.2015.10.006.
- [16] B. Karger, S.P. Rand, B. Brinkmann, Experimental bloodstains on fabric from contact and from droplets, *Int. J. Legal Med.* 111 (1998) 17–21. doi:10.1007/s004140050104.
- [17] Y. Cho, F. Springer, F.A. Tulleners, W.D. Ristenpart, Quantitative bloodstain analysis: Differentiation of contact transfer patterns versus spatter patterns on fabric via microscopic inspection, *Forensic Sci. Int.* 249 (2015) 233–240.

doi:10.1016/j.forsciint.2015.01.021.

- [18] M. Holbrook, Evaluation of Blood Deposition on Fabric: Distinguishing Spatter and Transfer Stains, *Int. Assoc. Bloodstain Pattern Anal. News.* 26 (2010) 3–12.
- [19] J. Slemko, Bloodstains on fabric- the effects of droplet velocity and fabric Composition, (1999).
- [20] E.M.P. Williams, M. Dodds, M.C. Taylor, J. Li, S. Michielsen, Impact dynamics of porcine drip bloodstains on fabrics, *Forensic Sci. Int.* 262 (2016) 66–72.  
doi:10.1016/j.forsciint.2016.02.037.
- [21] H.F. Miles, R.M. Morgan, J.E. Millington, The influence of fabric surface characteristics on satellite bloodstain morphology, *Sci. Justice.* 54 (2014) 262–266. doi:10.1016/j.scijus.2014.04.002.
- [22] British Standards Institution, Textiles - Domestic washing and drying procedures for textile testing, BS EN ISO 6330. (2012).
- [23] British Standards Institution, Textiles - Standard atmospheres for conditioning and testing, BS EN ISO 139. (2005).
- [24] British Standards Institution, Textiles - Determination of thickness of textiles and textile products, BS EN ISO 5084. (1997).
- [25] British Standards Institution, Textiles - Woven fabrics - Determination of mass per unit length and mass per unit area, BS 2471. (2005).
- [26] British Standards Institution, Textiles - Woven fabrics - Construction - Methods of analysis Part 2: Determination of the number of threads per unit length, BS EN 1049-2. (1994).
- [27] L. Dicken, C. Knock, D.J. Carr, S. Beckett, Investigating bloodstain dynamics at impact on the technical rear of fabric, (2018) Submitted for publication.
- [28] R.D. Deegan, O. Bakajin, T.F. Dupont, G. Huber, S.R. Nagel, T.A. Witten, Capillary

flow as the cause of ring stains from dried liquid drops, *Nature*. 389 (1997) 827–829. doi:10.1038/39827.

- [29] A.B. Nyoni, D. Brook, Wicking mechanisms in yarns—the key to fabric wicking performance, *J. Text. Inst.* 97 (2006) 119–128. doi:10.1533/joti.2005.0128.
- [30] Metris, CT Pro User Manual, (2008).
- [31] Volume Graphics, VGStudio Max 3.0, (2014).

## **4 Investigating bloodstain dynamics at impact on the technical rear of fabric**

Dicken, L., Knock, C., Carr, D. J., Beckett, S.

Submitted for publication in *Forensic Science International*, July 2018.

### **4.1 Abstract**

Using high speed video, the impact of blood drops falling at three velocities (1.9, 4.2 and 5.8 ms<sup>-1</sup>) were filmed from both the technical face and for the first time the technical rear of three different mass per unit areas (85.1, 163.5 and 224.6 g/m<sup>2</sup>) of 100% cotton calico. It was seen that there were two stages in the creation of a bloodstain on fabric; the impact dynamics, followed by wicking along the intra-yarn spaces. In the first stage, once the blood impacted the fabric, blood was visible on the technical rear of the fabrics with the medium and lightest mass per unit area within as little as 0.067 ms after impact. No blood was visible on the technical rear of the fabric with the heaviest mass per unit area following impact or the medium mass per unit area from 1.7 ms<sup>-1</sup> impacts. On the technical face of the fabric, the blood drop spread laterally and then receded for 8 ms following impact. The dynamics on the technical face were not affected by what was occurring on the technical rear of the fabric. The bloodstain on the technical rear initially only increased until 0.8 ms following impact. The increase in technical rear bloodstain area was caused by continued movement of the blood through to the rear of the fabric as the blood drop spread on the technical face. Once the impact dynamics were concluded within 8 ms of impact, there was no further change in the bloodstain for the remaining 67 ms of high speed video. Following this the blood wicked into and along the yarns, resulting in a dry technical rear bloodstain on all fabrics at all velocities.

### **4.2 Keywords**

- Bloodstain analysis
- High speed video

- Impact dynamics
- Plain woven fabric
- Technical rear

### **4.3 Highlights**

- Blood penetrated to the technical rear of the fabric prior to surface spreading.
- The penetrated blood spread for no more than 0.6 ms after impact.
- Penetration of blood to the technical rear was fabric and velocity dependent.
- Wicking of the blood led to a dry technical rear bloodstain for all fabrics.

### **4.4 Introduction**

In recent years research in blood pattern analysis (BPA) has increased rapidly [1–6]. An area which has been investigated within BPA is the impact dynamics of a blood drop on fabric. When porcine blood was allowed to fall vertically 200 mm onto 100% cotton plain woven and jersey knit fabrics, a number of stages were seen to occur following impact [4]. The drop spread on the surface of the fabric, followed by a crown and ligaments and satellite stains forming. The drop then retracted before stabilising. The drop area remained nearly constant for 0.5 s before increasing again owing to lateral wicking. What was not described in this previous work was what occurred on the technical rear of the fabric, and whether this affected the dynamics on the technical face.

The two most utilised mounting methods within BPA research are either fixing the fabric to a hard surface (such as foam core board) [1,2,4] or mounting the fabric on an embroidery hoop [3,4,7]. Research has shown that the surface on which the fabric is mounted for BPA research affects the impact dynamics of the blood drop, and therefore the resultant dry bloodstain. Passive bloodstains were created by dropping blood from between 100 and 110 cm onto three different fabrics (100% cotton plain woven bed sheeting, technical face and technical rear of cotton single jersey knit t-shirt fabric and 100% cotton denim) [5]. No impact velocities were provided. For a 'hard' surface, the fabrics were placed directly onto a piece of blotting paper on a concrete floor. The 'hard' surface resulted in the drop initially spreading on the surface

of the fabric before retracting and spines and satellite stains forming. The blood then 'wicked' into the textile, merging with many of the surrounding spines and satellite stains [5]. It has been suggested [3] that the use of a hard backing can create capillary bridges of blood between the fabric and the hard surface and affect the wicking pattern.

For a 'semi-hard' surface the woven and knit fabrics were placed on top of denim on the concrete floor. This softened the impact, resulting in fewer satellite stains and spines than for the hard surface. For a taut mounting, the woven and knit fabrics were stretched tautly in an embroidery hoop. The tautness was not measured, even though different levels of stretching could lead to different bloodstains owing to both the tautness of the fabric and the increase in the inter-yarn spaces. The fabrics were draped over the embroidery hoop for a 'loose' mounting. For a 'taut' mounting, some of the impacting blood was seen to bounce off the fabric, altering the bloodstain. This has also been reported to occur when fabrics were mounted on foam core board [8]. For the 'loose' mounting the fabric deformed and absorbed much of the kinetic energy, resulting in very few spines and satellite stains. In this previous work [5] bloodstains which resulted on the opposite side of the fabric to that impacted were not described, and only mentioned in terms of blood passing through the fabric resulting in bloodstains on the backing material.

The impact dynamics on the technical face of the fabric are well understood [4,8]. However, how the impact dynamics are affected by what is occurring on the technical rear of the fabric is not as well understood. The aim of the current work is to determine what dynamics occur on the technical rear of the fabric as the blood impacts the technical face. Two high speed cameras were used in this work to simultaneously video the technical face and technical rear of the fabrics.



## 4.5 Materials and methods

### 4.5.1 Materials

Three calico fabrics (100% cotton, plain woven) were chosen for the experiments (85.1 g/m<sup>2</sup> (light), 163.5 g/m<sup>2</sup> (medium) and 224.6 g/m<sup>2</sup> (heavy)). The fabric specimens were prepared as per [8]. Briefly, the fabrics were made dimensionally stable by laundering six times [9] before line drying and pressing to remove creases. The fabrics were cut into 100 x 100 mm specimens [10] which were then conditioned for 24 hours at 20 ± 2 °C and 65 ± 4 % relative humidity [11].

Fabric thickness [12], mass per unit area [13] and sett [14] were measured. Yarn linear density was estimated by the removal of ten 1m long yarns from the fabric and weighing them using an Oxford A2204 balance accurate to four decimal places (table 4-1) (appendix C).

	Light calico		Medium calico		Heavy calico	
Thickness (mm)	0.38 ± 0.03		0.46 ± 0.02		0.56 ± 0.03	
Mass per unit area (g/m <sup>2</sup> )	85.1 ± 1.54		163.5 ± 2.26		224.61 ± 1.56	
Sett (yarns per 10 mm)	27 x 23		25 x 26		26 x 26	
Yarn type <sup>16</sup>	Ring spun		Ring spun		Ring spun	
	Warp:	Weft:	Warp:	Weft:	Warp:	Weft:
Twist (turns per m) <sup>1</sup>	650	650	756	756	650	624
Linear density (tex)	14	18	33	31	43	47

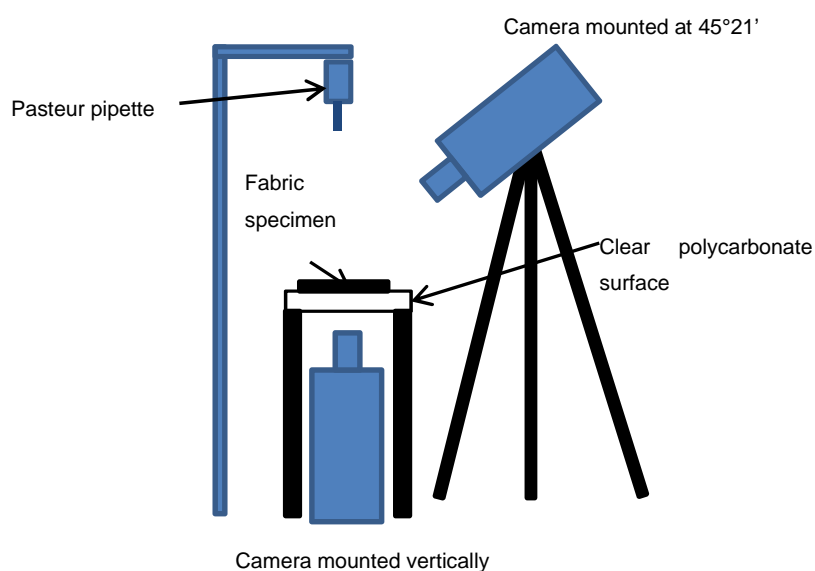
**Table 4-1 mean fabric properties and standard deviations where available (n = 5).**

<sup>16</sup> Yarn type and twist were provided by the fabric company; Whaleys Bradford Ltd, Harris Court, Great Horton, Bradford, West Yorkshire, BD7 4EQ <http://www.whaleys-bradford.ltd.uk>

Defibrinated horse blood was sourced from Southern Group Laboratory<sup>17</sup> to create the bloodstains. The blood was stored below 4°C, and was used within one week of delivery.

#### 4.5.2 Methods

A diagram of the set-up of the cameras and fabric specimen is given in figure 4-1. A phantom V12 high-speed video was mounted vertically beneath a stand with a clear polycarbonate surface. A second high-speed video, a Phantom V7, was mounted above the surface at an angle of 45°21'. This allowed simultaneous filming of the face and rear of the drop as it impacted the surface. The cameras were connected to the same trigger so both would trigger at the same time.



**Figure 4-1 camera set-up**

The camera settings are given in table 4-2. The frame rate for the technical rear was a multiple of the technical face so that frames from the two resulting videos could be matched to compare the bloodstain on the technical rear to that on the technical face. Between 90 and 100 ms of high-speed video was saved for each impact.

<sup>17</sup> E-H Cavendish Courtyard, Sallow Road, Weldon North Industrial Estate, Corby, Northants.  
[www.sglab.co.uk](http://www.sglab.co.uk)

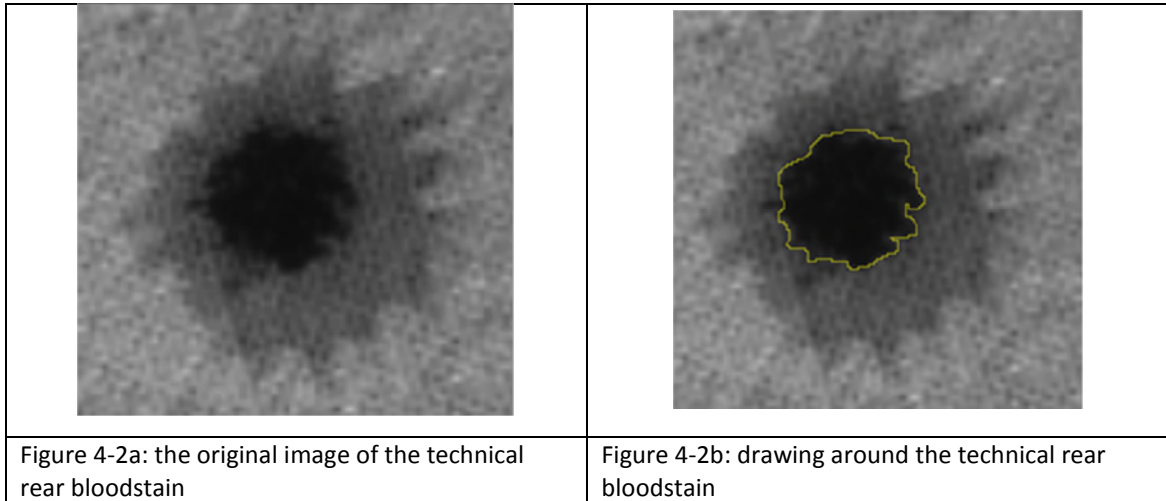
	V12 (technical rear)	V7 (technical face)
Resolution	512 * 512	512 * 512
Frame rate (frames per second)	15000	5000
Exposure ( $\mu$ s)	60	80

**Table 4-2 the setting for the high speed cameras.**

In order to simulate body temperature, the horse blood was heated in a water bath to 37°C. The calico was placed on the clear polycarbonate surface above the phantom V12 camera before bloodstains were created by dropping the blood vertically using a Pasteur pipette. Three different heights were used; 200 mm, 1000 mm and 2000 mm. The resulting high-speed video was analysed using Phantom Camera Control software<sup>18</sup> to measure the impact velocity and drop diameter. The mean drop diameter was  $3.8 \pm 0.17$  mm, cross-sectional area was  $11.3 \text{ mm}^2$ . The velocities were  $1.9 \pm 0.06 \text{ ms}^{-1}$ ,  $4.2 \pm 0.06 \text{ ms}^{-1}$  and  $5.7 \pm 0.07 \text{ ms}^{-1}$ . Five repeats were done at each height on each fabric, resulting in a total of 45 specimens. The areas of the technical rear bloodstains 1 ms after impact were obtained by drawing around the visible bloodstain using the freehand drawing tool in ImageJ<sup>19</sup> (figure 4-2) (appendix D). The dry technical face and technical rear bloodstains were measured using the inbuilt tools in ImageJ.

<sup>18</sup> <https://www.phantomhighspeed.com/resourcesandsupport/phantomresources/pccsoftware> page accessed 27<sup>th</sup> September 2018.

<sup>19</sup> ImageJ is a public domain Java image processing programme <https://imagej.nih.gov/ij/> page accessed 27<sup>th</sup> September 2018.

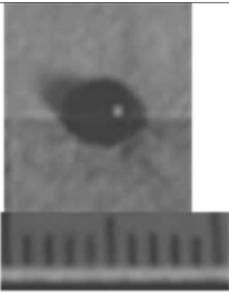
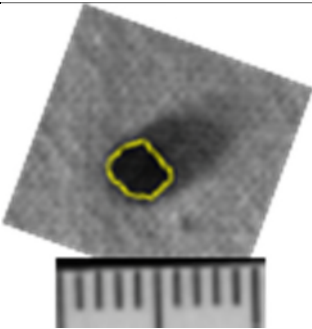
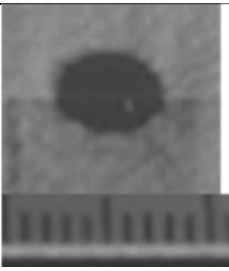
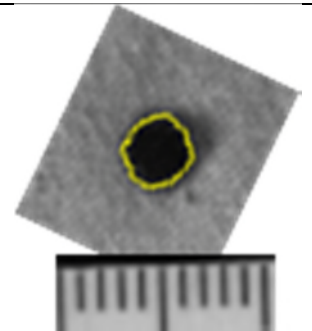
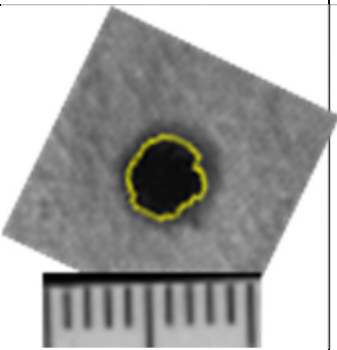


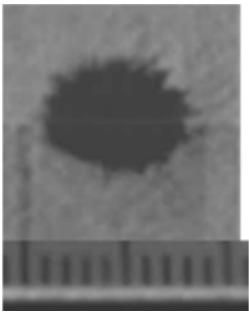
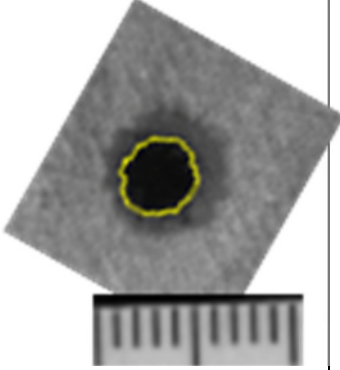
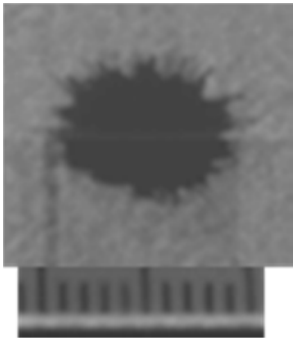
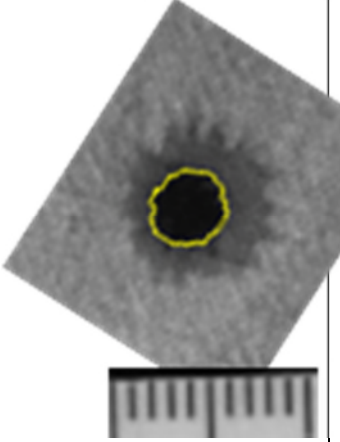
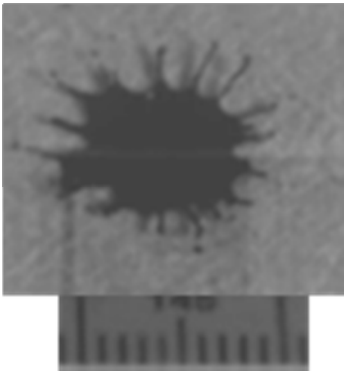
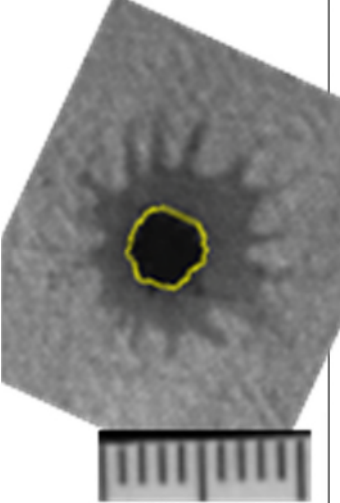
**Figure 4-2 measuring the area of an example technical rear bloodstain image. The darkest central area is where the blood has passed through to the technical rear of the fabric, while the light surrounding area is blood on the surface of the fabric.**

## 4.6 Results

### 4.6.1 Impact dynamics

Example high-speed video stills of the technical face and technical rear from a drop impacting the light calico at  $4.2 \text{ ms}^{-1}$  are given in figure 4-3. The marked area was where the blood was visible on the technical rear of the fabric, and is the area measured in figure 4-2b. Surrounding this, the blood which was spreading on the technical face of the fabric can be seen.

Time following when impact can be seen on the technical face	Technical face	Technical rear with blood which has passed through the fabric indicated	Technical rear bloodstain area
Impact visible on technical face			7 mm <sup>2</sup>
0.2 ms			16 mm <sup>2</sup>
0.335 ms			21 mm <sup>2</sup>

0.6 ms			21 mm <sup>2</sup>
1 ms			21 mm <sup>2</sup>
2 ms			21 mm <sup>2</sup>

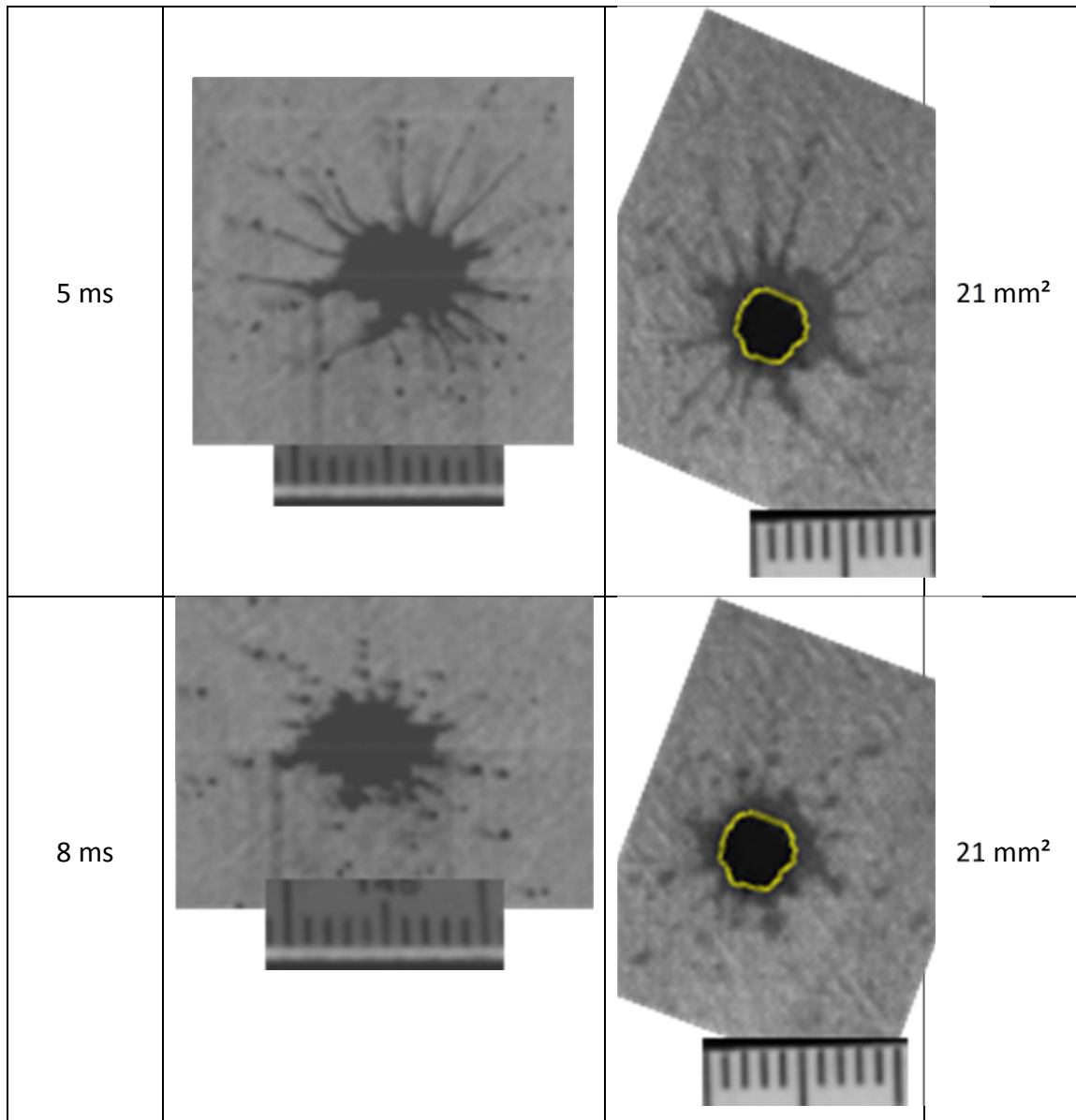


Figure 4-3 impact stages on the technical face and technical rear of the light calico of a single specimen from  $4.2 \text{ ms}^{-1}$ . The technical face and technical rear bloodstains are orientated to the same angle but appear as mirror images owing to being filmed from the top and bottom respectively. The additional technical rear image at 0.335 ms is between two technical face frames. Scale is 20 mm.

On the technical face of the fabric by 0.2 ms the blood drop was spreading laterally in all directions across the surface of the fabric (figure 4-3). By 1 ms following impact (figure 4-3) ligaments began to form, which continued to grow until 5 ms. At this point the main bloodstain began to retract, with satellite stains breaking off from the end of the ligaments. By 8 ms (figure 4-3) the blood drop settled, with spines and satellite stains formed around the edge of the bloodstain. For the following 67 ms of high speed video there was no further change in the technical face bloodstain. From this

point, previous work [4] has indicated the blood may wick along the yarns, further increasing the bloodstain area.

On the technical rear of the fabric, the frame speed for the high speed camera was faster than for the technical face, every 0.067 ms compared to every 0.2 ms for the technical face camera. On the example specimen shown in figure 4-3, blood appeared on the technical rear of the fabric in the high-speed video on the frame prior to the frame when impact could be seen in the technical face video. If impact occurred at the earliest point between the two frames on the technical face camera, the time for the blood to reach the technical rear of the fabric may have taken up to 0.134 ms. This was not consistent across all specimens. On the light calico, the longest potential time from impact to blood appearing on the technical rear was between 0.5 ms and 0.7 ms.

The amount of blood on the technical rear of the fabric increased from 8 mm<sup>2</sup> to 21 mm<sup>2</sup> by 0.335 ms after impact (figure 4-3). This occurred as the blood on the technical face of the fabric spread laterally. The longest time taken for a technical rear bloodstain to reach maximum area was 0.8 ms, which was a medium calico specimen. Following this, although the blood on the surface of the fabric was still spreading and retracting, there was no further increase in the size of the bloodstain on the technical rear in the remaining 45 ms of high speed video.

#### **4.6.2 Effect of fabric mass per unit area**

An example technical rear bloodstain for each fabric at each velocity is shown in figure 4-4. This shows that the amount of blood which was visible on the technical rear of the fabric 1 ms after impact varied depending on the mass per unit area of the fabric and the impact velocity of the blood drop.



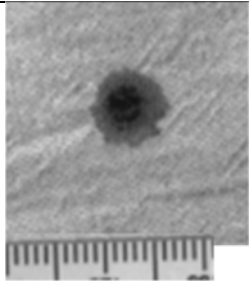
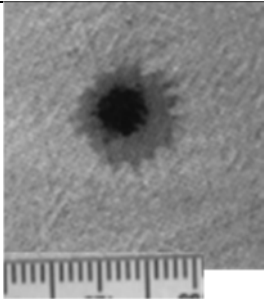
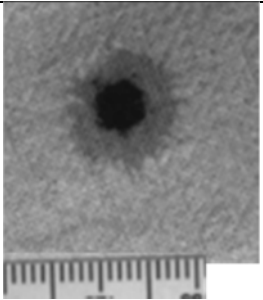
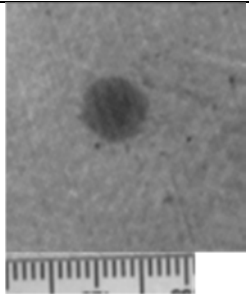
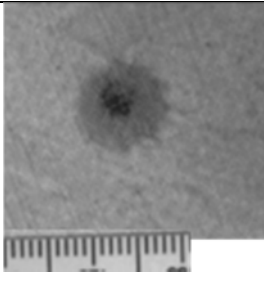
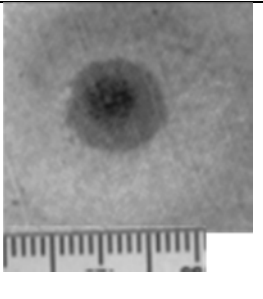
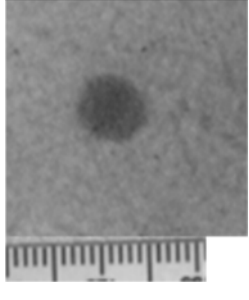
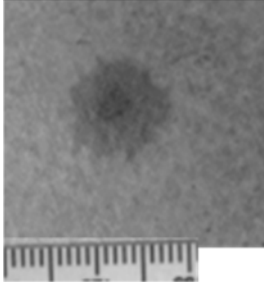
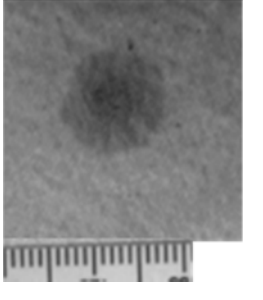
	1.9 ms <sup>-1</sup>	4.2 ms <sup>-1</sup>	5.8 ms <sup>-1</sup>
Light			
Mean technical rear bloodstain area	7.2 mm <sup>2</sup>	18.6 mm <sup>2</sup>	21.1 mm <sup>2</sup>
Medium			
Mean technical rear bloodstain area	0 mm <sup>2</sup>	7.2 mm <sup>2</sup>	12.6 mm <sup>2</sup>
Heavy			
Mean technical rear bloodstain area	0 mm <sup>2</sup>	0 mm <sup>2</sup>	0 mm <sup>2</sup>

Figure 4-4 a typical example of a high speed video still from each fabric and each velocity from 1 ms after impact. The light areas surrounding the darker technical rear bloodstains is the blood on the surface of the fabric, which can be seen from the technical rear. Scale is 2 cm.

For the light calico, blood was visible on the technical rear of the fabric at all three velocities (figure 4-4) on the high speed video. For the slowest velocity (1.9 ms<sup>-1</sup>) blood was visible on the technical rear of the fabric, for only four out of the five specimens, by between 0.2 to 0.67 ms following impact. For the fastest velocity (5.8 ms<sup>-1</sup>), blood was visible on the technical rear between 0.067 ms and 0.268 ms. The mean technical

rear bloodstain was statistically significantly smaller ( $F_{2, 12} = 22.89, p \leq 0.01$ ) for the specimens from  $1.9 \text{ ms}^{-1}$  ( $7.2 \text{ mm}^2$ ) than for the other two velocities ( $4.2 \text{ ms}^{-1}$ :  $18.6 \text{ mm}^2$ ;  $5.8 \text{ ms}^{-1}$ :  $21.1 \text{ mm}^2$ ).

For the medium calico the amount of blood which was visible on the technical rear of the fabric by 1 ms after impact increased with the increase in impact velocity (figure 4-4). The mean technical rear bloodstain area from  $4.2 \text{ ms}^{-1}$  was statistically significantly smaller than that from  $5.8 \text{ ms}^{-1}$  ( $t_8 = -3.211, p \leq 0.05$ ). From  $4.2 \text{ ms}^{-1}$ , blood was visible on the technical rear by between 0.268 to 0.469 ms following impact. For the fastest velocity ( $5.8 \text{ ms}^{-1}$ ) blood was visible by between 0.067 and 0.335 ms, with just one specimen taking 0.67 ms. The technical rear bloodstains were patchier for the medium calico than the light calico (figure 4-4), as blood did not reach the technical rear of the medium calico across the entire bloodstain.

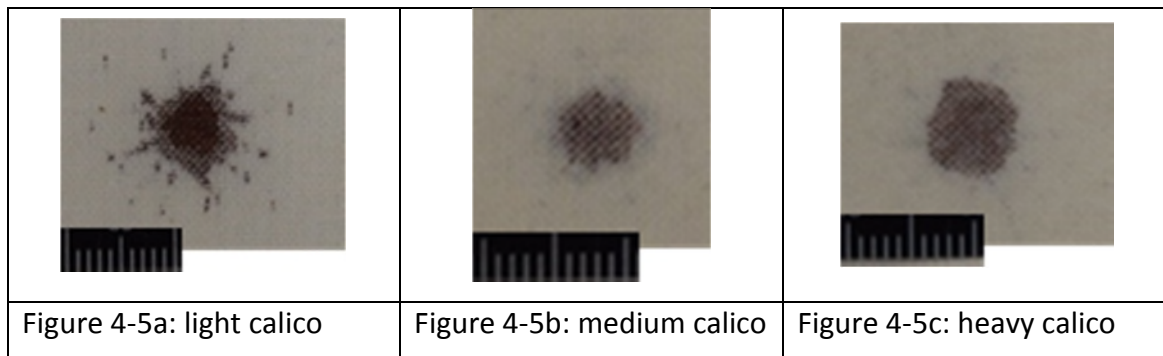
For the heavy calico, no blood was visible on the technical rear of the fabric within the high speed video for any of the three impact velocities (figure 4-4). Although there is a small area of slightly darker blood visible in the centre of the heavy calico video stills, this appears to be where blood has penetrated into the fabric, but not all the way through to the technical rear.

#### **4.6.3 Dry technical face and technical rear area**

The mean dry technical face and technical rear bloodstain areas for all three fabrics and velocities are given in table 4-3. Both the mean dry technical face and dry technical rear bloodstain areas for all three fabrics increased with velocity. At all velocities, the light calico had the largest mean dry technical face and technical rear bloodstains, and the medium had the smallest. An example dry technical rear bloodstain for each fabric from  $4.2 \text{ ms}^{-1}$  is given in figure 4-5.

Velocity (ms <sup>-1</sup> )	Dry bloodstain areas (mm <sup>2</sup> )					
	Light calico		Medium calico		Heavy calico	
	Technical face	Technical rear	Technical face	Technical rear	Technical face	Technical rear
1.9	39.4 ± 8.2	37.3 ± 8.7	20.5 ± 2.9	6.7 ± 4.4	29.7 ± 7.1	15 ± 9.2
4.2	57.9 ± 8.6	52 ± 9.9	36.7 ± 3.5	14.6 ± 8.1	51.3 ± 8.4	23.3 ± 7.7
5.8	70.4 ± 12.6	58.3 ± 8.5	49.3 ± 3.4	28.9 ± 2.7	58.9 ± 8.2	37.2 ± 5.3

**Table 4-3** the mean and standard deviation dry technical face and technical rear bloodstains for all fabrics and velocities.



**Figure 4-5** an example dry technical rear bloodstain on each fabric from 4.2 ms<sup>-1</sup>. Scale is 1cm.

## 4.7 Discussion

The technical face and technical rear of three mass per unit areas of fabric were filmed using high speed video during blood drop impacts at three impact velocities. This was undertaken in an attempt to improve understanding of what was happening on the technical rear of the fabric, while the blood drop was spreading and receding on the technical face.

The impact dynamics on the technical face of the fabric in the current work agreed with those seen in previous work [4] (figure 4-6). Briefly, the blood drop spread on the surface of the fabric, a crown formed and broke up into ligaments and satellites, before the drop retracted. However, the only mention in Williams et al. [4] of what

may have occurred on the technical rear of the fabric was when a blood drop was allowed to fall 10 mm onto 100% cotton plain woven and single jersey fabrics. Very little wicking was seen to occur in the first 500 ms following impact [4]. The suggested reason for this was the time taken for penetration of the blood into the fabric prior to any in-plane wicking occurring. However, this was only mentioned when the blood drop impacted with very little velocity, and not in terms of the greater velocities also investigated in this previous work.

Penetration is used to describe the movement of blood vertically from the technical face to the technical rear of the fabric. On the light calico, blood had penetrated through to the technical rear of the fabric by as little 0.067 ms after impact, as shown in the timeline (figure 4-6). During the first 0.335 ms the technical rear bloodstain increased in area as the blood spread laterally on the technical face (figure 4-3, 4-6). The penetration of the blood caused the initial increase in bloodstain area on the technical rear, which always remained smaller than the technical face bloodstain (figure 4-3) on this particular fabric. From an impact velocity of  $1.9 \text{ ms}^{-1}$ , the mean technical rear bloodstain area on the light calico 1 ms after impact (figure 4,  $7.2 \text{ mm}^2$ ) was smaller than that of the cross-sectional area of the impact drop ( $11.3 \text{ mm}^2$ ). Therefore, the blood was only able to penetrate where the volume of blood was at its greatest. As the velocity increased, although the mean technical rear bloodstain area increased beyond that of the cross-sectional area of the blood drop, the area of the technical rear bloodstain only increased for the first 0.335 ms following impact (figure 4-3, 4-6). As the blood spread laterally across the surface of the fabric there was no longer enough volume for the blood to penetrate to the technical rear of the fabric, therefore no further increase in technical rear bloodstain area was seen at this point.

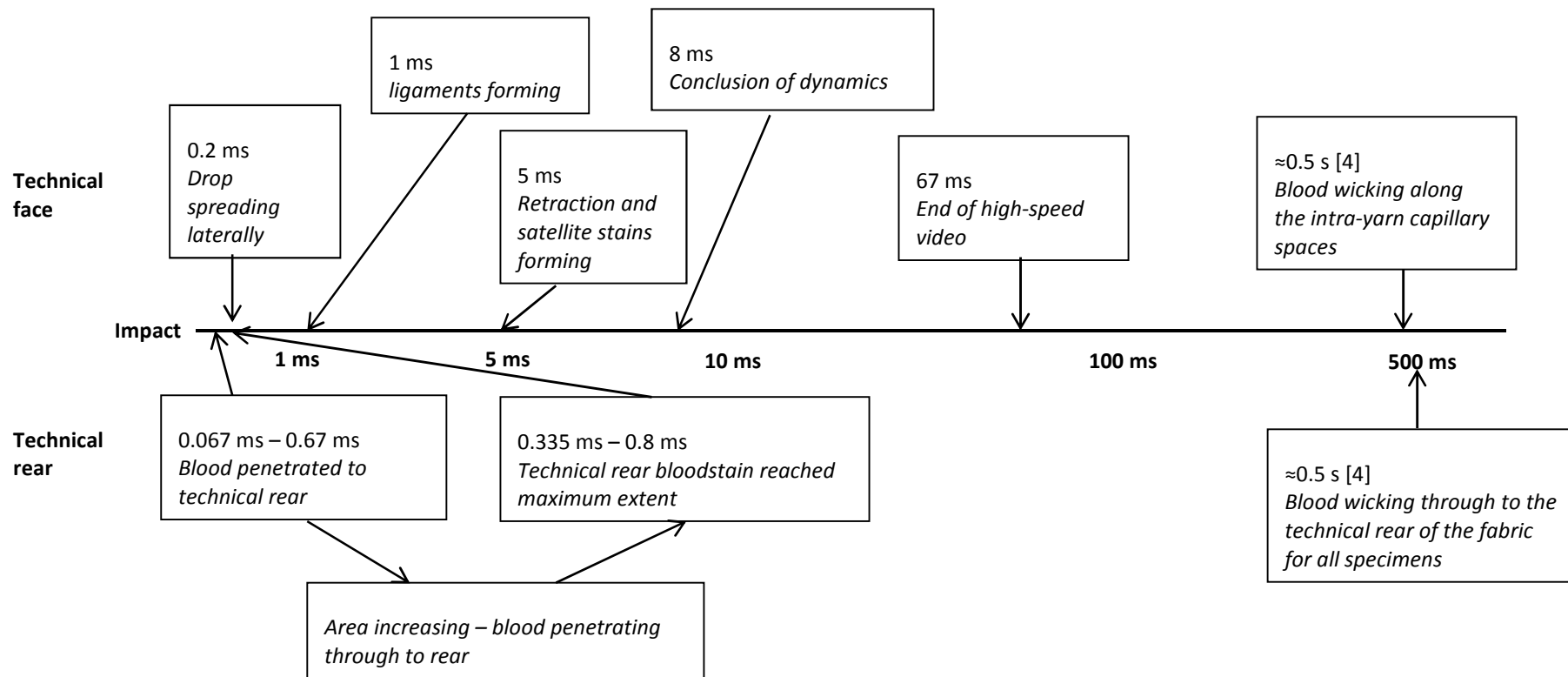


Figure 4-6 a timeline of what dynamics occurred following drop impact.

Whilst the technical rear bloodstain had ceased to spread by no later than 0.8 ms following impact, the blood on the technical face of the bloodstain continued to spread, before retracting and producing satellite stains and spines. The drop impact dynamics on the technical face of the fabric did not conclude until 8 ms (figure 4-6). For the following 67 ms of high speed video there was no further change in the bloodstain. Following this lateral wicking along the yarns occurred (figure 4-6).

It has previously been suggested [3,4] that blood on the technical rear of a fabric on a hard surface spreads independently of the blood on the technical face. The movement of blood on the technical rear of the fabric is caused by pooling and spreading on the hard surface, before wicking back into the fabric. This phenomenon has been mentioned as a reason for not using a hard backing in blood pattern research. During the initial penetration of the blood through to the technical rear, the period of time over which the technical rear blood was increasing (up to the first 0.8 ms after impact), compared to the length of time over which the impact dynamics on the technical face were occurring (8 ms) suggests that the effect on the technical face bloodstain would be minimal. Following this, wicking did increase the technical rear bloodstain area. Looking at figure 4-5a, the area in the centre of the bloodstain is a solid bloodstain, where the blood penetrated through to the technical rear of the fabric at impact. The area surrounding this is where the blood wicked along the yarns, primarily the warp yarns, increasing the technical rear bloodstain area. Any wicking which did occur on the technical rear was therefore movement along the yarns, rather than movement back from the hard surface beneath.

The amount of blood which penetrated through to the technical rear of the fabric was both fabric and velocity dependent (figure 4-4). The penetration through to the technical rear of the fabric at impact occurred to the greatest extent on the light calico owing to the low yarn linear density (14 and 18 tex) leading to a thin fabric (0.38mm) with large inter-yarn spaces. The blood therefore could easily penetrate both the inter-yarn spaces and the yarns. For the light calico, the mean dry technical rear areas (37.3,

52 and 58.3 mm<sup>2</sup>, table 4-3) were larger than those measured 1 ms following impact (7.2, 18.6 and 21.1 mm<sup>2</sup>, figure 4-4) as the blood wicked along the yarns.

The medium calico had a greater yarn linear density (33 and 31 tex) than the light calico, resulting in a thicker fabric (0.46mm) with smaller inter-yarn spaces, reducing the ease with which the blood could penetrate to the technical rear of the fabric. At 1.9 ms<sup>-1</sup>, the blood drop did not penetrate to the technical rear, as there was not enough kinetic energy at impact to force the blood into the inter-yarn spaces (figure 4-4). From 4.2 ms<sup>-1</sup> and 5.8 ms<sup>-1</sup> the increase in kinetic energy at impact forced a small amount of blood to penetrate to the technical rear of the fabric (figure 4-4). The greater yarn linear density and higher twist (756 turns per metre) of the medium than the light calico also reduced the ease with which the blood could then wick into the yarns. Increased twist has previously been shown to reduce wicking in yarns [15]. This resulted in the patchier technical rear bloodstains for the medium compared to the light calico, as well as the smallest dry technical rear bloodstain areas (table 4-3).

The heavy calico had the greatest yarn linear density (43 and 47 tex) and therefore the smallest inter-yarn spaces of the three fabrics investigated in this work. The blood did not penetrate the entire thickness of the fabric at impact from any of the impact velocities investigated. The blood drop did not reach a sufficient kinetic energy with which to force the blood into the inter-yarn spaces and through to the technical rear of the fabric at impact. However, the blood was able to wick through, or around, the yarns before drying. This meant that when the dry bloodstain was examined, there was a bloodstain on the technical rear of the fabric (figure 4-5, table 4-3). The dry technical rear bloodstain on the heavy calico was larger than that of the medium calico owing to the differences in yarn twist levels (650 x 624 tpm and 756 x 756 tpm for the heavy and medium calicos respectively). The lower twist level for the heavy calico meant once the blood was able to wick into the intra-yarn spaces, they were a more optimum size for wicking than those of the medium calico. This increased the dry bloodstain areas beyond those of the medium calico.

## **4.8 Conclusion**

Bloodstains formed on the technical face and technical rear of three 100% cotton plain woven fabrics with different yarn linear densities were filmed using high speed video. On the light calico, blood was visible on the technical rear of the fabric within as little as 0.067 ms of impact. As the blood was spreading on the technical face of the fabric, blood continued to penetrate through to the technical rear. The maximum technical rear bloodstain area from penetration was reached by no more than 0.8 ms after impact, as the blood was too spread out on the surface of the fabric for further penetration. The spreading and retraction of the blood drop on the technical face continued for 8 ms. The effect of the technical rear bloodstain on the dynamics on the technical face would therefore be minimal. Whether blood was visible on the technical rear of the fabric within the high speed video was dependent on both the fabric and the impact velocity of the drop. For the heavy calico, no blood penetrated through to the technical rear of the fabric at impact, for the medium calico it was velocity-dependent, and for the light calico blood penetrated through to the technical rear of the fabric at impact at all velocities. Once the impact dynamics were complete (8 ms) and following the conclusion of the high speed video (67 ms), the blood wicked through and along the yarns, resulting in a dry technical rear bloodstain on all fabrics at all velocities.

## **4.9 Ethical Statement**

All applicable international, national and institutional guidelines for the care and use of animals were followed.

## **4.10 References**

- [1] T.C. de Castro, M.C. Taylor, J.A. Kieser, D.J. Carr, W. Duncan, Systematic investigation of drip stains on apparel fabrics: The effects of prior-laundrying, fibre content and fabric structure on final stain appearance, *Forensic Sci. Int.* 250 (2015) 98–109. doi:10.1016/j.forsciint.2015.03.004.
- [2] T.C. De Castro, D.J. Carr, M.C. Taylor, J.A. Kieser, W. Duncan, Drip bloodstain



- appearance on inclined apparel fabrics: Effect of prior-laundering, fibre content and fabric structure, *Forensic Sci. Int.* 266 (2016) 488–501.  
doi:10.1016/j.forsciint.2016.07.008.
- [3] X. Li, J. Li, S. Michielsen, Effect of yarn structure on wicking and its impact on bloodstain pattern analysis (BPA) on woven cotton fabrics, *Forensic Sci. Int.* 276 (2017) 41–50. doi:10.1016/j.forsciint.2017.04.011.
- [4] E.M.P. Williams, M. Dodds, M.C. Taylor, J. Li, S. Michielsen, Impact dynamics of porcine drip bloodstains on fabrics, *Forensic Sci. Int.* 262 (2016) 66–72.  
doi:10.1016/j.forsciint.2016.02.037.
- [5] J.Y.M. Chang, S. Michielsen, Effect of fabric mounting method and backing material on bloodstain patterns of drip stains on textiles, *Int. J. Legal Med.* (2016). doi:10.1007/s00414-015-1314-z.
- [6] L. Dicken, C. Knock, S. Beckett, T.C. de Castro, T. Nickson, D.J. Carr, The use of micro computed tomography to ascertain the morphology of bloodstains on fabric, *Forensic Sci. Int.* 257 (2015) 369–375.  
doi:10.1016/j.forsciint.2015.10.006.
- [7] J. Li, X. Li, S. Michielsen, Alternative method for determining the original drop volume of bloodstains on knit fabrics, *Forensic Sci. Int.* 263 (2016) 194–203.  
doi:10.1016/j.forsciint.2016.04.018.
- [8] T. De Castro, T. Nickson, D. Carr, C. Knock, Interpreting the formation of bloodstains on selected apparel fabrics, *Int. J. Legal Med.* 127 (2013) 251–258.  
doi:10.1007/s00414-012-0717-3.
- [9] British Standards Institution, Textiles - Domestic washing and drying procedures for textile testing, BS EN ISO 6330. (2012).
- [10] British Standards Institution, Textiles. Sampling of fibres, yarns and fabrics for testing, BS EN 12751. (1999).

- [11] British Standards Institution, Textiles - Standard atmospheres for conditioning and testing, BS EN ISO 139. (2005).
- [12] British Standards Institution, Textiles - Determination of thickness of textiles and textile products, BS EN ISO 5084. (1997).
- [13] British Standards Institution, Textiles - Woven fabrics - Determination of mass per unit length and mass per unit area, BS 2471. (2005).
- [14] British Standards Institution, Textiles - Woven fabrics - Construction - Methods of analysis Part 2: Determination of the number of threads per unit length, BS EN 1049-2. (1994).
- [15] A.B. Nyoni, D. Brook, Wicking mechanisms in yarns—the key to fabric wicking performance, *J. Text. Inst.* 97 (2006) 119–128. doi:10.1533/joti.2005.0128.

## **5 The effect of reactive dyeing of fabric on the morphology of passive bloodstains**

**Dicken, L., Knock, C., Carr, D. J., Beckett, S.**

**Planning to submit to International Journal of Legal Medicine**

### **5.1 Abstract**

Although the majority of fabrics used in blood pattern analysis research are either bleached or optically brightened (chemicals which make fabrics look whiter), the effect of the surface treatments on the resultant bloodstains has not been considered. In this work, calico fabrics (100% cotton, plain woven), on which passive blood drop research had previously been undertaken in a not-coloured state, were reactively dyed. Three different mass per unit areas (after dyeing: 91 g/m<sup>2</sup>, 171 g/m<sup>2</sup> and 243 g/m<sup>2</sup>) of dyed fabric were used. Horse blood was dropped onto the dyed calico using five impact velocities (1.7 ms<sup>-1</sup>, 2.8 ms<sup>-1</sup>, 4.1 ms<sup>-1</sup>, 4.9 ms<sup>-1</sup> and 5.4 ms<sup>-1</sup>). The use of reactive dye increased the thickness (from 0.38 – 0.56 mm to 0.39 - 0.6 mm) and mass per unit area (from 85.1 – 224.6 g/m<sup>2</sup> to 91 – 243 g/m<sup>2</sup>) of the calico fabrics. The result of reactively dyeing the fabrics was larger bloodstains on the dyed (e.g. light calico 41.2 – 78.6 mm<sup>2</sup>) than the not-coloured fabrics (e.g. light calico 21.4 – 67.5 mm<sup>2</sup>) across all three mass per unit areas. The dyeing of the fabrics altered the intra-yarn spaces to a more optimum size for wicking, increasing the ease with which the blood could wick along the yarns in the dyed calico. The amount of wicking varied depending on individual variations within the fabrics and yarns. More variation in dry bloodstain area was seen among dyed calico specimens than for the not-coloured fabric. The amount of wicking which was seen on the dyed calico meant there was no correlation between dry bloodstain area and impact velocity, a correlation which was seen on the medium and heavy not-coloured calico in the previous work.

### **5.2 Keywords**

- Bloodstain analysis
- Wicking

- Wetting
- Absorbent surfaces
- Fabric surface treatments

### 5.3 Highlights

- The use of reactive dye affected the morphology of passive bloodstains.
- Larger bloodstains were seen on dyed fabric than not-coloured fabric.
- No correlation with velocity was seen for the dyed fabrics.

### 5.4 Introduction

Within blood pattern analysis (BPA), the earliest comprehensive study on bloodstains on fabric was undertaken in 1986 [1]. This work [1] indicated the complexity of understanding bloodstains on fabric, and showed further research needed to be undertaken. Subsequent work investigating bloodstains on fabric has differentiated between contact and projected drops [2,3], interpreted satellite stains on fabrics [4], studied the effect of impact velocity and fabric structure on bloodstains on fabric [5,6], the effect of backing materials [7] and the effect of the angle of impact [8]. These studies have shown that BPA on fabric is a complex process, with a multitude of variables affecting the morphology of the bloodstain.

De Castro et al. [6,8] investigated the effects of yarn type (100% cotton, 100% polyester and 65% cotton / 35% polyester blend) and fabric structure (plain woven, single jersey knit) on bloodstains. The blend plain woven fabric produced larger bloodstains than polyester plain woven, with the smallest bloodstains on the cotton plain woven. This was due to the thinness and low mass per unit area of the blend, meaning the blood spread laterally on the surface of the fabric rather than through the depth of the fabric. In terms of fabric structure, the plain woven resulted in larger bloodstains than the single jersey knit, most likely owing to the higher compliancy<sup>20</sup> of the latter resulting in less spreading across the surface of the fabric as it recovered elastically from the impact. The single jersey knit was also found to have a greater

---

<sup>20</sup> 'The property of a body or substance of yielding to an applied force'. Oxford English Dictionary (1989) 2nd edition, prepared by Simpson, J.A. and Weiner E.S.C

surface roughness than the plain woven, altering the wetting and wicking characteristics of the fabric which may also have led to a decrease in dry bloodstain area.

The yarn structure has also been shown to affect bloodstain morphology. Six 100% cotton plain woven fabrics were created from yarns made using three different methods; ring spun, open end and murata vortex [9]. The yarn linear density was  $164 \pm 2$  dtex and the twist multiplier (3.8) was the same for the ring spun and open end yarns. The yarns were each woven into two different fabrics with different sett counts; 100 x 100 yarns per inch (39.4 x 39.4 yarns per cm) and 130 x 70 yarns per inch (51.2 x 27.6 yarns per cm). Porcine blood was dropped onto the fabrics from 500 mm. The resulting bloodstains revealed that while the blood wicked into the fabric woven from ring spun yarns, it did not wick into the fabric woven from either the open end or vortex spun yarns. Instead, the blood largely remained on the surface of the fabric with very little increase in the bloodstain area (5% for open end spun yarns, 15 – 20% for vortex spun yarns). On commercial bed sheeting, which was found to have ring spun weft yarns and Murata vortex spun warp yarns, elliptical-shaped bloodstains were created owing to the uneven wicking with the different methods of yarn creation [9].

Dicken et al. [10] investigated the effect of different mass per unit areas of calico (100% cotton, plain woven) on bloodstain morphology. The mean dry bloodstain area increased with increased impact velocity for all three fabrics, although the correlation between dry bloodstain area and impact velocity was greater for the fabrics with the medium and heaviest mass per unit areas. This was due to an increase in the amount of lateral spreading on the fabric surface at impact with an increase in impact velocity. Owing to the greater yarn linear density of the medium and heaviest fabrics than the lightest fabric, following the lateral spreading at impact less wicking along the yarns then occurred. The greater yarn linear density of the medium and heaviest fabrics meant a greater volume of blood was required to fully wet and wick into the intra-yarn spaces, therefore less blood was available for wicking along the yarns. The lateral spreading was the key mechanism determining the bloodstain area of the medium and

heaviest fabrics. The fabric with the lowest mass per unit area (light: 85.1 g/m<sup>2</sup>) created the largest bloodstain. The low yarn linear density of this fabric meant the blood could easily fill the volume of the yarn, and therefore wick along the intra-yarn spaces, drawing from the reservoir of blood pooled in the inter-yarn spaces. The smallest bloodstains were seen on the fabric with the middle mass per unit area (medium: 163.5 g/m<sup>2</sup>). The twist level for this fabric was greater than for the calico with either the lighter or heavier mass per unit area. Therefore, the amount of wicking which occurred along the yarns was reduced owing to the tighter yarn structure, resulting in a smaller bloodstain area.

Within the literature on bloodstains on fabric, very little mention has been made as to the effect of fabric treatments and dyes on the resultant bloodstains. The effect of Scotchgard (a water repellent) has been mentioned in terms of preventing the blood from absorbing into the fabric, and the blood drop drying on the surface of the fabric [11]. Although fabric used in many of the aforementioned studies [6,8,9] may have been treated in various ways (e.g. optically brightened, bleached [7]), the effect of these treatments is not considered. Bleaching, for example, has been seen to increase the amount of absorption in cotton fibres owing to physical changes in the fibre structure [12].

The majority of bloodstained fabrics found at crime scenes will have had a finishing treatment. The properties of fabrics have previously been seen to change following processing. Fourteen 100% cotton single jersey knit samples were produced and subjected to bleaching, dyeing and softening [13]. The dyeing of the fabrics was seen to affect rigidity, tensile energy and resilience, mass per unit area and geometric roughness due to the shrinking of the fabric during dyeing, as well as the disruption of surface fibres and creation of surface irregularities. Therefore it is important to consider how the treatment could affect the bloodstain patterns seen.

Therefore, the work in this paper was undertaken in order to ascertain whether the dyeing of 100% cotton fabrics affected the resultant bloodstain morphology. Passive blood drops were allowed to fall from a number of heights onto three mass per unit

areas of dyed calico. The fabrics under consideration had been previously used in passive blood drop research in a not-coloured state [10] to allow direct comparison of the bloodstains on the fabric in a dyed and not-coloured state.

## 5.5 Materials and Method

### 5.5.1 Materials

To study the effect of reactively dyeing fabrics on bloodstains, three masses of calico, a 100% cotton plain woven fabric, were used for this research. Due to the use of a 100% cotton fabric, a reactive dye was used. Reactive dyes have become the most popular dye for dyeing cotton since their creation in the 1950s. Around 38% of the total cellulose dye market is taken up by reactive dye [14]. Reactive dyes are the only water-soluble dyes which produce a dye-fibre covalent bond [15]. As such, reactive dyes have extremely good wash-fastness, as well as being easy to apply and available in a wide shade gamut.

All three fabrics were dyed using Dylon Sunflower Yellow 05 fabric dye. This contains Colour Index (C.I.) reactive yellow 125. The fabrics were dyed according to the packet instructions; fabrics were washed with detergent<sup>21</sup> before the dye was added to the washing machine<sup>22</sup>, which was then run on a 40°C cotton cycle. The fabric was then washed again with detergent<sup>19</sup> to remove any excess fabric dye and washed a further four times to create a dimensionally stable fabric [16]. The fabrics were line-dried and cut into 100 mm x 100 mm specimens (n = 87), minimising the repetition of warp and weft yarns. The specimens were then pressed using a digital fabric steam press model PSP-202E on the 'cotton' setting, before conditioning to 20 ± 2°C and 65 ± 4% relative humidity for 24 hours [17].

Following conditioning, the thickness (mm) [18], mass per unit area (g/m<sup>2</sup>) [19] and sett [20] were measured, to assess whether the dyeing of the fabric had altered these parameters from those on the not-coloured fabric [10] (table 5-1).

---

<sup>21</sup> Persil non-bio small and mighty

<sup>22</sup> Samsung Ecobubble at 40°C cotton cycle

	Light dyed	Light not-coloured*	Medium dyed	Medium not-coloured*	Heavy dyed	Heavy not-coloured*
Thickness (mm)	0.39 ± 0.02	0.38 ± 0.03	0.51 ± 0.01	0.46 ± 0.02	0.6 ± 0.04	0.56 ± 0.03
Mass per unit area (g/m <sup>2</sup> )	91 ± 1.84	85 ± 1.54	171 ± 3.71	164 ± 2.26	243 ± 1.77	225 ± 1.56
Sett (yarns per 10mm)	27 x 23	27 x 23	25 x 27	25 x 26	26 x 26	26 x 26

**Table 5-1 mean fabric properties and standard deviation. \*taken from Dicken et al. [10].**

The bloodstains were created using defibrinated horse blood, obtained from Southern Group Laboratory<sup>23</sup>. The blood was stored below 4°C and used within one week of acquisition.

### 5.5.2 Method

In order to simulate a blood-letting event at body temperature, the horse blood was heated to 37°C. The blood was dropped from five heights onto the calico to create passive bloodstains (table 5-2). A Phantom V7 high-speed video filmed all the drops (256 x 256 resolution, 4796 fps and 80 µs exposure). Phantom Camera Control software<sup>24</sup> was used to analyse the high speed videos to measure impact velocity and droplet diameter. The mean droplet diameter was 3.4 ± 0.1 mm. Five repeats were taken at 200 mm, 500 mm, 1000 mm and 1500 mm on each fabric and three repeats at 2500 mm on each fabric resulting in a total of 69 specimens.

Drop height (mm)	Impact velocity and standard deviation (ms <sup>-1</sup> )
200	1.7 ± 0.02
500	2.8 ± 0.04
1000	4.1 ± 0.04
1500	4.8 ± 0.03
2500	5.3 ± 0.07

**Table 5-2 the mean and standard deviation impact velocity resulting from each drop height**

A second experiment was undertaken as per Dicken et al. [21] to film the technical face and technical rear of the fabric at impact. Blood was dropped from three heights; 200 mm, 1000 mm and 2000 mm. This resulted in velocities of 1.8 ms<sup>-1</sup>, 4.2 ms<sup>-1</sup> and 5.7

<sup>23</sup> E-H Cavendish Courtyard, Sallow Road, Weldon Industrial Estate, Corby, Northants. [www.sglab.co.uk](http://www.sglab.co.uk)

<sup>24</sup> <https://www.phantomhighspeed.com/resourcesandsupport/phantomresources/pccsoftware> page accessed 27<sup>th</sup> September 2018.



ms<sup>-1</sup> respectively. The blood drop diameter was 3.6 ± 0.24 mm<sup>2</sup>. Two repeats on each fabric from each height were undertaken resulting in a total of 18 specimens.

The wet bloodstains were photographed less than 30 seconds after impact. The dry bloodstains were photographed on both the technical face and technical rear at least 24 hours later. All photographs were taken using a Nikon D3300 camera.

A Nikon XTH225 micro computed tomography (μCT) scanner was used to analyse all the specimens (table 5-3). Following scanning, the data was manually reconstructed in CT Pro 3D (table 5-3). Using VGStudio Max, the reconstructed data was analysed and a 2D image of the 3D reconstruction and 2-dimensional cross-sectional data were saved [10].

Scanning values						Reconstruction	
<i>Target</i>	<i>Voltage (kV)</i>	<i>Current (μA)</i>	<i>Exposure (ms)</i>	<i>Projections</i>	<i>Frames per projection</i>	<i>Beam hardening</i>	<i>Noise reduction</i>
Tungsten	50	150	500	1080	2	1	1

**Table 5-3 μCT scanner parameters**

A Hitachi SU3500 scanning electron microscope (SEM) and EDAX TEAM microanalysis system<sup>25</sup> was used to examine two specimens from each velocity and fabric combination (15 kV, 60 Pa). Images were taken of the not-bloodstained fabric (x 50 and x 250) and of the bloodstains (x 42 and x 250).

The bloodstain areas from the technical face wet and dry and technical rear dry external photographs were measured using ImageJ.

Analysis of variance (ANOVA) (IBM SPSS statistics version 22) was carried out on the data to assess whether drop impact velocity or fabric type had a statistically significant effect on the dry technical face bloodstain area. To identify which variables contributed to any significant effects, Tukeys HSD analysis was carried out. Interactions were only reported if they were found to be significant. Equality of variances and normality of data were checked. An independent t-test was used to assess whether there were any statistically significant differences in external wet and dry technical

<sup>25</sup> <https://www.edax.com/products/eds/team-eds-system-for-the-sem> Page accessed 27<sup>th</sup> September 2018

face and technical rear bloodstain area between the dyed and not-coloured [10] calicos. Equal variances were assumed, unless Levene's test was significant.

## **5.6 Results and discussion**

### **5.6.1 Bloodstains on dyed fabric**

The resultant bloodstains from the passive blood drops were examined and compared among fabrics and velocities to understand the effect of these variables on the bloodstains.

#### **5.6.1.1 Overall trends**

Figure 1 shows a plot of dry bloodstain area against impact velocity. There was a wide variance in the data with variations in area up to 30 mm<sup>2</sup> (the dry bloodstain area for the medium calico for 1.7 ms<sup>-1</sup> impacts varied from 29.7 mm<sup>2</sup> to 59.6 mm<sup>2</sup>) and coefficients of variation (CVs) of up to 28%. Due to the large variance there was no observed correlation between dry bloodstain area and impact velocity, although there was a general trend for the dry bloodstain area to increase as the impact velocity increased. However, for the light dyed calico, the dry bloodstain areas did not increase consistently with impact velocity with a decrease in bloodstain area from 1.7 ms<sup>-1</sup> to 2.8 ms<sup>-1</sup> (mean areas: 63.3 mm<sup>2</sup> and 55.7 mm<sup>2</sup> respectively). The area then increased as the impact velocity increased to 4.1 ms<sup>-1</sup> (69 mm<sup>2</sup>) before decreasing with an impact velocity of 4.9 ms<sup>-1</sup> (64.9 mm<sup>2</sup>). This is discussed in more detail below. Generally, the dry bloodstain areas were largest on the light calico, with overlap between all three fabrics (figure 5-1).

Univariate analysis of variance (ANOVA) showed fabric ( $F_{14,54} = 16.931$ ,  $p \leq 0.01$ ) and impact velocity ( $F_{14,54} = 9.855$ ,  $p \leq 0.01$ ) affected dry bloodstain area. Tukey's HSD analysis revealed the mean dry bloodstain area on the light calico (64.4 mm<sup>2</sup>) was statistically significantly larger than that on the medium (50.9 mm<sup>2</sup>) and heavy (48.4 mm<sup>2</sup>) calicos. The dry bloodstain area on the specimens from an impact velocity of 1.7 ms<sup>-1</sup> (46.4 mm<sup>2</sup>) were statistically significantly smaller than those from 4.1 ms<sup>-1</sup> (56.5 mm<sup>2</sup>), 4.9 ms<sup>-1</sup> (63 mm<sup>2</sup>) and 5.3 ms<sup>-1</sup> (63.4 mm<sup>2</sup>). The dry bloodstain area on the

specimens from an impact velocity of 2.8 ms<sup>-1</sup> (47.1 mm<sup>2</sup>) were statistically significantly smaller than those from 4.9 ms<sup>-1</sup> and 5.3 ms<sup>-1</sup>.

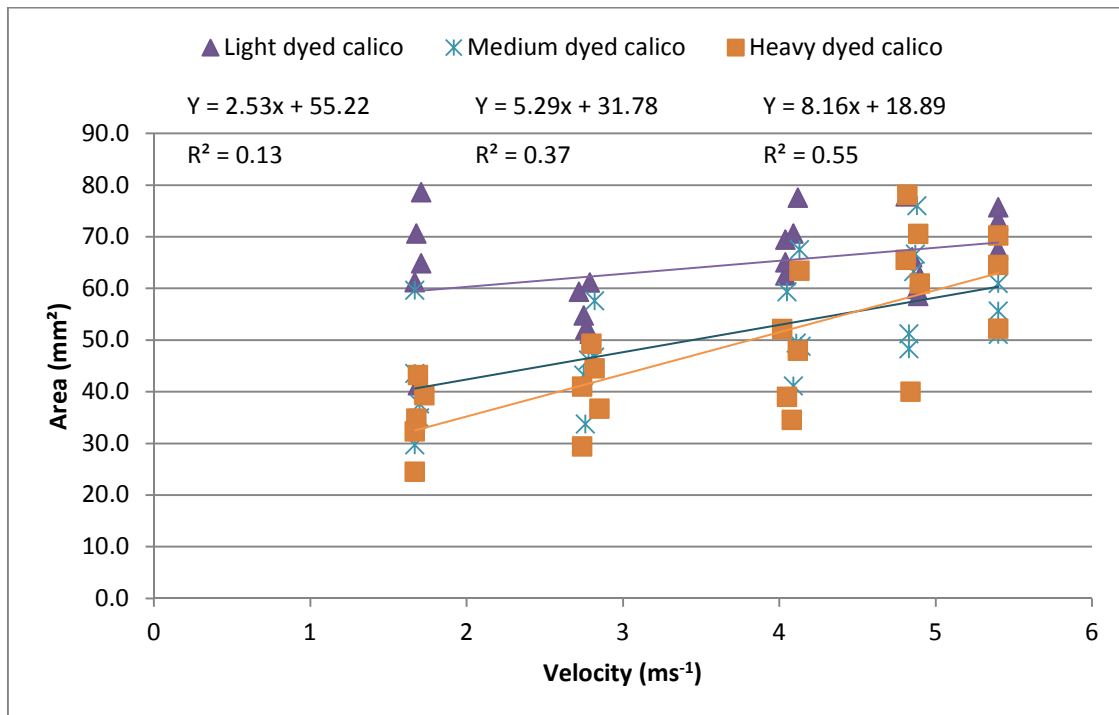


Figure 5-1 dry bloodstain areas plotted against velocity for all three mass per unit areas of calico.

### 5.6.1.2 Bloodstain formation

Bloodstains were formed on the fabrics in two stages. First, the dynamics of the blood drop immediately following impact, referred to in this paper as impact dynamics, and secondly wicking into and along the yarns. These stages are examined in more detail below.

Using the high-speed video of the technical face and technical rear of the fabric at impact, it was possible to ascertain the impact dynamics of the blood drop. Following impact, the blood initially penetrated through to the technical rear of the light calico at all velocities (1.8, 4.2 and 5.7 ms<sup>-1</sup>) as quickly as 0.067 ms after impact. For the medium and heavy calico, no blood penetrated through to the technical rear of the fabric as a result of the impact of the blood drop within the 50 ms of high speed video. For all three fabrics, the blood spread laterally on the surface of the fabric for between 2 and 4 ms, with an increase in impact velocity decreasing the length of time the blood spread for. The blood drop then retracted, and satellite stains and ligaments formed.

By between 8 and 14 ms after impact the impact dynamics had ceased and the blood drop had settled on the surface of the fabric.

For all three fabrics, as the impact velocity increased, the amount of lateral spreading which occurred following impact also increased. Stills from filming the technical face of each fabric following drops impacting at velocities of  $1.8 \text{ ms}^{-1}$  and  $4.2 \text{ ms}^{-1}$  (figure 5-2) show the greater amount of lateral spreading which occurred at the higher impact velocity.

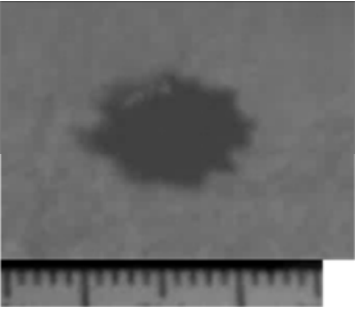
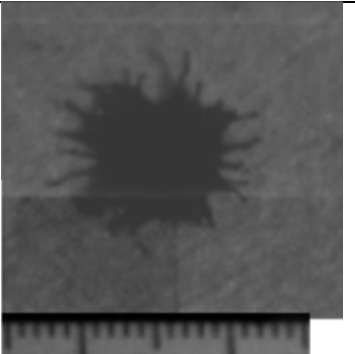
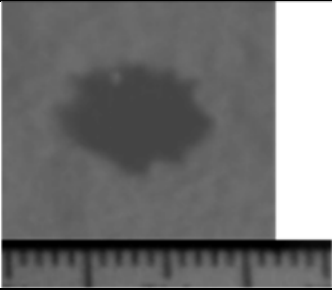
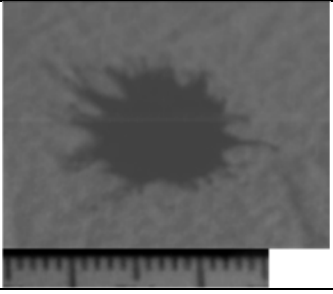
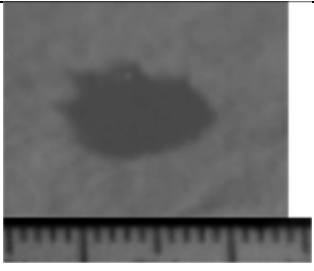
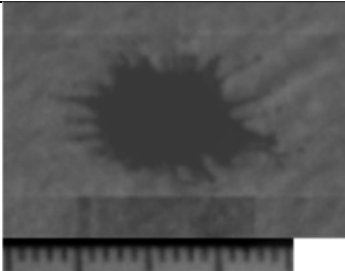
	
<p>Figure 5-2a: light calico from <math>1.8 \text{ ms}^{-1}</math> at 3ms following impact</p>	<p>Figure 5-2b: light calico from <math>4.2 \text{ ms}^{-1}</math> at 2ms following impact</p>
	
<p>Figure 5-2c: medium calico from <math>1.8 \text{ ms}^{-1}</math> at 3ms following impact</p>	<p>Figure 5-2d: medium calico from <math>4.2 \text{ ms}^{-1}</math> at 2ms following impact</p>
	
<p>Figure 5-2e: heavy calico from <math>1.8 \text{ ms}^{-1}</math> at 3ms following impact</p>	<p>Figure 5-2f: heavy calico from <math>4.2 \text{ ms}^{-1}</math> at 2ms following impact</p>

Figure 5-2 stills from filming the fabric technical face at impact on all three calicos from  $1.9 \text{ ms}^{-1}$  and  $4.2 \text{ ms}^{-1}$ . Scale is 2 cm.

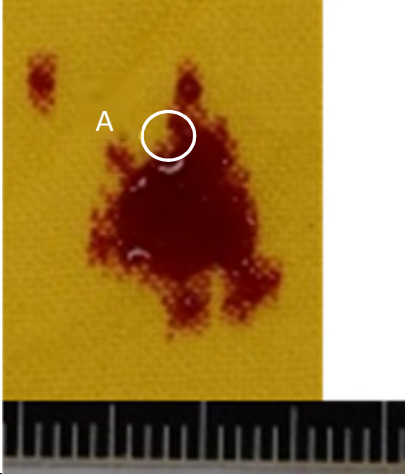
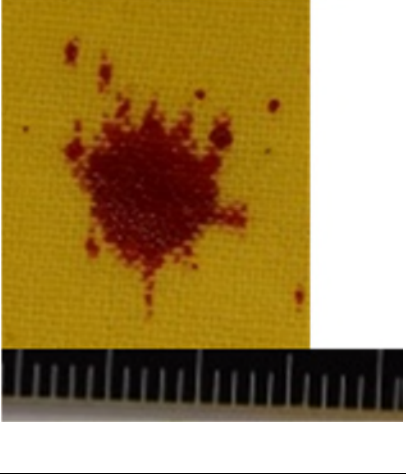
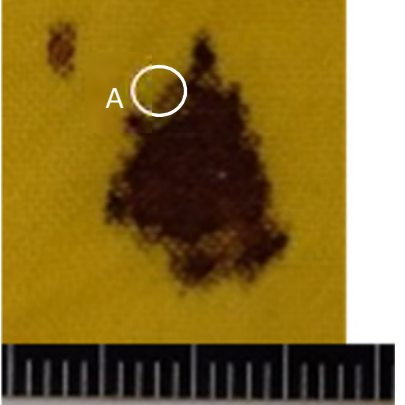
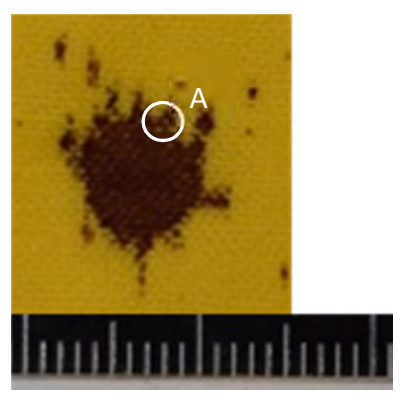
Once the blood drop had settled on the surface of the fabric, if the blood remained on the surface it then wicked vertically into the yarns, followed by wicking along the intra-yarn spaces. If the blood had already penetrated the yarns, the blood then wicked along the intra-yarn spaces. Less wicking occurred in the medium and heavy than the light calico. The greater yarn linear density of the medium and heavy than the light calico meant a greater volume of blood was required to fully wet and wick into the yarns, resulting in a smaller volume of blood being available to wick along the yarns. Therefore, the medium and heavy fabrics had smaller dry bloodstain areas than the light. The amount of wicking within a fabric can vary with variations within the fabric, yarns and fibres [22]. Therefore the amount of wicking was not consistent across specimens for any given fabric, which created the variation in the data.

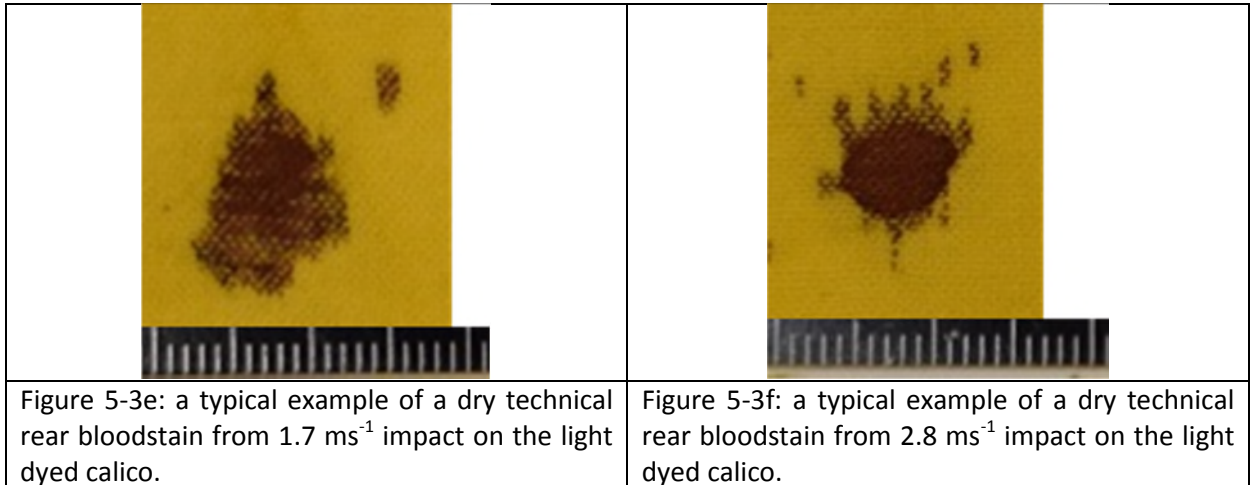
#### ***5.6.1.3 Fabric and velocity effects***

On the light calico the mean dry bloodstain area from impacts of  $1.7 \text{ ms}^{-1}$  ( $63.3 \text{ mm}^2$ ) was larger than that from impacts of  $2.8 \text{ ms}^{-1}$  ( $55.7 \text{ mm}^2$ ). This decrease in dry bloodstain area with increased velocity was likely caused by a difference in the amount of blood which was pooled on the surface of the fabric following impact (figure 5-3a and b). From  $1.7 \text{ ms}^{-1}$  the lack of lateral spreading at impact owing to the low kinetic energy resulted in a pool of blood remaining on the surface of the fabric. This resulted in a reservoir from which wicking occurred preferentially along the warp yarns around the edge of the bloodstain (figure 5-3a and c, marked 'A'). The preferential wicking along the warp yarns occurred owing to differences in yarn linear density between the warp (14 tex) and weft (18 tex) yarns. The lower yarn linear density of the warp yarns meant less blood was required to fill the volume of the yarns, and therefore more blood was available for wicking along them. The amount of wicking which was able to occur on the light calico at this velocity also altered the shape of the bloodstain from a typical 'circular' passive bloodstain [23] to a bloodstain which was a more irregular shape (figure 5-3c).

The increase in kinetic energy at impact from  $1.7 \text{ ms}^{-1}$  to  $2.8 \text{ ms}^{-1}$  resulted in no blood being pooled on the surface of the light calico after impact (figure 5-3b). Instead, a

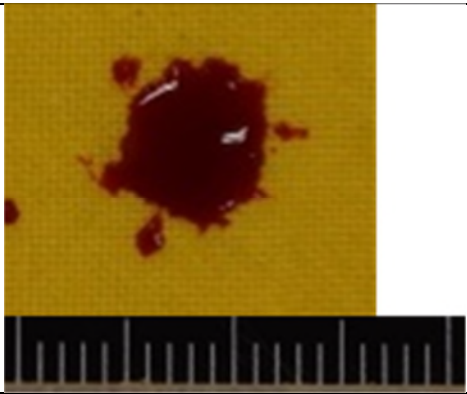
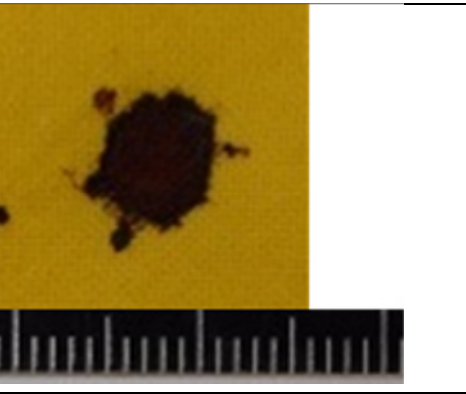
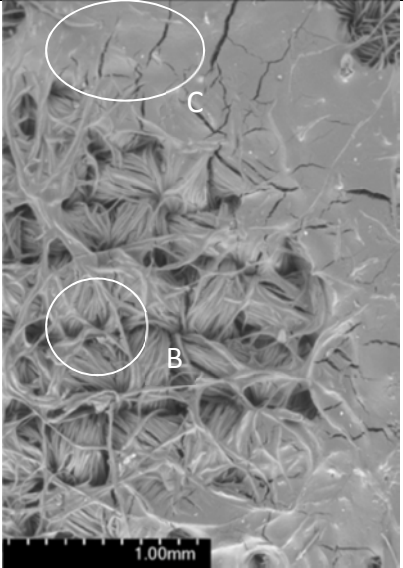
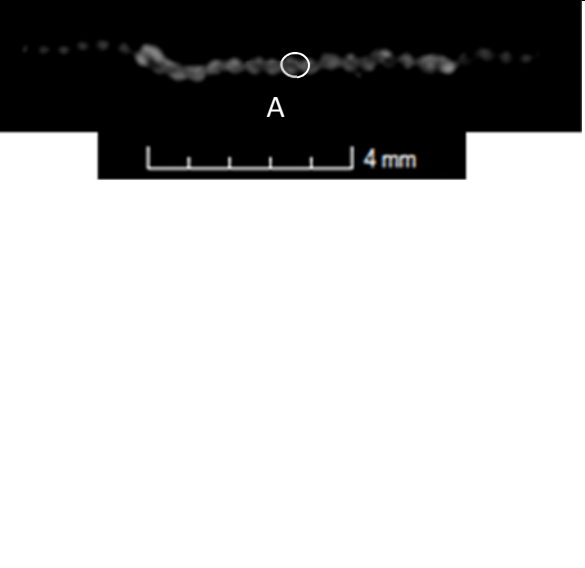
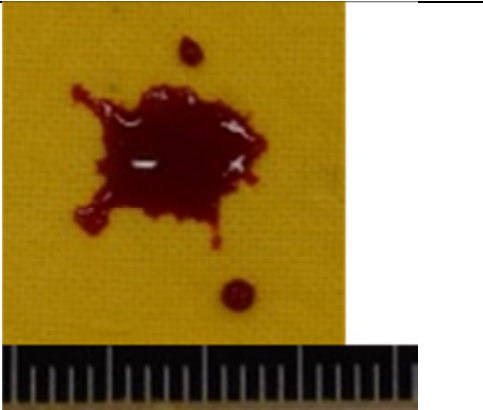
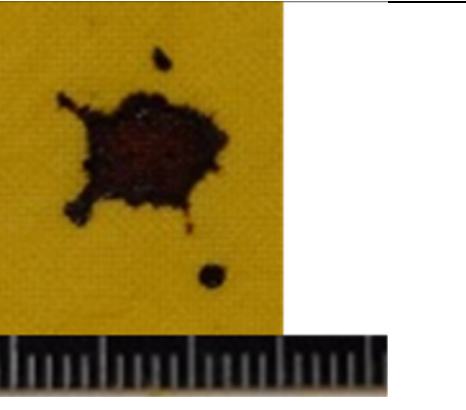
greater amount of blood penetrated through to the technical rear of the fabric (figure 5-3f). A small amount of blood still wicked preferentially along the warp yarns at the edge of the bloodstain for the specimens from  $2.8 \text{ ms}^{-1}$  (figure 5-3d, marked 'A'). However, as there was no reservoir of blood on the surface of the light calico this could not occur to the same extent as for the specimens from  $1.7 \text{ ms}^{-1}$  impacts. Therefore, the light calico bloodstains were smaller from  $2.8 \text{ ms}^{-1}$  impacts than from  $1.7 \text{ ms}^{-1}$  impacts.

	
<p>Figure 5-3a: a typical example of a wet bloodstain from <math>1.7 \text{ ms}^{-1}</math> impact on the light dyed calico.</p>	<p>Figure 5-3b: a typical example of a wet bloodstain from <math>2.8 \text{ ms}^{-1}</math> impact on the light dyed calico.</p>
	
<p>Figure 5-3c: a typical example of a dry bloodstain from <math>1.7 \text{ ms}^{-1}</math> impact on the light dyed calico.</p>	<p>Figure 5-3d: a typical example of a dry bloodstain from <math>2.8 \text{ ms}^{-1}</math> impact on the light dyed calico.</p>



**Figure 5-3 a typical example of a wet and dry bloodstain on the dyed light calico. 'A' indicates where the blood has continued to wick along the warp yarns beyond the main bloodstain. Scale is 2 cm.**

On the medium and heavy calicos, as for the light calico, the low kinetic energy at impact for the specimens from an impact velocity of 1.7 ms<sup>-1</sup> resulted in a lack of lateral spreading at impact (figure 5-2c and e). This resulted in the wet bloodstain remaining pooled on the surface of the fabric (figure 5-4a and e). In the middle of the bloodstain the blood wicked vertically into both the warp and weft yarns (figures 5-4d and h, marked 'A') and did not remain on the surface of the fabric (figure 5-4c and g marked 'B'). The blood which was inside the yarns was then able to wick along the intra-yarn spaces. However, some blood remained on the surface of the fabric and dried before it was able to wick away along the yarns. This is shown in the large rim of dense, dry blood around the edge of the bloodstain (figures 5-4b, c, f and g, marked 'C') where the blood which remained on the surface of the fabric dried in the manner of the coffee ring effect [24].

	
<p>Figure 5-4a: medium dyed calico wet bloodstain</p>	<p>Figure 5-4b: medium dyed calico dry bloodstain</p>
	
<p>Figure 5-4c: medium dyed calico SEM image</p>	<p>Figure 5-4d: medium dyed calico cross-section in the weft direction</p>
	
<p>Figure 5-4e: heavy dyed calico wet bloodstain</p>	<p>Figure 5-4f: heavy dyed calico dry bloodstain</p>



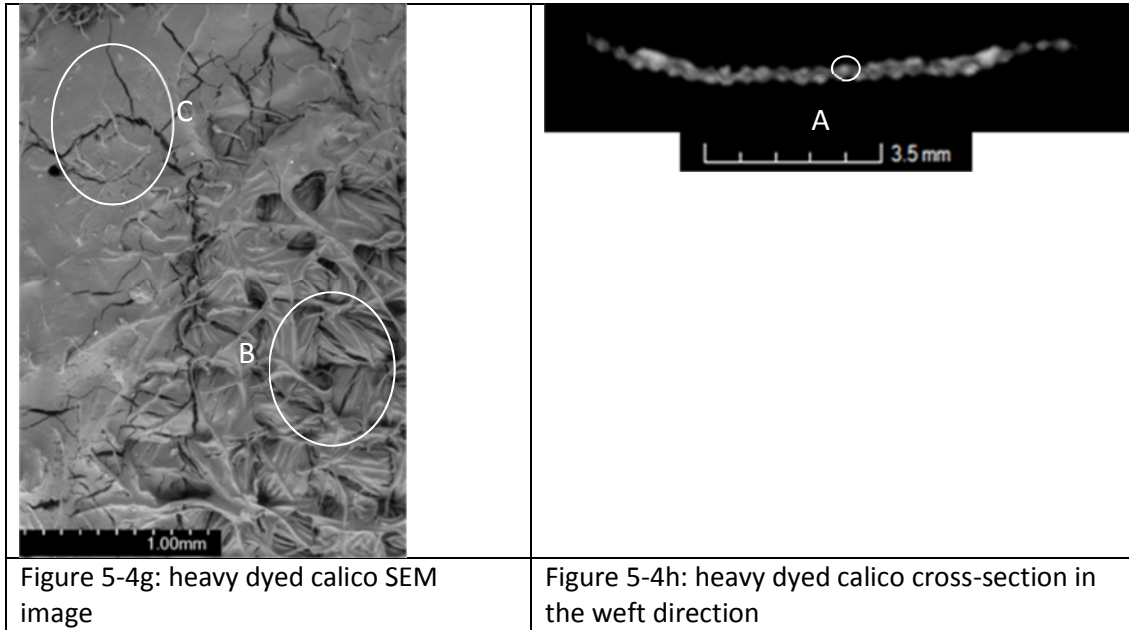
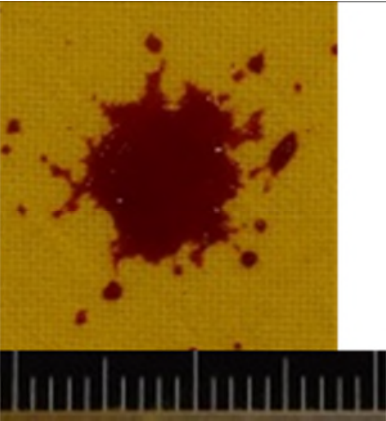
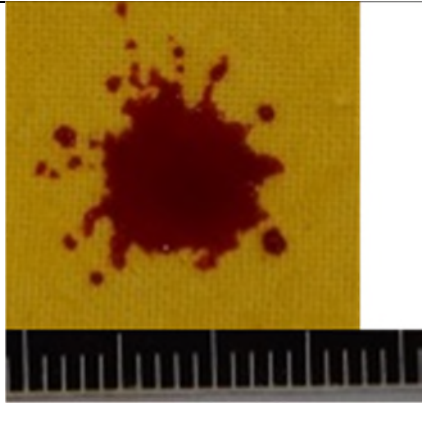
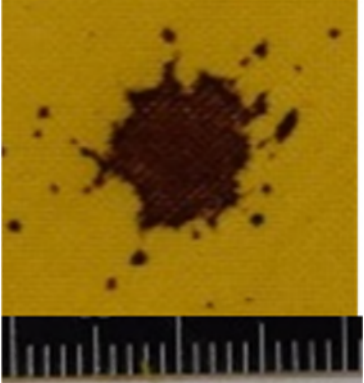
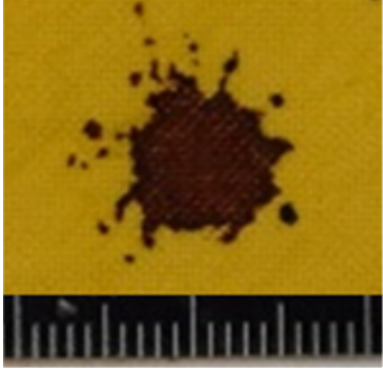
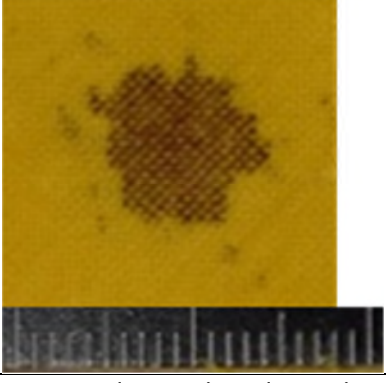
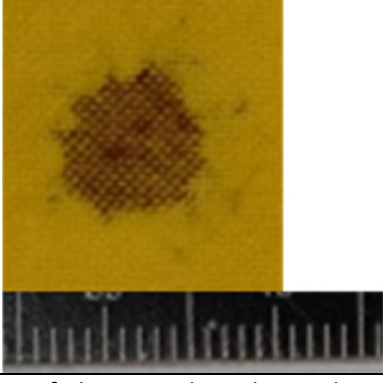
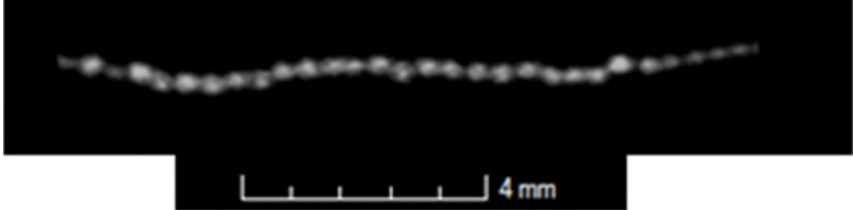


Figure 5-4 a typical example of a wet and dry bloodstain (scale: 2 cm) and SEM image at 42x magnification and CT cross section on the dyed medium and heavy calicos from an impact velocity of  $1.7 \text{ ms}^{-1}$ . 'A' is an example of blood in the warp and weft yarns at the centre of the bloodstain. 'B' is the blood in the centre of the bloodstain inside the yarns. 'C' is the blood at the edge of the bloodstain which remained on the surface of the fabric.

On the light calico, the greater amount of lateral spreading of the blood on the surface of the fabric with the increase in impact velocity resulted in the increase in mean dry bloodstain area from  $2.8 \text{ ms}^{-1}$  ( $55.7 \text{ mm}^2$ ) to  $4.1 \text{ ms}^{-1}$  ( $69 \text{ mm}^2$ ).

On the dyed medium and heavy calicos, for  $4.1 \text{ ms}^{-1}$  impacts the wet blood did not pool on the surface of the fabrics (figure 5-5a and b), owing to the increased lateral spreading at impact. Although the blood may have penetrated slightly into the yarns, the high speed video showed the blood did not penetrate through to the technical rear of the fabric following impact. However, after the end of the high speed video, the blood did wick into the yarns through to the technical rear of the fabric, as there is a dry technical rear bloodstain visible for both the medium (figure 5-5e) and heavy (figure 5-5f) calicos. The blood wicked through, rather than around, the yarns (figure 5-5g and h). Only a small amount of blood remained and dried on the surface of the fabric as there was only a small area of dense blood around the edge of the bloodstain (figure 5-5c and d). For the medium and heavy calicos, these trends continued for the higher velocities ( $4.9$  and  $5.3 \text{ ms}^{-1}$ ).

	
<p>Figure 5-5a: medium calico wet bloodstain</p>	<p>Figure 5-5b: heavy calico wet bloodstain</p>
	
<p>Figure 5-5c: medium calico dry bloodstain</p>	<p>Figure 5-5d: heavy calico dry bloodstain</p>
	
<p>Figure 5-5e: medium calico dry technical rear bloodstain</p>	<p>Figure 5-5f: heavy calico dry technical rear bloodstain</p>
	
<p>Figure 5-5g: medium calico CT cross-section</p>	

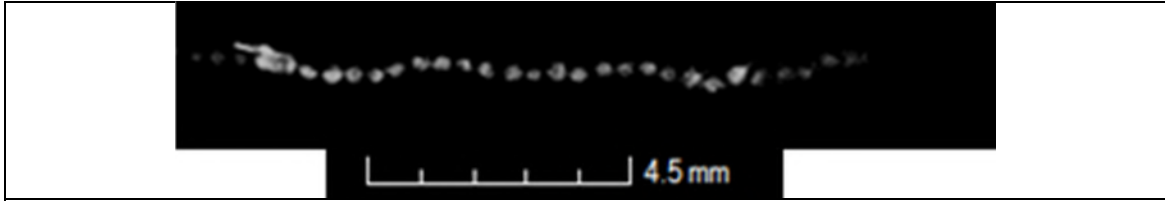


Figure 5-5h: heavy calico CT cross-section

Figure 5-5 a typical example of a wet and dry bloodstain (scale: 2 cm) and CT cross-section in the weft direction from the medium and heavy calico from  $4.1 \text{ ms}^{-1}$  impact.

However, for the light calico the mean dry bloodstain area decreased from  $69 \text{ mm}^2$  at  $4.1 \text{ ms}^{-1}$  impacts to  $64.9 \text{ mm}^2$  at  $4.9 \text{ ms}^{-1}$  impacts. The higher impact velocity forced the blood into the yarns, reducing the amount of blood which pooled in the inter-yarn spaces. The reservoir of blood from which wicking along the intra-yarn spaces could occur was therefore reduced. The similarity between the mean wet ( $68.3 \text{ mm}^2$ ) and dry ( $64.9 \text{ mm}^2$ ) bloodstain area for the light calico specimens from  $4.9 \text{ ms}^{-1}$  showed the lack of wicking which occurred at this velocity. The blood was spread evenly along the warp yarns throughout the entire bloodstain for the light calico specimens from an impact velocity of  $4.9 \text{ ms}^{-1}$  (figure 5-6b), which would have occurred when the blood was forced into the yarns at impact. On the other hand, the blood is patchy in the centre of the bloodstain in the light calico specimens from an impact velocity of  $4.1 \text{ ms}^{-1}$  as the blood wicked into and along the yarns, and would not have been as evenly spread out (figure 5-6a).

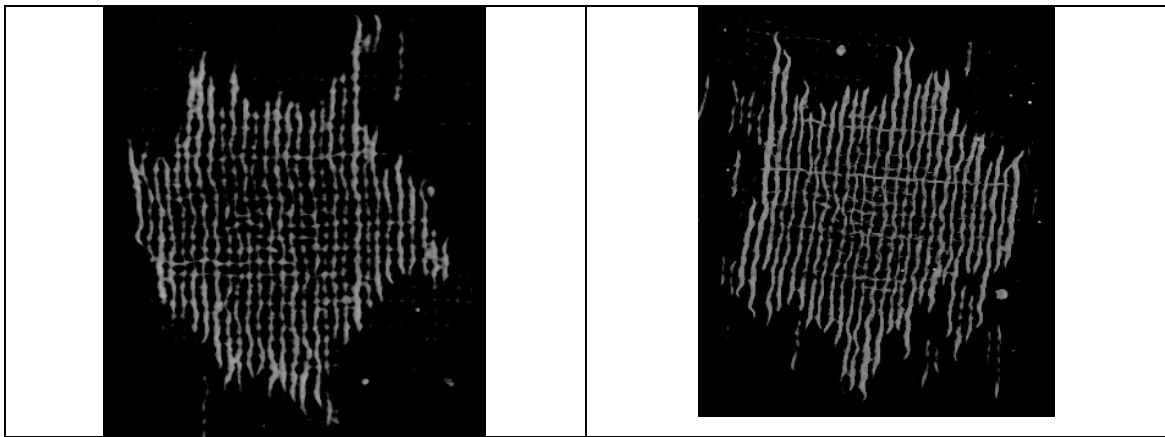


Figure 5-6a: light calico from  $4.1 \text{ ms}^{-1}$

Figure 5-6b: light calico from  $4.9 \text{ ms}^{-1}$

Figure 5-6 a typical example of a 2D image of the 3D CT reconstruction of a light calico specimen from an impact velocity of  $4.1 \text{ ms}^{-1}$  and  $4.9 \text{ ms}^{-1}$ .

The mean dry bloodstain area on the light calico specimens increased to 72.1 mm<sup>2</sup> with the increase in impact velocity to 5.3 ms<sup>-1</sup>. The increase in impact velocity to 5.3 ms<sup>-1</sup> resulted in a greater amount of lateral spreading at impact, and a large amount of wicking following this. The amount of wicking which occurred following impact at 5.3 ms<sup>-1</sup> was shown in the largest increase in light calico bloodstain area between the mean wet (64.7 mm<sup>2</sup>) and dry (72.1 mm<sup>2</sup>) bloodstains among the velocities investigated. The wicking occurred in both the warp and weft directions, evidenced by the bloodstains from 5.3 ms<sup>-1</sup> impacts being the only specimens where no wicking occurred along the warp yarns beyond the edge of the main bloodstain (figure 5-7).

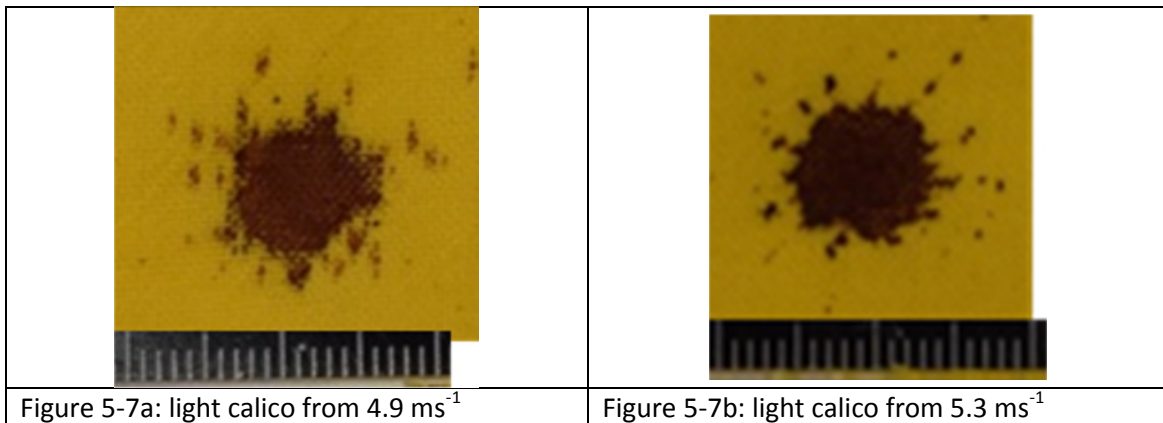


Figure 5-7a: light calico from 4.9 ms<sup>-1</sup>

Figure 5-7b: light calico from 5.3 ms<sup>-1</sup>

Figure 5-7 a typical example of a dry bloodstain on the light calico from impact velocities of 4.9 and 5.3 ms<sup>-1</sup>. Scale is 2 cm.

### 5.6.2 Effect of dyeing

The use of reactive dye resulted in chemical and physical changes to the fabric. Dyeing increased the thickness (light: from 0.38 to 0.39 mm; medium from 0.46 to 0.51 mm; heavy from 0.56 to 0.6 mm) and mass per unit area (light from 85 to 91 g/m<sup>2</sup>; medium from 164 to 171 g/m<sup>2</sup>; heavy from 225 to 243 g/m<sup>2</sup>) for all three calicos (table 5-1). The sett of the three fabrics is almost identical before and after dyeing (table 5-1), so the increase in thickness and mass per unit area was not owing to the yarns being closer to each other. Therefore, the size of the yarns themselves must have increased.

The SEM images of the dyed and not-coloured medium calico (x50 and x250) are given in figure 5-8. The dyed fabric (figure 5-8a) was more tightly compacted than the not-coloured fabric (figure 5-8b), with less evidence of inter-yarn spaces. This was due to the swelling of the fibres, and therefore the yarns. In order to dye a cotton fibre, the

dye molecules must enter the polymer structure of the fibre. The structure of a cotton fibre is partly crystalline and partly amorphous; as the crystalline regions do not alter when immersed in water [25], only the amorphous regions are responsible for the diffusion of dye into the fibre. When immersed in water, the amorphous regions of a cotton fibre swell, and allow the dye molecules entry into the fibre [25]. For a reactive dye, the molecules form a covalent bond with the cotton. Therefore upon drying, owing to the addition of the dye, the cotton fibres will remain swollen. This, in turn, will increase the diameter of the yarns, and alter the intra-yarn spaces between the fibres. As long as the intra-yarn spaces were changed to a more optimum size for wicking [26], the ease with which the blood could wick both into and along the yarns would increase. Coupled with this, as the amorphous regions of the cotton fibre reacted with the dye, the blood is less likely to be absorbed into the fibres. This would increase the amount of blood available to wick along the intra-yarn spaces, as the blood would only be able to wick between the fibres, not into them.

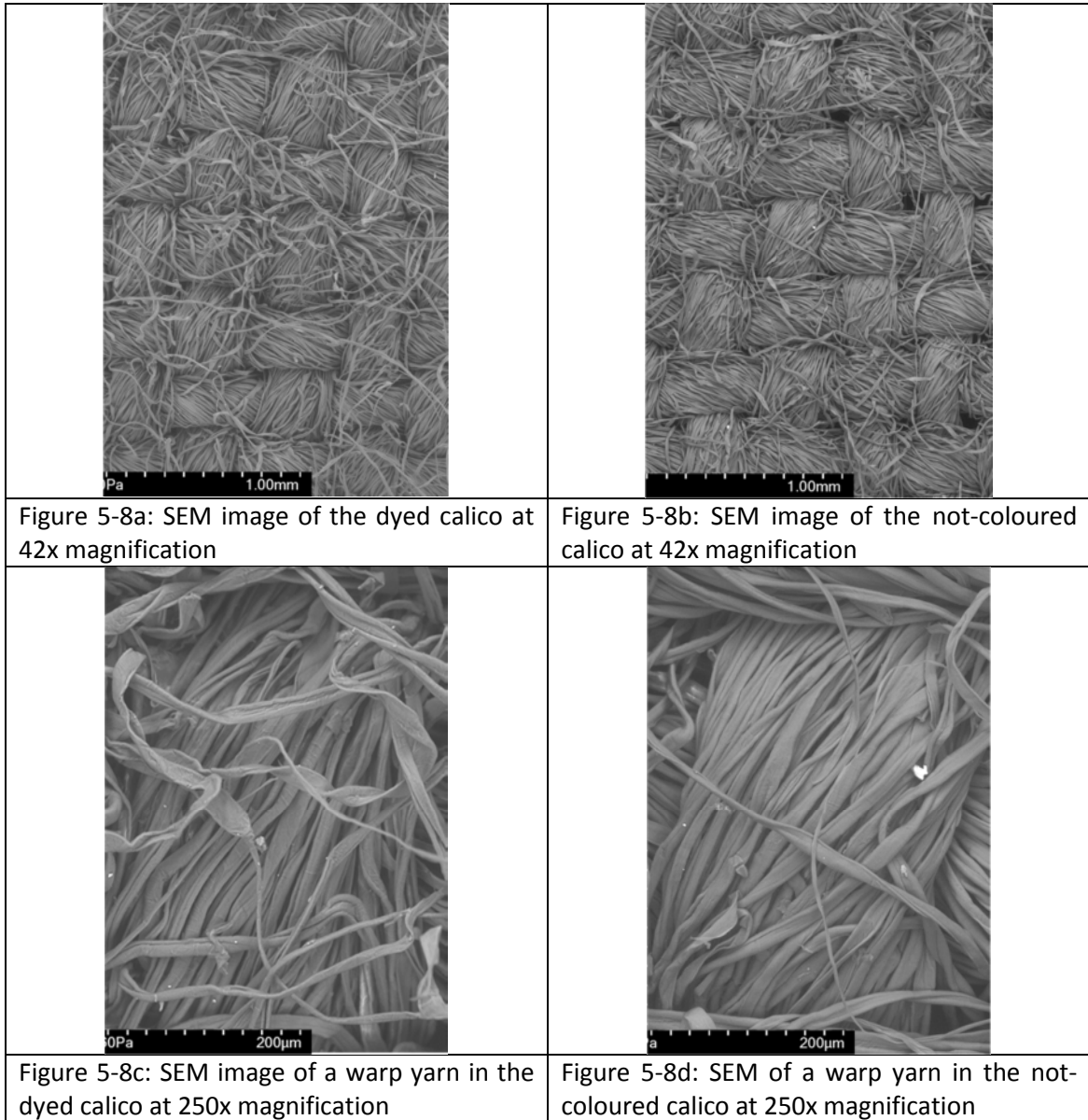


Figure 5-8 SEM images of the dyed and not-coloured [10] medium calico

### 5.6.3 Comparison to bloodstains on not-coloured fabric

Passive blood drop research had previously been undertaken on the three calicos used in this paper when they were in a not-coloured state [10]. Comparison of the bloodstains on the not-coloured and dyed calicos has been undertaken to assess the difference that dyeing the fabric created in the bloodstains.

The dry bloodstain areas of the dyed and the not-coloured calicos [10] are given in figure 5-9. Although there was some overlap between the two groups of bloodstains, the dry bloodstain areas on the dyed calicos tended to be larger than those on the not-

coloured calicos. An independent t-test showed that the dry bloodstain areas for the dyed calico were statistically significantly larger than the not-dyed calico for all fabrics (light:  $t_{46} = 6.219, p \leq 0.01$ , medium:  $t_{46} = 5.340, p \leq 0.01$ , heavy:  $t_{46} = 2.33, p \leq 0.05$ ) and all velocities ( $1.7 \text{ ms}^{-1}$ :  $t_{28} = 5.046, p \leq 0.01$ ,  $2.8 \text{ ms}^{-1}$ :  $t_{28} = 3.699, p \leq 0.01$ ,  $4.1 \text{ ms}^{-1}$ :  $t_{28} = 4.533, p \leq 0.01$ ,  $4.9 \text{ ms}^{-1}$ :  $t_{28} = 4.985, p \leq 0.01$ ,  $5.3 \text{ ms}^{-1}$ :  $t_{22} = 2.956, p \leq 0.01$ ).

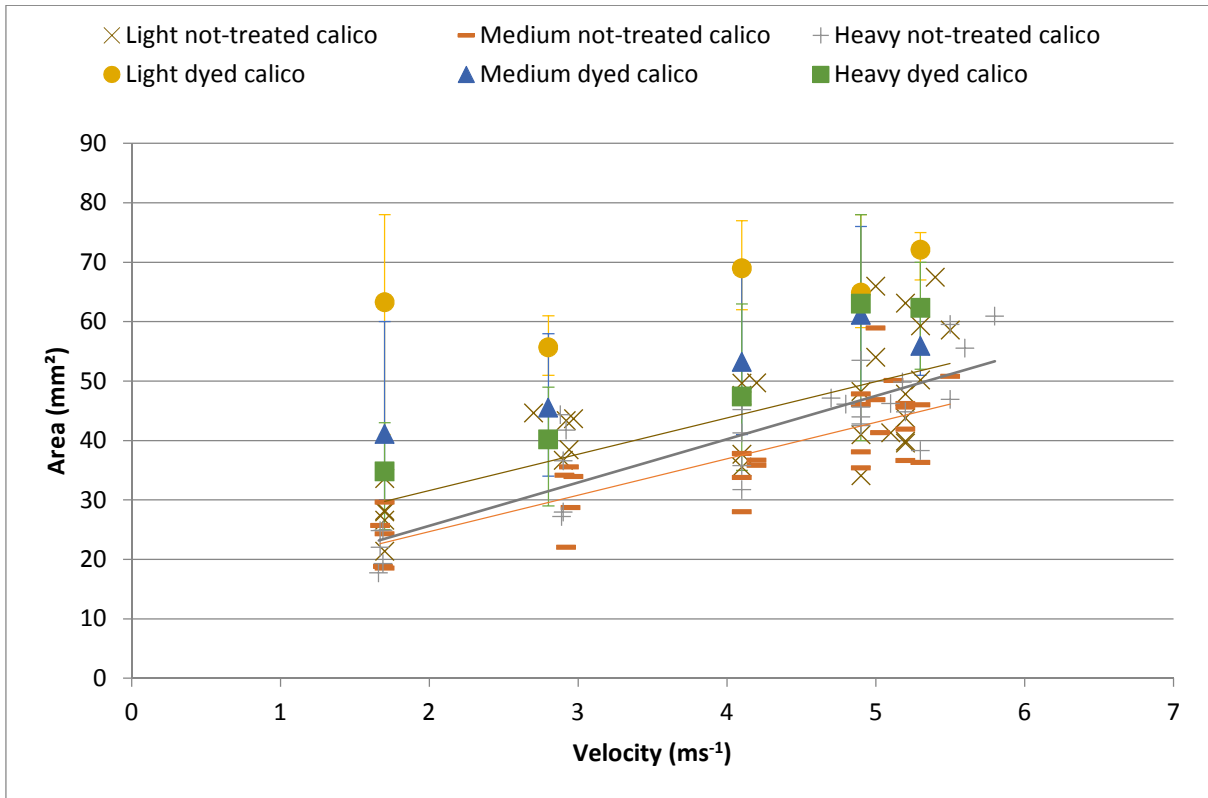


Figure 5-9 Dry bloodstain area for the not-coloured calicos [10] and the mean dry bloodstain area and range for the dyed calicos plotted against impact velocity

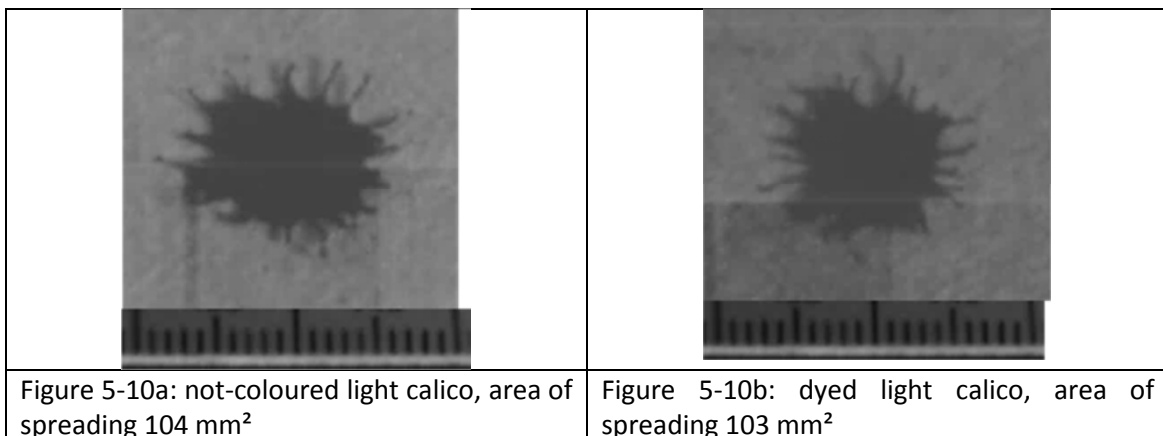
The correlations ( $R^2$  values) of a straight line fitted to the data using a least squares fit for each of the dyed and not-coloured fabrics are given in table 5-4. The only correlations between dry bloodstain area and velocity are for the medium and heavy not-coloured fabrics.

	Not-coloured	Dyed
Light	0.51	0.13
Medium	0.68	0.37
Heavy	0.76	0.55

Table 5-4 the  $R^2$  values for each of the not-coloured [10] and dyed fabrics

For the medium and heavy not-coloured calico, the greatest influence on the dry bloodstain area was the amount of lateral spreading of the blood drop on the fabric surface at impact [10], which increased with higher velocities. This resulted in a slight correlation between dry bloodstain area and velocity (figure 5-9, table 5-4). The not-coloured medium and heavy calicos had smaller dry bloodstain areas than the dyed fabrics [10]. This indicates the blood was not able to wick along the intra-yarn spaces in the medium and heavy not-coloured calico to the same extent as in the dyed fabrics, as dye entering the amorphous regions in the cotton fibres altered the intra-yarn spaces. The greater amount of wicking for the medium and heavy dyed fabrics increased the variation among specimens and therefore reduced the correlation with velocity.

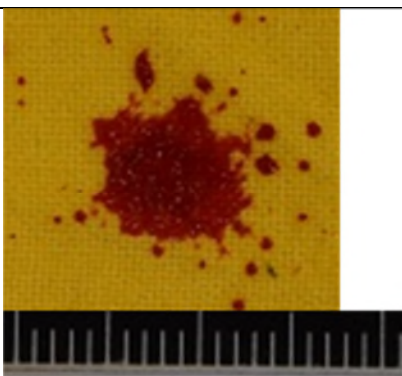
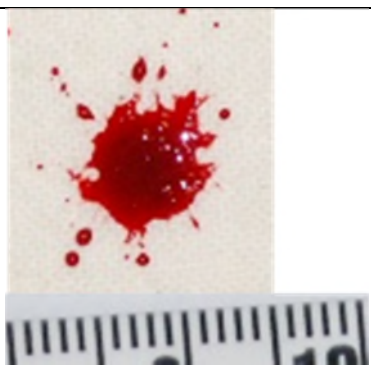
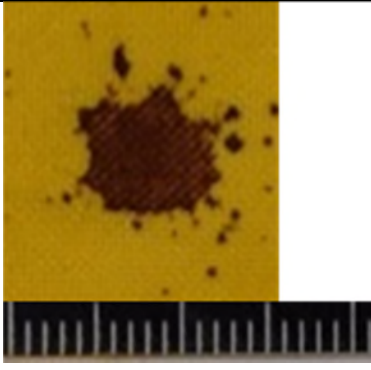
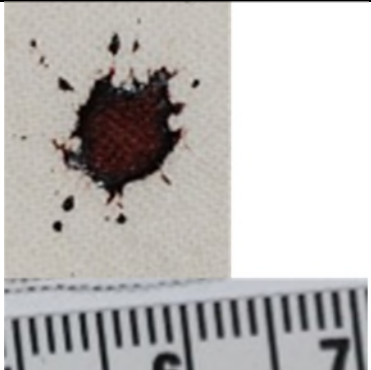
Initially at impact, the amount of lateral spreading which occurred was comparable between the dyed and the not-coloured calicos (e.g. figure 5-10, areas of spreading were 103 and 104 mm<sup>2</sup> 2 ms after impact respectively). However, after impact the interaction between the blood and the fabric differed between the dyed and the not-coloured fabrics. A greater amount of blood remained pooled on the surface of the not-coloured calico [10] than the dyed calico. On the not-coloured calico, pooled blood was present on the surface of the medium and heavy fabrics up to an impact velocity of 4.1 ms<sup>-1</sup> [10] (figure 5-11b), while pooling only occurred on the dyed calico up to 2.8 ms<sup>-1</sup> impacts.



**Figure 5-10 a typical example of a high speed video still from 2ms following impact on a light dyed and not-coloured calico [20] from 4.2 ms<sup>-1</sup>. Scale is 2 cm.**



On the not-coloured calico, the blood which pooled on the surface was not able to wick into the yarns before drying occurred, resulting in a rim of dense, dry blood [10] (figure 5-11d and f). On the dyed calico the blood was able to wick into the yarns before it dried on the surface of the fabric. This resulted in a smaller rim of dense blood around the edge of the bloodstain (figure 5-11c and e). The blood was inside the yarns in the dyed calico; both the warp and weft yarns are blood soaked for the dyed calico (figure 5-11g), while they are patchy for the not-coloured calico [10] (figure 5-11h). The blood which was inside the yarns in the dyed calico was then able to wick along the intra-yarn spaces, resulting in a larger dry bloodstain area for the dyed than the not-coloured fabrics. The greater ease with which the blood could wick into the yarns, resulting in less blood on the surface of the dyed calico, and along the yarns, creating larger dry bloodstain areas, suggests the alteration of the intra-yarn spaces following dyeing resulted in them being a more optimum size for wicking.

	
<p>Figure 5-11a: medium dyed calico wet bloodstain</p>	<p>Figure 5-11b: medium not-coloured calico wet bloodstain</p>
	
<p>Figure 5-11c: medium dyed calico dry bloodstain</p>	<p>Figure 5-11d: medium not-coloured calico dry bloodstain</p>

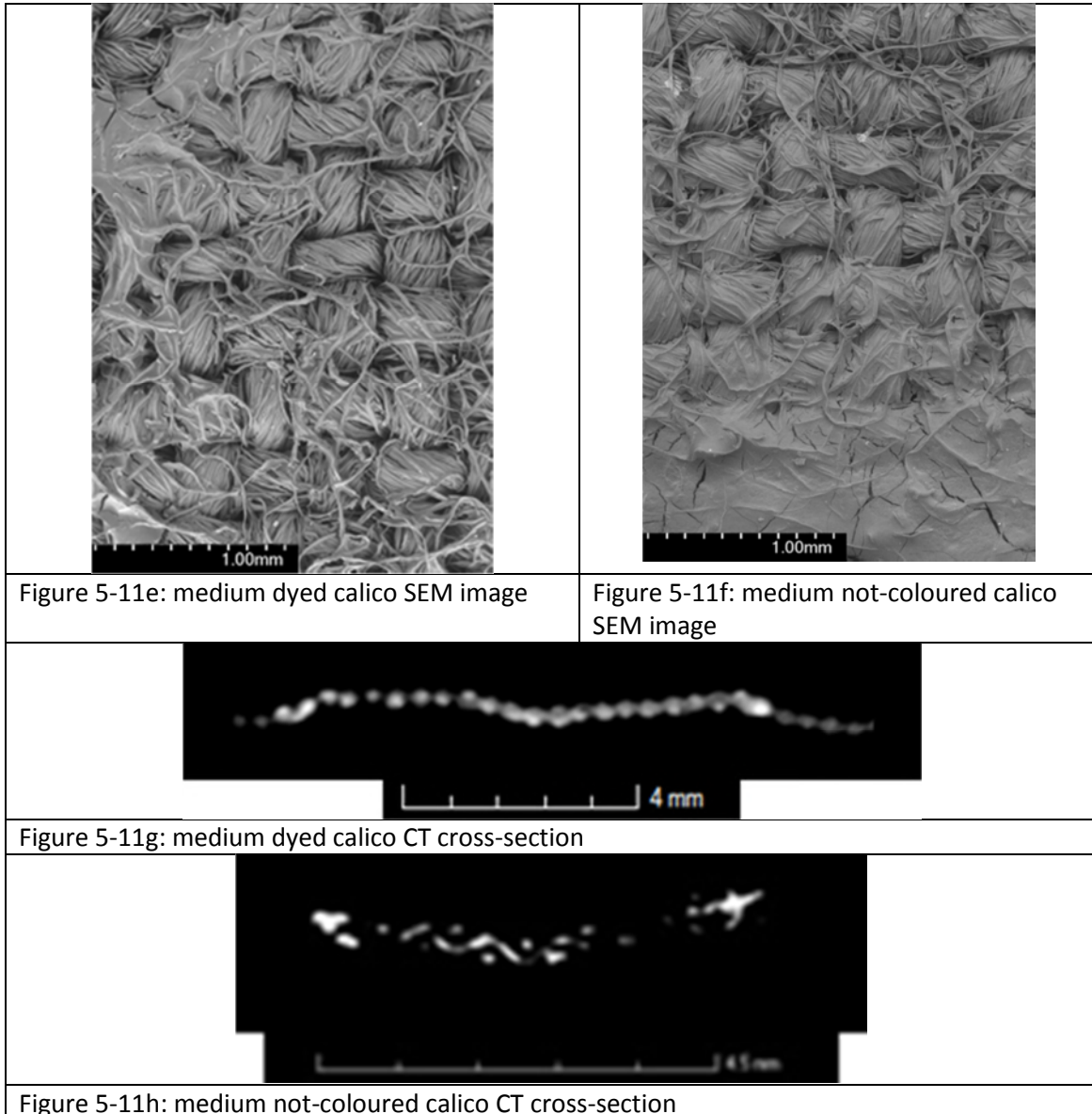


Figure 5-11 an example wet and dry bloodstain photograph (scale: 2 cm), SEM image at 42x magnification and CT cross-section in the weft direction on the medium dyed and not-coloured calico (images taken for research done in [10] but not used in publication) from  $4.1 \text{ ms}^{-1}$ .

In summary, differences in dry bloodstain area were seen among the light, medium and heavy dyed fabrics owing to differences among the fabrics. The greater yarn linear density of the medium and heavy calico resulted in smaller dry bloodstain areas than on the light calico. The dyeing of the calico resulted in the blood being able to wick more easily into and along the intra-yarn spaces. This was most likely owing to the intra-yarn spaces becoming a more optimum size for wicking following the dyeing process. When compared to the not-coloured fabrics [10], the greater amount of

wicking resulted in larger dry bloodstain areas for the dyed calico, and no correlation with velocity.

## 5.7 Conclusions

Passive bloodstains were created on three mass per unit areas (91 g/m<sup>2</sup>, 171 g/m<sup>2</sup> and 243 g/m<sup>2</sup>) of reactively dyed 100% cotton plain woven calico. Five drop heights were used, which resulted in five impact velocities (1.7 ms<sup>-1</sup>, 2.8 ms<sup>-1</sup>, 4.1 ms<sup>-1</sup>, 4.9 ms<sup>-1</sup> and 5.3 ms<sup>-1</sup>). The reactive dyeing of the fabric resulted in the blood being able to wick more easily along the yarns, resulting in a larger dry bloodstain area across all three dyed calicos than on the not-coloured calico [10]. The increase in wicking for the dyed calico also removed any correlation with velocity, as the wicking increased the variability in dry bloodstain area among specimens. The amount of wicking which was able to occur, most notably on the light dyed calico, altered the shape of the parent bloodstain from the typical 'circular' bloodstains seen on the not-coloured calico [10] to a more irregular shape (e.g. figure 5-3c). This could have implications in assessing bloodstains at a crime scene, as typically passive bloodstains are thought to have an approximately circular shape [23], while bloodstains from an angled impact would be more elongated [23]. The work undertaken in this paper shows an irregular-shaped bloodstain can occur without an angled impact, and indicates great care needs to be taken in analysing bloodstains on fabric when a lot of wicking can occur. Therefore, at a crime scene the manner in which the fabric has been processed would need to be taken into consideration when assessing the morphology and area of the dry bloodstains. Different surface treatments may alter the dry bloodstain area and the likelihood of a correlation with velocity.

## 5.8 References

- [1] B. White, Bloodstain pattern on fabrics: the effect of drop volume, dropping height and impact angle, *Can. Soc. Forensic Sci. J.* 19 (1986) 3–36.
- [2] B. Karger, S.P. Rand, B. Brinkmann, Experimental bloodstains on fabric from contact and from droplets, *Int. J. Legal Med.* 111 (1998) 17–21. doi:10.1007/s004140050104.

- [3] Y. Cho, F. Springer, F.A. Tulleners, W.D. Ristenpart, Quantitative bloodstain analysis: Differentiation of contact transfer patterns versus spatter patterns on fabric via microscopic inspection, *Forensic Sci. Int.* 249 (2015) 233–240. doi:10.1016/j.forsciint.2015.01.021.
- [4] H.F. Miles, R.M. Morgan, J.E. Millington, The influence of fabric surface characteristics on satellite bloodstain morphology, *Sci. Justice.* 54 (2014) 262–266. doi:10.1016/j.scijus.2014.04.002.
- [5] T. De Castro, T. Nickson, D. Carr, C. Knock, Interpreting the formation of bloodstains on selected apparel fabrics, *Int. J. Legal Med.* 127 (2013) 251–258. doi:10.1007/s00414-012-0717-3.
- [6] T.C. de Castro, M.C. Taylor, J.A. Kieser, D.J. Carr, W. Duncan, Systematic investigation of drip stains on apparel fabrics: The effects of prior-laundrying, fibre content and fabric structure on final stain appearance, *Forensic Sci. Int.* 250 (2015) 98–109. doi:10.1016/j.forsciint.2015.03.004.
- [7] J.Y.M. Chang, S. Michielsen, Effect of fabric mounting method and backing material on bloodstain patterns of drip stains on textiles, *Int. J. Legal Med.* (2016). doi:10.1007/s00414-015-1314-z.
- [8] T.C. De Castro, D.J. Carr, M.C. Taylor, J.A. Kieser, W. Duncan, Drip bloodstain appearance on inclined apparel fabrics: Effect of prior-laundrying, fibre content and fabric structure, *Forensic Sci. Int.* 266 (2016) 488–501. doi:10.1016/j.forsciint.2016.07.008.
- [9] X. Li, J. Li, S. Michielsen, Effect of yarn structure on wicking and its impact on bloodstain pattern analysis (BPA) on woven cotton fabrics, *Forensic Sci. Int.* 276 (2017) 41–50. doi:10.1016/j.forsciint.2017.04.011.
- [10] L. Dicken, C. Knock, S. Beckett, D.J. Carr, The effect of fabric mass per unit area and blood impact velocity on bloodstain morphology, (2018) Submitted for publication.

- [11] J. Slemko, Bloodstains on fabric- the effects of droplet velocity and fabric Composition, (1999).
- [12] A.P. D'Silva, G. Harrison, A.R. Horrocks, D. Rhodes, Investigation into cotton fibre morphology Part II: Effect of scouring and bleaching treatments on absorption, *J. Text. Inst.* 91 (2000) 107–122.
- [13] H. Hasani, Effect of different processing stages on mechanical and surface properties of cotton knitted fabrics, *Indian J. Fibre Text. Res.* 35 (2010) 139–144.
- [14] D.M. Lewis, The chemistry of reactive dyes and their application processes, in: M. Clark (Ed.), *Handb. Text. Ind. Dye. Vol. 1 Princ. Process. Types Dye.*, Woodhead Publishing, Cambridge, 2011: pp. 303–364. doi:10.1111/cote.12114.
- [15] D.M. Lewis, Dyestuff-fibre interactions, *Rev. Prog. Color.* 28 (1998) 12–17.
- [16] British Standards Institution, *Textiles - Domestic washing and drying procedures for textile testing*, BS EN ISO 6330. (2012).
- [17] British Standards Institution, *Textiles - Standard atmospheres for conditioning and testing*, BS EN ISO 139. (2005).
- [18] British Standards Institution, *Textiles - Determination of thickness of textiles and textile products*, BS EN ISO 5084. (1997).
- [19] British Standards Institution, *Textiles - Woven fabrics - Determination of mass per unit length and mass per unit area*, BS 2471. (2005).
- [20] British Standards Institution, *Textiles - Woven fabrics - Construction - Methods of analysis Part 2: Determination of the number of threads per unit length*, BS EN 1049-2. (1994).
- [21] L. Dicken, C. Knock, D.J. Carr, S. Beckett, Investigating bloodstain dynamics at impact on the technical rear of fabric, (2018) Submitted for publication.
- [22] A.B. Nyoni, D. Brook, Wicking mechanisms in yarns—the key to fabric wicking performance, *J. Text. Inst.* 97 (2006) 119–128. doi:10.1533/joti.2005.0128.

- [23] S.H. James, P.E. Kish, T.P. Sutton, Principles of Bloodstain pattern analysis: Theory and Practice, CRC Press, Florida, 2005.
- [24] R.D. Deegan, O. Bakajin, T.F. Dupont, G. Huber, S.R. Nagel, T.A. Witten, Capillary flow as the cause of ring stains from dried liquid drops, *Nature*. 389 (1997) 827–829. doi:10.1038/39827.
- [25] S. Grishanov, Structure and properties of textile materials, in: M. Clark (Ed.), *Handb. Text. Ind. Dye. Vol. 1 Princ. Process. Types Dye.*, Woodhead Publishing, Cambridge, 2011: pp. 28–63.
- [26] N. Erdumlu, C. Saricam, Wicking and drying properties of conventional ring- and vortex-spun cotton yarns and fabrics, *J. Text. Inst.* 104 (2013) 1284–1291. doi:10.1080/00405000.2013.799258.

## **6 The effect of the digital printing of fabric on the morphology of passive bloodstains**

**Dicken, L., Knock, C., Carr, D. J., Beckett, S.**

**Planning to submit for publication in Textile Research Journal.**

### **6.1 Abstract**

Bloodstained fabrics found at crime scenes are likely to have had processing treatments, such as dyeing or printing, but the effect of the treatments on bloodstain morphology is not always considered. In order to study the effect of digital printing on bloodstain morphology, passive bloodstains were created from five impact velocities (1.9 to 5.4 ms<sup>-1</sup>) on three different mass per unit areas (88 to 226 g/m<sup>2</sup>) of 100% cotton calico which had been digitally printed using reactive dye. Across all three printed fabrics, the bloodstains appeared visually similar, and no correlation was found between the dry bloodstain area and the impact velocity. When comparing the bloodstains on the printed fabric to those which had been created previously on the same fabric in a dyed and not-coloured state, the dry bloodstains on the printed fabric were statistically significantly larger (e.g. for the calico with the lightest mass per unit area, mean dry bloodstain area was 126.6, 64.4 and 44.3 mm<sup>2</sup> for the printed, dyed and not-coloured fabrics respectively). The larger bloodstains on the printed calico, and examination of the bloodstains with the micro computed tomography scanner and scanning electron microscope, suggested that the printing process decreased the surface roughness, and therefore increased the wettability of the fabric, so the blood could spread more easily on the surface. This allowed the blood to coat the yarns, and wick into them before wicking along the intra-yarn spaces.

### **6.2 Keywords**

- Bloodstain analysis
- Absorbent surfaces
- Wicking
- Wetting

### **6.3 Highlights**

- Bloodstains for all printed fabrics were visually similar
- Bloodstains on not printed face larger than bloodstains on printed face of fabric
- No correlation of dry bloodstain area with velocity was seen
- Bloodstains on printed calico were larger than those on dyed or not-coloured calico

### **6.4 Introduction**

An area of interest within bloodstain pattern analysis (BPA) is the interaction of blood and fabrics, as bloodstained clothing and household textiles are frequently encountered at crime scenes. The interaction of blood and fabric was found to be more complex than that of blood and non-absorbent surfaces in the first comprehensive study of bloodstains on fabrics in 1986 [1]. Since then, with the reliability and scientific integrity of BPA under question [2], further research has been undertaken to improve the understanding of the interaction of blood and fabrics. A number of variables have been found to affect the resultant bloodstains on fabrics. These include fibre content and fabric structure [3,4], the mounting method of the fabric [5], impact angle [4], mass per unit area and thickness [6] and yarn structure [7]. However, an area which has not been thoroughly investigated in BPA is the effect of finishing treatments on the interaction of blood and fabric. When blood impacts a fabric at a crime scene, it is unlikely the fabric in question will be loom-state. More likely, it will have undergone a number of processing stages including bleaching, scouring, dyeing and/or printing to produce the end-use fabric. Therefore, investigating the effects of processing is important to BPA.

Work which has been carried out within textile science can be used to understand what is occurring following the impact of a blood drop onto fabric. Some experimentation has been undertaken within textile science to assess the effect of processing treatment methods on yarn wicking. Differences in cotton knitted fabrics were seen to occur following bleaching, dyeing and softening [8]. Dyeing affected the rigidity, mass per unit area and geometric roughness of the fabrics as a result of the



shrinkage and disruption of the fabric during dyeing. Cotton yarns with a yarn count of 30 tex and various twist levels (350 and 550 turns per metre) were subjected to bleaching, prewashing and plasma treatment to assess the effect of these treatments on the wicking of the yarns [9]. Both prewashing and plasma treatment improved the amount of wicking from none, owing to the hydrophobicity of the raw fibre, to  $0.5 \text{ cm s}^{-1}$  after plasma treatment due to the increased wettability of the cotton fibre. This previous work [8,9] showed that processing treatments affected the structure and wettability of yarns and fabrics. This suggests that the bloodstains on fabrics which have been subjected to processing will differ depending on the treatments.

The effect of reactive dye on passive bloodstains on three 100% cotton fabrics with different mass per unit areas (91, 171 and  $243 \text{ g/m}^2$ ) has been investigated [10]. The bloodstains on the dyed fabric were statistically significantly larger than the equivalent bloodstains on the not-coloured fabric, owing to the intra-yarn spaces becoming a more optimum size for wicking as a result of the dyeing process. Therefore, BPA research which has been undertaken on bleached and/or optically brightened textiles [5,7,11,12], while providing a basis for understanding the interaction of blood and fabric, cannot be directly applied to fabric which has been dyed [10]. Each of the various methods of colouring fabrics needs to be examined individually to assess the effect on the resultant bloodstains.

An area of increasing growth within the textiles market is that of digitally printed textiles. Although in 2016 digitally printed textiles accounted for only 2.8% of the textile market, this is predicted to grow by 12.3% every year until 2021, much higher than the industry average growth of 3% [13]. Digitally printed textiles can be used for anything from cushions, tea towels and table cloths to bespoke clothing fabrics [14]. Therefore, the likelihood of encountering a blood-soaked fabric at a crime scene which has been digitally printed will increase, and therefore an understanding of how this method of dyeing affects the interaction of blood and fabric is important.

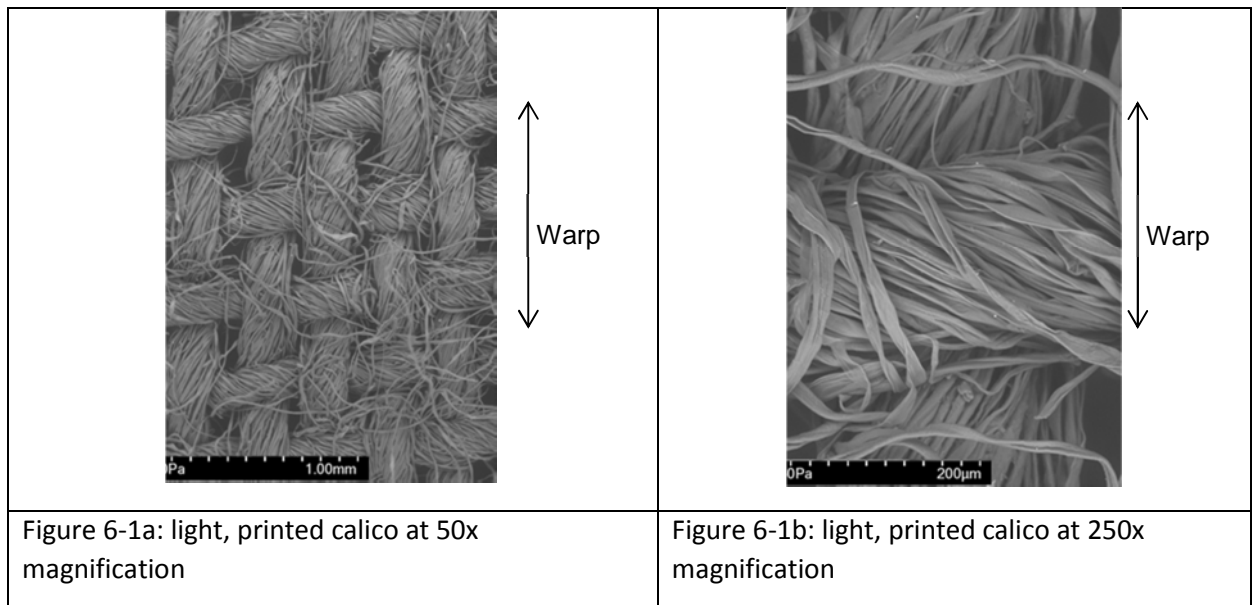
The current work investigated the effect of digital inkjet printing on the morphology of passive bloodstains. In order to do this, passive bloodstains were created on three


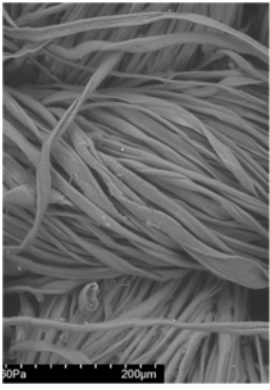
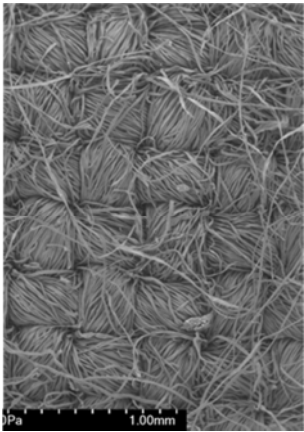
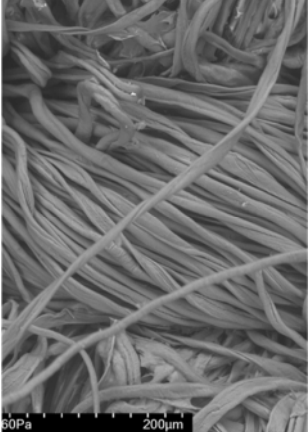
different mass per unit areas of inkjet printed 100% cotton fabric. The resultant bloodstains were analysed with the use of micro computed tomography ( $\mu$ CT) and scanning electron microscopy (SEM). This allowed a detailed examination of the internal structure of the bloodstains. Differences among the fabrics, impact velocities and between the printed fabrics and previous work which was undertaken on dyed [10] and not-coloured [6] fabrics were examined.

## 6.5 Materials and Method

### 6.5.1 Materials

The fabrics used in this research were three different mass per unit areas of calico, a 100% cotton plain woven fabric (88 g/m<sup>2</sup> (light), 165 g/m<sup>2</sup> (medium) and 226 g/m<sup>2</sup> (heavy)). An SEM image of each printed fabric at 50x and 250x magnification is given in figure 6-1. These fabrics have been previously used in both a not-coloured [6] and dyed [10] state.



	
<p>Figure 6-1c: medium printed calico at 50x magnification</p>	<p>Figure 6-1d: medium printed calico at 250x magnification</p>
	
<p>Figure 6-1e: heavy printed calico at 50x magnification</p>	<p>Figure 6-1f: heavy printed calico at 250x magnification</p>

**Figure 6-1 example SEM images of the printed calicos at 50x and 250x magnification.**

All fabrics were inkjet printed using the drop on demand technique by Magic Textiles<sup>26</sup>. The inks used were Huntsman reactive dyes<sup>27</sup> designed for digital textile printing. The side of the fabric which was printed was the technical face. The printed fabrics were prepared as per Dicken et al. [6]. The mass per unit area, thickness and sett of the printed fabrics are given in table 6-1, along with those of the dyed and not-coloured fabrics [6,10].

<sup>26</sup> Unit 1A, Churnet Works, James Brindley Rd, Leek, Staffordshire, ST13 8YH <https://www.magictextiles.co.uk/> (accessed 5<sup>th</sup> September 2018).

<sup>27</sup> <http://www.huntsman.com> (accessed 5<sup>th</sup> September 2018)

		Thickness (mm)	Mass per unit area (g/m <sup>2</sup> )	Sett (yarns per 10 mm)
Light calico	Printed	0.35 ± 0.02	88 ± 2.3	27 x 23
	Dyed* <sup>1</sup>	0.39 ± 0.02	91 ± 1.84	27 x 23
	Plain* <sup>2</sup>	0.38 ± 0.03	85 ± 1.54	27 x 23
Medium calico	Printed	0.45 ± 0.01	165 ± 2.6	25 x 26
	Dyed* <sup>1</sup>	0.51 ± 0.01	171 ± 3.71	25 x 27
	Plain* <sup>2</sup>	0.46 ± 0.02	164 ± 2.26	25 x 26
Heavy calico	Printed	0.53 ± 0.005	226 ± 3.1	26 x 26
	Dyed* <sup>1</sup>	0.6 ± 0.04	243 ± 1.77	26 x 26
	Plain* <sup>2</sup>	0.56 ± 0.03	225 ± 1.56	26 x 26

**Table 6-1 mean fabric properties and standard deviation. \*1 [10] \*2 [6]**

Defibrinated horse blood was used to create the bloodstains, sourced from Southern Group Laboratory<sup>28</sup>. The blood was stored below 4°C until required and was used within one week of delivery.

### 6.5.2 Method

The horse blood was heated to 37°C prior to use to simulate a blood-letting event at body temperature. A Pasteur pipette was used to drop the blood onto the printed face (PF) of the fabric from five different heights (table 6-2) to create passive bloodstains. All blood drops were filmed using a Phantom V12 high-speed video (1280 x 800 resolution, 6273 fps, exposure 70 µs). The high-speed videos were analysed using Phantom Camera Control software<sup>29</sup> to measure droplet diameter and impact velocity (table 6-2). The mean droplet diameter was 3.5 ± 0.2 mm. Five repeats were undertaken at drop heights of 200 – 1500 mm, and three at 2500 mm, resulting in 69 specimens.

<sup>28</sup> E-H Cavendish Courtyard, Sallow Road, Weldon Industrial Estate, Corby, Northants. [www.sglab.co.uk](http://www.sglab.co.uk) (accessed 5<sup>th</sup> September 2018) .

<sup>29</sup> <https://www.phantomhighspeed.com/resourcesandsupport/phantomresources/pccsoftware> (accessed 5th September 2018) .

Passive bloodstains were also created by dropping blood from three heights (table 6-2) onto the not-printed face (NPF) of the fabric. The mean droplet diameter was  $3.6 \pm 0.1$ . Five repeats were undertaken on each fabric at each of the three drop heights, resulting in 45 specimens.

The terms technical face and technical rear will not be used to describe the side of the bloodstain being examined, as the technical face is determined by the side of the fabric which was printed on. When the bloodstains were therefore created on the NPF of the fabric, the ‘technical rear’, the use of the terms technical face and technical rear could lead to some confusion as to which side of the bloodstain was being examined. Therefore, to describe bloodstains on the side of the fabric which the blood drop impacted, ‘impact face’ will be used. For bloodstains on the opposite side of the fabric, ‘penetrated face’ will be used.

Drop Height (mm)	Impact velocity and standard deviation ( $\text{ms}^{-1}$ ) drops onto PF	Impact velocity and standard deviation ( $\text{ms}^{-1}$ ) drops onto NPF
200	$1.9 \pm 0.07$	$1.7 \pm 0.03$
500	$3 \pm 0.1$	
1000	$4.1 \pm 0.1$	$4.1 \pm 0.05$
1500	$5 \pm 0.2$	$4.8 \pm 0.1$
2500	$5.4 \pm 0.1$	

**Table 6-2 the mean and standard deviation impact velocity resulting from each drop height.**

Further experiments simultaneously filmed the technical face and the technical rear of the fabric for drop impacts on the printed face as per Dicken et al. [15] for a limited number of impact velocities. Three different heights were used; 200 mm, 1000 mm and 2000 mm resulting in impact velocities of  $1.8 \text{ ms}^{-1}$ ,  $4.3 \text{ ms}^{-1}$  and  $5.7 \text{ ms}^{-1}$ . The blood drop diameter was  $3.7 \pm 0.15 \text{ mm}^2$ . Two repeats were undertaken on each fabric from each height, resulting in 18 specimens.

All subsequent analysis was undertaken as per Dicken et al. [6]. Briefly, the wet impact face and dry impact face and penetrated face bloodstains were photographed. The

bloodstain areas were measured from the photographs with the use of the inbuilt tools in ImageJ. All 69 specimens from the initial experiment were scanned in a Nikon XTH225 micro computed tomography ( $\mu$ CT) scanner, the parameters of which, which differed from Dicken et al. [6], can be seen in table 6-3. Two specimens on each fabric from each of the five velocities were examined using a Hitachi SU3500 SEM with the EDAX TEAM microanalysis system<sup>30</sup> (15 kV, 60 Pa).

Scanning values						Reconstruction	
<i>Target</i>	<i>Voltage (kV)</i>	<i>Current (<math>\mu</math>A)</i>	<i>Exposure (ms)</i>	<i>Projections</i>	<i>Frames per projection</i>	<i>Beam hardening</i>	<i>Noise reduction</i>
Tungsten	50	160	500	1080	2	1	1

**Table 6-3  $\mu$ CT scanner parameters.**

Analysis of variance (ANOVA) (IBM SPSS statistics version 22) was used to assess whether drop impact velocity or fabric type had a statistically significant effect on the wet and dry impact face and dry penetrated face bloodstain area for both the PF and NPF, as well as dry impact face area among the PF, dyed and not-coloured fabrics. Tukey's HSD analysis identified which variables contributed to any significant effects. An independent samples t-test was used to assess whether there were any statistically significant differences between wet and dry impact face and dry penetrated face bloodstains between the PF and NPF. Repeated measures ANOVA was undertaken to assess whether there were statistically significant differences between the impact face and the penetrated face of the bloodstains. Interactions are only reported in the results section if they were found to be significant. Equality of variances and normality of data were checked.

## 6.6 Results

The photographs of the wet and dry bloodstains and the  $\mu$ CT and SEM images were examined to study the effects of fabric mass per unit area and impact velocity on the bloodstain area of the printed fabrics.

<sup>30</sup> <http://www.edax.com/products/eds/team-eds-system-for-the-sem> (Accessed 5th September 2018)

### 6.6.1 Wet impact face bloodstains

A high-speed video still showing the maximum spread of a blood drop impacting the PF of each fabric at three impact velocities (1.8, 4.3 and 5.7 ms<sup>-1</sup>) is shown in figure 6-2. For all three fabrics the lateral spreading of the blood drop increased as the velocity increased from 1.8 ms<sup>-1</sup> to 4.3 ms<sup>-1</sup>.

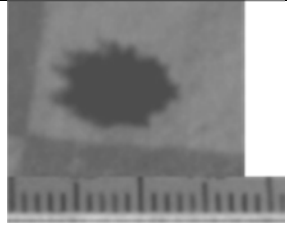
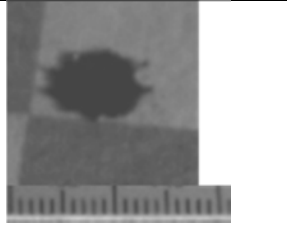
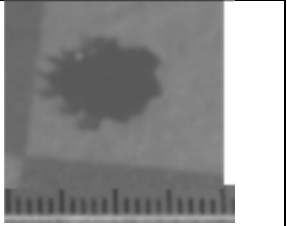
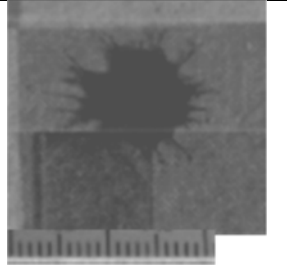
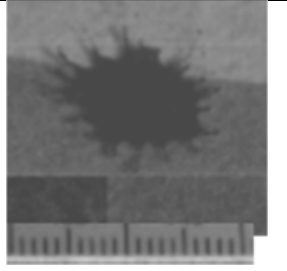
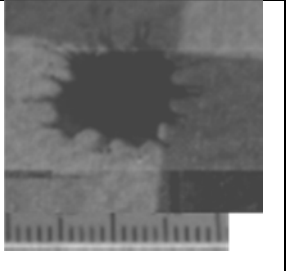
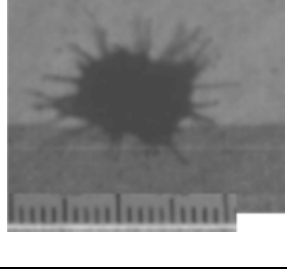
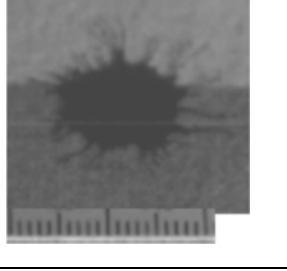
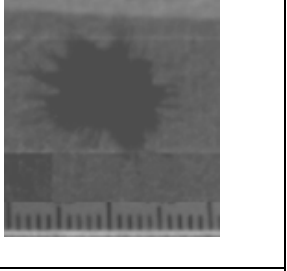
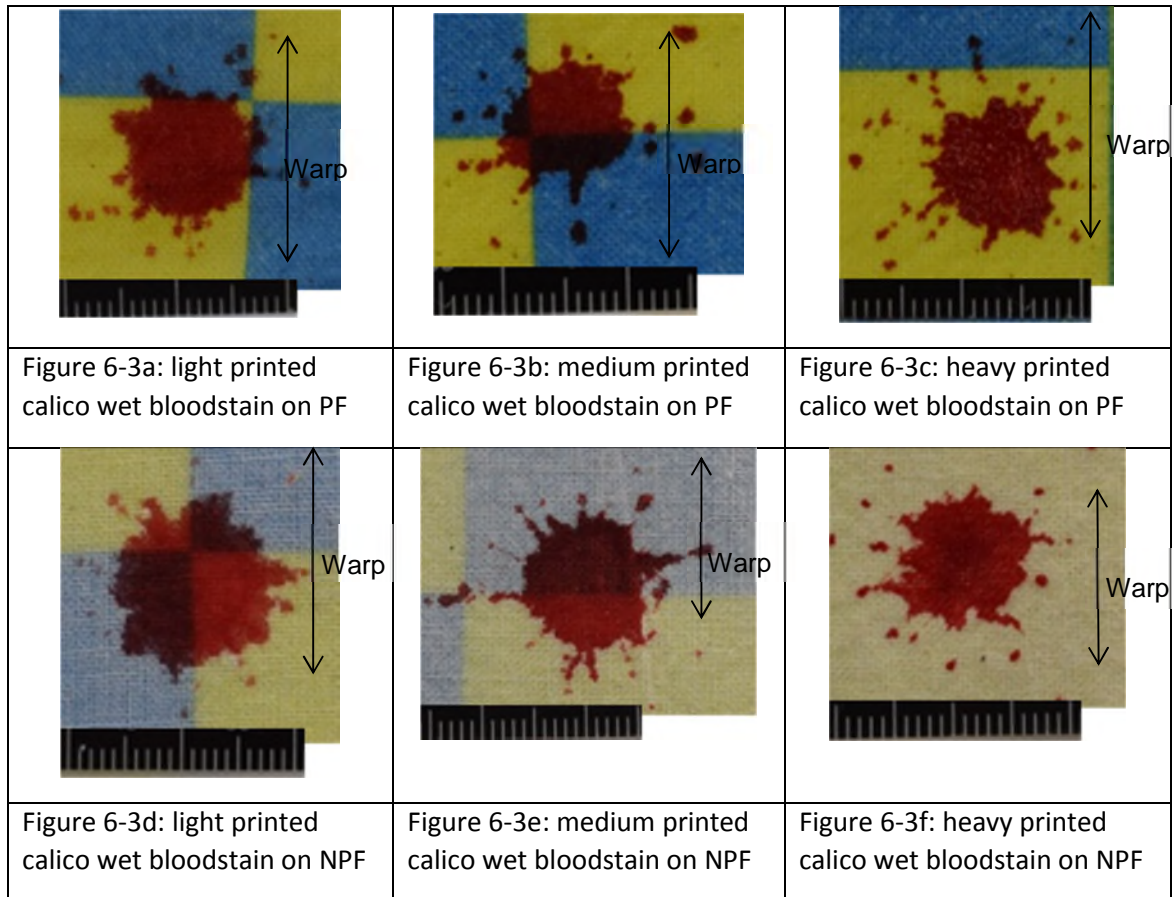
	Light calico	Medium calico	Heavy calico
1.8 ms <sup>-1</sup>			
	6-2a: 2.6 ms after impact	6-2b: 2.6 ms after impact	6-2c: 2 ms after impact
4.3 ms <sup>-1</sup>			
	6-2d: 2 ms after impact	6-2e: 1.8 ms after impact	6-2f: 1.8 ms after impact
5.7 ms <sup>-1</sup>			
	6-2g: 2 ms after impact	6-2h: 1.6 ms after impact	6-2i: 1.4 ms after impact

Figure 6-2 a high speed video still of the maximum spread of the blood drop following impact onto each fabric from each velocity. Scale is 20 mm.

Visually, the wet bloodstains from the blood drops on both the PF (figure 6-3a-c) and NPF (figure 6-3d-f) had a similar consistent colour, and therefore density, of blood across the bloodstain. No blood remained pooled on the surface of the light or

medium calico specimens. For the heavy printed calico from blood drops on both the PF and NPF, blood only remained pooled on the surface of the specimens from  $1.9 \text{ ms}^{-1}$  impacts.



**Figure 6-3** an example wet impact face bloodstain on each of the three printed fabrics from drops onto both the PF and NPF from  $4.1 \text{ ms}^{-1}$ . Scale is 20 mm.

The wet bloodstain areas of the blood drops on the PF and NPF of the fabric are shown in figure 6-4. For the medium and light calico, the wet bloodstain areas from blood drops on the NPF were larger than those on the PF of the fabric. For the heavy calico, however, there was overlap between the wet bloodstain areas from the blood drops onto both the PF and NPF. The heavy calico bloodstains also overlap with those on the PF of the medium calico; these three groups produced the smallest wet bloodstains. An independent samples t-test compared the wet bloodstain area on the PF and NPF. The wet bloodstain areas from drops on the NPF were statistically significantly larger than those on the PF for the light calico ( $t_{28} = 10.36, p \leq 0.01$ ) and the medium calico



( $t_{28} = 7.81, p \leq 0.01$ ). There was no statistically significant difference for the heavy calico between wet bloodstains on the PF and NPF.

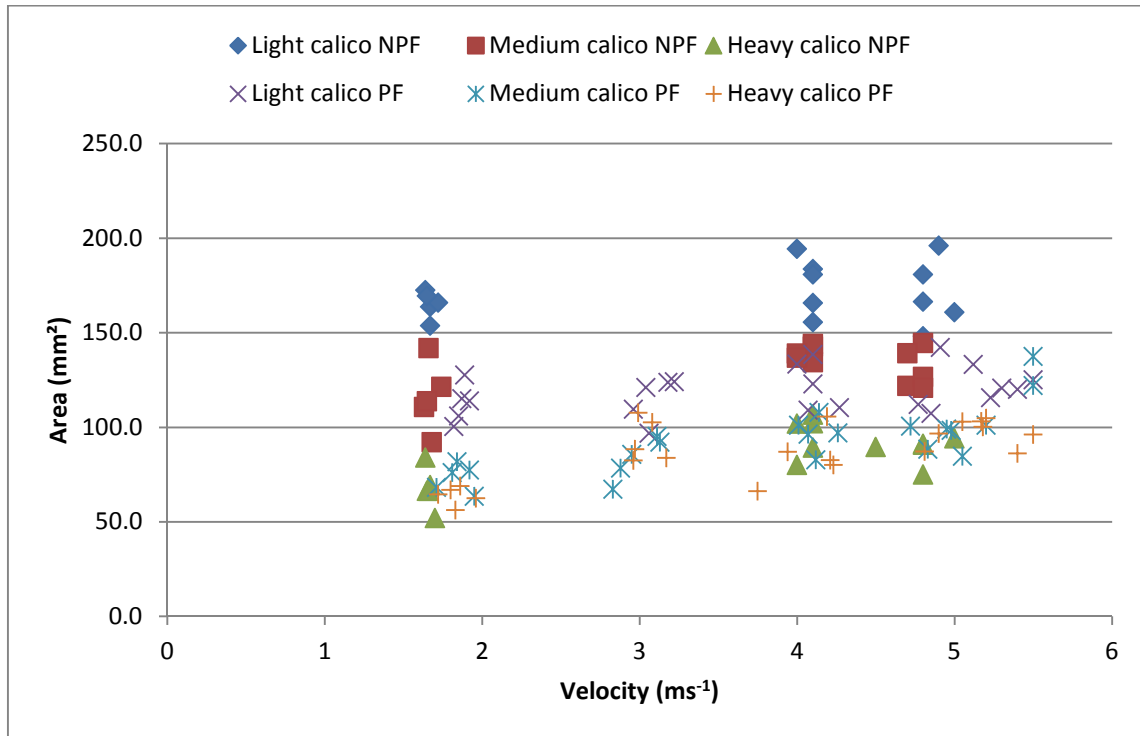


Figure 6-4 the wet bloodstain areas from the blood drops on the PF and NPF of the light, medium and heavy calicos.

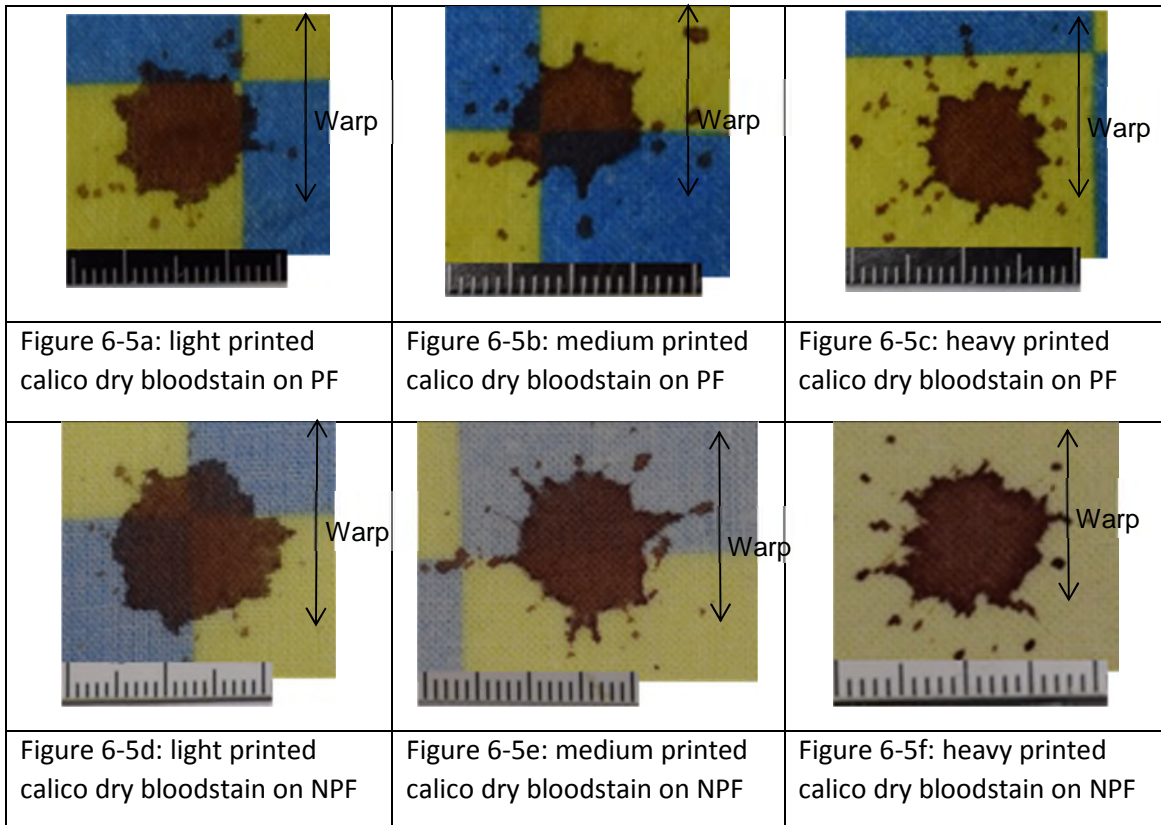
The results of univariate analysis of variance (ANOVA) and Tukey's HSD analysis on the wet bloodstain area among fabrics and velocities are given in table 6-4.

		F statistic and significance	Tukey's HSD
PF	Among fabrics	$F_{14,54} = 53.627, p \leq 0.01$	Light larger than medium and heavy calicos.
	Among velocities	$F_{14,54} = 12.894, p \leq 0.01$	1.9 $\text{ms}^{-1}$ smaller than all other velocities, 3 $\text{ms}^{-1}$ smaller than 5.4 $\text{ms}^{-1}$ .
NPF	Among fabrics	$F_{8,36} = 181.944, p \leq 0.01$	Light larger than medium and heavy, medium larger than heavy calico.
	Among velocities	$F_{8,36} = 10.914, p \leq 0.01$	1.7 $\text{ms}^{-1}$ smaller than 4.1 and 4.8 $\text{ms}^{-1}$ .

Table 6-4 results of ANOVA on the wet impact face bloodstain area.

### 6.6.2 Dry impact face bloodstains

The dry impact face bloodstains (figure 6-5) from drops on both the PF and NPF had even colouration across the majority of the bloodstain, with a very small area of darker blood surrounding the bloodstain. Very little, if any, pooled blood dried on the surface of the fabric.



**Figure 6-5** an example dry impact face bloodstain on each of the three printed fabrics from drops onto both the PF and NPF from  $4.1 \text{ ms}^{-1}$ . Scale is 20 mm.

Generally, for the blood drops on the PF, the light calico had the largest and the heavy calico the smallest dry impact face bloodstains (figure 6-6). However, there was large variation and overlap in the data. For example there was a difference of  $55.4 \text{ mm}^2$  between the largest ( $126.7 \text{ mm}^2$ ) and smallest ( $71.3 \text{ mm}^2$ ) dry bloodstain area for the medium calico specimens from an impact velocity of  $3 \text{ ms}^{-1}$  (a coefficient of variation (CV) of 21%). Although there was a slight increase in dry bloodstain area on the PF with velocity, using a least squares fit there was no correlation between dry bloodstain area and velocity for any of the printed fabrics (figure 6-6).

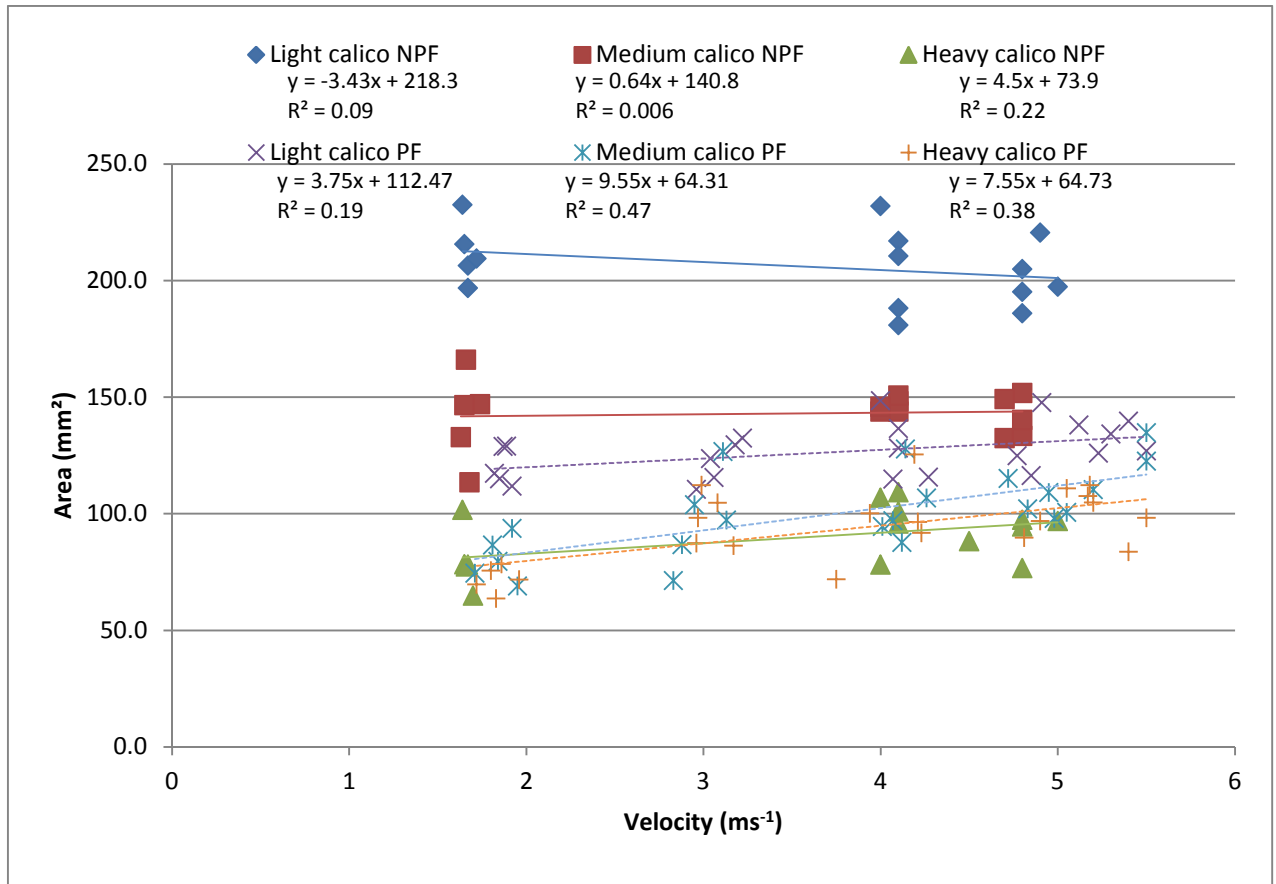


Figure 6-6 the dry bloodstain areas from the blood drops on the PF and NPF of the light, medium and heavy calicos.

The dry bloodstain areas from the blood drops on the PF and NPF were compared in figure 6-6. The dry bloodstain areas were largest on the light calico from blood drops on the NPF. As for the wet bloodstain areas, the dry bloodstains from the blood drops on the NPF of the medium and light calico were larger than their counterparts on the PF of the fabric. Again, there was overlap for the heavy calico between the dry bloodstain areas of the blood drops onto both the PF and NPF of the fabric. An independent samples t-test compared the dry bloodstain area on the PF and NPF. The dry bloodstain area from drops on the NPF was statistically significantly larger than those on the PF for the light calico ( $t_{28} = 13.526, p \leq 0.01$ ) and the medium calico ( $t_{28} = 9.336, p \leq 0.01$ ). There was no statistically significant difference for the heavy calico.

The results of ANOVA and Tukey's HSD analysis on the dry bloodstain area among fabrics and velocities are given in table 6-5.

		F statistic and significance	Tukey's HSD.
PF	Among fabrics	$F_{14,54} = 44.551, p \leq 0.01$	Light larger than medium and heavy calicos.
	Among velocities	$F_{14,54} = 8.773, p \leq 0.01$	$1.9 \text{ ms}^{-1}$ smaller than all other velocities.
NPF	Among fabrics	$F_{8,36} = 277.571, p \leq 0.01$	Light larger than medium and heavy, medium larger than heavy calico.
	Among velocities	Not significant.	

**Table 6-5 results of ANOVA on the dry impact face bloodstain area**

### 6.6.3 Dry penetrated face bloodstain

For the blood drops on either side of the fabric, the amount of blood penetrating through the fabric decreased from the light calico to the heavy calico (figure 6-7). Visually, bloodstains on the penetrated face from the drops on the NPF (figure 6-7d-f) appeared patchier than those from the drops on the PF (figure 6-7a-c). The results of ANOVA and Tukey's HSD analysis on the dry penetrated face bloodstain area among fabrics and velocities are given in table 6-6.

		F statistic and significance	Tukey's HSD.
PF	Among fabrics	$F_{14,54} = 135.127, p \leq 0.01$	Light larger than medium and heavy, medium larger than heavy calico.
	Among velocities	$F_{14,54} = 3.763, p \leq 0.01$	$1.9 \text{ ms}^{-1}$ smaller than $5 \text{ ms}^{-1}$ .
NPF	Among fabrics	$F_{8,36} = 255.214, p \leq 0.01$	Light larger than medium and heavy, medium larger than heavy calico.
	Among velocities	Not significant.	

**Table 6-6 results of ANOVA on the dry penetrated face bloodstain area**

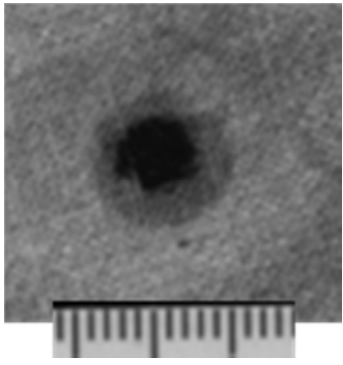
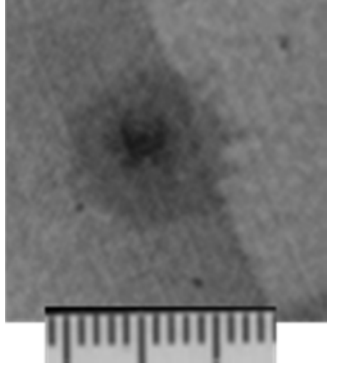
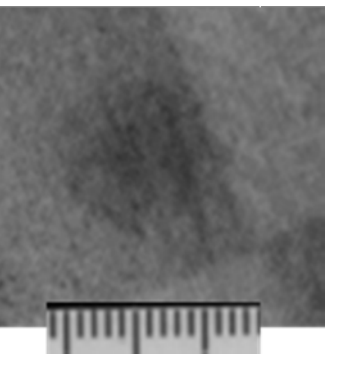
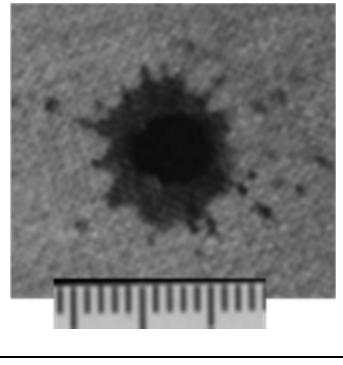
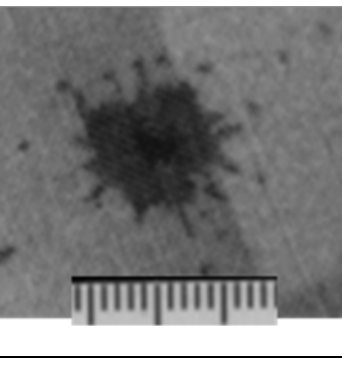
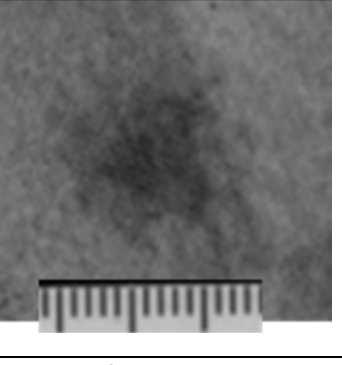
An independent samples t-test compared the penetrated face bloodstain area on the PF and NPF. The penetrated face bloodstain area from drops on the NPF was statistically significantly larger than those on the PF for the light calico ( $t_{28} = 9.643, p \leq$

0.01) and the medium calico ( $t_{28} = 8.969, p \leq 0.01$ ). There was no statistically significant difference for the heavy calico.

<p>Figure 6-7a: light printed calico from drop on PF</p>	<p>Figure 6-7b: medium printed calico from drop on PF</p>	<p>Figure 6-7c: heavy printed calico from drop on</p>
<p>Figure 6-7d: light printed calico from drop on NPF</p>	<p>Figure 6-7e: medium printed calico from drop on NPF</p>	<p>Figure 6-7f: heavy printed calico from drop on NPF</p>

**Figure 6-7** an example dry penetrated face bloodstain on each of the three printed fabrics from drops onto both the PF and NPF from  $4.1 \text{ ms}^{-1}$ . Scale is 20 mm.

On the light calico for the blood drops impacting the PF, blood passed through to the rear of the specimen across the entire bloodstain. High-speed video of the technical rear of the fabric at impact from blood drops on the PF showed that the blood quickly penetrated to the rear of the light and medium calicos (figures 6-8a and b). By 20 ms following impact for the light calico and 50 ms for the medium calico blood had penetrated through the fabric across the entirety of the bloodstain (figure 6-8d and e). For the heavy calico no blood penetrated through the fabric at impact (figure 6-8c), and had not penetrated by 50 ms following impact (figure 6-8f).

		
Figure 6-8a: light printed calico 1ms following impact	Figure 6-8b: medium printed calico 1ms following impact	Figure 6-8c: heavy printed calico 1ms following impact
		
Figure 6-8d: light printed calico 20ms following impact	Figure 6-8e: medium printed calico 50ms following impact	Figure 6-8f: heavy printed calico 50ms following impact

**Figure 6-8** stills from filming the penetrated face of the fabric at impact on each printed fabric PF following impact from  $4.3 \text{ ms}^{-1}$ . Scale is 15 mm.

On the light calico for blood drops impacting the PF both the penetrated face and impact face bloodstains had consistent colouring and a slightly denser area around the edge (figure 6-5a and 6-7a). The penetrated face bloodstain was superimposed on top of the impact face bloodstain (figure 6-9) to show the similarity in shape and area between the two bloodstains, although the penetrated face bloodstain was slightly larger than the impact face bloodstain. Repeated measures ANOVA from blood drops on the PF of the light calico showed the penetrated face bloodstain ( $135.9 \text{ mm}^2$ ) was statistically significantly larger than the impact face bloodstain ( $126.6 \text{ mm}^2$ ) ( $F_{4,18} = 49.976$ ,  $p \leq 0.01$ ). On the NPF of the light calico the penetrated face bloodstain ( $194.1 \text{ mm}^2$ ) was statistically significantly *smaller* than the impact face bloodstain ( $206.2 \text{ mm}^2$ ) ( $F_{2,12} = 41.414$ ,  $p \leq 0.01$ ).




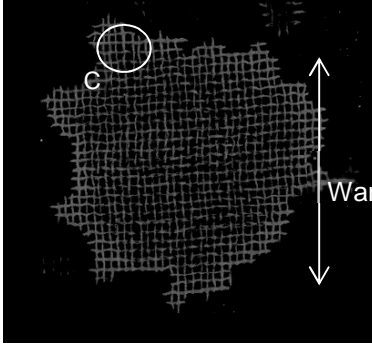
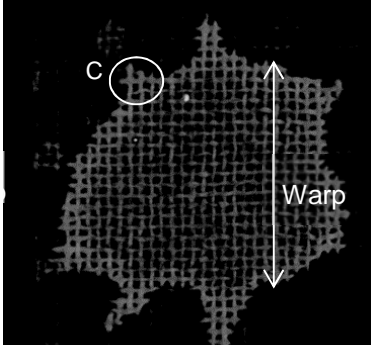
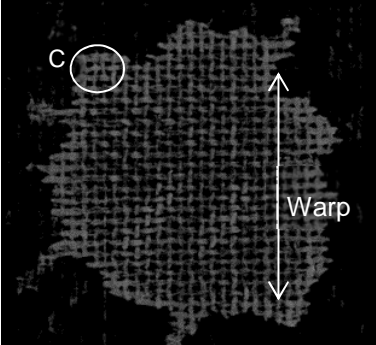
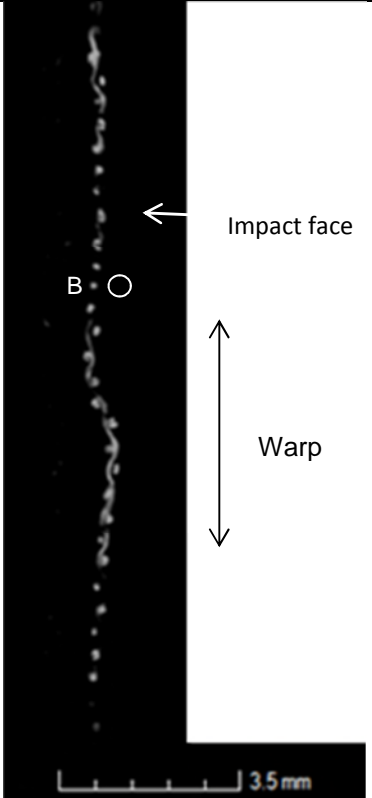
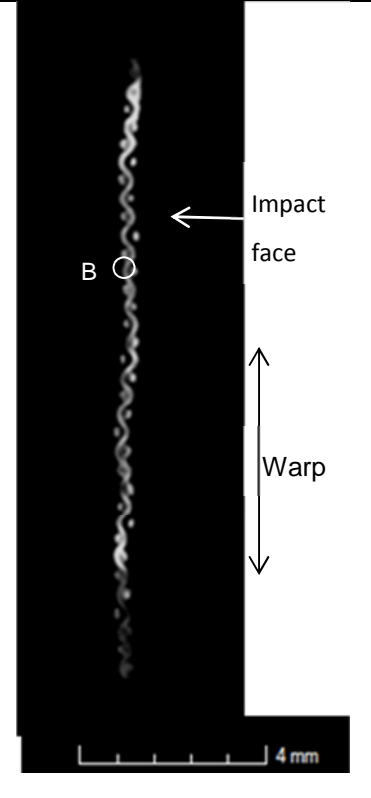
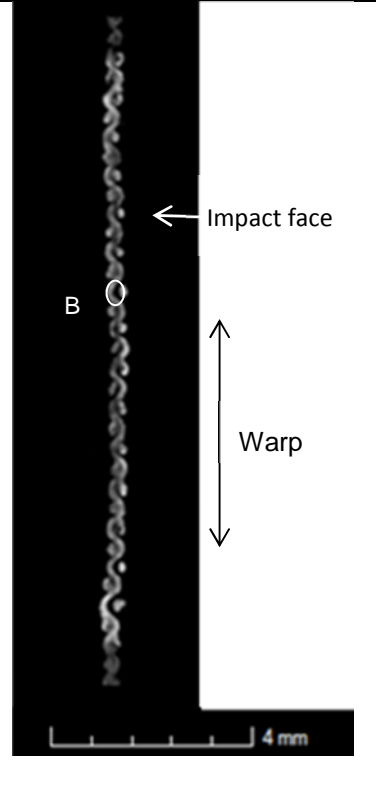
		
Figure 6-9a: light calico bloodstain from 1.9 ms <sup>-1</sup>	Figure 6-9b: light calico bloodstain from 4.1 ms <sup>-1</sup>	Figure 6-9c: light calico bloodstain from 5.4 ms <sup>-1</sup>

Figure 6-9 a typical example of a light calico (PF) penetrated face bloodstain (translucent, red) superimposed on the equivalent impact face bloodstain (opaque, black) from 1.9 ms<sup>-1</sup>, 4.1 ms<sup>-1</sup> and 5.4 ms<sup>-1</sup> showing the similarity in shape between the two bloodstains.

For blood drops onto the PF and NPF of the both medium (PF:  $F_{4,18} = 29.077$ ,  $p \leq 0.01$ ; NPF:  $F_{2,12} = 73.63$ ,  $p \leq 0.01$ ) and heavy (PF:  $F_{4,18} = 130.645$ ,  $p \leq 0.01$ , NPF:  $F_{2,12} = 132.846$ ,  $p \leq 0.01$ ) calicos, the impact face bloodstain was statistically significantly larger than the penetrated face bloodstain. For the medium and, in particular, the heavy calico, the penetrated face bloodstain is patchy as the blood has not penetrated through the fabric across the entire bloodstain.

#### 6.6.4 CT printed face bloodstains

The yarns in both the warp (marked 'A') and weft (marked 'B') directions (figure 6-10d-i) were soaked in blood for all three fabrics. For the heavy calico this occurred to a greater extent on the impact face than the penetrated face, as the blood was denser towards the impact face. Blood-soaked yarns were present across the entire bloodstain for all three fabrics (figures 6-10a-c) with only a small area around the edge of the bloodstain where the blood appeared denser, indicative of the coffee ring effect (marked 'C'). However, even in this area of denser blood there were no inter-yarn spaces filled for any of the three fabrics.

		
<p>Figure 6-10a: light printed calico 2D image of 3D reconstruction</p>	<p>Figure 6-10b: medium printed calico 2D image of 3D reconstruction</p>	<p>Figure 6-10c: heavy printed calico 2D image of 3D reconstruction</p>
		
<p>Figure 6-10d: light printed calico CT cross-section in the warp direction</p>	<p>Figure 6-10e: medium printed calico CT cross-section in the warp direction</p>	<p>Figure 6-10f: heavy printed calico CT cross-section in the warp direction</p>



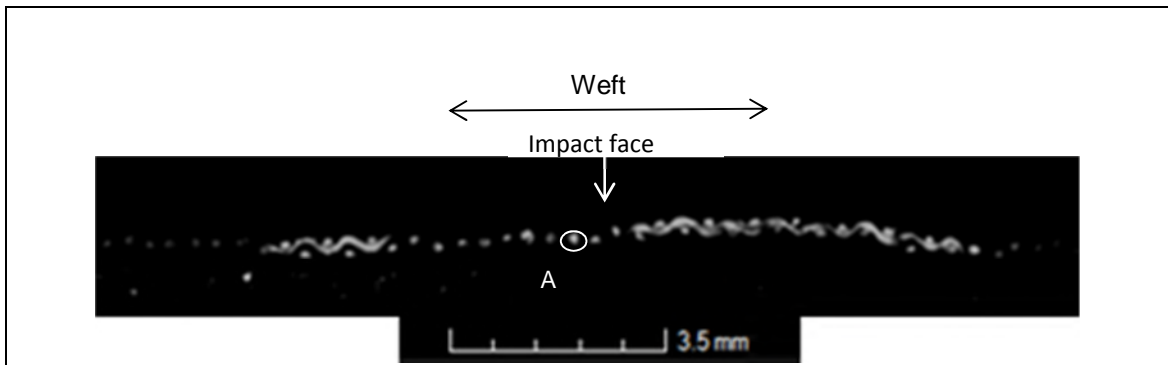


Figure 6-10g: light printed calico CT cross-section in the weft direction

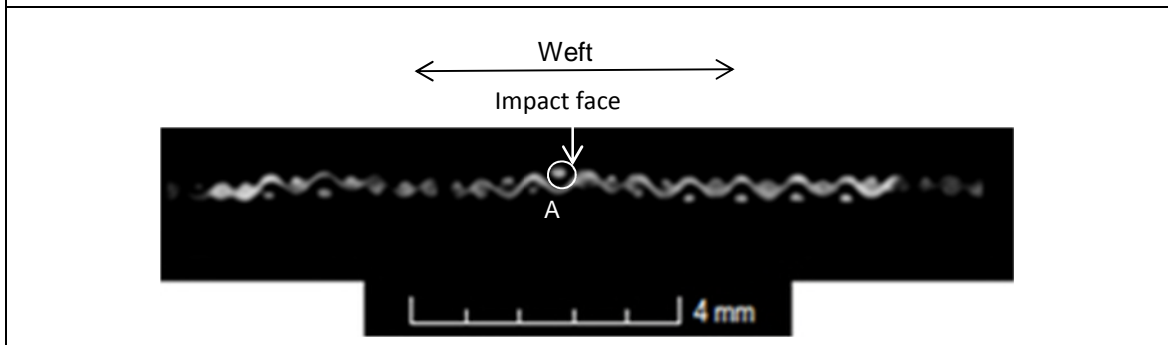


Figure 6-10h: medium printed calico CT cross-section in the weft direction

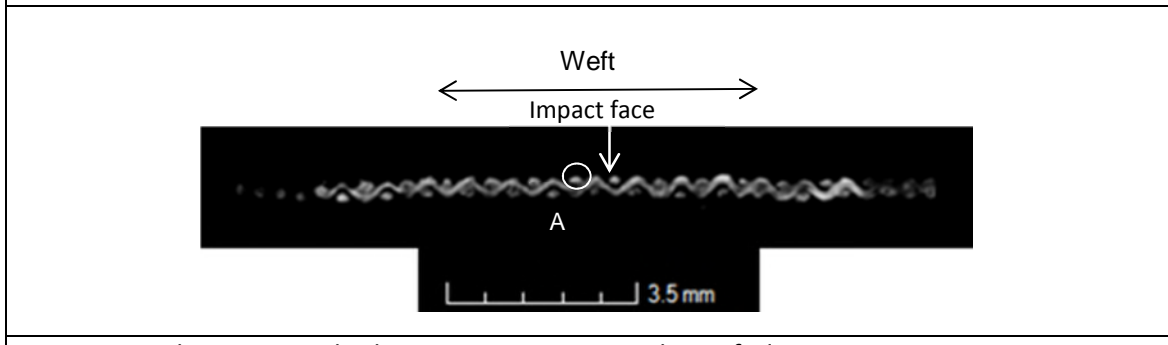


Figure 6-10i: heavy printed calico CT cross-section in the weft direction

Figure 6-10 A 2D image of the complete 3D reconstruction and cross-sections from a specimen from the printed calico from  $4.1 \text{ ms}^{-1}$ . 'A' is a blood-soaked warp yarn, 'B' a blood-soaked weft yarn. 'C' is an example of the denser blood at the edge of the bloodstain.

### 6.6.5 SEM printed face bloodstains

For all three printed fabrics from blood drops on the PF the SEM images (figure 6-11a-c) showed the blood was entirely contained within the yarns themselves and there were no inter-yarn spaces filled. There does not appear to be any blood coating the yarns (figures 6-11d-f) as the external fibres were relatively free of blood. The blood therefore was inside the intra-yarn spaces.

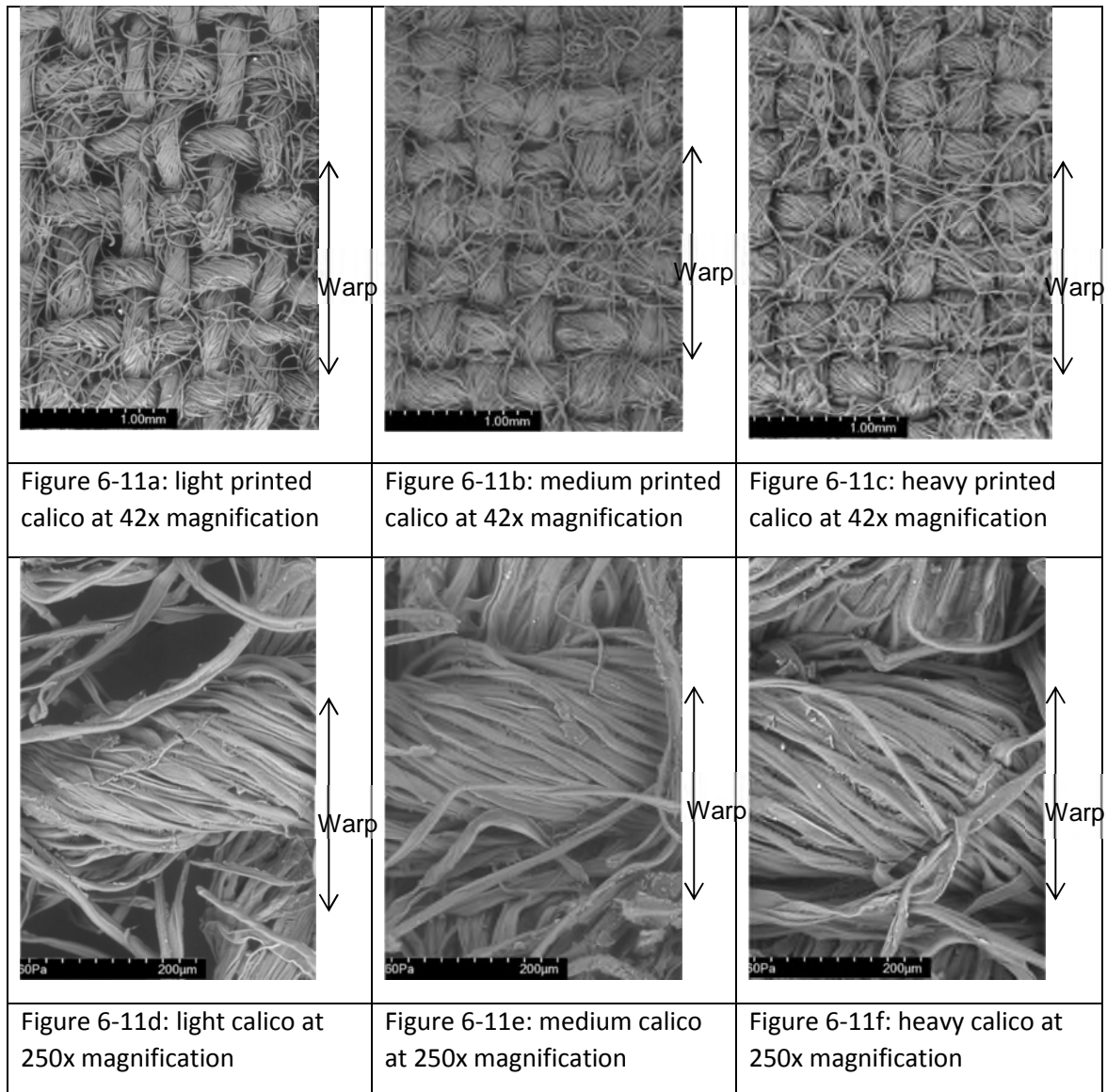


Figure 6-11 a typical example of an SEM image of a bloodstain on each fabric from  $4.1 \text{ ms}^{-1}$

## 6.7 Discussion

The discussion will be separated into four sections to investigate the issues revealed in the results above:

- The trends seen in the bloodstains from blood drops on the PF.
- Comparison between the bloodstains from blood drops on the PF and NPF.
- The effect of the printing on the fabric.
- Comparison to not-coloured [6] and dyed [10] calicos.

### 6.7.1 Bloodstains from blood drops on the PF

When the blood initially impacted the printed calico, the amount of lateral spreading which occurred on the surface of the fabric depended on the impact velocity (figure 6-2). On the light and medium printed calico blood penetrated through the fabric following impact (figure 6-8). The maximum lateral spread on the surface of the medium and light calicos was reached by between 1.6 and 2.6 ms after impact (figure 6-2). The lack of blood which pooled on the surface of the medium and light calicos (figure 6-3) suggests the blood was able to wet and swiftly spread over the surface of the fabric.

On the light and medium calicos, owing to the lower thickness and yarn linear density of these fabrics than the heavy calico, the blood wicked through to the penetrated face of the fabric across the entire bloodstain by 20 ms and 50 ms after impact respectively (figure 6-8). Although blood did not reach the penetrated face of the heavy calico within the high speed video (figure 6-8), the blood did reach the penetrated face of the heavy calico before drying (figure 6-7c). For all three fabrics, as the blood was within the intra-yarn spaces in both the warp and weft yarns, (figure 6-10d-i), it could wick along the intra-yarn spaces. This resulted in the large bloodstain area seen across all three printed fabrics.

The large amount of wicking affected the correlation of the dry bloodstain area with velocity. At impact the amount of lateral spreading which occurred varied depending

on the impact velocity (figure 6-2). However, the amount of wicking which occurred following this was not dependent on the impact velocity. How much wicking can occur within a fabric varies with any irregularities within the yarns and fabric [16]. This resulted in CVs of up to 21% within any given velocity, and very little difference among the velocities for all three fabrics (figure 6-6). In a crime scene situation it could not be assumed that a larger bloodstain seen on a printed fabric impacted at a higher velocity than that of a smaller bloodstain.

The only impact face dry bloodstain areas which were statistically significantly different were the specimens from an impact velocity of  $1.9 \text{ ms}^{-1}$ , which were significantly smaller than all other velocities. From  $1.9 \text{ ms}^{-1}$  the amount of spreading at impact was considerably less than for the other velocities (figure 6-2a-c). Although wicking occurred following this, as the bloodstain was initially small, it remained statistically significantly smaller than all the other velocities.

The dry bloodstain images (figure 6-5a-c) and SEM images (figure 6-11) showed very little blood remained pooled on the surface of the printed fabrics. The CT scans (figure 6-10) showed the particulates were evenly spread out throughout the bloodstains. There was therefore very little evidence of the blood drying in the manner of the coffee ring effect [17].

The effect of the amount of wicking on the bloodstain area can be seen most clearly in the light, printed calico. The low yarn linear density of the light calico allowed the blood to more easily coat the yarns and wick into them. The low yarn linear density also meant there was less volume in each yarn for the blood to fill, and therefore the blood could wick further along the yarns. Similar bloodstain sizes were seen at each velocity, with more variation within a velocity than among the velocities. This was due to the large amount of wicking along the intra-yarn spaces at every velocity. The difference between the mean dry impact face bloodstain area from a velocity of  $1.9 \text{ ms}^{-1}$  ( $120.4 \text{ mm}^2$ ) and that from  $5.4 \text{ ms}^{-1}$  ( $133.6 \text{ mm}^2$ ) was  $13.2 \text{ mm}^2$ , while the variation of bloodstain areas for specimens from a velocity of  $2.9 \text{ ms}^{-1}$  was  $22 \text{ mm}^2$ .

The other result of the amount of wicking seen on the light calico was the similarity between the impact face (figure 6-5a) and penetrated face (figure 6-7a) bloodstains, as both had a consistent colouring across the bloodstain with a slightly denser area around the edge. For all but one specimen, the penetrated face bloodstain was larger than the impact face bloodstain. There were no obvious differences between the two to ascertain from which side the blood impacted. Therefore, for bloodstains from impacts on the PF of the light dyed calico, the penetrated face bloodstain, as the larger of the two sides, could easily be interpreted as the side which the blood impacted. Without any contextual clues at a crime scene, such as the way in which the fabric was lying, it would be extremely difficult to ascertain on this particular printed fabric on which side the blood drop impacted. This could, therefore, lead to misinterpretation of the evidence seen, for example whether an item of clothing was being worn at the time of bloodshed, or whether it was discarded inside out.

The greater yarn linear density of the heavy calico meant the blood could not penetrate the fabric across the entire bloodstain (figure 6-7c). The blood was able to penetrate to the centre of the yarns which lay on the impact face of the fabric (figures 6-10f and i). As the heavy calico yarns were a high yarn linear density there were a greater number of intra-yarn spaces for the blood to fill than in the lower density yarns of the medium and light calico. Therefore, to wick into the centre of the heavy calico yarns a large volume of blood would be required. Owing to the finite amount of blood on each specimen (the blood drop volume), the more blood which was required to completely penetrate the yarns, the less blood which was available for wicking along the intra-yarn spaces. This resulted in the heavy calico having the smallest mean dry bloodstain area at all but one velocity.

### **6.7.2 Comparison between bloodstains from blood drops on the PF and NPF**

For three velocities (1.7, 4.1 and 4.8 ms<sup>-1</sup>) bloodstains were created by allowing drops to fall onto the NPF of each of the three calicos. For the medium and light calico, the wet and dry impact face and dry penetrated face bloodstains created on the NPF were statistically significantly larger than those on the PF. The larger bloodstains suggests

the blood was able to wick along the intra-yarn spaces with greater ease when the blood impacted the NPF than when it impacted the PF.

For the light calico specimens from the blood drops on the PF, the penetrated face area was larger than the impact face area. This suggests the blood was able to wick further along the yarns towards the penetrated face of the fabric. When the blood drops impacted the NPF, the penetrated face bloodstains on the light calico (figure 6-7d) were smaller and patchier than the impact face bloodstains (figure 6-3d). This suggests less wicking was occurring as the blood moved through to the penetrated face. Together, these points imply the blood was able to wick more easily along the yarns on the NPF of the fabric than the PF.

There were no statistically significant differences for the heavy calico between the bloodstains created from drops on the PF and NPF. The volume of blood which was required to create the penetrated face bloodstains on the heavy calico (figure 6-7c and f) was greater than for either the medium or light calico owing to the greater thickness (0.53 mm). Therefore, the volume of blood available for wicking in the heavy calico would be depleted owing to the volume required to reach the penetrated face of the fabric. The similarity in the dry bloodstain area for drops on both the PF and NPF of the heavy calico was due to there being not enough blood available for further lateral wicking to occur following blood drop impacts on the NPF.

### **6.7.3 Effect of printing on the bloodstains**

Following drop impacts at all velocities (apart from  $1.9 \text{ ms}^{-1}$  impacts on the heavy calico), there was no blood pooled on the surface of the fabric in the wet bloodstains (figure 6-3) as the blood was able to swiftly spread over the surface of the fabric. Therefore, the primary reason for the similarity among all fabrics and velocities on the printed calico is initially the ease with which the blood could wet the fabric. This was followed by the blood penetrating or wicking into the intra-yarn spaces, and wicking along them.

To represent the wettability of a material, the cosine of the contact angle is often used [18]. The contact angle  $\theta$  is the angle between the solid-liquid interface and the tangent to the liquid-vapour interface. If the contact angle is less than  $90^\circ$ , then the liquid will wet the surface [19]. The smaller the contact angle, the greater the wettability of the surface. This also applies to the wicking of fluids along capillaries; the smaller the contact angle, the greater the capillary rise. As the printing of the calico fabric appeared to increase the ease with which the blood could wet the fabric, the contact angle between the fabric and the blood drop must have decreased. This allowed the blood to more easily wet the yarns and the fibres, and then move along the intra-yarn spaces.

The blood drops on the NPF of the calico resulted in larger dry bloodstains than the PF, suggesting a greater amount of wicking occurred in the former. Therefore, it is not the addition of the reactive dye which increased the wetting and wicking properties of the fabric, but something else within the inkjet printing process. The inkjet dye itself slightly decreased the ability of the blood to wick along the intra-yarn spaces evidenced by the smaller impact face bloodstains on the PF than the NPF. This possibly occurred as a result of the dye filling the intra-yarn spaces slightly and therefore reducing them to smaller than optimum size for wicking.

Within a typical inkjet printing process, a number of stages occur: singe > desize > scour > bleach > mercerise > dry > print > steam > wash > roll [20]. A number of these stages (scouring, bleaching, mercerising) are undertaken in order to remove the hydrophobic wax layer from the cotton fibres, increasing the wettability of the fabric and therefore the dye uptake. Although these methods are undertaken in order to improve the dye uptake within the yarns, they will also have a longer term effect on the wettability of the fabric, therefore increased the ease with which the blood drop spread on the surface of the fabric.

Once the fabric was wetted, the blood was able to enter and wick along the intra-yarn spaces. In order to increase the ease with which this could happen, the fibres and yarns would have to have been altered by the inkjet printing process. The surface

roughness of a yarn has an effect on the contact angle between water and the yarn, and therefore on transport rates in fibre assemblies [21]. The contact angles between water drops and fibres and yarns of polyethylene, nylon, Dacron and wool were measured [21]. Although the contact angles of the fibres varied only between 79 and 86°, the contact angles of the yarns were very different. The lowest contact angle was 25° for the polyethylene yarn, while the contact angle for the wool yarn was 108°, and therefore hydrophobic. The explanation for this difference lies in the rough yarns created from the wool fibres because of the natural crimp and random distribution of fibres within the yarns. Yarns of synthetic fibres, on the other hand, are compact and well-aligned [21]. Within inkjet printing, following the addition of the dye the fabric is then steamed, washed and fed onto a roll, all of which may decrease the surface roughness of the fabric. It is this possible decrease in surface roughness, with the concurrent decrease in contact angle, which may have increased the ease with which the blood could wick along the intra-yarn spaces. Larger dry impact face bloodstains were seen from blood drops on the NPF of the fabric as the surface roughness of the impact face was decreased, without the corresponding addition of the dye.

#### **6.7.4 Comparison to not-coloured and dyed calico**

The three mass per unit areas of calico investigated in the current work had previously been subjected to passive blood drops from the same drop heights when they were not-coloured [6] and following reactive dyeing [10].

The dry impact face bloodstain areas for the blood drops onto both the PF and NPF of the printed fabric, dyed [10] and not-coloured [6] fabrics are shown in figure 6-12. Although there was overlap between the dyed and not-coloured fabrics, there was very little overlap between these and the printed fabrics. The not-coloured medium and heavy calicos were the only sets of specimens where the dry bloodstain area was correlated with velocity [6].



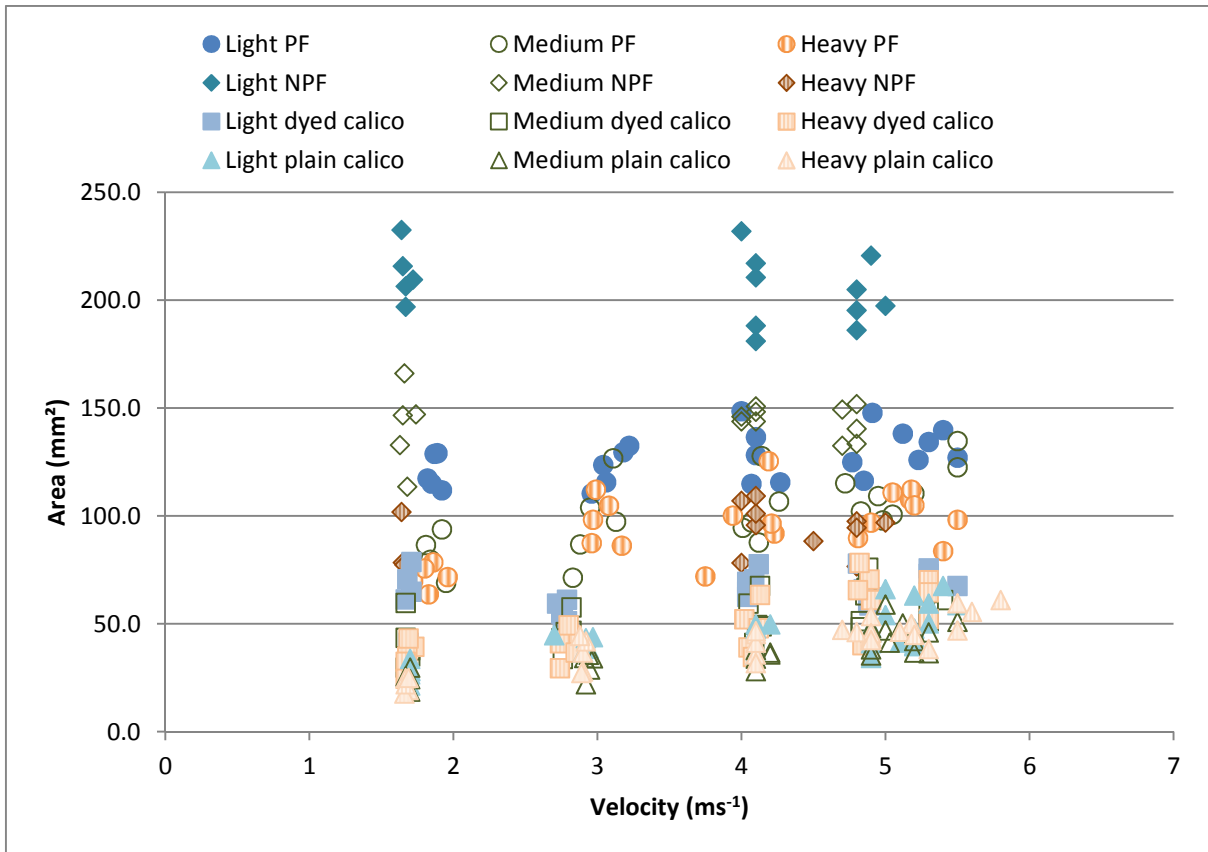


Figure 6-12 the dry impact face bloodstain areas for all specimens from blood drops on the PF and NPF of the printed calico, dyed [10] and not-coloured [6] calicos.

The amount of lateral spreading at impact did not alter between the dyed and not-coloured calicos [10]. When comparing the heavy printed and dyed calico from a drop impact of  $1.8 \text{ ms}^{-1}$ , the maximum area of spreading was  $62 \text{ mm}^2$  for the printed calico, and only  $43 \text{ mm}^2$  for the dyed calico (figure 6-13).

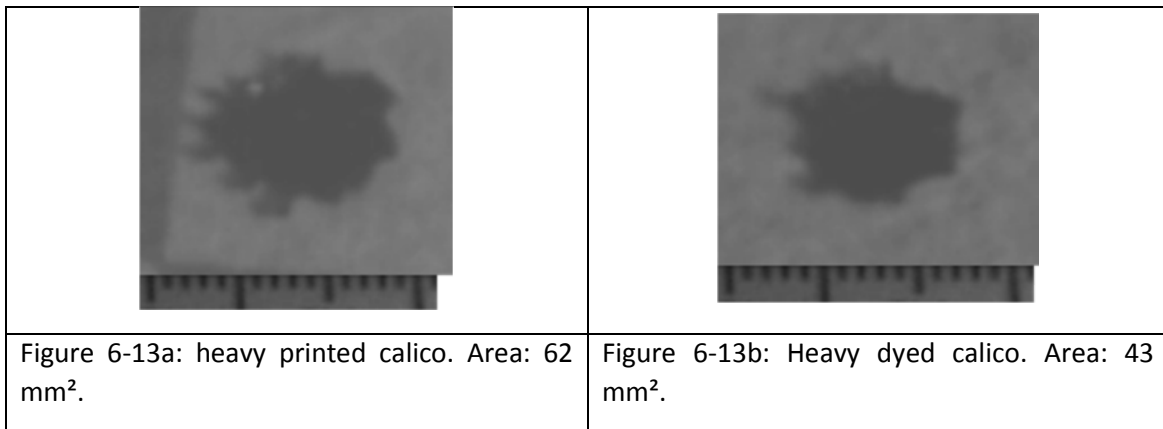

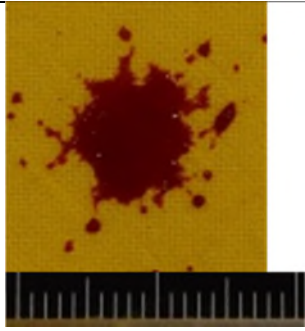
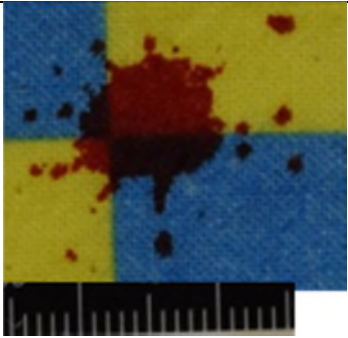
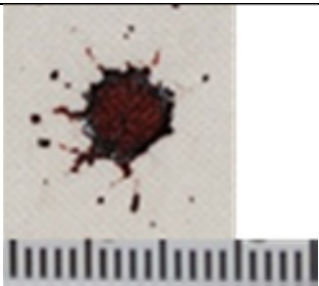
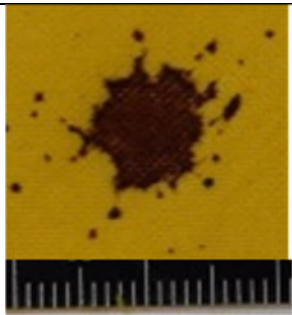
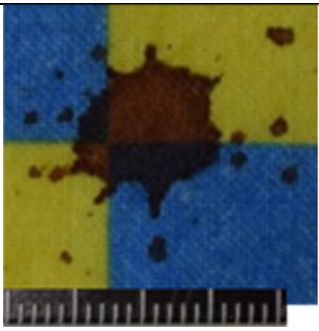


Figure 6-13 High speed video stills showing the maximum area of spreading on the dyed (image taken for research done in [10] but not used in publication) and printed heavy calico from a drop impact at  $1.8 \text{ ms}^{-1}$ . Scale:  $15 \text{ mm}$ .

Differences were seen in the wet impact face bloodstains (figure 6-14a-c) amongst the not-coloured [6], dyed [10] and printed fabrics. For the medium and heavy not-coloured calico, blood was pooled on the surface of the fabric up to and including the specimens from  $4.1 \text{ ms}^{-1}$  [6]. On the medium and heavy dyed calico, blood was only pooled on the surface of the fabric up to and including the specimens from  $2.8 \text{ ms}^{-1}$  [10]. The only pooling of wet blood which occurred on the PF and NPF of the printed calico was the specimens on the heavy calico from  $1.9 \text{ ms}^{-1}$ .

The blood which remained on the surface of the not-coloured calico dried in the manner of the coffee ring effect [6]. The large area of dense blood surrounding the central area of the bloodstain is indicative of the blood which remained on the surface of the fabric (figure 6-14d). Less pooling of blood was seen on the dyed than the not-coloured calico, with less evidence of the coffee ring effect on the surface of the fabric as a result [10] (figure 6-14e). The almost complete lack of pooling of blood on the surface of the printed calico resulted in the lack of a ring of dense blood surrounding the dried bloodstain (figure 6-14f). The dry impact face bloodstains on the PF of the printed calico were statistically significantly larger than those on the not-coloured and the dyed calicos across the light ( $F_{2,68} = 351.909, p \leq 0.01$ ), medium ( $F_{2,68} = 151.822, p \leq 0.01$ ) and heavy ( $F_{2,68} = 93.025, p \leq 0.01$ ) fabrics.

		
<p>Figure 6-14a: medium not-coloured calico, wet bloodstain</p>	<p>Figure 6-14b: medium dyed calico, wet bloodstain</p>	<p>Figure 6-14c: medium printed calico PF, wet bloodstain</p>
		
<p>Figure 6-14d: medium not-coloured calico, dry bloodstain</p>	<p>Figure 6-14e: medium dyed calico, dry bloodstain</p>	<p>Figure 6-14f: medium printed calico PF, dry bloodstain</p>

**Figure 6-14** a typical example of a wet and dry bloodstain on each of the medium not-coloured, dyed and printed calicos from  $4.1 \text{ ms}^{-1}$  [6,10]. Scale 20 mm.

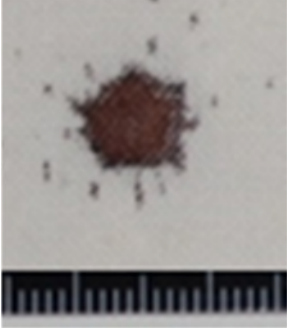
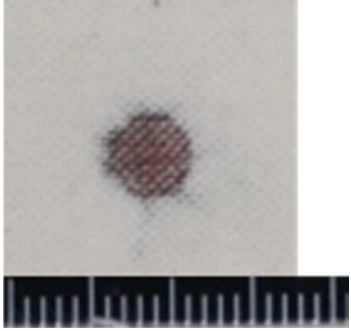
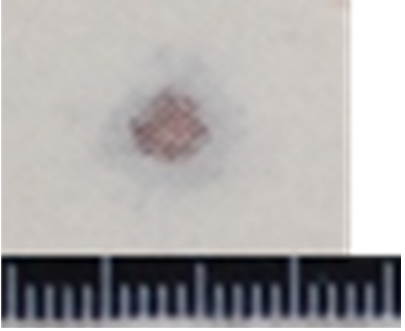
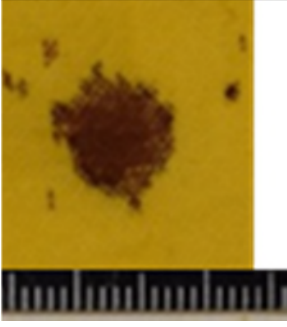
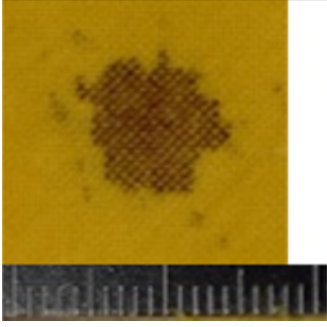
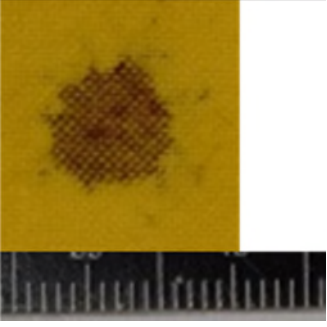
The amount of blood which penetrated through the fabric differed among the different treatments (figure 6-15). Owing to the different yarn linear densities, the light calico consistently had the largest penetrated face bloodstain area and the heavy calico the smallest across all treatments (table 6-7). For all three fabrics, the largest penetrated face bloodstains were seen from blood drops on the NPF of the printed calico, and the smallest on the not-coloured fabric.

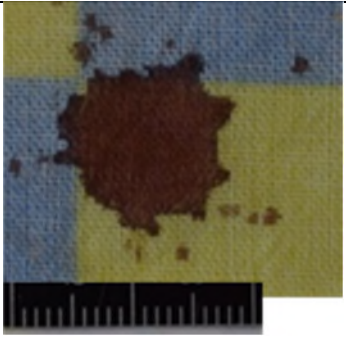
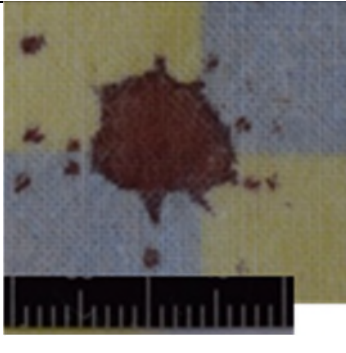
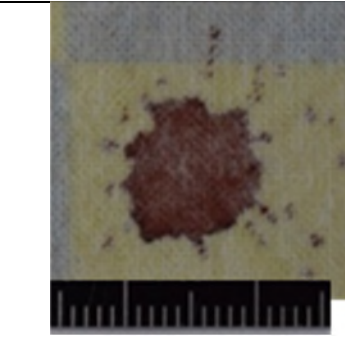
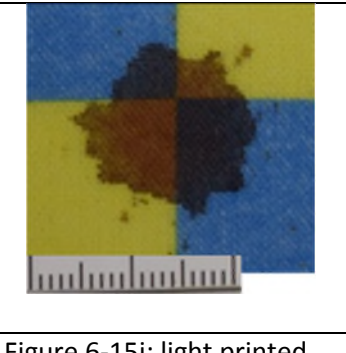
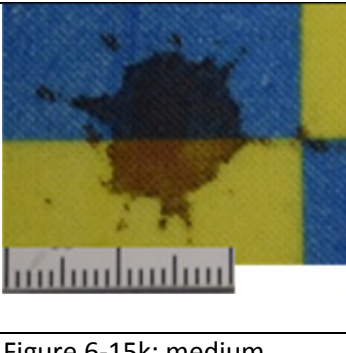
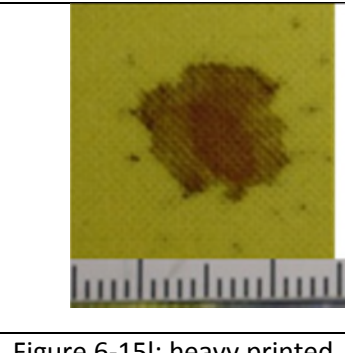
The light, printed calico from blood drops on the PF produced the only specimens where the mean penetrated face bloodstain was larger than the mean impact face bloodstain. On each of the not-coloured [6] and dyed [10] light calicos, there were only two specimens across all velocities where the penetrated face bloodstain on the light calico was larger than the impact face bloodstain. For blood drops on the NPF of the

light, printed calico, only one specimen across all velocities had a larger penetrated face than impact face bloodstain.

Fabric state	Light	Medium	Heavy
PF	136 mm <sup>2</sup>	95 mm <sup>2</sup>	72.5 mm <sup>2</sup>
NPF	194 mm <sup>2</sup>	134.7 mm <sup>2</sup>	79.7 mm <sup>2</sup>
Dyed	62.3 mm <sup>2</sup>	40.9 mm <sup>2</sup>	26.1 mm <sup>2</sup>
Not-coloured	37.9 mm <sup>2</sup>	15.2 mm <sup>2</sup>	14.9 mm <sup>2</sup>

**Table 6-7 the mean penetrated face bloodstain area for each fabric state and each mass per unit area [6,10].**

		
Figure 6-15a: light not-coloured calico	Figure 6-15b: medium not-coloured calico	Figure 6-15c: heavy not-coloured calico
		
Figure 6-15d: light dyed calico	Figure 6-15e: medium dyed calico	Figure 6-15f: heavy dyed calico

		
Figure 6-15g: light printed calico from drops on PF	Figure 6-15h: medium printed calico from drops on PF	Figure 6-15i: heavy printed calico from drops on PF
		
Figure 6-15j: light printed calico from drops on NPF	Figure 6-15k: medium printed calico from drops on NPF	Figure 6-15l: heavy printed calico from drops on NPF

**Figure 6-15** a typical example of a penetrated face bloodstain from an impact velocity of  $4.1 \text{ ms}^{-1}$  on each mass per unit area and treatment of fabric [6,10] (figure 6-15d not used in publication). Scale 20 mm.

The differences in the wet and dry impact face and dry penetrated face bloodstains among the four groups of specimens were indicative of differences in the interaction of the blood and the fabric. The blood drops on the printed fabric initially spread on the surface of the fabric to a greater extent than on the dyed calico (figure 6-13). This was indicative of the blood being able to wet the surface of the fabric to a greater extent for the printed calico than for the dyed calico. This was a result of the procedures in the inkjet printing process (e.g. scouring, bleaching, mercerising) which removed the hydrophobic layer from the cotton yarns in order to increase the dye uptake.

The larger wet and dry bloodstains for the printed calico (PF and NPF) than either the dyed or not-coloured fabrics indicate the blood was also able to wick into and along

the yarns to a greater extent for the printed calico. This was indicative of a lower surface roughness for the printed fabric. The larger dry penetrated face bloodstain for the printed than either of the other two fabrics further suggests a decrease in the surface roughness of the yarns themselves, which allowed the blood to penetrate the inter- and intra-yarn spaces and wick along the yarns with greater ease. Larger bloodstains on fabric with a lower surface roughness have previously been seen when comparing 100% cotton plain woven and single jersey knit fabrics [3]. Bloodstains were larger on the plain woven fabrics, in part owing to the lower geometric roughness of the woven ( $3.3 \mu\text{m}$ ) as compared to the knitted ( $4 \mu\text{m}$ ) fabric.

The blood was not able to wet and wick into the dyed [10] and not-coloured [6] fabrics as easily as the printed fabric, possibly owing in part to the greater surface roughness of the former fabrics. Previous research [8] has shown that dyeing may increase the surface roughness of a fabric owing to the creation of surface irregularities in the fabric as a result of the dyeing process. Therefore, the bloodstains on the dyed calico were smaller than those on the printed calico. However, it was thought that the bloodstains on the dyed calico were larger than those on the not-coloured calico owing to differences in the intra-yarn spaces created as a result of the dyeing process, making them a more optimum size for wicking [10].

Although the mechanisms were different, blood was able to wick more easily into and along the yarns for the dyed (owing to more optimally sized capillary spaces) [10] and printed (owing to increased wettability) than for the not-coloured [6] calico. This led to no correlation with velocity being seen for either of the printed (PF and NPF) or dyed fabrics, as variations within the fabrics and yarns themselves would have had an effect on the amount of wicking which occurred [16]. This increased the variability of dry bloodstain area among specimens. The correlation between dry bloodstain area and velocity which was seen for the heavy and medium not-coloured calico was a result of the smaller amount of wicking which occurred for these fabrics. The primary mechanism which created the dry bloodstain area for the medium and heavy not-

coloured fabrics was the increase in lateral spreading with increase in impact velocity [6].

## **6.8 Conclusion**

Passive bloodstains were created from five different impact velocities (1.9, 3, 4.1, 5 and 5.4 ms<sup>-1</sup>) on three different mass per unit areas (light: 88 g/m<sup>2</sup>, medium: 165 g/m<sup>2</sup> and heavy 226 g/m<sup>2</sup>) of 100% cotton plain woven calico which had been digitally printed with reactive dye. Three impact velocities (1.7, 4.1 and 4.8 ms<sup>-1</sup>) were also used to create passive bloodstains on the not printed face (NPF) of the fabrics. Among the three mass per unit areas of fabric (printed face (PF) and NPF) the dry impact face bloodstains appeared visually similar. The bloodstains had even colouration across the majority of the bloodstain, with a very small area of darker blood surrounding the bloodstain. The dry impact face bloodstains on the NPF of the medium and light calicos were statistically significantly larger than those on the PF. Owing to the lower yarn linear density the largest dry impact face bloodstains were seen on the light calico, and the smallest on the heavy calico with the highest yarn linear density. For the light calico from blood drops on the PF, the mean penetrated face bloodstain was larger than the mean impact face bloodstain. This may make it difficult to ascertain onto which side the blood drop impacted.

When comparing the dry bloodstains between the printed calico and those which had been previously produced on dyed [10] and not-coloured [6] fabrics, those on the printed fabrics were statistically significantly larger. The similarities among the printed fabrics, and the differences between the printed fabrics and the dyed and not-coloured fabrics were as a result of the increased wicking seen in the printed fabrics. The amount of wicking seen on the printed calico, as a result of the greater wettability of this fabric, would need to be taken into account when bloodstains on printed fabrics were assessed at crime scenes. Comparison between printed fabrics and fabrics with other, or no, processing treatment would be difficult as regardless of the impact velocity the area of the bloodstains would vary depending on the treatment.

## 6.9 References

- [1] B. White, Bloodstain pattern on fabrics: the effect of drop volume, dropping height and impact angle, *Can. Soc. Forensic Sci. J.* 19 (1986) 3–36.
- [2] National Research Council, *Strengthening Forensic Science in the United States: A Path Forward*, Washington, 2009.
- [3] T.C. de Castro, M.C. Taylor, J.A. Kieser, D.J. Carr, W. Duncan, Systematic investigation of drip stains on apparel fabrics: The effects of prior-laundrying, fibre content and fabric structure on final stain appearance, *Forensic Sci. Int.* 250 (2015) 98–109. doi:10.1016/j.forsciint.2015.03.004.
- [4] T.C. De Castro, D.J. Carr, M.C. Taylor, J.A. Kieser, W. Duncan, Drip bloodstain appearance on inclined apparel fabrics: Effect of prior-laundrying, fibre content and fabric structure, *Forensic Sci. Int.* 266 (2016) 488–501. doi:10.1016/j.forsciint.2016.07.008.
- [5] J.Y.M. Chang, S. Michielsen, Effect of fabric mounting method and backing material on bloodstain patterns of drip stains on textiles, *Int. J. Legal Med.* (2016). doi:10.1007/s00414-015-1314-z.
- [6] L. Dicken, C. Knock, S. Beckett, D.J. Carr, The effect of fabric mass per unit area and blood impact velocity on bloodstain morphology, (2018) Submitted for publication.
- [7] X. Li, J. Li, S. Michielsen, Effect of yarn structure on wicking and its impact on bloodstain pattern analysis (BPA) on woven cotton fabrics, *Forensic Sci. Int.* 276 (2017) 41–50. doi:10.1016/j.forsciint.2017.04.011.
- [8] H. Hasani, Effect of different processing stages on mechanical and surface properties of cotton knitted fabrics, *Indian J. Fibre Text. Res.* 35 (2010) 139–144.
- [9] Q. Li, J.J. Wang, C.J. Hurren, A Study on Wicking in Natural Staple Yarns, *J. Nat. Fibers.* 14 (2017) 400–409. doi:10.1080/15440478.2016.1212763.
- [10] L. Dicken, C. Knock, D.J. Carr, S. Beckett, The effect of reactive dyeing of fabric



on the morphology of passive bloodstains, (2018) Submitted for publication.

[11] J. Li, X. Li, S. Michielsen, Alternative method for determining the original drop volume of bloodstains on knit fabrics, *Forensic Sci. Int.* 263 (2016) 194–203.

doi:10.1016/j.forsciint.2016.04.018.

[12] E.M.P. Williams, M. Dodds, M.C. Taylor, J. Li, S. Michielsen, Impact dynamics of porcine drip bloodstains on fabrics, *Forensic Sci. Int.* 262 (2016) 66–72.

doi:10.1016/j.forsciint.2016.02.037.

[13] J. Hayward, Smithers Pira Forecasts 17.5% annual growth for digital textile print, *Futur. Text. Print. to 2021.* (2016).

<https://www.smitherspira.com/news/2016/november/growth-for-digital-textile-print-market> (accessed December 4, 2017).

[14] Magic Textiles, Finished Products, (2016).

<https://www.magictextiles.co.uk/bespoke-printing/> (accessed March 28, 2018).

[15] L. Dicken, C. Knock, D.J. Carr, S. Beckett, Investigating bloodstain dynamics at impact on the technical rear of fabric, (2018) Submitted for publication.

[16] A.B. Nyoni, D. Brook, Wicking mechanisms in yarns—the key to fabric wicking performance, *J. Text. Inst.* 97 (2006) 119–128. doi:10.1533/joti.2005.0128.

[17] D. Brutin, B. Sobac, B. Loquet, J. Sampaol, Pattern formation in drying drops of blood, *J. Fluid Mech.* 667 (2011) 85–95. doi:10.1017/S0022112010005070.

[18] A. Patnaik, R.S. Rengasamy, V.K. Kothari, A. Ghosh, Wetting and wicking in fibrous materials, *Text. Prog.* 1 (2006) 1–105. doi:10.1533/tepr.2006.0001.

[19] P.W. Atkins, *Physical Chemistry*, 6th Edition, Oxford University Press, Oxford, 1998.

[20] C. Hawkyard, Substrate preparation for ink-jet printing, in: H. Ujiie (Ed.), *Digit. Print. Text.*, Woodhead Publishing, Cambridge, 2006: pp. 201–217.

[21] N. Hollies, M. Kaessinger, H. Bogarty, *Water Transport Mechanisms in Textile*

Materials Part I: The Role of Yarn Roughness in Capillary-Type Penetration, *Text. Res. J.*  
26 (1956) 829–835.

## **7 Discussion**

Bloodstains on fabric are frequently found at crime scenes, on both clothing fabrics and upholstery, however a thorough understanding of how blood and fabric interacts is lacking. Although the amount of research being undertaken in this area is increasing, the effect of a number of fabric properties is still not fully understood. Therefore, the overall aim of the work in this thesis was to improve understanding of the interaction of blood and fabric. The work described in this thesis studied the effect of different fabric properties on the resultant bloodstains. Passive blood drops were allowed to fall vertically onto three different mass per unit areas (85.1 g/m<sup>2</sup>, 163.5 g/m<sup>2</sup> and 224.6 g/m<sup>2</sup>) of calico (100% cotton, plain woven) which was either not-coloured, reactively dyed or digitally printed. The falling blood drops were filmed using high-speed video to measure the droplet diameter and impact velocity. The resultant wet and dry bloodstains were photographed, and the bloodstain areas measured using the in-built tools in ImageJ. The dry bloodstains were then examined using  $\mu$ CT scans and SEM images, which were novel techniques to BPA, to understand how the blood was interacting with the fabrics.

### **7.1 Bloodstain formation**

Bloodstains were found to form on the fabric in two stages; the dynamics of the blood drop immediately following impact, including wetting the surface of the fabric and penetration to the technical rear of the fabric, followed by wicking into and along the yarns.

#### **7.1.1 Wetting**

Following impact, the blood spread laterally, wetting the surface of the fabric. The current work has confirmed that the amount of lateral spreading increased with an increase in impact velocity (figures 5-2 pg109 and 6-2 pg136), as was previously found in work on solid surfaces [1,2]. The increase in lateral spreading at impact was owing to the kinetic energy at impact being converted to surface energy [3]. The amount of lateral spreading at impact was consistent between the dyed and not-coloured fabrics (figure 5-10 pg121), but not between the dyed and printed fabrics (figure 6-13 pg154).

Although the kinetic energy at impact was a key mechanism determining the amount of spreading which occurred on the surface on the fabric, it was not the sole mechanism.

The effect of digital printing on the wetting properties of fabric does not appear to have been previously reported. An increase in the wettability of the fabric would result in the blood being able to spread more easily on the surface of the fabric (figure 6-13 pg154). One or a number of factors within the printing process caused this difference to occur.

A number of different processes are undertaken in order to inkjet print a fabric: singe<sup>31</sup> > desize<sup>32</sup> > scour<sup>33</sup> > bleach > mercerise<sup>34</sup> > dry > print > steam > wash > roll [4]. Cotton is a naturally hydrophobic fibre, owing to the waxes present on the surface of the fibre [5]. The fabric is scoured, bleached and mercerised to remove the hydrophobic layer on the fibres, improving the wettability of the fabric and therefore the dye-uptake [4]. As well as improving dye-uptake, the wettability of the fabric would also be improved in terms of the spreading of the blood drop on the surface of the fabric.

The large amount of spreading at impact assisted in the printed fabrics having the largest dry bloodstains (figure 6-12 pg154). The differences between the dry bloodstains formed on the printed fabrics to those on the dyed and not-coloured fabrics emphasised the importance of understanding that different finishing treatments can result in very different dry bloodstains. This would be imperative at a

---

<sup>31</sup> 'To remove, in a flame, or by infra-red radiation, or by burning against a hot plate, unwanted surface fibres'. Textile Terms and Definitions (2002) 11<sup>th</sup> edition (revised) edited by Denton, M.J. and Daniels P.N.

<sup>32</sup> 'The removal of size from woven fabrics'. Textile Terms and Definitions (2002) 11<sup>th</sup> edition (revised) edited by Denton, M.J. and Daniels P.N.

<sup>33</sup> 'The treatment of textile materials in aqueous or other media in order to remove natural fats, waxes, proteins and other constituents'. Textile Terms and Definitions (2002) 11<sup>th</sup> edition (revised) edited by Denton, M.J. and Daniels P.N.

<sup>34</sup> 'The treatment of cellulosic fibres...with a concentrated solution of caustic alkali whereby fibres are swollen, the moisture regain, strength and dye affinity of the materials are increased, and their handle is modified'. Textile Terms and Definitions (2002) 11<sup>th</sup> edition (revised) edited by Denton, M.J. and Daniels P.N.

crime scene, where blood could land on a fabric which has been treated in any number of ways. Without understanding the effects of the finishing treatment on the interaction of blood and the fabric, any bloodstains could easily be misinterpreted. The larger size and more even colouration of the bloodstains on the printed fabric could easily be interpreted as having come from a different impact mechanism than the smaller and denser bloodstains seen on the other fabrics.

### **7.1.2 Penetration**

Whether or not blood penetrated through to the technical rear of the fabric as a result of the impact dynamics depended on the impact velocity of the blood drop and the fabric mass per unit area (figure 4-4 pg90 and figure 6-8 pg143). On the light not-coloured, printed and dyed calicos and the medium not-coloured (at 4.2 and 5.7 ms<sup>-1</sup>) and printed (at 1.8, 4.3 and 5.7 ms<sup>-1</sup>) fabrics, blood had penetrated through to the technical rear of the fabric by no more than 1 ms following impact. The blood was able to penetrate the lower mass per unit area fabrics as a result of the kinetic energy at impact, forcing the blood into the inter-yarn spaces. Blood did not penetrate through to the technical rear of the heavy calico as a result of the impact of the blood drop for any of the three treatments. This was due to the greater mass per unit area and yarn linear density of the heavy calico, so the blood was not able to penetrate the smaller inter-yarn spaces.

Following the drop spreading laterally on the surface of the fabric, the blood then retracted, before the impact dynamics finished by no more than 14 ms after impact.

### **7.1.3 Wicking**

Following the completion of the impact dynamics, once the blood drop had settled on the surface of the fabric, wicking was able to occur. If the blood had remained on the surface of the fabric following impact (e.g. not-coloured calicos at 1.7 ms<sup>-1</sup>, figure 3-5 pg50), the blood first had to wick vertically into the yarns. Once the blood had wicked into the yarns, or if the blood had penetrated the yarns at impact (e.g. light, printed calico, figures 6-3a pg137 and 6-8a pg143), the blood was then able to wick along the intra-yarn spaces.

## **7.2 Effect of yarn and fabric properties on the wicking of blood**

### **7.2.1 Summary of interaction of blood and fabric**

Variables within the fabrics and yarns themselves affected the interaction of the blood and fabric, and therefore the dry bloodstain area, following the conclusion of the lateral spreading and receding at impact. Even a simple fabric like a 100% cotton plain woven fabric can have many variables which affect the way in which blood wicks into and along the fabric. In the work discussed in this thesis, a number of yarn variables in 100% cotton plain woven fabrics were found to affect the ease with which the blood could wick into and along the yarns: intra-yarn capillary spaces, yarn twist, yarn linear density and inter-yarn spaces. In the current study, the combination of properties for the light calico, most notably the low yarn linear density and high porosity of the fabric, resulted in a fabric which was able to wick blood to a greater extent than either the medium or the heavy calico. The wicking ability of all the fabrics was increased by the dyeing and printing of the fabric, as shown in the statistically significantly larger dry bloodstains for each of these finishing treatments than the not-coloured fabric. This indicates the importance of understanding every aspect of a fabric; its yarn structure, weave and processing treatments, and the effect that each of these variables will have on the ability of blood to wet and wick into and along the fabric. A bloodstain on a fabric cannot be understood without first understanding the fabric itself.

Therefore, the effect of a number of important variables (intra-yarn capillary spaces, yarn twist, yarn linear density and inter-yarn spaces) on the interaction of blood and fabric, as revealed in chapters 2 – 6, is discussed in more detail below.

### **7.2.2 Intra-yarn capillary spaces**

In chapter five 'the effect of reactive dyeing of fabric on the morphology of passive bloodstains', it was found that the dry bloodstain areas for all three dyed calicos were statistically significantly larger than the dry bloodstain areas for the not-coloured calicos (figure 5-9 pg120). Previous work found that dyeing a 100% cotton single jersey knitted fabric created surface irregularities, increasing the surface roughness of the fabric [6]. Yarns with high surface roughness have previously been found to exhibit

poor wetting properties [7] and therefore an increase in surface roughness following dyeing would not result in an increase in dry bloodstain area as the blood would not be able to spread as easily on the surface of the fabric. The previous work [6] did not discuss an alteration to the fabric following dyeing which would alter the wicking properties of the fabric. Therefore, the work discussed in chapter five revealed a further effect of reactively dyeing the fabrics, in terms of an increase in the wicking properties of the fabric following dyeing.

The initial analysis of the fabric properties following dyeing revealed an increase in the fabric thickness and mass per unit area, with very little difference in the sett of the fabrics (table 5-1 pg105). Therefore, the yarns within the fabric were altered to result in an increase of the thickness and mass per unit area.

Previous work [8] has shown that the addition of a finishing treatment can produce an increase in the vertical wicking height of a 100% cotton fabric. When assessing the wicking height in cotton before and after treatment with durable press finishes<sup>35</sup>, an increase in vertical wicking rate was found after the treatment [8]. Examination of the total pore volume found an increase from 0.679 to 0.882 cm<sup>3</sup>, which explained the increase in vertical wicking. The larger capillary spaces seen following the addition of the durable press finish were a more optimum size for wicking. However, it is unlikely a similar increase in pore volume would have occurred following the addition of the dye to the calico fabrics. When a cotton fabric is reactively dyed, the dye enters the amorphous regions in the fibres, and covalently bonds with the cellulose [9]. Therefore, the fibres in dyed fabric are likely to have swollen following the addition of the reactive dye. This would explain the increase in the mass per unit area and thickness of the fabrics, but would have likely resulted in a decrease, rather than an increase, in the intra-yarn capillary spaces.

---

<sup>35</sup> 'A finishing treatment designed to impart to a textile material or garment the retention of specific contours...resistant to normal usage, washing and/or dry-cleaning.' Textile Terms and Definitions (2002) 11<sup>th</sup> edition (revised) edited by Denton, M.J. and Daniels P.N.

Larger than optimum capillary spaces have also been seen to reduce the amount of wicking. When comparing the wicking of ring-spun and vortex-spun yarns, ring spun yarns had higher wicking values [10]. The lower fibre-packing density of the vortex-spun yarns was thought to result in larger than optimum capillary spaces, therefore reducing the amount of wicking [10]. The capillary spaces in the not-coloured calicos may have been a larger than optimum size, with the addition of the dye to the calico fabrics decreasing the size of the capillary spaces to a more optimum size for wicking. The smaller capillary spaces would have increased the capillary pressure, increasing the amount of wicking which occurred along the yarns and therefore increasing the dry bloodstain area.

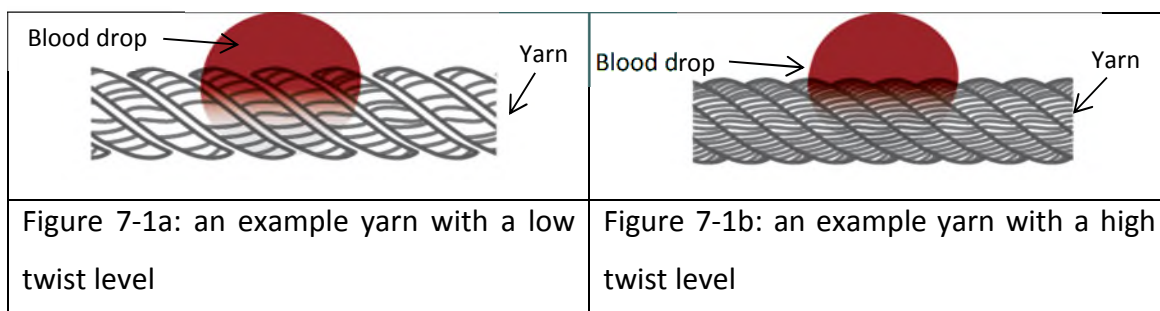
Previous work within BPA has pointed to the fact that the different capillaries created when a yarn has been spun using different methods (ring spun, open-end spun or vortex spun) alter the ability of the yarn within a fabric to wick blood [11]. However, although the effect of different capillary sizes on the wicking of blood within a fabric is known, the work presented in this thesis has shown reactively dyeing a cotton fabric also alters the capillary spaces, and therefore the wicking of the blood. The differences between bloodstains on a not-coloured fabric and those on a reactively dyed fabric is an important consideration for forensic science, as it emphasises the importance of not comparing bloodstains which have been found on fabrics with different finishing treatments. Understanding what is causing the differences seen between the two types of fabrics can provide further detail as to why the bloodstains seen may be different.

### **7.2.3 Twist**

Within textile science, it has been found that a higher twist level reduces the amount of wicking along a yarn (figure 7-1 ) [7,12]. Within a twisted yarn, the fibres are packed closely together, therefore reducing the size of the capillary spaces between the fibres [13]. The greater the twist, the smaller the capillary spaces, therefore the more difficult it is for the liquid, in this case blood, to wick along the yarns. Hollies [7] found that between a twist range of 4 to 12 turns per inch (tpi) (157.5 to 472.4 turns per



metre (tpm)), water transport rates decreased with the increase in twist. At a twist level below 4 tpi the water transport rates also decreased, owing to the reduction in the number and continuity of intra-fibre capillary spaces. Therefore, in Hollies' work [7], 4 tpi was the optimum amount of twist for water transport rates. All fabrics used in this thesis had a greater twist level (624 – 756 tpm) than the yarns investigated in Hollies [7] work. Therefore, any further increase in twist would reduce the wicking rates, as seen in the previous work [7].



**Figure 7-1 illustrating the different twist levels of yarns. In figure 7-1a, the blood is able to enter the capillary spaces between the fibres owing to the reduction in twist, while the blood cannot easily enter the capillary spaces when the fabric is more highly twisted (figure 7-1b).**

The medium not-coloured calico had the smallest mean dry bloodstain area for four out of the six velocities investigated (figure 3-3 pg46). The medium not-coloured calico had a higher twist level (756 x 756 tpm) than both the light (650 x 650 tpm) and heavy (650 x 624 tpm) not-coloured calicos (table 3-1 pg40). The smaller bloodstains on the medium calico than the heavy and light calicos at these velocities was likely caused by the reduced ease with which the blood could wick along the yarns owing to the higher twist for the medium calico. The two velocities where the smallest mean dry bloodstain area was not seen on the medium calico were  $1.7 \text{ ms}^{-1}$ , where the low energy at impact resulted in the blood pooled on the surface of the fabric, and  $5.1 \text{ ms}^{-1}$ , where the high energy at impact forced the blood into the yarns table 3-4 pg48). This resulted in other variables among the light, medium and heavy fabrics having a greater effect than the twist level on the dry bloodstain area.

When the calico fabrics were dyed and printed, it was the heavy calico which was most likely to produce the smallest mean dry bloodstain area, despite the higher twist level for the medium calico (figure 5-1 pg108 and figure 6-6 pg140). This suggests that other

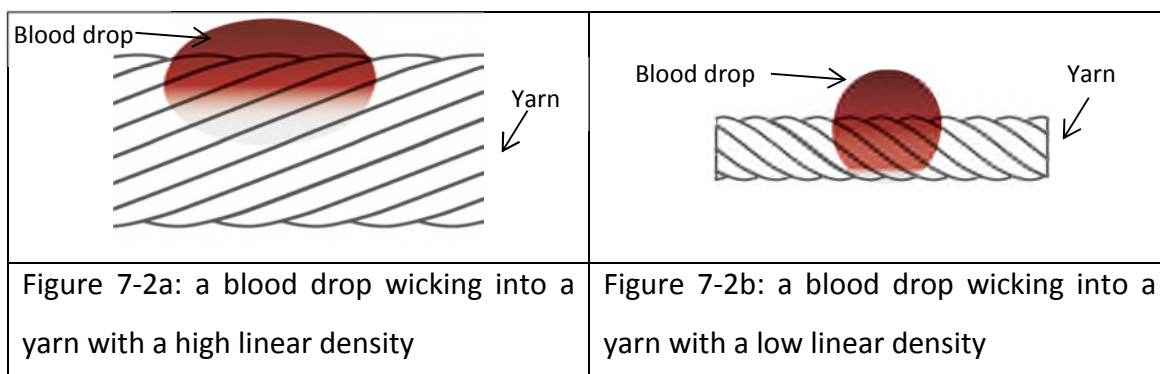
variables, such as the greater yarn linear density of the heavy calico (discussed below), had more of an effect on the amount of wicking which occurred within the yarns than the twist level. The effect of the higher twist level for the medium calico decreased as the amount of wicking which occurred within the fabric increased (from the not-coloured to the printed calico). This introduced a possible order of importance among the variables investigated in this thesis, as a greater yarn linear density may be more likely to result in a smaller bloodstain area than a greater twist level.

#### **7.2.4 Yarn linear density**

A difference among the fabrics in the work described in this thesis, which occurred across all three finishing treatments, was that seen between the light, and the medium and heavy calicos. The light calico consistently produced larger dry bloodstain areas than the medium and heavy calicos (figures 3-3 pg46, 5-1 pg108 and 6-4 pg138), with the blood more spread out throughout the bloodstain. In the current work the light calico had a lower yarn linear density (14 x 18 tex) than the medium (33 x 31 tex) and heavy (43 x 47 tex) calicos (table 3-1 pg40). Previous research has shown that for a vertical wicking test, the wicking height decreases as the yarn linear density decreases. This is owing to the lower number of fibres used in a finer yarn, and therefore a decrease in the total number of capillary spaces within the yarn [14].

However, these previous experiments were undertaken by placing the yarns in an 'infinite' liquid reservoir [14], rather than a finite reservoir (the blood drops) as used in the current work. The yarns in the heavy calico had the greatest yarn linear density of the three fabrics investigated in this thesis, therefore according to the previous work [14] the heavy calico should result in the largest bloodstain. However, in order to wet the greater surface area of the heavy calico yarns and wick into the centre of the yarns, a greater amount of liquid blood was required owing to the greater yarn linear density. In the wicking experiments [14], when drawing from an infinite reservoir of liquid, this was not a problem. However, the amount of liquid blood in the finite reservoir (the blood drop) in the current work would be greatly depleted by wetting the surface and wicking into the centre of the yarns (figure 7-2a). Therefore less wicking along the

yarns would have been able to occur, despite the greater number of capillary spaces. In the time taken for the liquid blood to wick into the yarns, it would also have begun to dry on the surface of the fabric, again reducing the amount of blood available for wicking along the yarns. On the other hand, only a very small volume of blood was required to wet and wick into the light calico yarns (figure 7-2b), reserving a larger volume of blood for subsequent wicking along the yarns.

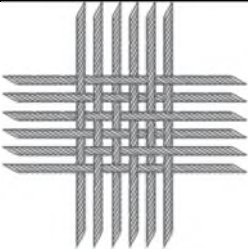
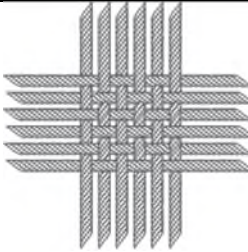


**Figure 7-2 the effect of yarn linear density on wicking with a finite reservoir. Only a small volume of blood is required to wet and wick into the yarn with a low linear density (figure 7-2b), but the same volume of blood cannot as easily wet and wick into a yarn with a higher linear density (figure 7-2a).**

The importance of the effect of yarn linear density on dry bloodstain area has been emphasised throughout this work. The differences in dry bloodstain area seen among the light, medium and heavy fabrics for all three treatments attest to the effect of the difference in yarn linear density. This emphasises the importance of understanding the effect of yarn linear density on a bloodstain within a forensic context. A blood drop of the same volume, impacting at the same velocity, can appear very different depending on the yarn linear density. A low yarn linear density, on a 100% cotton plain woven fabric, would likely result in a larger bloodstain, with a more even colouration as the particulates are more spread out within the bloodstain. A higher yarn linear density, on the other hand, would result in a smaller, denser bloodstain, with more blood remaining on the surface of the fabric. If the differences between the fabrics were not considered, it would be easy to assume the bloodstains resulted from very different mechanisms, when in reality it is the fabrics themselves creating the differences seen.

### 7.2.5 Inter-yarn spaces

When yarns are woven into a fabric, the yarn linear density and sett will affect the size and number of the inter-yarn spaces within the fabric. Vertical wicking height in fabric samples has been found to increase when the fabric was woven from finer yarns [10]. The finer the yarns a fabric is woven from, assuming the sett is kept constant, the greater the fabric porosity (figure 7-3) [10]. When the sett is kept the same, there will be larger spaces between the yarns for a fabric woven from finer yarns than for a fabric woven from coarser yarns. The similarity of the sett (yarns per 10 mm) for the light (27 x 23), medium (26 x 26) and heavy (26 x 26) calicos with the increase in yarn linear density from the light to the heavy calico resulted in the light calico having the highest fabric porosity, with the heavy having the lowest (table 3-1 pg40). The higher fabric porosity for the light calico allowed the blood to more easily enter the fabric, coating the yarns entirely and wicking into the intra-yarn spaces from all sides. For the medium and heavy not-coloured and dyed calico, the lower fabric porosity prevented the blood from coating the yarns, and instead the blood remained on the surface of the fabric except when the impact energy was great enough to force the blood into the intra-yarn spaces, for example on the not-coloured calico at  $5.1 \text{ ms}^{-1}$  (figures 3-11 pg65 and 3-12 pg67).

	
<p>Figure 7-3a: a plain woven fabric woven from fine yarns</p>	<p>Figure 7-3b: a plain woven fabric woven from coarse yarns</p>

**Figure 7-3 illustrating the effect of yarn linear density on the fabric construction. The greater the yarn linear density, assuming the sett is kept the same, the lower the fabric porosity.**

In combination with the yarn linear density, the differences in fabric porosity seen among the light, medium and heavy calicos resulted in the differences seen in the dry bloodstain area among the three fabrics. The greater fabric porosity for the light calico

resulted in larger dry bloodstain areas. As for the yarn linear density, differences in fabric porosity could result in different bloodstains even when the impact velocity and blood drop volume were kept constant.

### **7.3 Advantages and disadvantages of the $\mu$ CT and SEM**

Neither a  $\mu$ CT nor SEM had previously been used to investigate bloodstains on fabrics. Therefore, the current work introduced the use of a  $\mu$ CT and SEM to provide a more detailed examination of bloodstains on fabric, as a new technique. Overall, the use of both a  $\mu$ CT and SEM did enable a better understanding of the interaction of blood and fabric.

The  $\mu$ CT allowed the form of the bloodstain inside the fabric to be assessed, which was not possible by visual examination alone. For example, an important consideration was whether the blood had wicked into the centre of the yarns, or only coated the yarns as this assisted in understanding how the blood moved through the different fabrics at different impact velocities. Distinguishing between different impact velocities is important for BPA. Knowing whether a blood drop impacted at a low or high velocity can assist in the determination of the creation mechanism and area of origin of the bloodstain.

For the heavy not-coloured calico, comparing the CT scans from specimens from impacts of 1.7 and 4.1  $\text{ms}^{-1}$  revealed noticeable differences in where the blood was within the fabric. From 1.7  $\text{ms}^{-1}$  impacts, both the warp and weft yarns were visible in the CT cross-sections as complete dense circles, indicating the yarns were completely soaked in blood (figure 3-7c pg54). In the wet bloodstain photographs, blood was pooled on the technical face at this velocity (figure 3-5c pg50). Therefore, the fact the warp and weft yarns were soaked in blood indicates the blood had wicked vertically from the technical face. This only occurred from 1.7  $\text{ms}^{-1}$ , and so would be strongly suggestive of a low impact velocity bloodstain. From an impact velocity of 4.1  $\text{ms}^{-1}$  a large amount of blood still dried on the surface of the fabric (figures 3-9f pg56 and 3-10i pg61). However, from 4.1  $\text{ms}^{-1}$  impacts, the CT cross-sections were patchy, with blood only surrounding the yarns (figure 3-10g pg61). The blood, therefore, had not

been able to wick into the centre of the yarns before drying, which was very different to what occurred at an impact velocity of  $1.7 \text{ ms}^{-1}$ . Therefore, although the pooled blood which dried on the surface of the heavy calico could point an examiner towards a lower velocity impact, the form of the bloodstain within the fabric showed the different dynamics which created the bloodstain at the higher velocity. At an impact velocity of  $4.1 \text{ ms}^{-1}$  the blood was more spread out and therefore dried before being able to wick into the centre of the yarns. This level of detail about the bloodstains could only be known with the use of a  $\mu\text{CT}$  scanner, and aided in differentiating between bloodstains which impacted at different velocities.

The detail of the bloodstain that was visualised with the SEM enabled better understanding of whether the blood filled the inter-yarn spaces (figure 3-10c and i pg61), and where it was within the yarns (figure 6-11 pg147). Differences in the density of blood throughout the bloodstain could also be examined. This was especially useful for the medium and heavy dyed calico from  $1.7 \text{ ms}^{-1}$  impacts. With the use of the dry bloodstain images alone it was difficult to ascertain whether there was a denser ring of blood around the edge of the bloodstain, and the dry bloodstains appeared to have a consistent density of blood across the surface of the fabric (figures 5-4 b and f pg114). However, the use of the SEM confirmed a dense ring of blood at the edge of the bloodstain, and blood which was able to wick into the yarns in the centre of the bloodstain (figures 5-4 c and a pg114). This greatly aided understanding of how the blood had interacted with the dyed fabric at this velocity, as it was able to wick into the yarns in the centre of the bloodstain to an extent to remove any blood pooled on the surface of the fabric. This indicated a difference from the not-coloured calico, as a much greater amount of blood remained pooled on the surface of the medium and heavy not-coloured calico from  $1.7 \text{ ms}^{-1}$  impacts (figure 3-8 b and c pg55), which may otherwise have been missed.

Neither of these methods were destructive, so any specimens used could be retained. The use of non-destructive methods within forensic science is important, as it allows specimens to be used for further analysis. In the case of blood spatter this could

involve DNA testing. The retention of specimens also means that if the case was not solved, or if the guilt of an individual later came into question, the evidence could be revisited.

However, despite the extra information which was provided with the use of a  $\mu$ CT and SEM, the use of this equipment did also have disadvantages:

- The amount of time involved in the use of both a  $\mu$ CT and SEM; a single CT scan took an hour, an SEM scan 20 minutes (although this could vary depending on the machine and settings chosen), followed by analysis time. When dealing with large numbers of samples, the amount of time each of these methods required would be an important consideration.
- The limit on the size of specimens which fitted into both the  $\mu$ CT and SEM used in this work. Although the techniques themselves were not destructive, any large samples would need to be cut down to fit into the machines, although different models are available which can accommodate larger samples. For the  $\mu$ CT, in order to get as high a resolution as possible it was necessary to have smaller specimens. This avoided possible anomalies caused by scanning only part of the specimen.
- The qualitative nature of the data. Although it is possible to take measurements from the  $\mu$ CT images, this was not always practical. Area measurements were taken from the  $\mu$ CT cross-sections in chapter 2 (paper: The use of micro computed tomography to ascertain the morphology of bloodstains on fabric). However, this technique was not repeated with the work on the calico fabric owing to the fabric deforming as the bloodstains dried. Any difference seen in the area throughout the depth of the fabric was therefore partly due to the deformed fabric rather than differences in the bloodstain. Although this problem could potentially be solved using complex geometry, this was beyond the scope of this research. Therefore, the  $\mu$ CT scans were then

only used qualitatively to visually examine where the blood was within the fabric.

As one of the objectives of the current research was to develop a thorough understanding of what occurred after the blood impacted these particular fabrics, the use of a  $\mu$ CT and SEM was imperative to this research. It would not have been possible to gain an understanding of how the blood moved through the yarns and fabrics without being able to see the internal structure of the bloodstain. However, the time which goes into running the machines and interpreting the data and the availability of equipment would limit the use of this technique to very specific circumstances. While it may be ideal to examine the internal structure of every bloodstain found at a crime scene, which could provide information as to the formation mechanism of the bloodstain, this is not always a realistic scenario due to time, money and the availability of equipment. The use of this method is most applicable in research situations, where a thorough understanding of the bloodstain structure is required.

#### **7.4 Impact for forensic science**

The work undertaken in this research emphasises the importance for a practitioner of BPA to have an understanding of the different fabric structures. Prior to doing a full analysis on any blood patterns which were found on fabric at a crime scene, it is necessary to understand the fabrics on which they were found. What is the fibre content? The fabric structure (woven, knit, non-woven, other)? The thickness, sett, mass per unit area and yarn linear density? Has the fabric been dyed or subjected to any finishing treatments? All of these differences will have an effect on the bloodstain, and without understanding the structure of the fabric, understanding the bloodstains will be considerably more difficult.

Once the structure of the fabric is understood to the greatest possible extent, the examination of the bloodstains can begin. There are a number of key points which this work has produced which may be pertinent to crime scene situations, although the scope of this is limited to the fabrics which were investigated in the current work:



- Determining the impact velocity of passive blood drops could enable the observer to assess the distance the blood drop fell; for example, whether it came from an individual standing or lying down. The current work found a correlation between the mean dry bloodstain area and velocity on the not-coloured calico, most notably for the medium and heavy fabrics (figure 3-3 pg46). Correlations between dry bloodstain area on fabrics and the velocity with which the blood drop impacted do exist, but only in very specific circumstances; when the primary mechanism behind the bloodstain area is the spreading which occurred on the surface of the fabric at impact, and not the amount of wicking which then followed. This could only be confirmed on specific fabrics by experimentation, but it cannot be assumed a larger bloodstain means a higher impact velocity or a larger blood drop.
- Comparison of bloodstains at a crime scene across different fabrics may not always be possible, as any processing treatments of the fabrics may affect the bloodstains. An understanding of what the treatment has done to the fabric would be necessary, again experimentation could help provide an understanding.
  - o Some processing treatments, such as the dyeing in the current work, may alter the intra-yarn spaces to a more or less optimum size for wicking, thereby altering the bloodstain area.
  - o Some processing treatments, such as the digital printing in the current work, may alter the wettability of the fabric, increasing or decreasing the amount of spreading which will occur on the surface of the fabric, and the ease with which the blood can wet the yarns.
- In certain cases, for example when fabrics with a low yarn linear density have a very low contact angle, the blood may penetrate to the technical rear of the fabric across the entirety of the bloodstain, as for the light, printed calico from impacts on the printed face (figure 6-9 pg144). This would result in bloodstains which looked extremely similar on both the technical face and technical rear of the fabric, and could raise questions as to which side of the fabric the

bloodstain impacted. The context of the fabric at the crime scene may help to answer those questions.

Overall, there is a need for analysis of bloodstains at a crime scene to have a more scientific approach. By beginning to understand what is occurring following impact of a blood drop on fabric, with use of the research which has previously been undertaken in textile science, a better understanding of the dried bloodstains which are seen at crime scenes can be gained. Only by truly understanding the fabric onto which the blood drop has impacted could an understanding of what occurred to cause that bloodstain begin to be formed.

## 7.5 References

- [1] L. Hulse-Smith, N.Z. Mehdizadeh, S. Chandra, Deducing drop size and impact velocity from circular bloodstains, *J. Forensic Sci.* 50 (2005) 54–63. doi:10.1520/JFS2003224.
- [2] C. Knock, M. Davison, Predicting the position of the source of blood stains for angled impacts, *J. Forensic Sci.* 52 (2007) 1044–1049. doi:10.1111/j.1556-4029.2007.00505.x.
- [3] E.M.P. Williams, M. Dodds, M.C. Taylor, J. Li, S. Michielsen, Impact dynamics of porcine drip bloodstains on fabrics, *Forensic Sci. Int.* 262 (2016) 66–72. doi:10.1016/j.forsciint.2016.02.037.
- [4] C. Hawkyard, Substrate preparation for ink-jet printing, in: H. Ujiie (Ed.), *Digit. Print. Text.*, Woodhead Publishing, Cambridge, 2006: pp. 201–217.
- [5] A.P. D’Silva, G. Harrison, A.R. Horrocks, D. Rhodes, Investigation into cotton fibre morphology Part II: Effect of scouring and bleaching treatments on absorption, *J. Text. Inst.* 91 (2000) 107–122.
- [6] H. Hasani, Effect of different processing stages on mechanical and surface properties of cotton knitted fabrics, *Indian J. Fibre Text. Res.* 35 (2010) 139–144.

- [7] N. Hollies, M. Kaessinger, H. Bogarty, Water Transport Mechanisms in Textile Materials Part I: The Role of Yarn Roughness in Capillary-Type Penetration, *Text. Res. J.* 26 (1956) 829–835.
- [8] H. Rhee, R.A. Young, A.M. Sarmadi, The Effect of Functional Finishes and Laundering on Textile Materials Part II: Characterization of Liquid Flow, *J. Text. Inst.* 84 (1993) 406–418.
- [9] S. Grishanov, Structure and properties of textile materials, in: M. Clark (Ed.), *Handb. Text. Ind. Dye. Vol. 1 Princ. Process. Types Dye.*, Woodhead Publishing, Cambridge, 2011: pp. 28–63.
- [10] N. Erdumlu, C. Saricam, Wicking and drying properties of conventional ring- and vortex-spun cotton yarns and fabrics, *J. Text. Inst.* 104 (2013) 1284–1291. doi:10.1080/00405000.2013.799258.
- [11] X. Li, J. Li, S. Michielsen, Effect of yarn structure on wicking and its impact on bloodstain pattern analysis (BPA) on woven cotton fabrics, *Forensic Sci. Int.* 276 (2017) 41–50. doi:10.1016/j.forsciint.2017.04.011.
- [12] A.B. Nyoni, D. Brook, Wicking mechanisms in yarns—the key to fabric wicking performance, *J. Text. Inst.* 97 (2006) 119–128. doi:10.1533/joti.2005.0128.
- [13] Q. Li, J.J. Wang, C.J. Hurren, A Study on Wicking in Natural Staple Yarns, *J. Nat. Fibers.* 14 (2017) 400–409. doi:10.1080/15440478.2016.1212763.
- [14] M. Taheri, M. Vadood, M.S. Johari, Investigating the effect of yarn count and twist factor on the packing density and wicking height of lyocell ring-spun yarns, *Fibers Polym.* 14 (2013) 1548–1555. doi:10.1007/s12221-013-1548-7.

## 8 Conclusions

### 8.1 Summary

The work undertaken in this thesis involved dropping blood from a number of different heights onto three different mass per unit areas (85, 164 and 225 g/m<sup>2</sup>) of 100% cotton plain woven calico. The fabric was either not-coloured (velocities: 1.7, 2.9, 4.1, 4.9, 5.1 and 5.4 ms<sup>-1</sup>), reactively dyed (velocities: 1.7, 2.8, 4.1, 4.9 and 5.4 ms<sup>-1</sup>) or digitally printed (velocities: 1.9, 3, 4.1, 5 and 5.4 ms<sup>-1</sup>). All drops were filmed using high speed video to measure blood drop size and impact velocity. The resultant wet and dry bloodstains were photographed and the bloodstain area measured using the inbuilt tools in ImageJ. The dry bloodstains were analysed using the  $\mu$ CT and SEM.

The aim of this thesis was to improve understanding of the interaction of blood and fabric by undertaking a thorough investigation, using novel techniques, into what occurs when a blood drop impacts a 100% cotton plain woven fabric. This was achieved in the current work as the results obtained from the investigation into the interaction of blood and a 100% cotton plain woven fabric revealed the effects of three key variables: the yarn linear density, the surface treatments and the impact velocity, on the bloodstain morphology.

#### **8.1.1 Objective one – to investigate the applicability of the use of the $\mu$ CT and SEM to BPA.**

The use of  $\mu$ CT allowed the internal structure of the bloodstains to be assessed, and therefore an understanding of where the blood was within the fabric and whether it had coated or penetrated the yarns could be gained. The SEM provided a magnified view of the external bloodstain, enabling a detailed look at the different densities of blood within the bloodstain, whether the blood was in the inter-yarn spaces, and whether it had coated the external surface of the yarns. Both the  $\mu$ CT and SEM provided details on the formation of the bloodstains which it would not have been possible to ascertain by external visual examination alone. These techniques provided information as to differences between the bloodstains, for example those created by

different velocity impacts, which could potentially be of use to forensic science in distinguishing creation mechanisms of bloodstains.

### **8.1.2 Objective two – to investigate the effect of fabric mass per unit area and thickness on bloodstain morphology.**

For all three different processing treatments, the light calico had the largest dry bloodstain area. This was owing to the lower yarn linear density of this fabric. The blood could therefore penetrate the inter-yarn spaces more easily, coating the yarns from all directions. The volume of blood required to wet and wick into the yarns themselves was lower than for the fabrics with greater yarn linear density, meaning there was more blood than available to wick along the yarns.

Blood remained more on the surface of the medium and heavy calicos as they had a greater yarn linear density than the light calico. Any blood which remained on the surface of the fabrics dried by means of the coffee ring effect.

### **8.1.3 Objective three – to investigate the effect of the impact velocity of the blood drop on the bloodstain morphology.**

On the not-coloured calico, the mean dry bloodstain area increased with impact velocity, with a better correlation for the medium and heavy calico. This was owing to the dependency of the dry bloodstain area on the amount of lateral spreading at impact, which increased with an increase in impact velocity, as opposed to the amount wicking which occurred following this. The work in this thesis confirmed that dry bloodstain area on fabrics can increase with increased impact velocity, which could assist forensic science in determining the creation mechanism of a bloodstain.

On the dyed and printed calico, owing to a greater amount of wicking which occurred than on the not-coloured calico, no correlation with velocity was seen for any of the fabrics.

#### **8.1.4 Objective four – to investigate how reactive dyeing affects the resultant bloodstains.**

Dyeing the calico increased the dry bloodstain area from that seen on the not-coloured calico, as well as removing the correlation with velocity. This was owing to the greater amount of wicking which was able to occur on the dyed than on the not-coloured calico. The dye filled the amorphous regions of the cotton fibres, bonding with the cellulose and causing the fibres to swell. This decreased the intra-yarn spaces and therefore increased the ease with which the blood could wick along the yarns.

#### **8.1.5 Objective five – to investigate how digital printing affects the resultant bloodstains.**

Digitally printing the fabrics increased the dry bloodstain area beyond that of the not-coloured or dyed fabrics and resulted in bloodstains which were visually similar across all three fabrics. The printing of the fabric increased the wettability, and therefore the ease with which the blood could spread on the fabric surface and wick into and along the yarns.

### **8.2 Limitations and suggestions for future work**

- The work undertaken in this study was only done on fabrics which were 100% cotton and plain woven. It cannot be directly applied fabrics of different structures or fibre types. Therefore, a similar study could be undertaken on fabrics of different structures (more complicated weaves and knits) and fibre types (wool, blends, polyester etc.). This would allow an assessment of how blood interacted with the differing structures and fibres types and whether similar or different factors affected the wicking of the blood within the fabrics.
- Only two out of a large number of processing treatments were examined in the current work. These treatments were chosen because reactive dyeing (used in both treatments) is the most commonly used dye for cotton. The treatments were also readily available and could easily be applied to the calico fabrics which had already been examined. A further surface treatment which would be of interest is dyeing the yarns prior to weaving or knitting, as this is also a

common occurrence in clothing fabrics. However, this was not possible in the current work as it would not have been possible to weave a fabric identical to the not-coloured calico which had already been examined.

- In the current work it was found that inkjet printing of the fabrics decreased the surface roughness and increased the wettability of the fabrics. The dry bloodstains from the blood drops on the not-printed surface of the fabric were larger than those on the printed surface. This indicated it was something in the printing process other than the addition of the dye itself which caused the increase in wettability. It was beyond the scope of this work to further investigate what caused the increase in wettability, but this would warrant further investigation. A fabric could be put through each stage of the printing process, with the effect on dry bloodstain area examined after each stage.
- The current work was only undertaken using passive blood drops falling vertically onto fabrics angled at 90°. Although the most practical solution for primarily understanding the interaction of blood and the fabrics, it is not the most realistic scenario in terms of finding bloodstains at a crime scene. Therefore the work could be extended to look at the effect of angling the fabric or the blood drops on the resultant bloodstains.
- Finally, it would be worth investigation whether the conclusions drawn from the current work could be applied in a crime-scene situation. This would involve a blind study, deciphering bloodstains on the fabrics investigated in the current work when the impact velocity is not known.

# Appendix A – Poster Presentation from International Association of Bloodstain Pattern Analysts Conference Rome 2015.

## The use of computed tomography in the analysis of bloodstain morphology

Lisa Dicken



### Introduction

There is a paucity of information in the literature regarding the interaction of blood and absorbent surfaces such as fabrics. Reported work has focused on the visible bloodstain on the fabric surface, treating it in the same way as a bloodstain on a non-absorbent surface.

The movement of liquids into and through a fabric depends on wetting and wicking processes. Wetting is the displacement of the solid-air interface with the solid-liquid interface. The surface fibres must be wetted before the liquid can then be transported through the inter-fibre and inter-yarn pores by means of capillary action, known as wicking. As wetting and wicking only occur on absorbent surfaces they need to be treated differently to non-absorbent surfaces.

### Aim

The aim of this work was to investigate the use of a micro computed tomography (CT) scanner to examine the morphology of the bloodstain inside fabrics.

### Materials and Methods

#### Materials

- Two fabric specimens were used i) 100% cotton rib knit fabric and ii) 100% cotton bull drill (a woven fabric).
- Bloodstains were created by dropping a single blood drop from heights of i) 500mm, ii) 1000mm and iii) 1500mm. Five specimens of each fabric / height combination were used.
- The mean impact velocities were:
  - for the rib knit : i) 3.2 ms<sup>-1</sup>, ii) 4.5 ms<sup>-1</sup> and iii) 5.3 ms<sup>-1</sup>
  - for the bull drill: i) 2.9 ms<sup>-1</sup> ii) 4.2 ms<sup>-1</sup> and iii) 5.0 ms<sup>-1</sup>.
- The mean drop diameter for the rib knit was 4.1mm (s.d. = 0.01mm), for the bull drill it was 3.4mm (s.d. = 0.01mm).

#### Methods

- Specimens were examined using a Nikon XTH225 micro CT scanner which exploited the difference in density between the higher density dried blood and the lower density air-filled fabric. The two fabrics were analysed using difference voltage (kV), current (µA) and exposure (ms) settings to optimise contrast. The samples were analysed between 30 - 35kV, 30 - 330µA and 500 - 1000ms exposure.
- Scanning data was manually reconstructed using CT Pro, and then two-dimensional and three-dimensional data were gathered using VGStudio Max. The data was then imported into ImageJ to measure i) area ii) y (wale or warp) measurement iii) x (course or weft) measurement.
- Univariate ANOVA was undertaken on the first area on the technical face, the maximum area and the last area at the technical rear of the cross-sections in the z-direction.

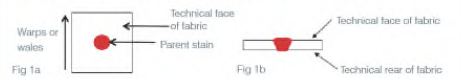


Figure 1: a technical drawing of the resultant specimens, indicating the direction of the warp (woven) and wales (knitted) (1a), and a possible cross-section of a specimen, indicating the two faces of the fabric (1b).



Figure 2: the direction of the measurements taken from the bloodstain. The area measurements were taken on the cross-sections marked in figure 2a from the technical face to the technical rear in direction z, depth. The resultant images were approximately circular, as seen in figure 2b, and measurements were taken in the wale or warp direction and course or weft direction on the cross-section with the largest area.

### General Observations

- Figure 3 shows a typical cross-section from the micro CT in the z-direction of the bloodstains formed on the rib knit and bull drill fabrics.
- From these images it is possible to see the blood-soaked and blood-void areas, the latter of which are most likely the air spaces between the yarns. There are more of these voids in the knit fabric (3a) than the bull drill (3b).
- It is also possible to see some variation in the intensity of the blood, with the external edges having a brighter colouration, suggesting denser blood in these areas.

### General Observations cont.

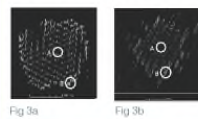


Figure 3: an example of a cross-sectional slice in the z-axis from the rib knit from a depth of 0.8mm (3a) and bull drill from a depth of 0.6mm (3b). An example of a blood-void section is indicated by 'A', an example of an area of denser blood is indicated by 'B'.

### Results

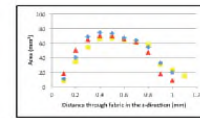
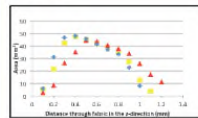
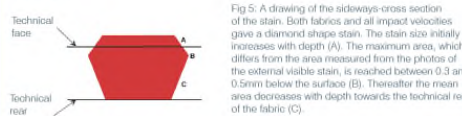


Figure 4a: the mean area for all impact velocities for the rib knit (3.2ms<sup>-1</sup> = ■, 4.5ms<sup>-1</sup> = ▲, 5.3ms<sup>-1</sup> = ◆)  
 Figure 4b: the mean area for all impact velocities for the bull drill (2.9ms<sup>-1</sup> = ■, 4.2ms<sup>-1</sup> = ▲, 5.0ms<sup>-1</sup> = ◆)  
 Figure 4: The mean of the area of the parent bloodstain for cross-sections taken every 0.1mm throughout the depth of the bloodstain in the z-direction for three velocities for both rib knit and bull drill fabrics.



- For the rib knit fabric the lowest and highest impact velocities, 3.2 ms<sup>-1</sup> and 5.3 ms<sup>-1</sup> gave the largest cross sectional areas and at a shallower depth than the middle impact velocity of 4.5 ms<sup>-1</sup>. The middle impact velocity penetrated the furthest into the fabric.
- For the drill fabric a different pattern was observed. The largest mean area was at the same depth (0.4mm) for the specimens from the middle impact velocity of 4.2 ms<sup>-1</sup> and the fastest impact velocity of 5 ms<sup>-1</sup>. The largest mean area for the slowest impact velocity of 2.9 ms<sup>-1</sup> was seen at a greater depth (0.5mm).
- ANOVA revealed only one statistically significant difference due to impact velocity, for the area of the cross-section on the technical face of the rib knit ( $F_{2,11} = 5.523, p = \leq 0.05$ ). Tukey HSD analysis revealed a significant difference between only two of the means; 4.5 ms<sup>-1</sup> (2.7mm<sup>2</sup>) and 5.3 ms<sup>-1</sup> (6mm<sup>2</sup>). No significant difference was found between either of these two means and the mean area of the bloodstain formed at 3.2 ms<sup>-1</sup> (5.4mm<sup>2</sup>).
- For the bloodstain area formed on the technical face of the drill fabric the data was transformed as it was not normal (log10), but no significant difference was found ( $F_{2,10} = 3.803, p = NS$ ). No significant difference was found for the maximum bloodstain area (knit:  $F_{2,11} = 1.66, p = NS$ ; drill:  $F_{2,10} = 2.088, p = NS$ ) or the area of the last bloodstain cross-section at the technical rear (knit:  $F_{2,11} = 0.454, p = NS$ ; drill:  $F_{2,10} = 0.058, p = NS$ ).

### Discussion

- The use of the micro CT scanner has enabled the internal morphology of the bloodstain to be examined, by showing the shape which the blood forms within the fabric and therefore indicating how the blood has moved through the fabric.
- For all impact velocities and both fabrics the combination of wetting and wicking resulted in a diamond shaped stain. When the blood initially hit the fabric it spread, wetting the top of the fabric and allowing wicking to occur. The mass of the remaining drop resulted in capillary action through the depth of the fabric, which did not occur around the extremities.
- For the bull drill fabric the lack of variability among the cross sectional areas at velocity varied was most likely due to the smaller capillary spaces which meant the blood could not disperse to a great extent regardless of the velocity.

### Conclusions

- This pilot study has demonstrated that micro CT scanning can improve the understanding of the morphology of bloodstains on and within fabrics. The technique has allowed extra measurements to be taken regarding the size and shape of the bloodstain inside the fabric.
- The results have shown that the wetting and wicking processes result in a diamond shaped stain within the fabric with the maximum cross-sectional area below the surface.
- This work has shown that the blood stain on fabrics varies depending on the impact velocity and fabric structure.

www.cranfield.ac.uk/cds  
 www.cranfield.ac.uk/cds

Centre for Defence Engineering, Cranfield University  
 Defence Academy of the United Kingdom, Shrivenham, Swindon, SN6 6LA, UK

Acknowledgments:  
 This work was produced with the help of Dr Clare Knock (Cranfield University),  
 Dr Debra Carr (Cranfield University), Dr Sophie Beckett (Cranfield University),  
 Theresa de Castro (University of Guelph), Tania Nickson (JGC Forensics).

Designed by CDS Learning Services, Cranfield University 15021413



**Appendix B – Presentation from International Association of Bloodstain Pattern Analysts Warsaw 2017. Presented by Dr. Clare Knock on the work done in Chapter 3 by the author.**

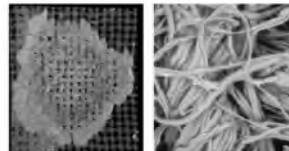


**Use of CT scanner and SEM to determine the effect of fabric density on the flow of blood within a fabric.**

Dr Clare Knock  
44 (0) 1793 785335 [c.knock@cranfield.ac.uk](mailto:c.knock@cranfield.ac.uk)  
Lisa Dicken  
[l.dicken@cranfield.ac.uk](mailto:l.dicken@cranfield.ac.uk)

June 2017

[www.cranfield.ac.uk](http://www.cranfield.ac.uk)

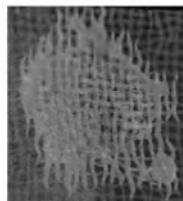
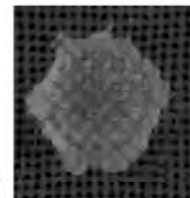
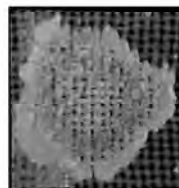


1



### Introduction

- Extensive, recent work on blood on fabrics
- What happens inside the fabric?
- How does this affect the stains observed?
- Scanning electron microscope
- CT scanner



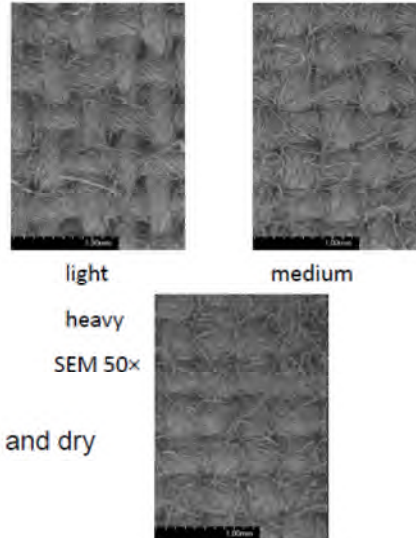
Impact velocity  $1.7 \text{ ms}^{-1}$

2



## Experimental methodology

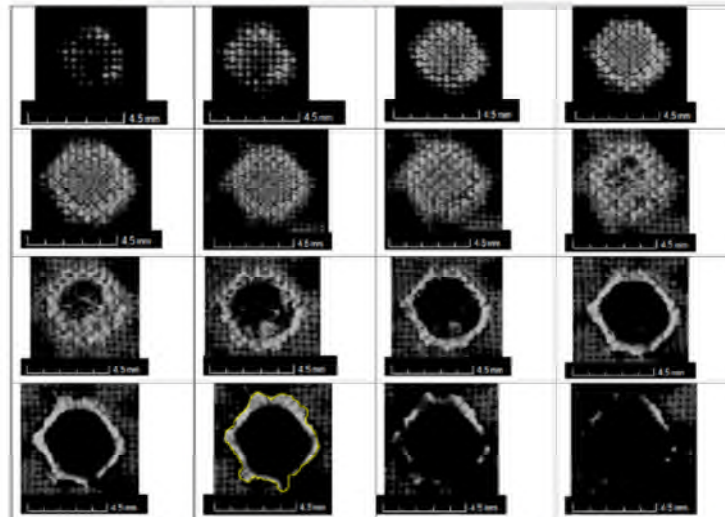
- 3 fabric densities cotton calico
  - 85 g m<sup>-2</sup> (light)
  - 164 g m<sup>-2</sup> (medium)
  - 225 g m<sup>-2</sup> (heavy)
- Vertical drops
- Drop size: 3.31 ± 0.17 mm
- 5 impact velocities
  - 1.7, 2.9, 4.1, 4.9, 5.1 m s<sup>-1</sup>.
- 5 replicates
- Analysis
  - Photographed technical face. Wet and dry
  - Photographed technical rear dry
  - CT scanner
  - SEM



3



## Example CT results, heavy calico (225 g m<sup>-2</sup>), 1.7 ms<sup>-1</sup>.

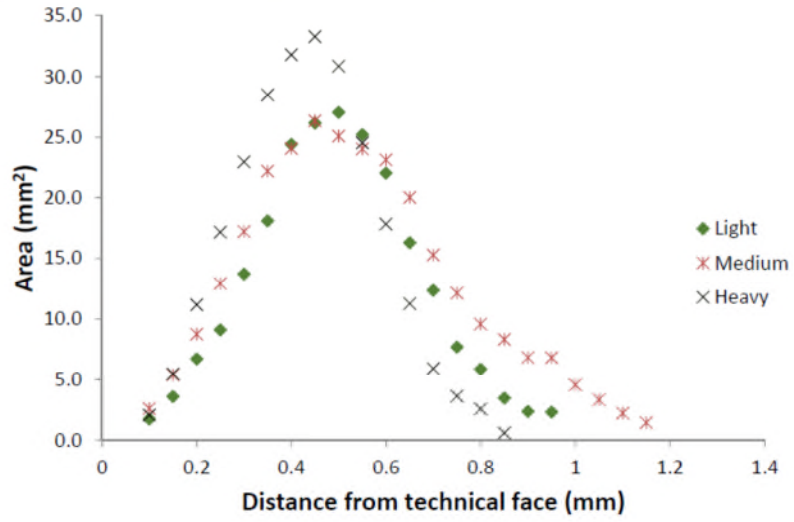


- Cross section every 0.05 mm, Technical rear to technical face

4



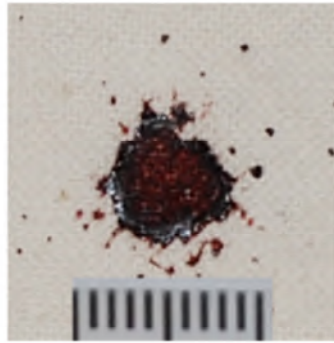
### Example CT results – 5.1 ms<sup>-1</sup>



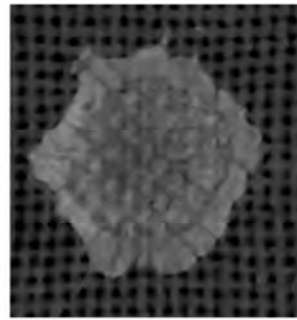
5



### Coffee ring effect



4.1 ms<sup>-1</sup>



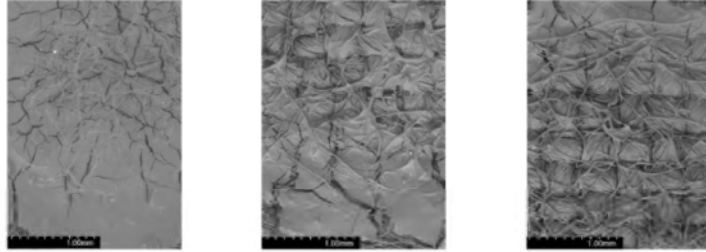
1.7 ms<sup>-1</sup>

Heavy calico

6



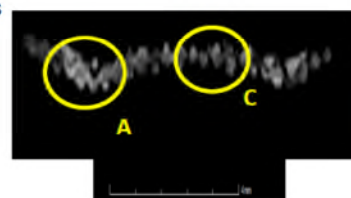
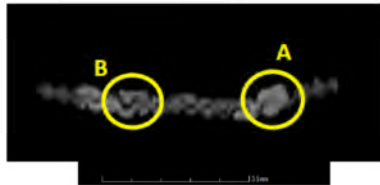
## Effect of impact velocity – heavy calico



1.7 ms<sup>-1</sup>

SEM 42X  
4.1 ms<sup>-1</sup>  
CT scans

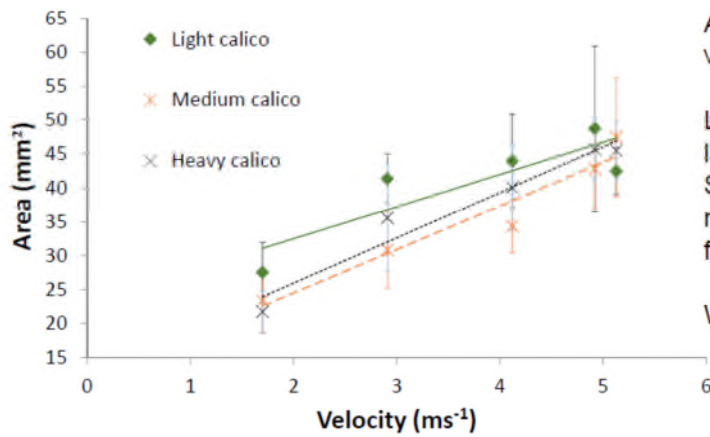
5.1 ms<sup>-1</sup>



7



## Results – effect of velocity



Area increases with velocity

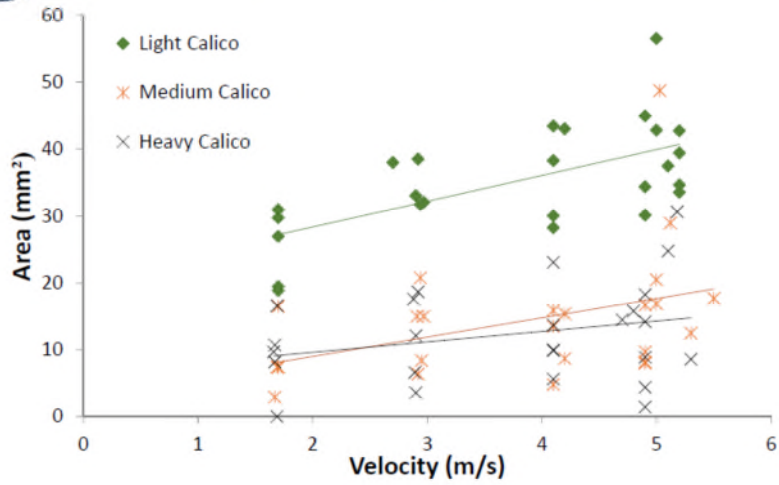
Largest stain – least dense fabric  
Smallest for – medium density fabric.

Why?

8



### Effect of impact velocity – technical rear

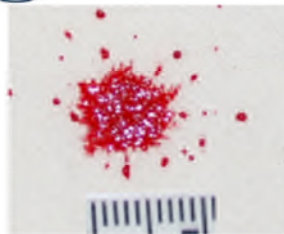


Fabric density key factor.

9

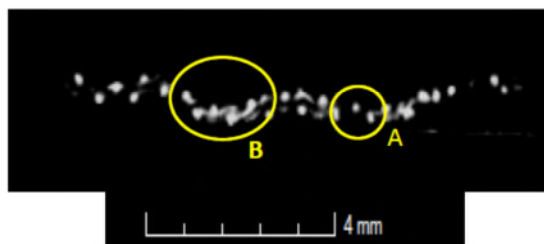
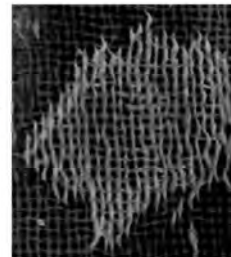


### Effect of fabric density – light fabric



Wet photograph  
4.1 ms<sup>-1</sup>.

CT  
5.1 ms<sup>-1</sup>.

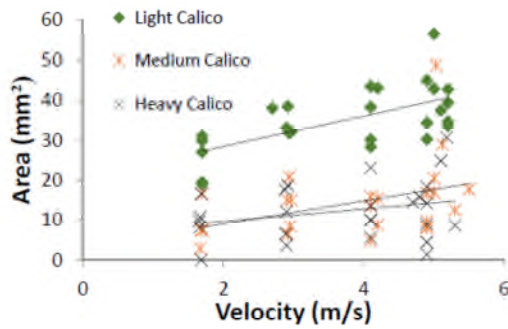


CT 5.1 ms<sup>-1</sup>.

10



## Rear face

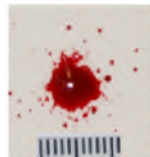


- Light calico
- Thin, low density allows blood to travel easily along yarns – quick wicking
- Penetrates further into fabric.
- Largest surface stain area (except 5.1 ms<sup>-1</sup>)

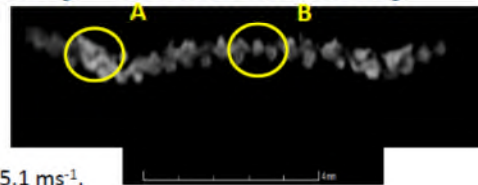
11



## Effect of fabric density – medium and heavy calico

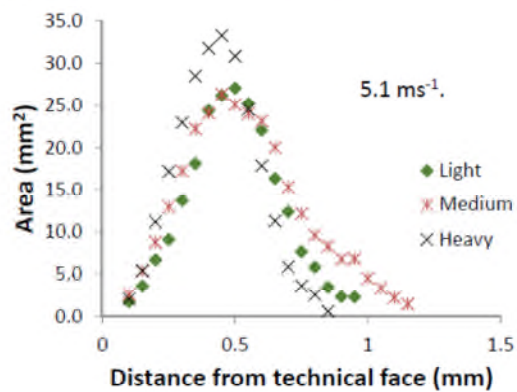


Heavy 4.1 ms<sup>-1</sup>.



Heavy 5.1 ms<sup>-1</sup>.

- Blood remains on surface as it dries
- Greater linear density and smaller capillary spaces so blood could not wick as easily into fabric

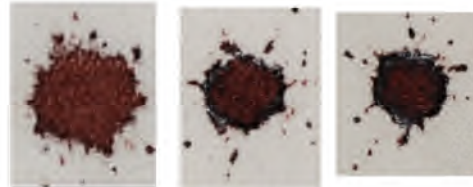


12



## Effect of fabric density – medium and heavy calico

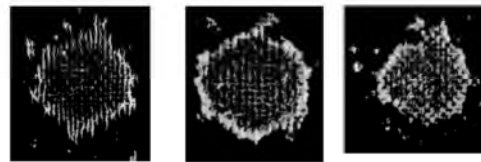
- Heavy calico blood on surface and spreads on surface
- Medium calico blood slightly wicks into fabric but then too dense for it to wick along the yarns
- Coffee ring effect pronounced



Light

Medium  
 $4.1\text{ms}^{-1}$ .

Heavy

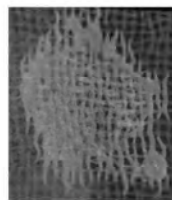


13

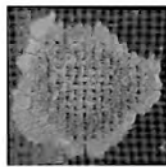


## Effect of fabric density

- Light calico – largest stain wicks into the calico and along warp yarns
  - Except  $5.1\text{ms}^{-1}$  smallest stain
  - Except  $1.7\text{ms}^{-1}$  when less energy, blood on surface
- Heavy calico – can not wick into dense fabric, spreads on surface of the calico
- Medium calico – Wicks slightly into the fabric but too dense for it to spread

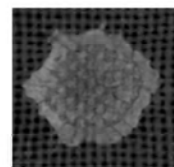


Light



Medium

$1.7\text{ms}^{-1}$ .



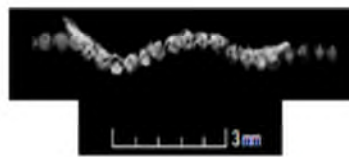
Heavy

14

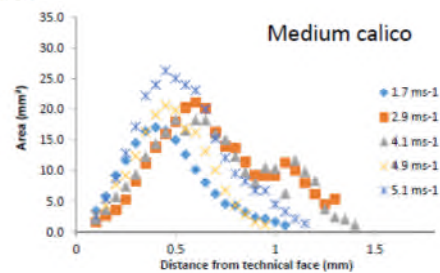


## CT scanner – advantages and disadvantages

- Allows study of internal structure of bloodstains
  - How blood has moved along weft and warp yarns
- Issues
  - Warping of fabric
  - Blood above surface, so how define an “origin”



Medium calico 4.1 ms<sup>-1</sup>



15



## Conclusions

- Cross sectional area increases with velocity
- Largest cross sectional area seen from lightest fabric
  - Open weave allows the blood to wet and then wick along the warp yarns
- Second largest cross sectional area for heaviest fabric
  - Too dense for the blood to penetrate and blood remains on the surface
- Smallest cross sectional area for the medium density fabric
  - Blood can penetrate slightly, but then prevented from wicking by density of fabric.

16





[www.cranfield.ac.uk](http://www.cranfield.ac.uk)

T: +44 (0)1234 750111

 @cranfielduni

 @cranfielduni

 /cranfielduni

## **Appendix C – Fabric testing**

Prior to using the fabrics for any testing, they had to be prepared in accordance with British Standards to create dimensionally stable fabrics to reduce the variability among specimens. The fabrics were also subjected to a number of tests to measure the fabric sett, mass per unit area, thickness and yarn linear density, so the effect of these variables on the bloodstains could be compared among fabrics.

### **C-1 Creating dimensionally stable fabrics**

In order to create dimensionally stable fabrics and remove any external coating on the fabrics, the fabrics were first machine-washed for six cycles [1]. In order to mimic a real-life situation, a domestic washing machine<sup>36</sup> was used. The specimens were laundered on a cotton cycle at 40°C using a widely available detergent<sup>37</sup>. The specimens were not dried between washes.

Following all six cycles, the fabrics were line-dried [1]. The fabrics were line-dried in such a way as to mimic how clothing would be hung with their length (warp) in the vertical direction. The fabrics were ironed using a PSP-202E digital steam press on the cotton setting to remove any creases which may have formed during the washing process.

The laundered fabrics were then cut into specimens 100mm x 100mm minimising the repetition of warp and weft among specimens. A strip of fabric one metre long and 10cm wide was cut from the warp and weft direction of each fabric for the estimation of yarn linear density. The specimens were not cut from within 50mm of the manufactured edge. The specimens were then conditioned to 20±5°C and 65±2% relative humidity for 24 hours [2].

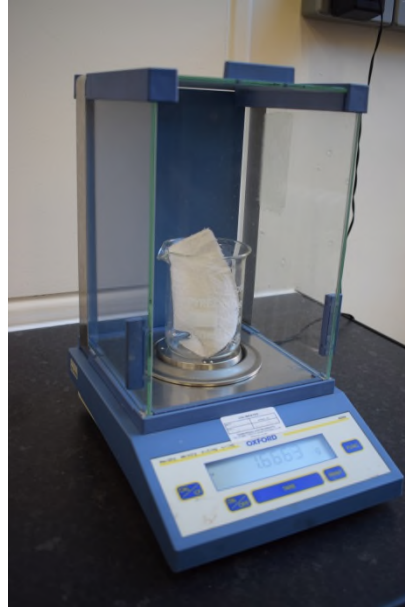
---

<sup>36</sup> Samsung Ecobubble

<sup>37</sup> Persil non-bio Small and Mighty

## C-2 Mass per unit area

The conditioned mass of five specimens from each of the three different calicos was measured on a balance accurate to four decimal places [3]. The balance was an Oxford A2204 (figure C-1).



**Figure C-1 measuring the mass of a fabric specimen**

The width and length of the specimen was then measured at three points in both directions in millimetres, and the mean taken. This information was then fed into equation C-1 to calculate the mass per unit area of the fabric [3]. The results of this can be seen in tables C-1-3.

$$M_{ua} = \frac{M_c}{L_c \times W_c}$$

**Equation C-1 calculating the mass per unit area of a fabric specimen**

Where:

$L_c$  = the conditioned length of the specimen, in metres.

$M_c$  = the conditioned mass of the specimen, in grams.

$M_{ua}$  = the mass per unit area, in grams per square metre.

$W_c$  = the conditioned width of the specimen, in metres.

Fabric	Mass (g)	Warp (mm)	Weft (mm)	Area (m <sup>2</sup> )	Mass/per unit area
L1	0.87	100.3	101.3	0.010	85.63
L2	0.86	99	102	0.010	85.56
L3	0.88	100.1	100.3	0.010	87.13
L4	0.84	100.1	99.6	0.010	84.01
L5	0.84	100.3	100.6	0.010	83.17
MEAN	0.859				85.10
STDEV	0.018				1.543
M1	1.63	100.6	100.6	0.010	159.79
M2	1.62	100.3	98.6	0.010	163.64
M3	1.59	100	97.3	0.010	163.92
M4	1.66	100.3	100.6	0.010	166.00
M5	1.64	100.3	100	0.010	164.00
MEAN	1.628				163.47
STDEV	0.026				2.262
H1	2.23	99.6	100.3	0.010	225.25
H2	2.23	10	99.6	0.010	223.00
H3	2.27	101	100.3	0.010	227.00
H4	2.26	101.6	99.6	0.010	223.81
H5	2.24	100.3	100.3	0.010	224.00
MEAN	2.246				224.61
STDEV	0.018				1.560

**Table C-1 calculating the mass per unit area for each specimen and the mean and standard deviation for each not-coloured fabric.**

Fabric	Mass (g)	Warp (cm)	Weft (cm)	Area (m <sup>2</sup> )	Mass/per unit area
L1	0.97	103.6	102.3	0.011	91.24
L2	0.91	102.3	98	0.010	90.97
L3	0.92	103	101	0.010	88.15
L4	0.88	97.3	99	0.010	91.77
L5	0.95	103	99.3	0.010	93.18
MEAN	0.927				91.06
STDEV	0.033				1.838
M1	1.77	101	101	0.010	171.31
M2	1.75	100.3	101.6	0.010	171.83
M3	1.81	102.6	101	0.010	174.28
M4	1.82	102	103	0.010	173.42
M5	1.65	97	103	0.010	164.85
MEAN	1.7592				171.14
STDEV	0.069				3.714
H1	2.53	101	103	0.010	243.58
H2	2.65	103.6	106	0.011	241.68
H3	2.44	103	96	0.010	246.36
H4	2.41	100	99.3	0.010	242.50
H5	2.448	100.6	100	0.010	243.34
MEAN	2.496				243.49
STDEV	0.1				1.77

**Table C-2 calculating the mass per unit area for each specimen and the mean and standard deviation for each dyed fabric.**

Fabric	Mass (g)	Warp (mm)	Weft (mm)	Area (m <sup>2</sup> )	Mass/per unit area
L1	0.75	90.3	95	0.009	87.43
L2	0.75	91	95.6	0.009	86.21
L3	0.78	90	94.6	0.009	91.61
L4	0.75	91	95.3	0.009	86.48
L5	0.79	91.3	96.3	0.009	89.56
MEAN	0.764				88.26
STDEV	0.019				2.29
M1	1.44	91.3	95.6	0.009	164.44
M2	1.45	92.6	96.6	0.009	162.1
M3	1.44	92	95	0.009	164.76
M4	1.43	90.3	96.6	0.009	163.93
M5	1.45	90	95.3	0.009	169.06
MEAN	1.442				164.86
STDEV	0.008				2.563
H1	1.95	90	94.6	0.009	229.03
H2	1.96	91.3	94	0.009	228.38
H3	1.94	91.6	94.695	0.009	222.94
H4	1.97	92	94.384.6	0.009	226.35
H5	1.92	91.6	94.3	0.009	222.28
MEAN	1.948				225.8
STDEV	0.019				3.083

**Table C-3 calculating the mass per unit area for each specimen and the mean and standard deviation for each printed fabric.**

### **C-3 Thickness**

In order to measure the thickness [4], a specimen was placed between a reference plate and a presser foot connected to a thickness gauge (figure C-2). The gauge was read once the value had settled. This was repeated once on each of the five different test specimens for each fabric. The mean of the results was then determined (tables C-4-6).



**Figure C-2 a fabric sample on the thickness gauge**

Light calico	Thickness	Medium calico	Thickness	Heavy calico	Thickness
L1	0.42	M1	0.44	H1	0.59
L2	0.39	M2	0.46	H2	0.53
L3	0.36	M3	0.48	H3	0.54
L4	0.36	M4	0.46	H4	0.56
L5	0.37	M5	0.48	H5	0.58
MEAN	0.38	MEAN	0.46	MEAN	0.56
STDEV	0.025	STDEV	0.017	STDEV	0.025

**Table C-4 the thickness measurements for all specimens and the mean and standard deviation for each not-coloured fabric.**

Light calico	Thickness	Medium calico	Thickness	Heavy calico	Thickness
L1	0.41	M1	0.5	H1	0.56
L2	0.37	M2	0.53	H2	0.6
L3	0.39	M3	0.5	H3	0.65
L4	0.37	M4	0.51	H4	0.62
L5	0.39	M5	0.5	H5	0.55
MEAN	0.386	MEAN	0.508	MEAN	0.596
STDEV	00.17	STDEV	0.013	STDEV	0.042

**Table C-5 the thickness measurements for all specimens and the mean and standard deviation for each dyed fabric.**

Light calico	Thickness	Medium calico	Thickness	Heavy calico	Thickness
L1	0.36	M1	0.47	H1	0.53
L2	0.37	M2	0.44	H2	0.52
L3	0.36	M3	0.44	H3	0.53
L4	0.33	M4	0.45	H4	0.52
L5	0.33	M5	0.46	H5	0.53
MEAN	0.35	MEAN	0.452	MEAN	0.526
STDEV	0.019	STDEV	0.013	STDEV	0.005

**Table C-6 the thickness measurements for all specimens and the mean and standard deviation for each printed fabric.**

### **C-4 Sett**

The sett (yarns per centimetre) of the fabrics was assessed [5]. Using a sett counter the number of yarns in a centimetre was counted in the warp and weft directions. This was undertaken once on each of the five specimens for each fabric. The results can be seen in table C-7.

Light Calico	Sett (warp)	Sett (weft)	Medium Calico	Sett (warp)	Sett (weft)	Heavy Calico	Sett (warp)	Sett (weft)
L1	27	22	M1	26	26	H1	26	26
L2	27	23	M2	26	27	H2	26	26
L3	27	22	M3	24	26	H3	26	26
L4	27	23	M4	25	26	H4	26	26
L5	27	23	M5	26	27	H5	25	26
MEAN	27	22.6	MEAN	25.4	26.4	MEAN	25.8	26
STDEV	0.000	0.548	STDEV	0.894	0.548	STDEV	0.447	0.000

**Table C-7 the sett for each specimen and the mean and standard deviation for each fabric.**



### C-5 Linear Density

The linear density of the yarns of each not-coloured fabric was estimated using the one metre long strips of fabric from the warp and weft direction. Ten complete yarns were removed from each strip of fabric and weighed on a balance accurate to four decimal places (figure C-3).



**Figure C-3 measuring the linear density of ten yarns**

The linear density in tex was then calculated using equation (C-2) [6]. The results of this can be seen in table C-8.

$$\frac{\text{Mass of yarns taken from fabric in grams} \times 1000}{\text{Length of yarns, in metres}}$$

**Equation C-2 calculating the linear density of the yarns**

Fabric	Warp yarns (g)	Tex	Weft yarns (g)	Tex
Light Calico	0.143	14.3	0.176	17.6
Medium Calico	0.329	32.9	0.308	30.8
Heavy Calico	0.429	42.9	0.466	46.6

**Table C-8 the weight of 10 yarns from each fabric and the resultant tex.**

## C-6 References

- [1] British Standards Institution, Textiles - Domestic washing and drying procedures for textile testing, BS EN ISO 6330. (2012).
- [2] British Standards Institution, Textiles - Standard atmospheres for conditioning and testing, BS EN ISO 139. (2005).
- [3] British Standards Institution, Textiles - Woven fabrics - Determination of mass per unit length and mass per unit area, BS 2471. (2005).
- [4] British Standards Institution, Textiles - Determination of thickness of textiles and textile products, BS EN ISO 5084. (1997).
- [5] British Standards Institution, Textiles - Woven fabrics - Construction - Methods of analysis Part 2: Determination of the number of threads per unit length, BS EN 1049-2. (1994).
- [6] British Standards Institution, Textiles - Woven fabrics - Construction - Methods of analysis - Part 5: Determination of linear density of yarn removed from fabric, BS ISO 7211-5. (1984).

## Appendix D - Post-processing

Following blood drop experiments, the high speed video and wet and dry bloodstain photographs were subjected to post-processing to retrieve measurement data.

### D-1 Analysing high-speed videos in Phantom Camera Software

All blood drops were filmed using a Phantom high speed camera, the video from which was analysed using Phantom Camera Control software to measure the impact velocity and blood drop diameter.

Before doing any measurements, the scale was set by calibrating with the ruler in all videos (figure D-1). A 50mm length of the ruler was measured, and the length of the scale fed into the software. This then provides a calibration in mm/pixel.

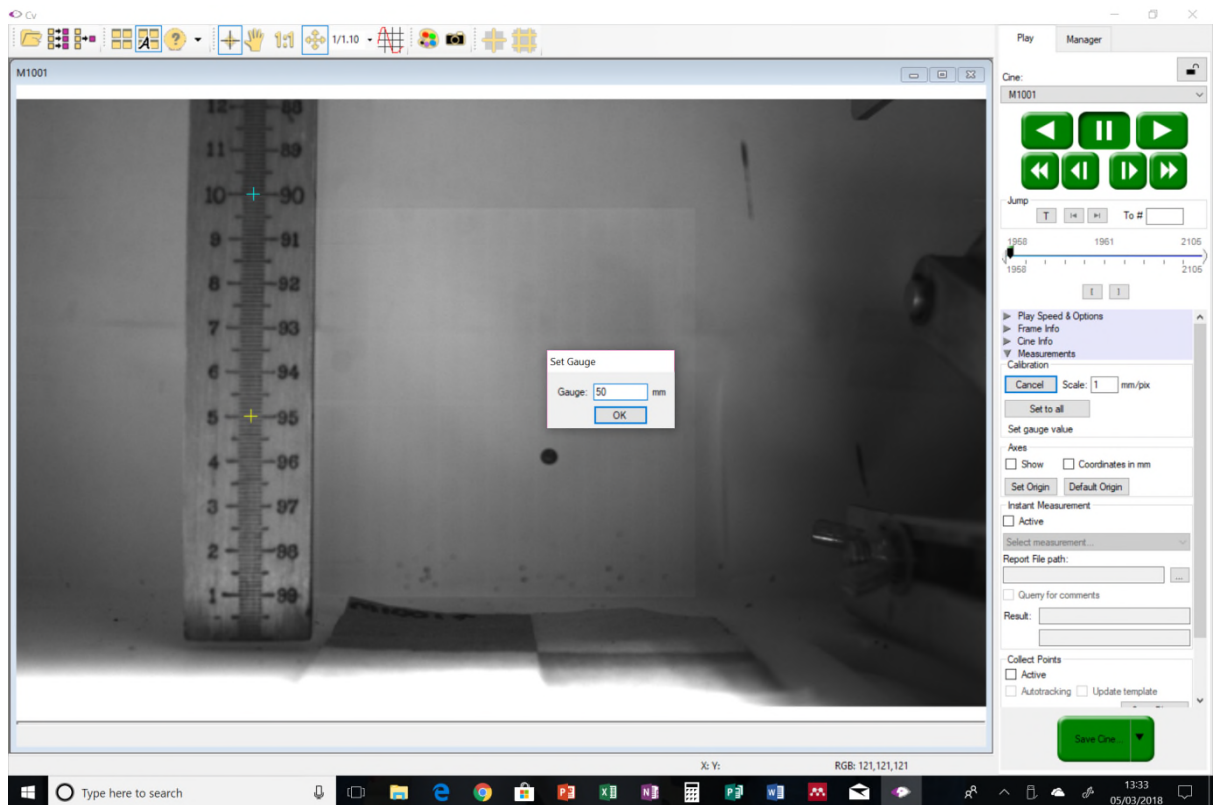
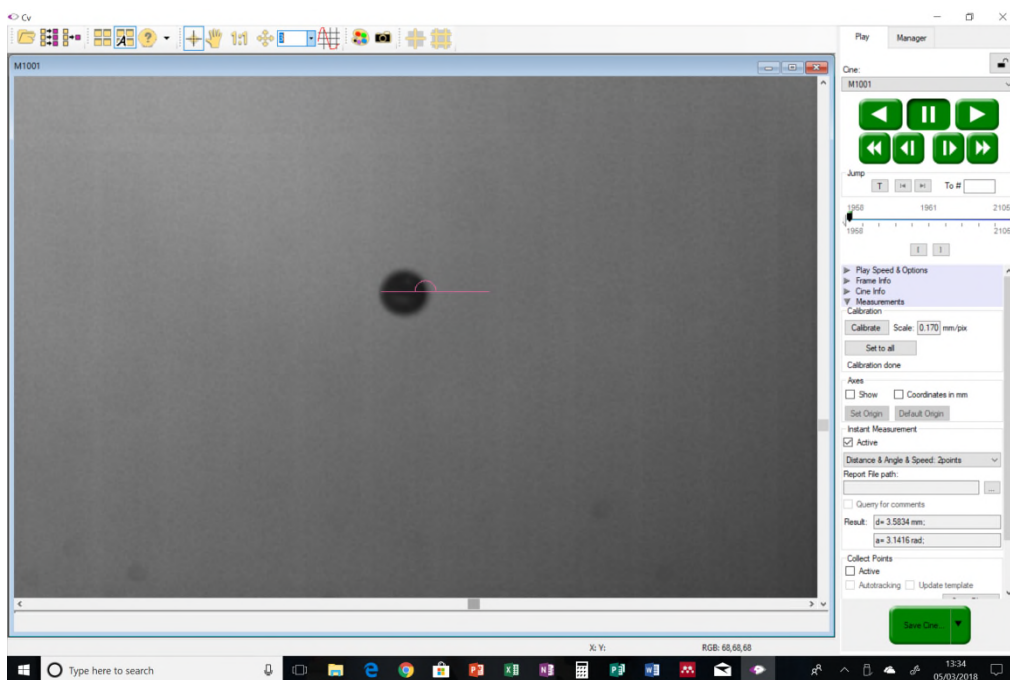


Figure D-1 calibrating the software with the ruler.

Following calibration, the diameter of the bloodstain was measured using the following method (figure D-2):

- 1) Zooming in on the video at least 3 times, in order to get a clearer view of the edges of the blood drop
- 2) Accessing the 'instant measurement' menu and selecting 'distance & angle & speed: 2 points'
- 3) Clicking on one side of the drop and then the other
- 4) The diameter is shown in the right-hand menu



**Figure D-2 measuring the diameter of a blood drop**

The velocity was measured using the following method (figure D-3):

- 1) Accessing the 'instant measurement' menu and selecting 'distance & angle & speed: 2 points'
- 2) Clicking on the centre of the blood drop when it is above the impact surface
- 3) Allow the video to play through until just before the drop is just above the surface of the fabric
- 4) Click on the centre of the drop again
- 5) The velocity is provided in the right-hand menu

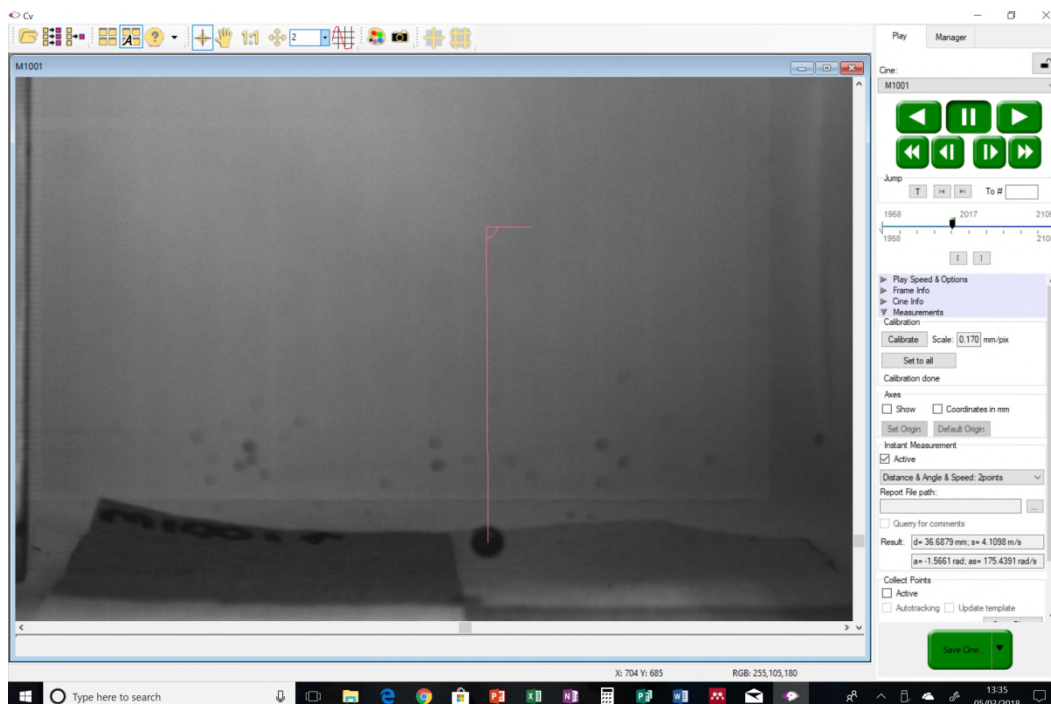


Figure D-3 measuring the impact velocity of a blood drop

For the drop videos when the technical face and the technical rear of the fabric were filmed simultaneously, the camera filming the impact of the blood drop was at an angle of 45°21'. Although the velocity was filmed using the same method as above, it was necessary to further process the data to transform it to take into account the angle of filming. This was done using equation (D-1).

$$x = \frac{V_m}{\cos(90 - 45.35)}$$

Equation D-1 transforming the impact velocity taking into account the angle of recording

Where  $V_m$  is the velocity measured from the high speed video. The velocities measured from the high speed video and respective transformed velocities for all fabrics can be seen in table D-1.

	Not-coloured calico		Dyed calico		Printed calico	
Drop height	Measured velocity	Transformed velocity	Measured velocity	Transformed velocity	Measured velocity	Transformed velocity
200mm	1.32 ms <sup>-1</sup>	1.86 ms <sup>-1</sup>	1.3 ms <sup>-1</sup>	1.83 ms <sup>-1</sup>	1.3 ms <sup>-1</sup>	1.83 ms <sup>-1</sup>
1000mm	3 ms <sup>-1</sup>	4.22 ms <sup>-1</sup>	3 ms <sup>-1</sup>	4.22 ms <sup>-1</sup>	3.05 ms <sup>-1</sup>	4.29 ms <sup>-1</sup>
2000mm	4.1 ms <sup>-1</sup>	5.8 ms <sup>-1</sup>	4.08 ms <sup>-1</sup>	5.74 ms <sup>-1</sup>	4.05 ms <sup>-1</sup>	5.69 ms <sup>-1</sup>

Table D-1 the velocities measured and transformed from the technical face filming.

## D-2 ImageJ

### D-2-1 Photos of the external bloodstains

The primary analysis which was done in ImageJ was measuring the area of the technical face wet and dry bloodstain, and the technical rear dry bloodstain.

#### D-2-1-1 Technical face wet and dry bloodstains

The area of the technical face wet and dry bloodstains across all fabrics were measured using the same method.

- 1) A 50mm scale was drawn using the camera scale included in all photographs.
- 2) The image was converted to 8 bit (figure D-4a).
- 3) The image was converted to binary (figure D-4b).
- 4) A rectangular box was drawn around the parent bloodstain (figure D-4c).
- 5) 'Analyse particles' was selected in the ImageJ menu; this measured all dark areas within the drawn box (figure D-4d).

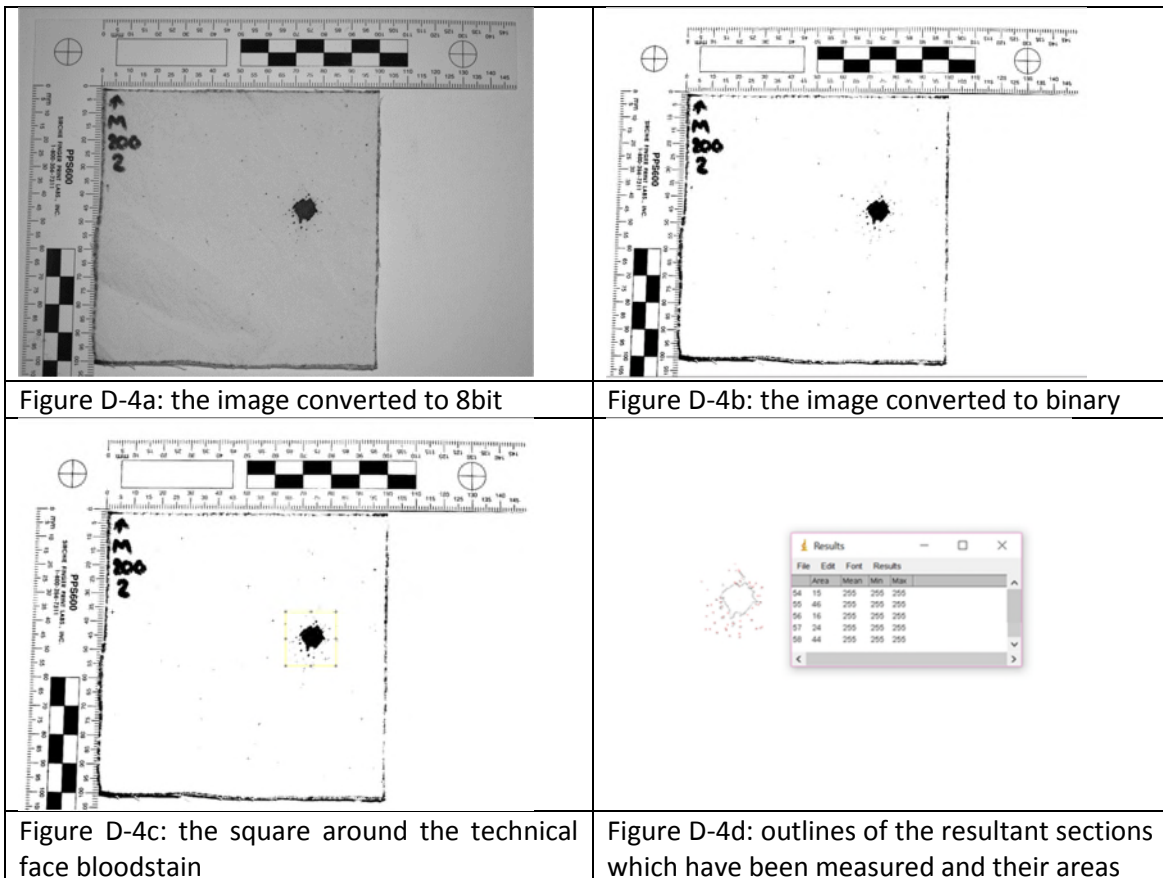
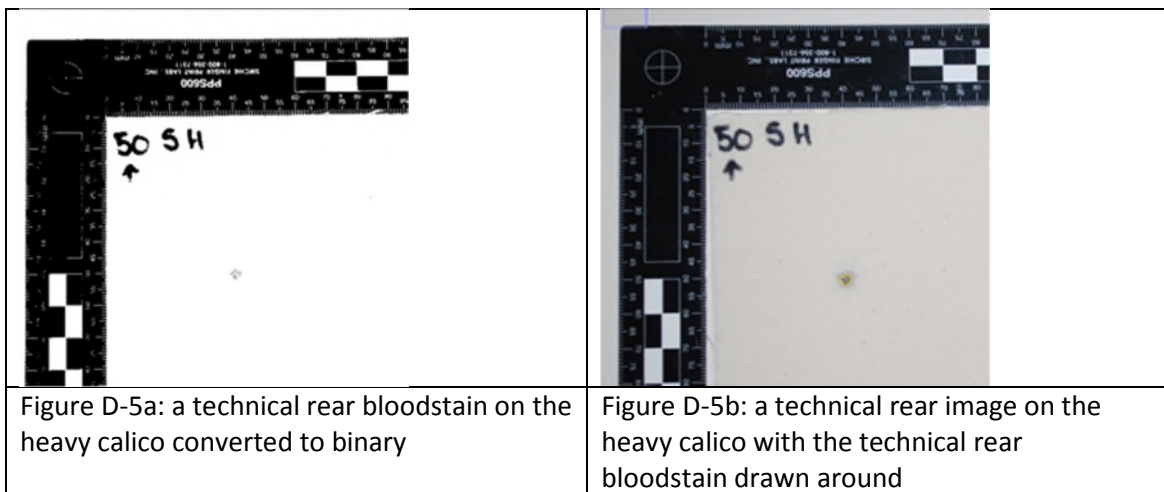


Figure D-4 measuring an example technical face dry bloodstain

### *D-2-1-2 Technical rear bloodstains*

The area of the technical rear bloodstains was measured using the same method as the technical face bloodstains for the majority of samples. However, some of the technical rear bloodstains on the heavy calico could not be seen when the images were changed to binary, so it was not possible to measure them in this method (figure D-5a). Instead, the 'freehand' and 'brush' tools in ImageJ were used to draw around the technical rear bloodstains, and the area measured from the selection (figure D-5b).

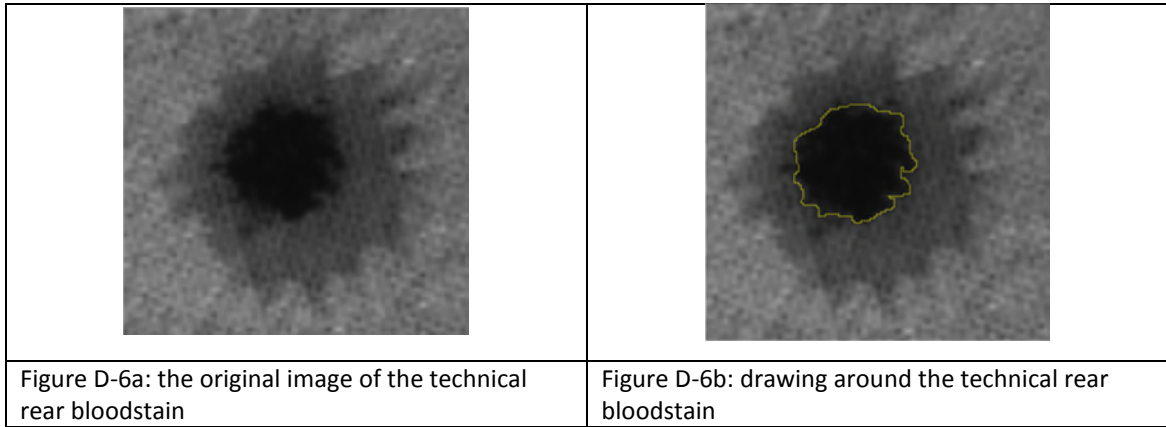


**Figure D-5 measuring the technical rear bloodstains on the heavy calico.**

### **D-2-2 Images from filming the technical rear bloodstain**

Stills were taken from the high-speed videos of the technical rear of the fabric at impact in order to measure the size of the bloodstain which had penetrated through to the technical rear of the fabric. The area of the technical rear bloodstain was measured in the following method:

- 1) A 50mm scale was drawn using the camera scale which was in all the stills.
- 2) The technical rear bloodstain was drawn around using the freehand tool in ImageJ (figure D-6), and the area was measured.



**Figure D-6 measuring the area of an example technical rear bloodstain image to measure the area. The darkest central area is where the blood has passed through to the technical rear of the fabric, while the light surrounding area is blood on the surface of the fabric.**



## Appendix E - Using the Micro Computed Tomography Scanner ( $\mu$ CT)

A CT scanner takes a series of conventional radiographs from a variety of angles. The x-rays exit the tube through an aperture located over an object of interest. As the x-rays pass through the object they are variably attenuated depending on differences in electron density of the constituent atoms [1]. This pattern is then captured by a detector on the other side of the object [1]. The sensitivity of CT to subtle differences in x-ray attenuation is at least 10 times greater than of a conventional x-ray [2]. The content of each of these individual radiographs is determined by the line of the x-ray path through the material. To gain multiple images, in a clinical CT machine the x-ray tube itself rotates, while in a  $\mu$ CT scanner the object rotates.

### E-2 Nikon XTH225

The micro computed tomography ( $\mu$ CT) scanner which was used in the current work was the Nikon XTH225. The specifications for this can be seen in table E-1.

XTH 225	
X-Ray Source	Open Tube UltraFocus Reflection Target
Target	Tungsten
Max kV	225kV
Power Rating	225W
X-Ray Spot Size	3 $\mu$ m
Geometric Magnification	>150x
Imaging System	Varian 2520 Flat Panel Detector
Manipulator	5 axes

Table E-1 Specification of the CT scanner [3]

### **E-3 Mounting the samples**

In order to get an accurate scan of the bloodstains, the specimen holder used in the  $\mu$ CT scanner had to keep the specimens as flat as possible. It also had to be made of a material of different density to the fabrics so it could be removed in post-processing.

Initially, a sample holder was created which sandwiched the samples between two sheets of polycarbonate. The sheets were each 3mm thick. Screws in each corner allowed the polycarbonate sheet to be pressed together to keep the sample flat. When this stand was used in the  $\mu$ CT scanner the specimen was not visible through the specimen holder. The removal of the polycarbonate in the CT scans during post-processing was time-consuming and introduced the possibility of removing some of the bloodstain. Thinner pieces of polycarbonate, 1.5mm thick each, were then used to sandwich the specimen. However, the polycarbonate still needed to be removed during post-processing.

As the polycarbonate in front of the specimen was appearing in the scans, this was then removed. Instead, the fabric specimens were taped to a single sheet of the polycarbonate. This kept the specimens flat without the need for a second sheet of polycarbonate.

However, the size of the specimen and holder mean the specimen had to be further away from the aperture than was necessary, reducing the resolution of the scan. Therefore, the samples were trimmed to a width just greater than that of the parent bloodstain and attached to a small piece of foam. This had the added benefit of being able to scan two specimens at once, one on either side of the foam block. Using the foam block enabled the specimens to be placed closer to the aperture, increasing the resolution of the scans.

All specimens were put in the CT scanner in the same orientation, with the wale (knitted) or warp (woven) orientated vertically.

## E-4 CT Settings

The voltage (kV) and current ( $\mu\text{A}$ ) at which the specimens were scanned was optimised for each of the fabrics (table E-2). The values were decided qualitatively in order to get the highest possible contrast between the blood and the fabric when looking at the live imaging from the scanner. Ideally, the blood stain needs to be visible in the live image, distinct from the fabric background.

Fabric	Target	Voltage (kV)	Current ( $\mu\text{A}$ )	Exposure (ms)	Projections	Frames per projection
Rib knit	Tungsten	35/30	160/300	500	1080	2
Bull drill	Tungsten	35	330	1000	1080	2
Plain calico	Tungsten	120	30	500	1080	2
Dyed calico	Tungsten	50	150	500	1080	2
Printed calico	Tungsten	50	160	500	1080	2

Table E-2 the CT settings for each of the fabrics

## E-5 Post-processing

Following scanning, the data was imported into VGStudio Max 2.1<sup>38</sup>. In order to get the best visualisation on the data, processing was done within this programme:

- **Registering the data:** the data was registered to ensure that it is level, and each cross-section was viewed on the same plane.
- **Cropping the data:** using an inbuilt tool within VGStudio Max, the ellipse tool, the excess data was then removed from around the edge of the bloodstain, including the fabric and any noise from the stand, leaving only the parent bloodstain (figure E-1).
- **Saving images:** following the registration and cropping of the data, cross-sectional images were saved at intervals of 0.05mm in each of the three directions.

---

<sup>38</sup> VGStudio Max is high-end software of the visualisation and analysis of CT data (Volume Graphics 2014).

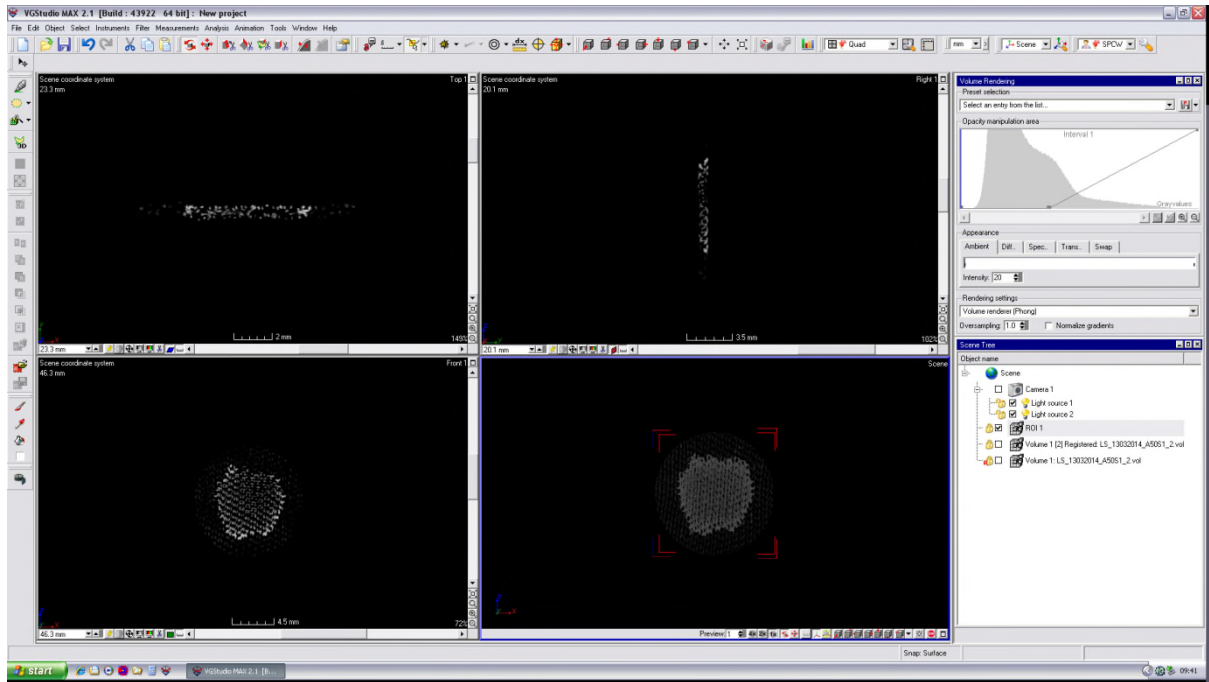


Figure E-1 A sample in VGStudio Max which has been registered and cropped

## E-6 References

- [1] M. Burke, Forensic pathology of fractures and mechanisms of injury: postmortem CT scanning, CRC Press, Florida, 2012.
- [2] M. Mahesh, MDCT Physics: the basics; technology, image quality and radiation dose, Wolters Kluwer, Philadelphia, 2009.
- [3] N. Metrology, I.V. Beyond, XT H Series X-ray and CT technology for industrial applications, (n.d.).

## Appendix F - Scanning electron microscope (SEM)

A scanning electron microscope (SEM) works by focusing an electron beam into a small diameter probe which is scanned across the specimen. A schematic of the basic components of an SEM can be seen in figure F-1. The electrons are accelerated to between 1 KeV and 30 KeV, passing through two or three condenser lenses to demagnify the electron beam. When it hits the specimen it will have a diameter of 2-10 nm [2]. Two perpendicular directions are scanned simultaneously, covering a square or rectangle area of specimen known as a raster [1].

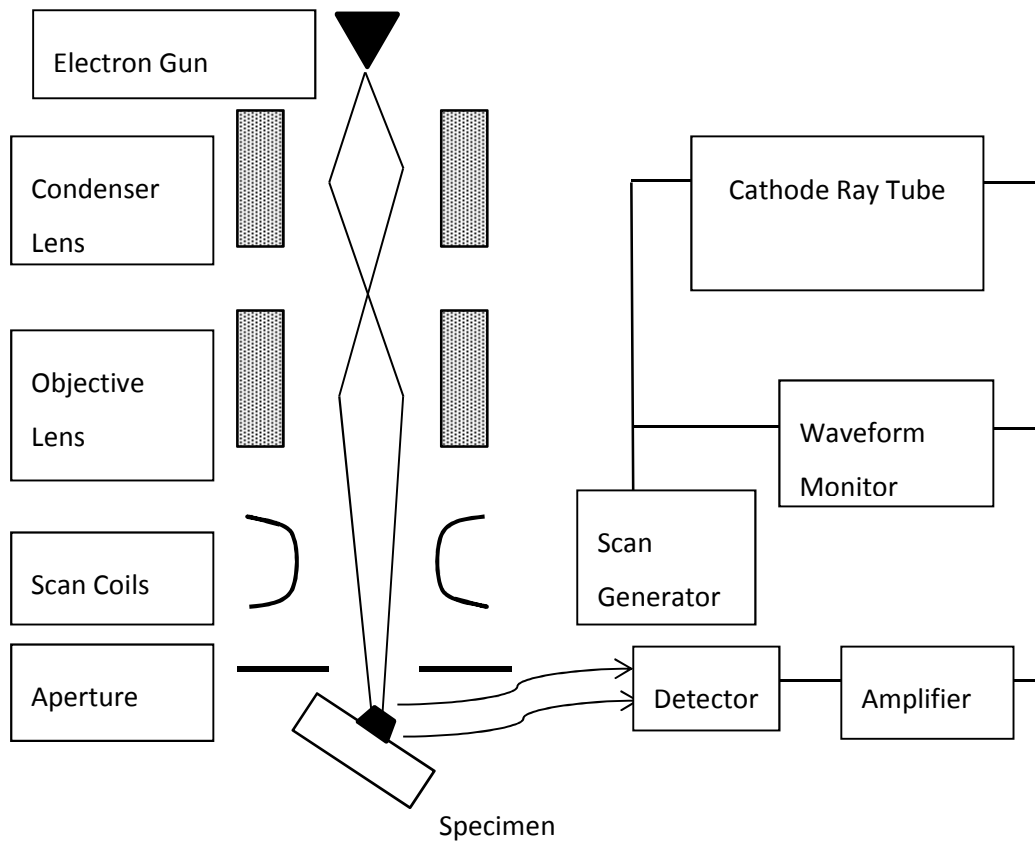


Figure F-1 Drawing of the main components on a scanning electron microscope. Recreated from [2].

When the accelerated electrons enter the solid specimen, they can either interact with the atomic nuclei (elastic scattering) or the atomic electrons (inelastic scattering). The region which contains the majority of the scattered electrons is known as the interaction volume [1]. SEMs normally have the capability of detecting secondary electrons and backscattered electrons [2], which can be distinguished on the basis of

their kinetic energy. Secondary electrons occur when the primary electrons lose energy to the atomic outer shell electrons, which can release them from the atom. If these are created close to the surface of the specimen they may escape into the vacuum. The secondary electrons detected by the SEM create an image of the surface structure of the specimen [1].

A backscattered-electron occurs when a primary electron is ejected from the solid with a scattering angle of greater than  $90^\circ$ . As this is elastic scattering, only a small energy exchange occurs and so most backscattered electrons have energies not far below the primary electron beam. As the backscattered electron coefficient increases with atomic number, these images can show contrast owing to variations in chemical composition [1].

### **F-1 References**

- [1] R. Egerton, *Physical Principles of Electron Microscopy: an introduction to TEM, SEM and AEM*, Springer, New York, 2005.
- [2] P. Goodhew, J. Humphreys, R. Beanland, *Electron Microscopy and Analysis*, Third Edit, Taylor and Francis, New York, 2001.

**Appendix G - Raw data for the not-coloured calico**

Fabric	Height	Specimen	Drop Size	Velocity	Wet area	Dry area	Difference	Reverse Dry	Face vs rear
Light	200mm	S1	3.5	1.7	32.2	28.0	-4.2	27	96%
		S2	3.5	1.7	31.2	28.2	-3.0	29.8	106%
		S3	3.45	1.7	30	26.6	-3.4	18.9	71%
		S4	3.3	1.7	26.3	21.4	-4.9	19.5	91%
		S5	3.5	1.7	32.1	33.6	1.5	31	92%
Medium	200mm	S1	3.31	1.69	24.6	18.8	-5.8	7.4	39%
		S2	3.3	1.7	23.5	18.5	-5.0	2.9	16%
		S3	3.4	1.7	29.7	24.3	-5.4	16.5	68%
		S4	3.3	1.67	31.9	25.7	-6.2	12.5	49%
		S5	3.3	1.7	35.7	29.6	-6.1	17.7	60%
Heavy	200mm	S1	3.45	1.69	23.8	19.3	-4.5	0	0%
		S2	3.2	1.66	22.1	17.7	-4.4	9.7	55%
		S3	3.3	1.67	30.2	24.8	-5.4	10.7	43%
		S4	3.45	1.67	28.8	22	-6.8	8.2	37%
		S5	3.45	1.69	30	24.9	-5.1	16.6	67%
Light	500mm	LS1	3.5	2.7	42.9	44.7	1.7	38	85%
		LS2	3	2.9	38.8	36.7	-2.1	33.1	90%
		LS3	3.01	2.97	55.4	43.7	-11.7	32.1	73%
		LS4	3.4	2.92	42.9	43.3	0.5	38.5	89%
		LS5	3.08	2.94	38.0	38.4	0.4	31.8	83%
Medium	500mm	MS1	3.4	2.91	40.3	34.1	-6.1	15	44%

		MS2	3.06	2.92	30.6	22.0	-8.6	6.4	29%
		MS3	3.06	2.94	41.8	35.5	-6.2	20.8	59%
		MS4	3.06	2.97	38.3	33.9	-4.4	15	44%
		MS5	3.4	2.95	35.1	28.7	-6.4	8.4	29%
Heavy	500mm	HS1	3.4	2.9	43.9	36.6	-7.4	12.1	33%
		HS2	3.06	2.9	38.1	27.9	-10.1	3.6	13%
		HS3	3.08	2.92	43.4	41.8	-1.6	18.7	45%
		HS4	3.06	2.88	47.6	44.3	-3.3	17.6	40%
		HS5	3.06	2.89	33.5	27.2	-6.3	6.6	24%
Light	1000mm	S1	3.4	4.1	46.7	49.6	3.0	43.4	87%
		S2	3.42	4.1	38.7	35.6	-3.2	28.3	80%
		S3	3.42	4.1	43.1	47.6	4.5	38.3	80%
		S4	3.42	4.2	47.8	49.7	1.9	43	87%
		S5	3.42	4.1	38.4	37.7	-0.7	30.1	80%
Medium	1000mm	S1	3.1	4.1	41.7	33.7	-7.9	13.5	40%
		S2	3.42	4.1	38.4	28.0	-10.3	4.8	17%
		S3	3.4	4.1	42.6	37.8	-4.8	15.9	42%
		S4	3.1	4.2	41.6	35.8	-5.8	15.4	43%
		S5	3.4	4.2	43.6	36.7	-7.0	8.7	24%
Heavy	1000mm	S1	3.1	4.1	42.0	35.8	-6.2	10	28%
		S2	3.1	4.1	43.1	31.7	-11.4	5.6	18%
		S3	3.42	4.1	43.6	45.2	1.6	23.1	51%
		S4	3.1	4.1	45.9	41.3	-4.7	9.9	24%
		S5	3.4	4.1	54.8	46.5	-8.3	13.7	29%



Light	1500mm	S1	3.1	4.9	44.8	48.3	3.5	44.9	93%
		S2	3.1	4.9	38.3	34.1	-4.2	30.2	89%
		S3	3.4	5	57.3	66.0	8.7	56.5	86%
		S4	3.4	5	50.3	54.0	3.8	42.8	79%
		S5	3.4	4.9	42.5	41.0	-1.5	34.4	84%
Medium	1500mm	S1	3.4	4.9	49.5	46.0	-3.5	9.7	21%
		S2	3.42	4.9	45.8	35.4	-10.4	8.2	23%
		S3	3.4	4.9	47.9	47.8	-0.1	16.7	35%
		S4	3.4	5	52.8	46.8	-6.0	16.9	36%
		S5	3.4	4.9	43.6	38.1	-5.5	8	21%
Heavy	1500mm	S1	3.42	4.9	45.7	44.0	-1.7	8.9	20%
		S2	3.4	4.9	52.3	42.8	-9.5	1.4	3%
		S3	3.1	4.9	55.0	53.5	-1.5	18.3	34%
		S4	3.4	4.9	50.2	45.6	-4.6	14.2	31%
		S5	3.4	4.9	45.8	42.5	-3.3	4.4	10%
Light	2000mm	S1	3.36	5.2	38.9	39.6	0.7	33.6	85%
		S2	3.35	5.2	40.5	39.9	-0.6	34.7	87%
		S3	3.5	5.2	51.5	47.8	-3.7	42.7	89%
		S4	3.5	5.1	46.3	41.3	-5.0	37.5	91%
		S5	3.5	5.2	40.8	43.8	3.0	39.4	90%
Medium	2000mm	S1	3.55	5.3	43.4	36.3	-7.1	20.5	56%
		S2	3.28	5.5	53.6	50.8	-2.8	29	57%
		S3	3.14	5	55.8	58.9	3.1	48.7	83%
		S4	3.33	5.12	52.6	50.1	-2.5	25.4	51%

		S5	3.2	5.03	46	41.3	-4.7	15.2	37%
Heavy	2000mm	S1	3.4	5.3	41.1	38.3	-2.8	8.6	22%
		S2	3.1	4.7	48.5	47.1	-1.4	14.5	31%
		S3	3.18	5.18	52.7	49.8	-2.9	30.7	62%
		S5	3.78	4.8	49.3	46.1	-3.2	15.8	34%
		S4	3.18	5.1	49.6	46.2	-3.4	24.8	54%
Light	2500mm	5-1	3.2	5.2	65.9	63.1	-2.8	52.1	83%
		5-2	3.2	5.3	68.2	59.3	-8.9	60.5	102%
		5-3	3.4	5.5	61.9	58.6	-3.3	49.1	84%
		5-5	3.4	5.4	72	67.5	-4.5	55.5	82%
		5-6	3	5.3	56.4	50.2	-6.2	40.7	81%
Medium	2500mm	5-1	3.4	5.2	54.3	46.2	-8.1	12.1	26%
		5-2	3.1	5.2	51.5	45.6	-5.9	6	13%
		5-3	3.1	5.2	43.8	36.6	-7.2	14.2	39%
		5-4	3.2	5.3	50.6	46	-4.6	22.2	48%
		5-5	3	5.2	45.2	41.9	-3.3	20.9	50%
Heavy	2500mm	5-1	3	5.2	46.4	44.8	-1.6	20.4	46%
		5-2	3.3	5.6	60.3	55.5	-4.8	32.4	58%
		5-3	3.4	5.5	48.6	46.9	-1.7	12.7	27%
		5-5	3.7	5.8	63.5	60.9	-2.6	42.1	69%
		5-6	3.4	5.5	62.8	59.5	-3.3	32.6	55%

**Appendix H - Raw data for the dyed calico**

Fabric	Height	Specimen	Drop Size	Velocity	Wet area	Dry area	Difference	Reverse Dry	Face vs rear
Light	200mm	S1	3.35	1.71	80.2	78.6	-1.6	76.2	97%
		S2	3.37	1.71	57.6	64.8	7.2	59.2	91%
		S3	3.33	1.69	40.2	41.2	1.0	38.6	94%
		S4	3.59	1.68	61.1	70.6	9.5	70.8	100%
		S5	3.27	1.67	60.9	61.2	0.3	62.6	102%
Medium	200mm	S1	3.31	1.67	30.1	29.7	-0.4	28.5	96%
		S2	3.57	1.7	38.1	34.9	-3.2	29.5	85%
		S3	3.33	1.67	42.2	43.5	1.3	39.6	91%
		S4	3.35	1.67	59.5	59.6	0.1	50.0	84%
		S5	3.68	1.7	37.4	37.6	0.2	33.0	88%
Heavy	200mm	S1	3.59	1.73	43.2	39.3	-3.9	18.0	46%
		S2	3.56	1.68	39.8	34.8	-5.0	23.3	67%
		S3	3.55	1.67	40.4	32.3	-8.1	18.5	57%
		S4	3.29	1.67	29.3	24.5	-4.8	11.7	48%
		S5	3.63	1.69	48.6	43.2	-5.4	25.6	59%
Light	500mm	S1	3.33	2.79	53.2	51.2	-2.0	47.6	93%
		S2	3.31	2.75	66.3	54.7	-11.6	52.9	97%
		S3	3.29	2.72	59.1	59.3	0.2	58.0	98%
		S4	3.33	2.76	52.9	52.0	-0.9	48.9	94%
		S5	3.33	2.79	67.2	61.1	-6.1	60.6	99%
Medium	500mm	S1	3.39	2.76	39.7	33.7	-6.0	29.5	88%
		S2	3.31	2.75	47.1	43.2	-3.9	35.0	81%

		S3	3.31	2.78	45.5	46.1	0.6	35.9	78%
		S4	3.39	2.82	59.7	57.6	-2.1	47.4	82%
		S5	3.33	2.82	51.5	46.7	-4.8	32.6	70%
Heavy	500mm	S1	3.37	2.82	48.5	44.5	-4.0	29.4	66%
		S2	3.59	2.74	43.3	41.0	-2.3	20.2	49%
		S3	3.35	2.74	34.8	29.4	-5.4	16.6	56%
		S4	3.37	2.85	43.6	36.7	-6.9	19.9	54%
		S5	3.39	2.8	54.2	49.3	-4.9	34.6	70%
Light	1000mm	S1	3.39	4.04	56.8	62.5	5.7	61.5	98%
		S2	3.39	4.04	72.4	69.4	-3.0	70.7	102%
		S3	3.39	4.04	68.2	65.0	-3.2	64.8	100%
		S4	3.45	4.12	74.6	77.5	2.9	70.0	90%
		S5	3.41	4.09	70.9	70.6	-0.3	67.8	96%
Medium	1000mm	S1	3.41	4.09	42.4	41.1	-1.3	31.3	76%
		S2	3.43	4.11	48.9	49.4	0.5	34.7	70%
		S3	3.43	4.13	71.6	67.5	-4.1	51.8	77%
		S4	3.39	4.05	60.9	59.3	-1.6	51.2	86%
		S5	3.46	4.14	50.4	48.8	-1.6	38.0	78%
Heavy	1000mm	S1	3.37	4.02	55.3	52.1	-3.2	27.8	53%
		S2	3.44	4.12	55.1	47.9	-7.2	25.6	53%
		S3	3.39	4.05	42.0	39.0	-3.0	25.9	66%
		S4	3.14	4.08	35.4	34.5	-0.9	18.7	54%
		S5	3.43	4.13	64.8	63.4	-1.4	47.8	75%
Light	1500mm	S1	3.43	4.81	76.8	77.8	1.0	75.1	97%

		S2	3.43	4.85	72.3	66.0	-6.3	62.3	94%
		S3	3.44	4.9	67.8	62.2	-5.6	61.4	99%
		S4	3.41	4.88	62.5	59.9	-2.6	58.9	98%
		S5	3.43	4.89	62.2	58.5	-3.7	56.7	97%
Medium	1500mm	S1	3.43	4.83	52.1	48.3	-3.8	41.0	85%
		S2	3.43	4.83	52.3	51.2	-1.1	43.2	84%
		S3	3.45	4.86	68.8	63.2	-5.6	56.8	90%
		S4	3.43	4.87	74.2	66.6	-7.6	60.7	91%
		S5	3.44	4.88	83.3	76.0	-7.3	47.7	63%
Heavy	1500mm	S1	3.45	4.9	68.3	60.9	-7.4	29.3	48%
		S2	3.45	4.89	73.8	70.5	-3.3	32.0	45%
		S3	3.43	4.81	75.5	65.5	-10.0	28.9	44%
		S4	3.12	4.84	45.9	40.0	-5.9	15.0	38%
		S5	3.45	4.82	86.4	78.1	-8.3	41.4	53%
Light	2500mm	1-2	3.2	5.5	61.3	67.5	6.2	65.4	97%
		1-3	3.2	5.3	64.9	73.1	8.2	64.9	89%
		1-5	3.1	5.3	68	75.7	7.7	69.8	92%
Medium	2500mm	1-1	3.1	5.4	55.7	60.9	5.2	48.1	79%
		1-2	3.2	5.3	57.1	55.6	-1.5	39.9	72%
		1-6	3.3	5.3	47.8	51.1	3.3	34.9	68%
Heavy	2500mm	1-1	3	5.3	55.8	52.2	-3.6	27.9	53%
		1-2	3.2	5.3	69.8	70.2	0.4	23.9	34%
		1-5	3.3	5.3	67	64.5	-2.5	33.0	51%

### Appendix I – Raw data for the printed calico drops on the printed face

Fabric	Height	Specimen	Drop Size	Velocity	Wet area	Dry area	Difference	Reverse Dry	Face vs rear
Light	200mm	S1	3.36	1.92	113.9	111.8	-2.1	121.6	-9.8
		S2	3.34	1.82	100.4	117.3	16.9	128.4	-11.1
		S3	3.5	1.89	127.6	129.0	1.4	132.0	-3.0
		S4	3.68	1.87	115.0	128.8	13.8	147.7	-18.9
		S5	3.34	1.85	105.9	115.0	9.1	122.3	-7.3
Medium	200mm	S1	3.5	1.71	68.2	74.5	6.3	75.3	-0.8
		S2	3.52	1.95	63.5	69.0	5.5	67.9	1.1
		S3	3.5	1.81	75.9	86.5	10.6	83.5	3.0
		S4	3.51	1.84	81.8	79.6	-2.2	75.1	4.5
		S5	3.54	1.92	77.3	93.7	16.4	87.5	6.2
Heavy	200mm	S1	3.66	1.96	62.4	71.7	9.3	61.7	10.0
		S2	3.53	1.86	68.8	78.5	9.7	60.1	18.4
		S3	3.33	1.72	64.5	69.7	5.2	59.5	10.2
		S4	3.52	1.83	56.2	63.6	7.4	58.9	4.7
		S5	3.55	1.8	66.9	75.6	8.7	68.8	6.8
Light	500mm	S1	3.52	3.06	96.8	115.5	18.7	118.9	-3.4
		S2	3.68	3.18	123.7	129.5	5.8	141.8	-12.3
		S3	3.71	3.04	121.0	123.6	2.6	141.1	-17.5
		S4	3.33	2.96	109.5	110.4	0.9	122.8	-12.4
		S5	3.87	3.22	124.0	132.4	8.4	141.2	-8.8

Medium	500mm	S1	3.72	3.11	95.1	126.7	31.6	98.5	28.2
		S2	3.7	2.95	85.7	103.9	18.2	104.0	-0.1
		S3	3.14	2.83	67.2	71.3	4.1	65.0	6.3
		S4	3.51	2.88	78.4	86.7	8.3	80.8	5.9
		S5	3.69	3.13	92.0	97.3	5.3	94.2	3.1
Heavy	500mm	S1	3.51	2.97	88.4	98.2	9.8	77.3	20.9
		S2	3.51	2.96	82.4	87.3	4.9	78.7	8.6
		S3	3.68	3.17	83.7	86.2	2.5	74.7	11.5
		S4	3.71	3.08	102.5	104.7	2.2	92.6	12.1
		S5	3.86	2.99	107.7	112.2	4.5	103.0	9.3
Light	1000mm	S1	3.4	4.1	138.4	136.5	-1.9	140.1	-3.6
		S2	3.34	4.07	108.9	114.8	5.9	129.8	-15.0
		S3	3.4	4.1	122.8	128.2	5.4	144.0	-15.8
		S4	3.57	4.27	110.3	115.6	5.3	127.4	-11.8
		S5	3.33	4	133.3	148.5	15.2	160.8	-12.3
Medium	1000mm	S1	3.56	4.12	82.8	87.6	4.8	79.9	7.7
		S2	3.5	4.01	101.0	94.5	-6.5	93.0	1.5
		S3	3.5	4.14	107.8	127.7	19.9	122.5	5.2
		S4	3.5	4.26	96.9	106.7	9.8	101.2	5.5
		S5	3.39	4.07	96.2	97.0	0.8	90.2	6.8
Heavy	1000mm	S1	3.1	3.75	66.1	71.9	5.8	39.4	32.6
		S2	3.14	3.94	87.0	100.1	13.1	53.2	46.9
		S3	3.5	4.23	80.1	91.8	11.7	83.8	8.0
		S4	3.56	4.21	82.6	96.4	13.8	82.3	14.1
		S5	3.56	4.19	105.6	125.4	19.8	93.0	32.4

Light	1500mm	S1	3.5	4.77	112.1	124.9	12.8	131.9	-7.0
		S2	3.32	4.85	107.3	116.3	9.0	126.0	-9.7
		S3	3.48	5.12	133.2	138.1	4.9	148.8	-10.7
		S4	3.48	5.23	115.5	125.9	10.4	123.0	2.9
		S5	3.66	4.91	142.1	147.7	5.6	168.0	-20.3
Medium	1500mm	S1	3.48	4.95	99.0	109.1	10.1	105.7	3.4
		S2	3.66	5.05	84.6	100.6	16.0	89.6	11.0
		S3	3.48	4.83	88.3	102.0	13.7	95.4	6.6
		S4	3.14	4.98	98.3	97.9	-0.4	91.7	6.2
		S5	3.48	4.72	100.5	115.1	14.6	107.5	7.6
Heavy	1500mm	S1	3.66	4.9	96.7	96.9	0.2	76.2	20.7
		S2	3.31	4.81	87.1	89.7	2.6	74.1	15.6
		S3	3.46	5.17	103.1	107.6	4.5	93.3	14.3
		S4	3.32	5.18	100.2	112.2	12.0	90.1	22.1
		S5	3.31	5.05	102.8	110.8	8.0	89.1	21.7
Light	2500mm	1-1	3.3	5.3	120.7	134.2	13.5	135.7	-1.5
		1-5	3.3	5.5	125.1	126.9	1.8	128.9	-2.0
		1-6	3.4	5.4	119.9	139.7	19.8	144.5	-4.8
Medium	2500mm	1-1	3.4	5.5	137.4	134.7	-2.7	124.5	10.2
		1-2	3.3	5.5	122.0	122.5	0.5	112.9	9.6
		1-6	3.3	5.2	101.1	110.3	9.2	102.9	7.4
Heavy	2500mm	1-1	3.3	5.2	104.7	104.8	0.1	64.1	40.7
		1-4	3.3	5.4	86.2	83.7	-2.5	51.6	32.1
		1-6	3.4	5.5	96.1	98.2	2.1	66.1	32.1



**Appendix J - Raw data for the printed calico drops on the not printed face**

Fabric	Height	Specimen	Drop Size	Velocity	Wet area	Dry area	Difference	Reverse Dry	Face vs rear
Light	200mm	3-2	3.6	1.67	153.6	206.4	52.8	194.8	11.6
		3-3	3.5	1.67	163.6	196.8	33.2	186.7	10.1
		3-4	3.6	1.64	172.4	232.5	60.1	220.7	11.8
		3-5	3.5	1.72	165.8	209.4	43.6	202.7	6.7
		3-6	3.5	1.65	169.4	215.6	46.2	203.2	12.4
Medium	200mm	3-1	3.6	1.74	121.4	147.0	25.6	140.9	6.1
		3-2	3.3	1.68	92.1	113.5	21.4	111.3	2.2
		3-3	3.6	1.66	141.8	166.0	24.2	163.5	2.5
		3-4	3.6	1.63	110.7	132.8	22.1	132.2	0.6
		3-5	3.5	1.65	113.7	146.5	32.8	140.1	6.4
Heavy	200mm	3-1	3.3	1.7	52.0	64.9	12.9	62.3	2.6
		3-2	3.5	1.67	69.4	78.2	8.8	79.6	-1.4
		3-3	3.5	1.65	66.3	78.3	12.0	81.4	-3.1
		3-5	3.8	1.64	84.0	101.7	17.7	95.1	6.6
		3-6	3.5	1.66	66.4	77.3	10.9	75.6	1.7
Light	1000mm	5-1	3.4	4.1	155.5	180.9	25.4	171.7	9.2
		5-2	3.4	4.1	165.7	188.1	22.4	177.5	10.6
		5-4	3.6	4.1	183.7	217.0	33.3	200.0	17.0
		5-5	3.6	4.1	180.8	210.5	29.7	200.8	9.7
		5-6	3.5	4	194.3	231.9	37.6	215.3	16.6
Medium	1000mm	5-1	3.7	4.1	142.6	148.2	5.6	144.9	3.3
		5-2	3.6	4.1	134.3	143.8	9.5	134.9	8.9

		5-3	3.8	4.1	144.0	150.7	6.7	139.9	10.8
		5-4	3.4	4	138.9	143.8	4.9	136.5	7.3
		5-5	3.6	4	136.7	145.9	9.2	143.6	2.3
Heavy	1000mm	5-1	3.4	4	80.1	78.2	-1.9	64.6	13.6
		5-3	3.3	4.1	89.1	95.7	6.6	82.0	13.7
		5-4	3.7	4.1	102.0	101.0	-1.0	86.2	14.8
		5-5	3.7	4.1	106.6	109.2	2.6	92.2	17.0
		5-6	3.6	4	101.9	106.9	5.0	89.1	17.8
Light	1500mm	4-1	3.6	4.9	195.9	220.5	24.6	225.9	-5.4
		4-2	3.6	4.8	148.1	186.0	37.9	172.9	13.1
		4-3	3.6	4.8	180.8	204.9	24.1	192.7	12.2
		4-4	3.5	4.8	166.4	195.2	28.8	175.9	19.3
		4-5	3.5	5	160.8	197.3	36.5	171.1	26.2
Medium	1500mm	4-1	3.6	4.8	144.6	151.7	7.1	129.2	22.5
		4-2	3.5	4.7	139.1	149.2	10.1	133.9	15.3
		4-3	3.5	4.7	121.8	132.4	10.6	119.8	12.6
		4-4	3.5	4.8	126.6	133.3	6.7	123.7	9.6
		4-5	3.6	4.8	120.9	140.3	19.4	125.5	14.8
Heavy	1500mm	4-1	3.5	4.5	89.5	88.2	-1.3	73.2	15.0
		4-2	3.6	4.8	91.2	97.4	6.2	86.2	11.2
		4-3	3.6	4.8	90.7	94.5	3.8	83.8	10.7
		4-4	3.8	5	94.1	96.8	2.7	77.7	19.1
		4-5	3.6	4.8	75.0	76.6	1.6	67.1	9.5